Geometric Simplification of a Distributed Rainfall-Runoff Model Over a Range of Basin Scales

Property of
Flood Control District of MC Library
Please Return to
2801 W. Durango
Phoenix, AZ 85009

GEOMETRIC SIMPLIFICATION OF A DISTRIBUTED RAINFALL-RUNOFF MODEL OVER A RANGE OF BASIN SCALES

by

David Charles Goodrich

A Dissertation Submitted to the Faculty of the

DEPARTMENT OF HYDROLOGY AND WATER RESOURCES

In Partial Fulfillment of the Requirements
For the Degree of

DOCTOR OF PHILOSOPHY
WITH A MAJOR IN HYDROLOGY

In the Graduate College

THE UNIVERSITY OF ARIZONA

1990

DEDICATED TO MY WIFE, KELLY

AND

MY PARENTS, DON AND MARILYN

ACKNOWLEDGEMENTS

Many have contributed directly or indirectly to the research effort reported here. Special thanks to Dr. David A. Woolhiser. I am forever in his debt for his thoughtful guidance, gracious patience, and largess of time, insight and wisdom. Dr. Soroosh Sorooshian's acumen and discerning judgement has contributed greatly to this effort. Many staff members of the Aridland Watershed Management Research Unit of USDA-Agricultural Research Service (ARS), Tucson, Arizona have provided valuable knowledge, assistance and diligent collection of high quality hydrologic data. Special thanks are extended to Carl Unkrich, Tim Keefer, Roger Simanton and Fatima Lopez. Financial assistance during the course of my graduate work has been provided by the National Science Foundation via a Graduate Research Fellowship, the American Society of Civil Engineers and the Hydrology Section of the American Geophysical Union for a Research Fellowships, the U. S. Geological Survey, USDA-Agricultural Research Service, and the U. S. Department of Energy (Los Alamos National Laboratory). Preparation and distribution of this report was made possible by a NASA/EOS interdisciplinary investigation (Sorooshian and Huerte, 1989). Without this assistance this effort could not have been undertaken and I gratefully acknowledge this support.

Property of
Flood Control District of MC Library
Please Return to
2801 W. Durango
Phoenix, AZ 85009

TABLE OF CONTENTS

Page

LIST OF ILLUSTRATIONS 10

LIST OF TABLES 18

ABSTRACT 20

1. INTRODUCTION 22

1.1 Problem Statement 22

1.2 Approach 23

1.3 Structural Overview 34

1.4 Literature Review 36

1.4.1 Geometric Simplification of Distributed Models 36

1.4.2 The Importance of Scale 43

1.4.3 Models and Model Complexity 46

1.4.4 Evidence of Subprocess Domination and Scale Thresholds 51

1.4.5 Spatial and Temporal Variability 55

1.4.6 Literature Review Summary 58

2. SMALL-SCALE INFILTRATION VARIABILITY AND RAINFALL-RUNOFF MODELING 59

2.1 Chapter Objectives 59

2.2 Introduction and Background 59

TABLE OF CONTENTS--Continued

Page

2.3 Approach 62

2.3.1 KINEROS: The Rainfall-Runoff Model 62

2.3.2 Review of Early Results 67

2.4 Model Reformulation and Improvements 72

2.4.1 Using Ks' and C_v from Field Estimates 72

2.4.2 Variable Strip Formulation 74

2.4.3 Estimation of the Model Required Soil Parameters from Textural Estimates of Ks' 77

2.5 Comparison to Other Model Representations of Infiltration Variability 81

2.6 Determination of the Number of Parallel Strips for the W-G Model 91

2.7 Summary and Conclusions 102

3. CHANNEL ATTENUATION EFFECTS ON SEVERAL TEMPORAL RAINFALL REPRESENTATIONS 104

3.1 Introduction 104

3.2 Background Review 106

3.3 Approach 110

3.4 Simulations to Assess Channel Attenuating Effects on Precipitation Distribution 117

3.5 Results 120

3.6 Random Storm Variation in the Woolhiser-Osborn Disaggregation Method 138

TABLE OF CONTENTS--Continued

Page

3.7 Conclusions 142

4. A METHOD FOR GEOMETRIC MODEL SIMPLIFICATION 145

4.1 Introduction 145

4.1.1 Channel and Overland Contributing Area Representation of Watershed 148

4.1.2 Evidence to Support a Simplified Slope Representation 150

4.2 Rules for Geometric Model Simplification 152

4.3 The Importance of Equilibruim Storage 157

4.3.1 Background 157

4.3.2 Storage Computations and Determination of Equivalent Roughness 159

4.3.3 The Basin Characteristic and Kinematic Equilibrium Time Relationship 162

4.4 Testing of the Simplification Procedure 165

4.5 Sensitivity of the Simplification Procedure to Computational Length and Initial Roughness 180

4.5.1 Sensitivity to Computational Length 180

4.5.2 Sensitivity to Initial Roughness 183

4.6 Summary 188

5. MODEL SENSITIVITY, CALIBRATION, AND VERIFICATION 191

TABLE OF CONTENTS--Continued

Page

5.1. Introduction and Background 191

5.2. Sensitivity to Selected Optimization Parameters 194

5.3. Model Calibration and Verification 216

5.3.1 Background 216

5.3.2. Calibration and Verification Data 217

5.3.3. Measuring Model Performance 221

5.3.4. The Search for Acceptable Model Parameters 226

5.3.5. Verification of Model Acceptability 231

5.4. Conclusions 247

6. SENSITIVITY AND GEOMETRIC MODEL COMPLEXITY AS A FUNCTION OF BASIN SCALE 250

6.1. Introduction 250

6.2. Model Performance as a Function of Basin Scale 251

6.3. Model Sensitivity as a Function of Basin Scale 257

6.3.1. Sensitivity of the Objective Function to Basin Scale for Calibration Multipliers 257

6.3.2. Hydrologic Subprocess Sensitivity as a Function of Scale 262

6.4. Geometric Model Simplification as a Function of Basin Scale and Storm Size 277

6.4.1. Geometric Model Simplification as a Function of Basin Scale 277

TABLE OF CONTENTS--Continued

Page

6.4.2. Geometric Model Simplification as a Function of Storm Size 295

6.5. Application of Study Results 302

6.6. Conclusions 305

7. CONCLUSIONS AND RECOMMENDATIONS FOR FUTURE RESEARCH 309

7.1. Major Conclusions and Contributions 309

7.2. Recommendations for Future Research 315

APPENDIX A: DETAILED DESCRIPTION OF HYDROLOGIC DATA FOR STUDY BASINS 318

APPENDIX B: ESTIMATION OF INITIAL SOIL MOISTURE FOR RUNOFF EVENTS 336

APPENDIX C: SPACE-TIME RAINFALL INTERPOLATION 342

LIST OF REFERENCES 348

LIST OF ILLUSTRATIONS

Figure		Page
1.1	USDA-ARS Walnut Gulch Experimental Watershed Location Map	25
1.2	Lucky Hills Subwatersheds	30
1.3	Walnut Gulch Subwatershed 11	31
2.1	Interplane Assignment of Ks'	68
2.2	Impacts of Climate, Degree of Spatially Variable Infiltration (C_v), and F_p* on the Hydrographs (from Woolhiser and Goodrich, 1988)	70
2.3	Composite Infiltration Curves with Lognormally Distributed Ks as a Function of C_v	83
2.4	Evolution of Time and Area-Dependent Infiltration Capacity (First Presented by Goodrich, Woolhiser, and Sorooshian, 1989)	85
2.5	Comparison of Methods to Treat Spatially Variable Infiltration in Surface Runoff: Small Runoff/Rainfall Ratio Case (from Smith, Goodrich, and Woolhiser, 1990)	87
2.6	Comparison of Methods to Treat Spatially Variable Infiltration in Surface Runoff: Large Runoff/Rainfall Ratio Case (from Smith, Goodrich, and Woolhiser, 1990)	87
2.7	Runoff Response as a Function of the Number of Parallel Strips (Storm 30, Soil 2).	94
2.8	Number of Strips Required to Maintain Volume to Within 10 Percent of the 50-Strip Case	100
3.1	Simple Catchment Geometry	111

LIST OF ILLUSTRATIONS--Continued

Figure		Page
3.2	Channel Slope vs. Length for Varying Lambda, Fixed n_c = 0.02, L_p = 30.5m, S_p = 0.1, and n_p = 0.01	115
3.3	Channel Slope vs. Length for Varying Lambda, Fixed n_c = 0.08, L_p = 30.5m, S_p = 0.1, and n_p = 0.01	115
3.4	Hydrograph from Pulsed Input for Two Different Catchments with Equal Lambda	118
3.5	Empirical Distributions Functions of Peak Discharge for a 30.5m Impervious Plane (Cases 1-4, T_* = 0.0345, F_{p*} = 0.0)	121
3.6	Empirical Distributions Functions of Peak Discharge for a 91.4m Infiltrating Plane (Cases 45-48, T_* = 0.308, F_{p*} = 0.574)	123
3.7	Empirical Distributions Functions of Peak Discharge for a 152.4m Impervious Plane (Cases 5-8, T_* = 0.585, F_{p*} = 0.0)	124
3.8	Empirical Distributions Functions of Peak Discharge for a 152.4m Infiltrating Plane (Cases 29-32, T_* = 0.585, F_{p*} = 1.15)	125
3.9	(a) Largest Storm Hyetograph and Resulting Hydrographs for All Lambda with 152.4m Infiltrating Planes (T_* = 0.585, F_{p*} = 1.15)	127
	(b) Largest Storm Hyetograph and Resulting Hydrographs for All Lambda with 91.4m Impervious Planes (T_* = 0.308, F_{p*} = 0.0)	127

LIST OF ILLUSTRATIONS--Continued

Figure		Page
3.10	(a-d) K-S D* Contour Plots for = 0, 0.5, 1.0, 1.5 Using Constant Storm Disaggregation	130
3.11	(a-d) K-S D* Contour Plots for = 0, 0.5, 1.0, 1.5 Using Isosceles Storm Disaggregation	131
3.12	(a-d) K-S D* Contour Plots for = 0, 0.5, 1.0, 1.5 Using Woolhiser-Osborn Storm Disaggregation	132
3.13	(a-c) Scatter Plots of Runoff Volume vs. Peak Rate for Fixed F_p* and Increasing T_*	136
3.14	(a-c) Scatter Plots of Runoff Volume vs. Peak Rate for Fixed T_* and Increasing F_p*	137
3.15	(a) Ten Realizations of Empirical Distribution Functions of Peak Rate for a Fast Responding Catchment (T_* = 0.0345); (b) Histogram for All Ten Realizations of Empirical Distribution Functions of Peak Rate for a Fast Responding Catchment (T_* = 0.0345)	139
3.15	(c) Ten Realizations of Empirical Distribution Functions of Peak Rate for a Slowly Responding Catchment (T_* = 0.585); (d) Histogram for All Ten Realizations of Empirical Distribution Functions of Peak Rate for a Slowly Responding Catchment (T_* = 0.585)	140
4.1	Basin Representation as a Function of Map Scale	146
4.2	Lucky Hills-106 Watershed: Base Map and Basin Segmentation	149

LIST OF ILLUSTRATIONS--Continued

Figure		Page
4.3	Model Representation as a Function of Map Scale (a) Elementary Watershed Base Map Representation (b) Model Representation (c) Model Slope Distribution	151
4.4	Slope Distributions as a Function of Basin Scale	153
4.5	Five Element vs. Single Equivalent Plane: Equilibrium Simulation	167
4.6	Five Element vs. Single Equivalent Plane: Partial Equilibrium Simulation	167
4.7	Five Element vs. Single Equivalent Plane: Measured Rainfall Event (Impervious)	168
4.8	Five Element vs. Single Equivalent Plane: Measured Rainfall Event (Infiltrating)	168
4.9	Five Element vs. Single Equivalent Plane: Partial Equilibrium Simulation (Infiltrating)	170
4.10	LH-106: Four Levels of Model Aggregation	173
4.11	Model Performance vs. Model Complexity	174
4.12	Event 2 Hydrographs	179
4.13	Model Aggregation Error vs. Model Complexity for Various Initial Roughness Values (C_v = 0.0)	185
5.1	Observed Versus Simulated Runoff for Event 53 (Roughness and Ks Parameter Multipliers Manually Adjusted)	196

LIST OF ILLUSTRATIONS--Continued

Figure		Page
5.2	Sensitivity of Tp, Qp, and VOL. of Simulated Runoff to a -/+ 10% Perturbation of Selected Model Parameters Over a Range of Ten Events	199
5.3	Variation in Tp, Qp, and Runoff Volume Caused by Using Rainfall Input from Two Adjacent Raingages (Approximately 300m Apart)	209
5.4	Runoff Simulations on LH-106 Using Rainfall from Adjacent Raingages for Event 3 (August 23, 1982)	212
5.5	Frequency Histograms of Runoff Volume and Peak Runoff Rate for LH-106 for the Selected Calibration and Verification Events	220
5.6	Calibration Event Selection Matrix for LH-106	222
5.7	Response Surface Plots of Volume and Peak Rate Calibration Efficiency at Fixed M_R for LH-104	230
5.8	Response of Volume and Peak Rate Calibration Efficiency to M_R for Fixed M_K and M_C for LH-104	232
5.9	LH-106: Observed Versus Simulated Volumes and Peak Rates for Calibration and Verification Event Sets	238
5.10	LH-102: Observed Versus Simulated Volumes and Peak Rates for Calibration and Verification Event Sets	239
5.11	LH-104: Observed Versus Simulated Volumes and Peak Rates for Calibration and Verification Event Sets	240

LIST OF ILLUSTRATIONS--Continued

Figure | Page

5.12 WG11: Observed Versus Simulated Volumes and Peak Rates for Calibration and Verification Event Sets 241

5.13 LH-106: Third Best and Worst Calibration Hydrographs Based on Volume and Comparable LH-104 Model Hydrographs Using LH-104 Multipliers 243

5.14 LH-102: Third Best and Worst Calibration Hydrographs Based on Volume and Comparable LH-104 Model Hydrographs Using LH-104 Multipliers 244

5.15 LH-104: Best and Worst Calibration Hydrographs Based on Volume 245

5.16 WG11: Best and Worst Calibration Hydrographs Based on Volume 246

6.1 Model Performance Versus Basin Area as Measured by the Forecast Coefficient of Efficiency 253

6.2 Observed and Simulated Means and Standard Deviations of Runoff Volume Versus Basin Area for the Calibration and Verification Event Set 254

6.3 Observed and Simulated Means and Standard Deviations of Peak Runoff Rate Versus Basin Area for the Calibration and Verification Event Set 255

6.4 Ec Response Surface for Runoff Volume as M_K and M_C Vary with Fixed M_R for the Lucky Hills Watersheds 258

6.5 Ec for Qp as a Function of M_R for All Study Basins 260

LIST OF ILLUSTRATIONS--Continued

Figure Page

6.6 Sensitivity of Runoff Response to Perturbations of Ks (Planes) and Ks (Channels) over a Range of Basin Scales 264

6.7 Illustration of the Importance of Channel Infiltration Losses on
(a) LH-104
(b) WG11 266

6.8 Sensitivity of Runoff Response to Perturbations of Roughness (Planes) and Roughness (Channels) over a Range of Basin Scales 267

6.9 Sensitivity of Runoff Response to Perturbations of C_v over a Range of Basin Scales 269

6.10 Ec for Qp and V as a Function of M_C for all Study Basins 270

6.11 Sensitivity of Runoff Response to +/-(15%) Perturbations of Rainfall over a Range of Basin Scales 274

6.12 Sensitivity of Peak Runoff Rate for Several Events to Perturbations of Rainfall over a Range of Basin Scales 275

6.13 Model Performance for Various Levels of Geometric Model Simplification for the Lucky Hills Watersheds 287

6.14 Model Performance for Various Levels of Geometric Model Simplification for WG11 288

6.15 Simplification and Percentage Simplification Error (30 to 1 Ele.) Versus Runoff Volume for LH-106 297

LIST OF ILLUSTRATIONS--Continued

Figure Page

6.16 Simplification and Percentage Simplification Error (68 to 1 Ele.) Versus Runoff Volume for LH-102 298

6.17 Simplification and Percentage Simplification Error (235 to 1 Ele.) Versus Runoff Volume for LH-104 299

6.18 Simplification and Percentage Simplification Error (243 to 1 Ele.) Versus Runoff Volume for WG11 300

LIST OF TABLES

Table		Page
1.1	Basic Research Watershed Characteristic	32
2.1	Summary of Regressions Relating Ks to Soil Parameters G, SR, and SFC	79
2.2	Test Storm Characteristics	95
2.3	Test Soil Characteristics	96
2.4	F_p* for ($\bar{I}$ - Soils) Combinations	97
2.5	Runoff Volume and Peak Rate Change as a Function of the Number of Parallel Strips	98
2.6	Runoff Volume Error from 50-Strip Case to Eight Strips for Four Lucky Hills Storms and the Minimum and Maximum Ks' Soil	101
3.1	Selected Plane and Channel Model Parameters	119
4.1	Equivalent Roughness Values for Various Rainfall Rates	166
4.2	Storm Characteristics for Test Events	171
4.3	Summary of Simplification Impacts	175
4.4	Sensitivity of Aggregation to Computational Length	182
5.1	KINEROSR Model Parameters Used in the Sensitivity Analysis	198
5.2	Lucky Hills Rainfall Depth Comparisons	210
5.3	Final Multipliers (Calibration Parameters)	229

LIST OF TABLES--Continued

Table | Page

5.4 Calibration and Verification Forecasting and Prediction Efficiencies for Runoff Volume and Peak Rate for All Study Basins 233

5.5 Mean and Standard Deviation for Volume and Peak Rates and Average Sum of Squared Deviations for Calibration and Verification Event Sets for All Study Basins 234

6.1 Calibration Set Runoff Ratio Statistics 271

6.2 LH-102 Simplification Error Components 282

6.3 Routing Simplification Errors for Individual Events for LH-102 (Impervious - Single Raingage) 284

6.4 Total Simplification Errors for Individual Events for LH-102 (Infiltrating Multi-Raingage Case) 285

6.5 Suggested Level of Percent Average Support Area to Maintain a Reasonable Level of Model Performance 290

ABSTRACT

Distributed Rainfall-Runoff models are gaining widespread acceptance; yet, a fundamental issue that must be addressed by all users of these models is definition of an acceptable level of watershed discretization (geometric model complexity). The level of geometric model complexity is a function of basin and climatic scales as well as the availability of input and verification data. Equilibrium discharge storage is employed to develop a quantitative methodology to define a level of geometric model complexity commensurate with a specified level of model performance. Equilibrium storage ratios are used to define the transition from overland to channel-dominated flow response. The methodology is tested on four subcatchments in the USDA-ARS Walnut Gulch Experimental Watershed in Southeastern Arizona. The catchments cover a range of basins scales of over three orders of magnitude. This enabled a unique assessment of watershed response behavior as a function of basin scale. High quality, distributed, rainfall-runoff data was used to verify the model (KINEROSR). Excellent calibration and verification results provided confidence in subsequent model interpretations regarding watershed response behavior. An average elementary channel support area of roughly 15% of the total basin area is shown to provide a watershed discretization level that maintains model performance for basins ranging in size from 1.5 to 631 hectares. Detailed examination of infiltration, including the role and impacts of incorporating small scale infiltration variability in a distribution sense, into KINEROSR, over a range of soils and climatic scales was also addressed. The impacts of infiltration and channel losses

on runoff response increase with increasing watershed scale as the relative influence of storms is diminished in a semiarid environment such as Walnut Gulch. In this semiarid environment, characterized by ephemeral streams, watershed runoff response does not become more linear with increasing watershed scale but appears to become more nonlinear.

CHAPTER 1

INTRODUCTION

1.1 Problem Statement

The content of this report is based on a dissertation by Goodrich (1990).

Distributed rainfall-runoff models are gaining widespread acceptance; yet, a fundamental issue that must be addressed by any user of these models is definition of an acceptable level of watershed discretization or geometric model complexity. The level of basin discretization relates directly to the degree of data averaging and parameter lumping that is permissible for a specified range of time-space scales. Some geometric and/or parameter lumping is inevitable, as distributed parameter systems formulated as partial differential equations are by definition of infinite dimension. This study will focus on geometric model complexity and not on process model complexity. For the purposes of this study, process model complexity refers to the type of transform equations used to model processes of routing and infiltration, nonlinear partial differential equations and their numerical representations being the most complex, and linear equations and simple regressions being less complex. Studies that have examined geometric model simplification in the context of watershed modeling are reviewed in detail in the literature review.

A scale-based quantitative framework to predict the proper level of geometric model complexity for a given modeling objective would allow one to simplify modeling and data collection efforts. This would enable the practitioner to introduce model complexity and collect data only to the extent that is required to meet his or

her needs. A firm basis of understanding this issue will serve as a foundation for the investigation of the dominant factors affecting runoff at a particular scale. A better grasp of the hydrology in semi-arid regions, as well as more reliable mathematical models for surface water management and control, will ultimately result from this line of research.

1.2 Approach

Defining the proper level of geometric model complexity is a subset of the larger problem of formulating a model building methodology that would easily enable a practitioner to construct a rainfall-runoff model which would meet desired accuracy requirements. Within this methodology, a theoretic framework and computational procedures would be developed to form measures characterizing basin-climatic space-time scales. Ideally, these measures could be obtained from existing data or from data collected at relatively little expense. The methodology would answer the basic question: What level of model complexity is sufficient to accomplish pre-stated modeling objectives and accuracies? It would allow the practitioner to assess data requirements and formulate the simplest rainfall-runoff model possible. This would enhance model calibration and parameter identifiability.

Many of the issues related to this larger problem will be addressed as part of a NASA-EOS effort (Sorooshian and Huerte, 1989). The present study concerning geometric model complexity and related issues highlighted in the literature review serves as a first step in addressing the larger modeling methodology problem. To further focus the study of geometric model complexity, a restricted climatic and

watershed regime will be examined. The study will focus on semi-arid watersheds prevalent at lower elevations in the southwestern United States. Summer air mass thunderstorms will be the type of climatic regime studied. The choice of this climate and region resulted from a preliminary study of the major processes responsible for runoff generation in this region and examination of data availability to verify study results.

Beck (1987) clearly stated that there are few practical case studies with extensive field data sets that address the problem of the appropriate level of geometric model complexity for adequate modeling. The need for a high quality rainfall-runoff data sets over a range of basin scales largely dictated the study location. The Walnut Gulch Experimental Watershed operated by the Agricultural Research Service (ARS) of the U.S. Dept. of Agriculture provided the necessary high-quality, long-term rainfall, runoff, topographic, and soils data used in this study. A general location map of the overall watershed is presented in Figure 1.1.

As a starting point of the investigation, initial analysis will concentrate on physically-based models to unlock the puzzle of hydrologic subprocess (overland routing, channel routing, channel infiltration, etc.) domination at various scales. The dominate subprocess is defined as the one which imparts the greatest degree of attenuation of the rainfall signal in its transformation to runoff. Of primary importance will be the subprocess transition from overland to channel dominated flow, as this will define the degree of geometric model complexity required. To more

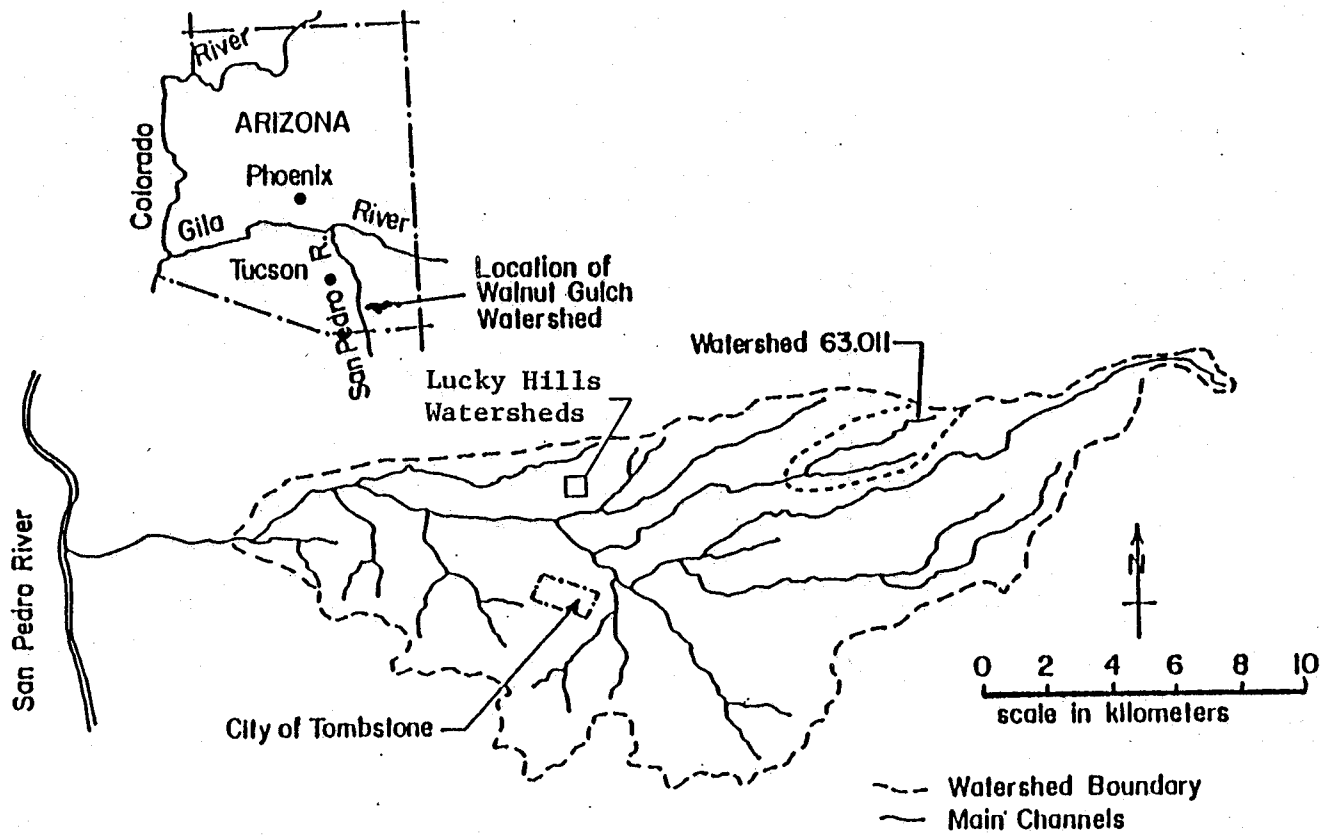

Figure 1.1. USDA-ARS Walnut Gulch Experimental Watershed Location Map

formally focus the geometric model complexity investigation, the following hypothesis is offered.

HYP (1): At a certain basin scale, represented by a base map of a given scale, in the climatic regime specified above, a maximum allowable size of overland flow elements will exist so that elements below this size will adequately model basin runoff and elements above this size will not.

This hypothesis translates directly into the required drainage density or first-order channel support area that must be maintained at a fixed map scale. A fixed drainage density defines the level of channel detail that will be modeled. If a specific drainage density must be maintained, it implies that the channel processes being modeled at that scale are important. This provides an indication of the transition between overland and channel dominated flow. Criteria to define the allowable size of an overland flow element must be established. To do so, a specified level of model performance will be set by way of an objective function to establish if model equivalence exists for a complex versus simple geometric basin representation.

Several specific subissues must also be examined to address hypothesis (1). The first concerns the scale of the climate or storm size. Investigation of this issue is posed by way of hypothesis 1A.

HYP (1A): The degree of allowable geometric model simplification is a function of storm size.

In the above hypothesis, "allowable" refers to a prespecified level of model performance as stated above. Storm size refers to the amount of rainfall compared to the amount of water abstracted by infiltration (excess runoff). A large storm has a small percentage of rainfall abstracted, and a small storm has a relatively high percentage of infiltration losses. Model representation of infiltration is the second subissue of hypothesis (1).

Two levels of overland runoff generation will be examined. At the first level, in very small basins, it is hypothesized that some representation of random variability of runoff-producing mechanisms must be incorporated into the model structure. At the second level, for larger basins, it is postulated that simple averages of properties or parameters can be used and still adequately model runoff. These two levels of model sophistication will be studied by way of the following hypotheses which are also a subset of hypothesis (1).

HYP (1B): For overland runoff generation, above a certain soils-climatic scale, hillslope positions will not be important to modeling runoff, but spatial variability must be considered.

HYP (1C): Above a certain basin-climatic scale, simple property or parameter averages of overland flow will be sufficient to model runoff.

KINEROSR (an extension of the work of Rovey et al., 1977 and Woolhiser et al., 1990) is the physically-based model that will be used in the investigation. This model uses a kinematic wave approximation to the dynamic flow equations for both overland and channel flow. Overland flow planes are used to approximate the watershed topography. Greater spatial variability can be incorporated by using a greater number of flow planes of smaller size. It employs an implementation of the Smith and Parlange (1978) interactive infiltration routine and allows explicit treatment of channel transmission losses. This particular model has been tested and widely used as a research tool on local semi-arid watersheds. Other implementations of kinematic routing are also used among practitioners and other federal agencies (HEC-1 of the Army Corps of Engineers; DR3M of the U.S. Geological Survey, Alley and Smith, 1982; WITWAT II of the South African Water Research Commission, Green, 1984, IIHR of the University of Iowa, Jain et al., 1982). In each

of these distributed model implementations, the key issue of the proper level geometric model complexity (basin discretization) must still be addressed.

The restriction to the semi-arid Walnut Gulch watershed will simplify the examination of some of the hydrologic subprocesses and complicate others. In these regions, with high-intensity thunderstorms, Hortonian overland flow is the predominant mechanism for runoff generation. Because of the ephemeral nature of runoff, throughflow and groundwater modeling of base flow components can, for practical purposes, be ignored. The spatial extent of thunderstorms is such that gauged, nested basins exist where the small basins are completely covered by the storm, and only partial storm coverage of the basin takes place in larger basins. The effect of vegetation on the distribution of infiltration will be indirectly investigated. Channel transmission losses are a critical component of runoff generation in semi-arid regions and must be studied in detail.

To facilitate the study of both the channel loss and climatic variability effects, four subwatersheds within Walnut Gulch have been selected for the study. Three of these watersheds are located in the Lucky Hills area, and the fourth is Walnut Gulch subwatershed 11 (WG11) (Figure 1.1). Figures 1.2 and 1.3 present larger scale maps of the Lucky Hills watersheds and WG11. Table 1.1 contains background information on each of the four watersheds. Detailed discussions of the basins and related data are presented in Appendix A.

The selection of the four watersheds specified above enables an examination of basin dynamics over a range of nearly four orders of magnitude of basin area.

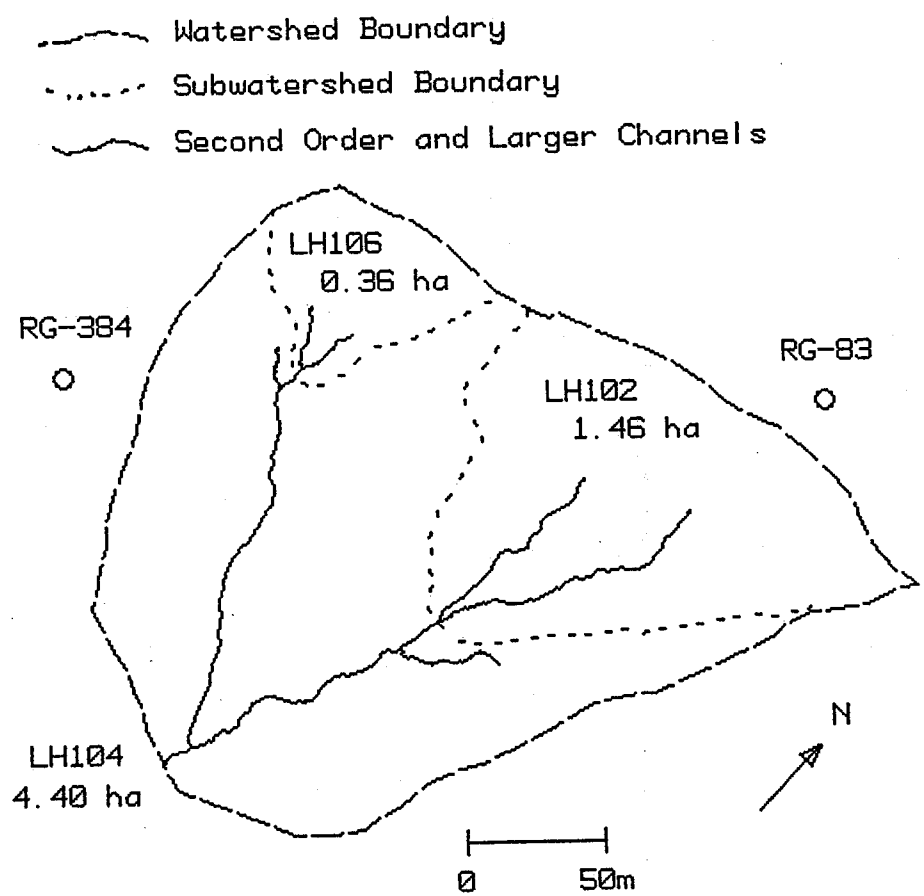

Figure 1.2. Lucky Hills Subwatersheds

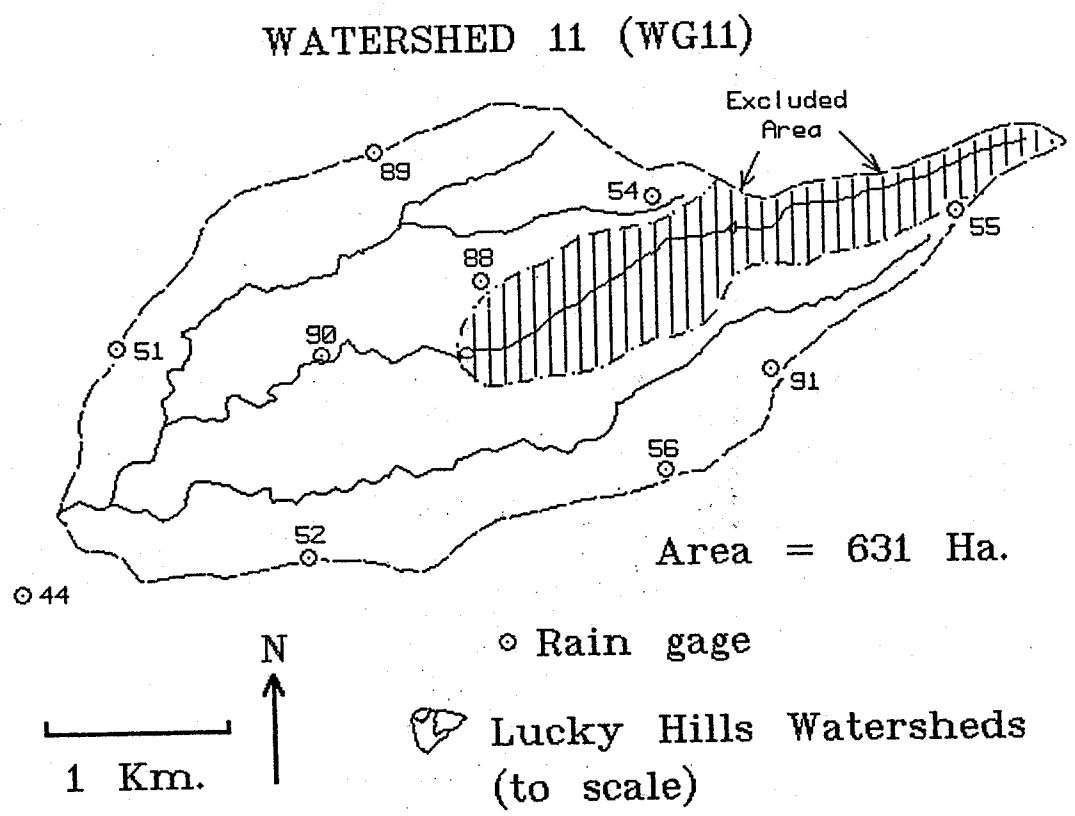

Figure 1.3. Walnut Gulch Subwatershed 11

Table 1.1 Basic Research Watershed Characteristics

Walnut Gulch Subwatershed	Drainage Area (ha)	Number of Applicable Raingages
Lucky Hills-106	0.36	2
Lucky Hills-102	1.46	2
Lucky Hills-104	4.40	2
Watershed 11	631.0	10

Over this range of scales, both precipitation and channel morphology change significantly. In the smaller Lucky Hills (LH) watersheds, channels are quite small and have little if any coarse sand in the beds that would contribute greatly to channel losses. WG11, however, does have wide sand bed channels, and channel losses can be expected to be significant. Climatic scales of spatial variability are also bridged over this range of basin scales. Within the LH watersheds, small-scale variability of rainfall due to gage catch, aspect, and wind effects is important, but little large-scale variability will be observed. In WG11, the large-scale structure of the air mass thunderstorms is apparent form the observed raingage network data. In addition, the three Lucky Hills (LH) watersheds with LH-106 and LH-102 nested within LH-104 allow distributed model verification for internal consistency. As Beven (1989) pointed out, without observed data internal to the basin being modeled, reliable conclusions concerning internal basin dynamics inferred using a distributed rainfall-runoff model are impossible.

Every effort was made to obtain data sets of exceptional quality from these watersheds. Careful screening of the data minimizes the risk of misinterpreting observed or model results. Staff at the USDA-ARS Aridland Watershed Research Management Unit have a high degree of confidence in the rainfall-runoff data for the four selected watersheds.

1.3 Structural Overview

The report of this investigation proceeds from small to large scale. Chapter 2 provides an overview of the rainfall-runoff model used in this study (KINEROSR) and reports on small-scale infiltration studies in an attempt to better understand the interaction between climate and soils as represented on a single overland flow plane (hypotheses 1B and 1C). Simulation methods were employed in Chapter 2 to investigate model behavior and to quantify model uncertainties in relation to other model representations of infiltration on overland flow planes. Chapter 3 extends the work in Chapter 2, again by way of simulation, by investigating the role that channel processes have on attenuating rainfall distributions in the transformation of rainfall to runoff with a first-order channel in an open-book geometry. The results presented in Chapter 3 lead directly into the basin geometric simplification strategy presented in Chapter 4 (hypothesis 1 and 1A).

In Chapter 4, the importance of watershed equilibrium storage as introduced by Wu et al. (1978) as a measure of characteristic basin response will be stressed. This measure integrates the effects of topography, slope convergence, and hydraulic roughness. Equilibrium storage concepts are employed to develop an objective, repeatable procedure to simplify (aggregate) distributed geometric model parameters. The simplification methodology enables the degradation in model performance to be quantified and assigned to specific hydrologic subprocesses. The sensitivity of the geometric aggregation procedures to initial roughness and the magnitude of

numerical errors encountered in the process of simplification are also addressed in Chapter 4.

Model sensitivity, calibration, and verification for four watersheds bridging a large range of scales are discussed in Chapter 5. Two of the selected watersheds are nested within a third watershed so that internal distributed model consistency and performance could be verified. During the calibration and verification analysis, methods of consistent parameter estimation by way of optimization over a calibration data set are applied to all basin model representations. Every effort was made to select calibration data sets which excite all aspects of various model components (Sorooshian et al., 1983). Model performance evaluation was then carried out on an independent set of rainfall-runoff events. Model performance was also examined for individual, distributed events to verify internal model behavior.

Chapter 6 addresses many of the issues raised in the earlier chapters but in the context of response change as a function of increasing basin scale as well as an investigation of hydrologic subprocess domination with changing basin scale. In addition, the effects of geometric model simplification over a range of basin and climatic scales are presented in Chapter 6 (hypotheses 1, 1A, and 1C). A specified level of model performance is used to define an acceptable level of basin discretization (geometric complexity). Equilibrium storage measures are used again in Chapter 6 to develop a priori methods to define the proper level of geometric model complexity. A brief discussion is then offered on incorporation of study results into common rainfall runoff modeling studies.

The research methodology stressed thorough model verification with observed data. This instills a high degree of confidence that model results and interpretations based on the model are soundly grounded in realism and reflect actual watershed runoff response behavior. Without such verification, any conclusions based on computer simulations, must be restricted to the realm of the computer.

1.4 Literature Review

The literature review is presented in five major sections. The first contains a review of prior work related to the central theme of this research effort, namely, geometric simplification of distributed rainfall-runoff models. However, the required level of geometric model complexity cannot be considered in isolation of other central rainfall-runoff modeling issues. These include: (1) basin scale, (2) model process complexity (the type of rainfall-runoff model), (3) hydrologic subprocess domination and scale thresholds, and (4) spatial and temporal variability. Relevant literature addressing each of these issues is presented in an individual section.

1.4.1 Geometric Simplification of Distributed Models

Geometric model simplification has been examined by several authors under situations ranging from urban to natural watersheds. Some studies have considered infiltration as well as routing in the aggregation (simplification) process and others have not. However, none of the studies reviewed has explicitly examined geometric simplification as a function of basin scale. Many of the studies also suffer from

either limited data sets and/or a lack of an objective methodology to simplify a complex basin representation. The various distinctions and limitations of these studies are presented below.

Heil and Brych (1978) attempted to answer the question "What is enough topographic detail?" for proper landform representation. They pointed out that the answer is application dependent but should support a consistent level of decision making. They go on to list drainage texture and landform identification as the primary criteria for defining the proper level of information. Drainage texture translates directly into stream representation and thus the demarcation between hillslope and channel processes in watershed discretization.

James (1972) alluded to the proper level of watershed discretization by noting that many models are "resolved in time and space beyond the integrity of available field observations." He also pointed out the dependence of model complexity on the modeling problem and its objectives. He presented a general flow chart to select the level of time-space model resolution but develops no methodology for simplification other than area weighted averaging. In a later paper, James and Robinson (1985) also discussed model simplification using SWMM3 in an urban setting. In that study, computational time step and precipitation intensites are varied, and the subsequent impacts on modeled runoff are studied but no rules are given for geometric model simplification. Hughes and Beater (1989) compared a lumped to a semi-distributed model and discuss the implications of the simplification. They have implied geometric simplifications by averaging and discussed the results of the two models

by stating which model behaves best for a given situation. Explanatory suggestions for model superiority are offered, but no criteria are given for the level of basin discretization required in the semi-distributed model.

Truschel and Campana (1983) used a kinematic wave runoff model with a Hortan infiltration model to calibrate CELLMOD, a conceptual storage model by Diskin and Simpson (1978). Geometric simplification is addressed by examining "unit area" catchments with different areas and drainage densities that are put together in series or parallel to represent a watershed. R-mode factor analysis of synthetic results was used to look at the relationship between each "unit area" configuration and basin geometric and hydraulic variables. An optimum unit area size was selected by examining the factor loading of the variables on the principal components. The two smallest unit basins (0.03125 and 0.125 sq. mi.) were eliminated because of small factor loadings and the fact that, for each of these areas, rainfall intensity was the principal factor. This alludes to the dominance of climate (storm size) over very small areas in the rainfall-runoff relationship. A unit area of 0.5 sq. mi. was selected purely on the basis of getting two significant factor loadings from hydraulic variables. This implies that, at this size, the basin is beginning to impart a substantial effect on the runoff. In the 0.5 sq. mi. unit area, drainage densities of two and six were considered. In each case, the overland flow parameters were the most dominant hydraulic parameters. Their analysis of optimum unit area size and drainage density complexity neglected infiltration, changes with scale and verification with observed data. However, for a given basin size, their results indicated that increased basin

discretization (smaller unit area) contributes little additional variance explanation and that, for a given unit area, channel processes have little influence on the rainfall-runoff relationship.

Lyngfelt (1985) studied the simplification of urban drainage areas without considering infiltration or the linkage to scale. For model simplification, he stressed that the simple model should maintain the velocity distribution along the flow system of the complex model. In his procedure for simplification of a plane to a trapezoidal gutter geometry to a single plane geometry, the area is maintained, the roughness is fixed to that of the plane, and the kinematic time to equilibrium (T_{eq}) is maintained. To maintain T_{eq}, the length of the plane is increased, and equations are given to determine the new length. However, these equations are a function of the rainfall intensity and, therefore, are storm dependent. He pointed out that as the length of the plane is increased, T_{eq} and the storage on the plane will increase but only one of the two can be maintained. Lyngfelt chose to maintain T_{eq}. This is a major distinction between Lyngfelt's work and the work presented here. By focusing on T_{eq}, the storm dependence problem mentioned above is presented, and optimization is often required to get a best simplified length. His procedure is well suited to simplification of a "base catchment" (similar to the unit area of Truschel and Campana, 1983) but not a complex watershed. When this is attempted, optimization is again required to determine simplified parameters. Given these limitations, there are still certain situations where Lyngfelt (1985) was able to attain significant

geometric model simplification without substantial degradation in model preformance.

Zaghloul (1981 and 1983) directly addressed the catchment discretization issue using the SWMM model in an urban setting. The effects of geometric simplification are first assessed by averaging the properties of 25 identical subwatersheds with later application to real watersheds for single events. In this study, the importance of maintaining storage between the complex and simple watershed representation is stressed. Adjustments to storage are made by adjusting the "hydraulic width". To aggregate overland flow elements, parameters are lumped using an area weighted average, and the hydraulic widths are summed. For channel or conduits, length weighted averages are used to lump parameters, but he recognized that, as small conduits are no longer represented in the simplified model, storage is not maintained. To compensate, the summed hydraulic widths from the overland flow planes are adjusted. Decreasing the hydraulic width is analagous to increasing the length of overland flow and thus increasing the storage. His adjustment was based on an arbitarily assumed level of storage in the conduits. When all conduits were replaced, optimization was required to obtain an adjusted hydraulic width. This will again introduce storm set dependence into his scheme. In comparing simplified to complex model results for tests with real basins with single events, generally good agreement was reached. Like Lyngfelt's (1985) simplification procedure, Zaghloul's (1983) procedure suffered from a lack of objective (non-optimizing) rules to obtain hydraulic and/or geometric parameters for the simplified system.

Shanholtz et al. (1981) examined the effects of spatial variability on rainfall-runoff performance for both a hypothetical and natural watershed. They noted that no criteria exist to determine the degree of permissible data averaging and evaluate the effect of several levels of watershed discretization on model results. They found that element length (longer implies fewer channels) and the treatment of precipitation had the greatest impact on model results. Hromadka (1987: I and II) also pointed out the importance of precipitation and the definition of the areal distribution of excess rainfall. He employed unit hydrograph (UH) concepts over storm classes forming a multilinear rainfall-runoff transformation. He argued that, without internal basin measurements of rainfall and runoff, additional model complexity is not warranted. However, in using UH concepts, change in basin management senarios cannot be evaluated nor can extrapolation to events outside the range of the calibration events be accomplished. The importance and sensitivity of modeling results to the spatial definition of precipitation will also be examined in this study.

Singh and Woolhiser (1976a) examined the use of a converging section as a possible method of watershed simplification but do not address scale dependence. However, they showed that a single, simple converging section was able to model the runoff dynamics from a variety of watersheds with only a single-fitting parameter.

More recently, Connors et al. (1989) used the SPUR model to assess impacts of geometric simplification on Walnut Gulch Watershed 15. They generated stream networks of various detail (order) using digital elevation data. For three levels of

stream network complexity, the SPUR model was used to predict runoff over a 15-year period. They found that for monthly averages, model performance became worse as the stream network was simplified but, from a flood frequency standpoint, the simplest network gave the best model results. Geometric simplification by way of stream order change used by Connors et al. (1989) is much like the methodolgy used in the current study, but they presented no objective procedure for distorting the hydraulic parameters during simplification.

Lane et al. (1975) presented the most thorough study of the geometric complexity issue for rainfall-excess routing. Their study proceeds in the opposite direction of the present study by starting with a simple overland flow plane and then increasing the complexity by adding additional elements and increasing the drainage density. The present study, like Connors et al. (1989), Lyngfelt (1985), and Zaghloul (1983), starts with a complex representation which is then simplified. Lane et al. (1975) used least squares to fit various geometric model elements to a sample of topographic points. They investigated the number of plane and channel elements to replicate various curvilinear forms of topography. They found that partial equilibrium cases show significant sensitivity to overland flow surface characteristics. This was recently reiterated by Moglen (1989). In the work by Lane et al. (1975), drainage density is used as an overall goodness-of-geometric-fit measure and is compared to hydrograph goodness-of-fit measures to assess the tradeoffs in simplification. In their simplification process, an a priori prediction of how the roughness will distort is predicted by a regression scheme. The current study will

present an analytically derived rule to predict the distortion in roughness. Lane et al. (1975) noted that storage represents the overall system performance at equilibrium. The importance of storage for the current study is also discussed in later chapters. Lane et al. (1975) concluded that as geometric complexity is increased, diminishing gains in model performance are attained. However, they noted that "as geometric complexity increases, so does the potential for distributing associated model parameters in space." This is illustrated later in the present study when infiltration is simultaneously considered in the simplification process.

None of the work reviewed related to geometric model simplification has addressed the topic as a function of basin scale. Those studies which simplify a complex basin representation do not present objective rules to distort hydraulic parameters, and none of the studies deal with infiltration in a detailed fashion. The current study attempts to address these issues and maintain objective, reproducible procedures in order to attain geometric model simpification and shed light on the relative importance of hydrologic subprocesses as a function of scale.

1.4.2 The Importance of Scale

Hydrologic basin response is the result of the interaction of stochastic climatic processes and deterministic and stochastic watershed processes. The deterministic watershed processes are regarded as those processes of directed flow defined by the topography and channel network (for the time scales of event rainfall-runoff modeling). Stochastic watershed processes include but are not limited to the

distribution of soils and vegetation, as well as antecedent moisture conditions. The temporal and spatial distribution of rainfall constitutes the major stochastic climatic process. These processes interact to a varying degree at different basin and climatic scales in the transformation of rainfall to runoff. Many hydrologic models attempting to emulate this transformation were developed for a particular basin and climatic regime. When these models are applied to basins with significantly different time-space scales, they often exhibit significant inaccuracies.

These model related scale issues as well as the overall importance of scale in the hydrologic process has received great attention in recent years within the literature. An entire issue of the *Journal of Hydrology* (August 1983) was devoted to this topic. In the introduction to the issue, the guest editors, Rodriguez-Iturbe and Gupta stated, "The understanding of the collective type of behavior which takes place in the basin (at basin scale) is one of the most challenging and crucial problems in hydrology." In the basin-scale approach, the focus is not on the individual components of the system, but their collective behavior. However, they add, "this does not imply that the role of dynamics in individual components is secondary, but that in the collective behavior, only a few of the individual characteristics play important roles . . .". This issue contained numerous articles of interest which will be referred to in later discussion.

In 1984, a conference (Gupta et al., 1986) devoted to scale problems in hydrology was held to examine the progress made toward solving problems at hydrologic scales and to put forth new ideas. The focus was still on collective basin

behavior, but individual hydrologic subprocess components (infiltration, hillslopes, and channel losses) were examined (Mesa and Mifflin, 1986; Kirkby, 1986; Diaz-Granados et al., 1986). Beven (1989) and Beven et al. (1988) also reviewed watershed scale considerations from the viewpoint of the individual hydrologic subprocess components and overall basin morphology. This direction of research indicates that, to acquire understanding at basin scale, more detailed information on the interaction of various components is required at different scales. This approach follows an upward conceptualization of scale from individual components. Klemes (1983) explored a downward approach to conceptualization by recognizing a "key hydrologic concept which can be related to natural constituents, followed by a search for the steps that could have lead to it from a lower level of scale."

The importance of scale and model complexity in hydrology was also reiterated in many articles of a special issue of *Water Resources Research* entitled "Trends and Directions in Hydrology" (August 1986). In particular, Dooge (1986) pointed out that, "To predict catchment behavior reliably, we must either solve extremely complex physically-based models which take full account of the spatial variability of various parameters or else derive realistic models on the catchment scale in which the global effect of these spatially variable properties is parameterized in some way. . . . The latter approach requires the discovery of hydrologic laws at the catchment scale that represent more than mere data fitting." He also noted that unlike hydraulic theory, which has the Reynolds and Froude numbers, in hydrology we have no principle of similarity for catchment behavior. A similarity relationship

would allow model results to be applied at different scales by maintaining certain ratios over a wide range of scales.

As Dooge pointed out, it is hoped that basin-scale relationships will cut through the complexity of including all the rainfall-runoff dynamics as numerical approximations to the governing partial differential equations. In a personal communication with Dooge (1986), he spoke of isolating the nonlinearities of rainfall-runoff response. For specified modeling requirements, both of these points imply the simple question: How complex must a model be to capture the essential system dynamics?

1.4.3 Models and Model Complexity

The role of scale and complexity is an integral part in both the reductionist and constructionist hypotheses in science. Anderson (1972) stated "that the reductionist hypothesis does not by any means imply a constructionist one: The ability to reduce everything to simple fundamental laws does not imply the ability to start from those laws and reconstruct the universe." He cited the difficulties of scale and complexity as the major roadblock to the construction hypothesis. Extending the behavior of elementary laws to large and complex systems does not necessarily aid in the understanding of the complex system. Often at each new level of complexity, entirely new properties appear (Anderson, 1972).

In a discussion of the roles of models in science, Rosenblueth and Wiener (1945) examined how models evolve as an abstraction of some small portion of the

universe. The models typically become more complex as further understanding of the system is acquired and as our desire for further understanding grows. Casti (1985) also addressed modeling and system complexity in an abstract manner. He discussed how complexity is perceived and the inherent human need to simplify in order to understand and control. This simplification arises in our models by way of various model assumptions or ignorance of relationships. At the simplest level, hydrologic models are empirical and relate cause and effect by way of regression. At greater levels of complexity, models attempt to better represent the physical processes as we understand them. This increase in complexity is typically accompanied by an increase in the number of model parameters. This often results in parameter identifiability problems and non-parsimony (Sorooshian and Gupta, 1983).

For this study, the proper level of geometric model complexity (discretization) used to represent the basin and rainfall data to adequately describe runoff dynamics will be investigated. Natural logic tells us that the more complex the model, the better. However, several studies indicate just the opposite. Miller and Mantey (1982) found that when using the TR-20 model, increased errors of estimation resulted when a basin was subdivded into ten subwatersheds. Beck (1987) offered the observation that a poor data set could explain this type of model behavior, because as greater numbers of highly uncertain parameters are introduced, an amplification of model prediction error takes place. Loague and Freeze (1985) found that more physically-based (more process complexity) models did not outperform a simple model. They compared a regression, unit hydrograph (UH), and quasi-physically-based models for

a number of events and found that the simple regression and UH model performed better than the more complex physical model in most cases in prediction. However, data errors (Gander, 1988, personal communication) will most likely prove that their conclusions are unjustifed. The importance of input data errors on model performance was illustrated by Singh and Woolhiser (1976). They demonstrated how input errors are amplified by a nonlinear system for a simple class of models. They state that "... even a perfectly identified nonlinear model cannot be uniformly better than an optimally identifed linear model. Under certain circumstances, a linear model may, in fact, be preferable to a nonlinear one, although the system is truly nonlinear. These circumstances occur when input errors overpower the nonlinearity of the runoff process." These studies underscore the paramount importance of distinguishing between model structure and data error contributions to prediction error. The following reviews briefly examine several types of models with varying degrees of both structural and geometric complexity and how they might be implemented to test for the necessary model complexity.

An ASCE Task Committee on quantifying land-use change effects (1985) evaluated 28 surface hydrologic models and rated their acceptability and accuracy for assessing land-use change effects when applied without calibration data. Primary and validation references were specified for all of the models evaluated along with specific model limitations. This reference and the model reviews by Renard et al. (1982) provide a good starting point to assess other simpler models or model components which might be used for various subprocess representations. The ASCE

study also pointed out that there is little justification for using a more complicated model than is necessary, as even very simple models can explain a large part of the discharge variance. The models reviewed in both studies ranged from very simple to quite complex. They did not review the class of models that follows.

In the middle ground of model complexity are probability distributed models. In this class of models, the frequency distribution of hydrologic variables is considered without regard to their position. Moore (1985) reviewed prior work in this area and developed an analytical solution for basin runoff for various assumed probability distributions. Models of storage capacity, infiltration capacity, and translation time, as well as the suitability of various distributions, are examined and discussed. Moore concluded that this approach may not be fruitful for operational use, but it should provide a useful tool to study basin scale.

At the most complex end of hydrologic models are the fully physically-based models such as the Systeme Hydrologique European (SHE). This model was developed by a consortium of European nations as a cell-based physical model that is capable of representing spatial variability (Abbott et al., 1986a,b). In each cell, all the major hydrologic inputs and abstractions are modeled. This leads to a highly parameterized system where 22 parameters per cell must be provided. An arbitrarily recommended cell size of less than one percent of basin size is recommended. Because the model is physically-based, all of these parameters should be measurable in the field. One must ask: Is this level of model sophistication and discretization required?

Abbott et al. (1986b) clearly stated that data requirements are extensive, but the model is formulated so that available data can be used. They also noted that this type of model formulation is ideally suited to investigate scale issues. For applications in which specific components are unimportant (non-dominant) the model can be easily simplified. To aid in the identification of important model components, they have incorporated routines to perform sensitivity analysis. Bathurst (1986a,b) applied the SHE model to a 10.55 km^2 catchment and performed a sensitivity analysis. Results were encouraging, and the sensitivity analysis showed that the model was most sensitive to overland flow roughness and hydraulic conductivity for both the saturated and unsaturated zone. The sensitivity of the model to just a few parameters indicates evidence of subprocess domination at the scale of their test basin. Indeed, Bathurst concluded that channel routing and spatial variability of rainfall were not important because the response was dominated by rapid surface and subsurface flow and the storm system was primarily frontal.

Using a less physically-based model than the SHE, Schilling and Fuchs (1986) examined how input rainfall resolution and the simplification of various model components affected urban basin outflow on a hypothetical catchment. Like Singh and Woolhiser (1976), they found that rainfall input errors were amplified by the nonlinear model and decreasing the resolution of rainfall data had the greatest impact on outflow. For the basin studied, they could easily simplify overland routing and conduit routing for special cases with little impact on reference outflows (reference outflows as computed from the most complex model).

For many of the models reviewed above, limited broad-scale applicability of the models is sometimes achieved after lengthy calibration procedures. Many of these procedures are widely criticized, as model parameters lose any physical significance and merely act as regression fitting parameters. The problem of model calibration is ubiquitous to most if not all of the models reviewed. Calibration problems often stem from model formulation, where more accurate physical representations introduce more complex transform equations and more model parameters resulting in non-parsimonious models. The problems of parameter calibration for large conceptual models have been well documented by Sorooshian and Dracup (1980) and Sorooshian and Gupta (1983).

1.4.4 Evidence of Subprocess Domination and Scale Thresholds

Process model simplification, by way of identification of subprocess domination, and geometric simplification are not entirely distinct issues. A major factor in geometric simplification and initial basin discretization hinges on the fundamental distinction between subprocesses of overland flow and channel flow. The primary distinction between the two depends on the perceived channel network for a given base map of the watershed. This of course is a function of map scale. Kirkby (1988) emphasized this point stating "there is no unambiguous method for determining the exact position of channel heads. . . A satisfactory hillslope hydrological model must, therefore, be insensitive to the exact density of channels chosen."

Because of a linkage between structural and geometric simplification, a brief review of subprocess domination and scale thresholds is presented. In small basins, the minor effect of channel routing on control of the storm hydrograph is noted by Woolhiser and Goodrich (1988), Iwagaki and Takasao (1956), and Beven (1986). Iwagaki and Takasao employed an open-book basin geometry and kinematic routing to illustrate the effects of various inputs and parameters on runoff. They showed that a change of channel conveyance from 0.8 to 1.6 has no effect on the ratio of peak flow to equilibrium flow for a basin length to width ratio of five or less. The same change in conveyance has only a small effect on the (time to peak)/(rainfall duration) ratio. Beven (1986) proposed that, in the case of overland flow domination, a linear routing scheme with constant wave velocity is adequate. This conclusion is supported with field evidence acquired from an earlier study (Beven, 1979). In the 1986 study, he applied a routing model with these simplifying assumptions to catchments with drainage areas of 4.3, 11.1, and 14.3 km^2. However, earlier works by Minshall (1960) and Izzard (1946) strongly refuted the assumption of a constant wave velocity which would enable a linear routing method. Wang et al. (1981) recognized the nonlineaity of basin response, and they incorporated it into geomorphological IUH concepts. They also presented empirical evidence that linearity of basin response increases with increasing basin size. Kirkby (1988) suggested that the water stores with the longest residence time are those processes that dominate the overall catchment response. Qualitative estimates are given for residence time related to various hydrologic subprocesses. Kirkby (1988) then

suggested identification of the major hydrologic subprocesses and only modeling the two processes with the longest residence times.

Golany and Larson's (1971) results showed that channel characteristics have a minor impact on the time characteristics of runoff for a synthetic stream network of order two or less. Their work also indicated that a significant increase in the effect of channel characteristics on runoff timing takes place during the transition between second- and third-order stream networks. This may indicate a threshold at which channel routing becomes the dominant process affecting runoff. Klein (1984) found a threshold in "peakedness index" at basins sizes of about 250 km^2. This index is defined as "mean flow as a percentage of the highest flow in the basin". He explained this threshold by arguing that, until an area of approximately 250 km^2 is reached, the catchment outflow (overland flow) is dominant. This is deduced from comparing the ratio of travel time in the channel to average subsurface travel time. For basins with area less than 250 km^2, runoff from overland flow will peak before the subsurface peak is observed. Klein also cited numerous other literature sources indicating that overland flow is dominant for basins up to about 250 km^2. These results indicate that including channel segments into the watershed representation for basins under a certain size may result in overkill of basin discretization and thus enable geometric simplification. The significant issue is, of course, the basin size at which explicit channel representation must occur.

At larger scales in semi-arid watersheds, the effect of channel losses will no doubt have a significant impact on runoff characteristics. These losses are well

documented in Keppel and Renard (1962) for the Walnut Gulch Experimental Watershed in southeastern Arizona. They also found that the magnitude of channel losses was highly dependent on antecedent conditions. Another interesting result of the study is that hydrograph rise time (the time from the start of runoff at a measuring point to the time of peak flow) decreases for increasing watershed areas. Because of large losses due to both turbulence and infiltration at the flow front on a dry channel, the flow velocity on the already wetted channel upstream of the front channel is greater than at the front. Greater flow depths also flow faster than shallow depths; therefore, upstream flow tends to overtake the flow front causing a very steep hydrograph rise as the front passes a gaging station. This indicates that a pure translational routing with constant velocity as used in the development of the geomorphologic instantaneous unit hydrograph, GIUH (Gupta and Waymire, 1983) is a poor assumption. The formation of translatory waves shows that channel routing is tied closely to the climate.

Troutman and Karlinger (1986) used branching theory to average properties of channel networks and show that linear channel routing may be adequate for routing through large networks. They concluded that all pertinent hydraulic information is contained in a single parameter: the wave celerity. Keppel and Renard's (1962) case study refutes this conclusion and may restrict Troutman and Karlinger's results to regions where channel losses are not significant and where the climate is not highly variable. To address channel losses in stream networks, Diaz-Granados et al. (1986) incorporated losses into a linear reservoir representation of

channel segments as a percentage loss. Their results, although elegant analytically, apply only to small channel lengths and probably would not be of use in semi-arid areas.

Model formulation and transferability would be greatly aided if one knew which rainfall to runoff subprocesses (infiltration, overland flow, channel routing, etc.) dominate at various time-space scales. Subprocess domination and basin similarity at in the context of basin scales has been recently examined by Pilgrim et al. (1982), Klemes (1983), Gupta et al. (1986), and Kirkby (1988), to mention just a few.

Wood et al. (1987) recently introduced promising work to find time-space scale thresholds using the concept of a Representative Elementary Area (REA). For basins below the REA size, the distribution and location of factors affecting runoff would have to be considered. Above the REA size, averages or simple property distributions that do not consider position could be employed. This concept was tested using topography from an actual watershed, but the hydrologic response was not verified using observed rainfall-runoff data.

1.4.5 Spatial and Temporal Variability

The importance of channel losses at larger scales and the observed domination of various subprocesses at other scales may, in many cases, be the result of spatial and temporal variation of inputs and basin characteristics. The interaction of rainfall and soil properties to produce excess precipitation which is subsequently routed is the

key interaction affected by variability. Loague and Freeze (1985) attributed poor model performance of a physically-based model to scale problems associated with the spatial variability of rainfall and basin soil properties. Cordova and Rodriguez-Iturbe (1983) reiterated the importance of excess precipitation production by stating "the problem is more what to route than how to route . . . what remains as a crucial and unsolved problem is the description of the infiltration process at basin scale." Beven et al. (1988) reiterated the same point.

Voluminous literature exists on the individual topics of variability in soils and in rainfall. Bonell and Williams (1986) found that the temporal variation of soil hydraulic parameters of the Phillips equation for infiltration were just as significant as the spatial variations. Beyond variability in either soils or rainfall alone, the linkage of variability in both processes has been considered only infrequently. This is, of course, a result of the extreme complexity of the problem. In an attempt to approach this problem by way of a pure simulation study, Freeze (1980) concluded that gross errors resulted when spatial variation of soil hydraulic properties was neglected. Smith and Hebbert (1979), Sharma et al. (1980), and Sivapalan and Wood (1986) also investigated the effects of spatially variable infiltration with various assumptions concerning rainfall variability. These studies used only a narrow range of rainfall intensities; therefore, few overall conclusions were drawn concerning the effect of spatially variable rainfall.

Woolhiser and Goodrich (1988) found that an equivalent saturated hydraulic conductivity (Ks) for spatially variable Ks cannot be obtained for infiltration excess

runoff when temporally varying rainfall is applied. This occurs because the rainfall rate fluctuates through the distribution of Ks, producing a different time history of infiltration over areas with different Ks values. This finding was confirmed by Binley et al. (1989) using a fully three-dimensional saturated-unsaturated model. For relatively uniform (temporally) rainfall rates, they were unable to obtain an equivalent Ks that would reproduce the spatially variable case for infiltration excess dominated runoff generation.

Hamlin (1983) specifically examined the significance of rainfall in the study of hydrologic response at basin scale. He concluded that application of research results from small basins to large "will not be possible without detailed analysis of the spatial and temporal variation of precipitation." O'Connell and Clarke (1981), in a review of adaptive hydrologic forecasting, concluded that expending additional effort to solve estimation problems may produce insignificant gains in comparison to obtaining a better representation of the spatial variation of rainfall and its effects on streamflow. Troutman (1983) showed how prediction errors and bias in parameter estimation are the direct result of spatial variability of rainfall. Woolhiser (1986) found that error in derived runoff distributions from a physically-based model on heavy textured soils was induced if a rainfall sampling interval of greater than five minutes was used. Woolhiser and Goodrich (1988) found that the relative size of the storm event in relation to the distribution of Ks also has a significant bearing on runoff response. For very large storms, the variability of the soils is washed out or overwhelmed by the high intensity rainfall rates.

Obviously, spatial and temporal variability of rainfall plays a key role in hydrologic response, but as Hamlin (1983) pointed out, that for many large basins "the general averaging which takes place balances out any significant variations in the catchment processes themselves and in the rainfall inputs." This points out the intimate link to scale when considering representation of spatial and temporal variability of rainfall and basin properties.

1.4.6 Literature Review Summary

The foregoing literature review illustrates that the level of geometric model complexity cannot be addressed in isolation. Because of the profound influence of basin size on hydrologic response, analysis over a range of scales is crucial. Within a range of basin scales, various levels of both spatial heterogeneities and temporal variability are encountered. The primary manifestation of these heterogeneities is in runoff production and subsequent channel losses in semi-arid regions. Adequate representation of spatial and temporal variability is essential if realistic conclusions regarding geometric model complexity are to be derived. Hydrologic subprocess domination is likely the result of the interaction of scale and spatial and temporal variability. The transition from overland flow to channel-dominated hydrologic response will point to proper level of geometric complexity for modeling runoff. Each of the issues raised in the literature review must be examined in concert. An attempt is made in this study to address each of these issues as they pertain to the central question of the proper level of distributed geometric model complexity.

CHAPTER 2

SMALL-SCALE INFILTRATION VARIABILITY AND RAINFALL-RUNOFF MODELING

2.1 Chapter Objectives

The primary objectives of this chapter are:

(1) Reformulate and generalize the small scale infiltration variability model of Woolhiser and Goodrich (1988);

(2) Compare the Woolhiser and Goodrich (1988) model to uniform and more complex spatial infiltration representations; and

(3) Assess the applicability of the Woolhiser and Goodrich (1988) model over a range of storm and soil types for rainfall-runoff modeling.

2.2 Introduction and Background

Many early rainfall-runoff studies were concerned strictly with routing of excess precipitation and neglected infiltration entirely (Bras, 1979). This is a far cry from reality, and this shortcoming has been noted by a number of investigators. Among them, Cordova and Rodriguez-Iturbe (1983), who stated that "the problem is more what to route than how to route . . . what remains as a crucial and unsolved problem is the description of the infiltration process at basin scale." Beven et al. (1988) reiterated the same point.

Including infiltration specifically in the modeling process provides a major

advance toward achieving physical realism. The level of infiltration process model complexity varies widely. However, representation of heterogeneities is typically accomplished by basin discretization. One commonly used criteria in discretization is the "Hydrologic Response Unit" (HRU) concept used by Li (1975). In this concept, discretization takes place until a unique combination of soil type, vegetation, and land use is achieved. The flaw in this procedure is the fact that, even within a single soil type, large variations in soil hydraulic properties occur over length scales on the order of meters (Grah et al., 1983; Nielsen et al., 1973; Loague, 1986). Hjelmfelt and Burwell (1984) presented field observations illustrating the large degree of spatial variability of runoff from 40 side-by-side 27.5 m x 3.2 m erosion plots within the same soil texture and treatment. They pointed out the implications to runoff modeling and practical problems of discretization. Basin discretization to this level and subsequent routing is impractical from a data input and parameter estimation viewpoint as well as from a computational viewpoint.

Using simulations, Freeze (1980) illustrated the importance of small-scale infiltration variability and concluded that the distribution of hydraulic conductivities should be incorporated into physically-based rainfall-runoff models. One approach to this task is to examine the distribution of runoff generation from a highly discretized hillslope and attempt to derive an effective hydraulic conductivity for a large area that produces a comparable response. This was the approach used by Binley et al. (1989) with a three-dimensional saturated-unsaturated model. They concluded that, for infiltration excess dominated runoff generation (Hortonian

runoff), an equivalent average effective hydraulic conductivity cannot be derived. Woolhiser and Goodrich (1988), using KINEROS, drew essentially the same conclusion by showing that geometric or arithmetic averages of Ks' could not reproduce distributed results.

Another approach to treat small-scale infiltration variability is to use scaling theory based on similar media concepts (Rajendran and Mein, 1986; Warrick et al., 1977). In this approach, a distribution of the scaling factor is assumed. Various soil parameters are then estimated from the distribution of the scaling parameter. Conceptual subareas of the watershed are assigned a scaling factor from a probability interval of the distribution. Because the scaling parameter cannot be measured in the field, the weakness of this approach is the necessary assumption of the distribution of the scaling parameter and estimation of its moments. Ahuja et al. (1984) also demonstrated that a one-to-one correspondence between the scaling factor for Ks and the suction head for different locations in a watershed does not exist. In this study, distributions of Ks are used directly and are not derived from an unmeasurable distribution of a scaling parameter.

More recently, Loague (1990) defined average soil hydraulic properties from a large number of field ring infiltrometer measurements. These average properties did not improve his earlier rainfall-runoff modeling results (Loague, 1986), as the model he employed (Engman, 1974) was unable to fully utilize the measured data. The absence of a methodology to incorporate small-scale infiltration variability into basin runoff models will continue to limit progress toward realistic simulation. Binley

et al. (1989) proposed, as future research, using a linear combination of the results of two independent simulations obtained from uniform soils with different properties. This is similar to the approach already presented by Woolhiser and Goodrich (1988), which incorporates small-scale infiltration variability in a simple and straightforward manner without resorting to more detailed basin discretization. A more detailed explanation as well as extension and refinement of the methodology used by Woolhiser and Goodrich (1988) is the focus of this chapter.

2.3 Approach

2.3.1 KINEROS: The Rainfall-Runoff Model

KINEROS will be used to investigate small-scale variability of infiltration. At this juncture, a brief description of the model is warranted. The information presented provides a basis for further development. For a more detailed explanation, refer to Woolhiser et al. (1990). This manual (Woolhiser et al., 1990) describes the theory and application of a "release" version of KINEROS. A "research" version of KINEROS was used in the majority of the analysis presented in the current study. The significant additions and enhancements to KINEROS for the research version "KINEROSR" will be explained in greater detail in this document where they are relevant.

KINEROSR employs the kinematic wave approximation to route both overland and channel flow. The program allows for the variation of geometric, soil, and hydraulic characteristics so that a drainage area is approximated by a cascade of

overland flow planes feeding channels. On an overland flow plane of length L and width W, a finite difference approximation to the kinematic wave equation is used. The kinematic wave equation is stated as:

$$\frac{\partial h}{\partial t} + \frac{\partial \alpha h^m}{\partial x} = r_i\ (t) - f_i(x,t) \qquad (2.1)$$

where:

h = flow depth

t = time

x = distance along the slope

$\alpha = 1.49\ S^{1/2}/n$

S = slope

n = Manning's roughness coefficient

m = 5/3

$r_i(t)$ = the rainfall rate

$f_i(x,t)$ = the infiltration rate

Channel flow can be routed in a trapezoidal channel cross section or a circular conduit. The kinematic wave equation is also used to describe unsteady channel flow and is written in the following form:

$$\frac{\partial A}{\partial t} + \frac{\partial Q(A)}{\partial x} = q_l(t) + r_i(t) - f_{c_i}(x,t) \qquad (2.2)$$

where:

A = cross-sectional area of flow

Q(A) = channel discharge as a function of area

$q_l(t)$ = uniform lateral inflow rate

$r_i(t)$ = the rainfall rate

$f_{ci}(x,t)$ = channel infiltration

This equation is also solved using a finite difference approximation. A Manning's roughness relationship was also used in channel routing. This treatment of overland flow and channel routing is typical of numerous other programs (DR3M of the U.S. Geological Survey, Alley and Smith, 1982; HEC-1 of the Army Corps of Engineers; WITWAT II of the South African Water Research Commission, Green, 1984, IIHR of the University of Iowa, Jain et al., 1982). Implementations differ, and treatment of infiltration varies widely from program to program.

KINEROSR treats infiltration using the physically-based model of Smith and Parlange (1978). This model is based on an approximation of the one-dimensional form of Richards' equation in a homogeneous unsaturated porous medium. It is applicable to cases of infiltration excess runoff generation (Hortonian overland flow). Simplification of the Richards equation is made by assuming that soil water flux

varies little with relative position within the wetted soil column with a remote lower boundary. At ponding time (t_p), the model assumes:

$$\int_0^{t_p} r_i(t)dt = \frac{A}{Ks'} \ln\left\{\frac{r_i\ (t_p)}{r_i\ (t_p)-Ks'}\right\} - F_p \qquad (2.3)$$

where:

Ks' = effective saturated hydraulic conductivity under imbibition

A = soil sorptivity related parameter

= $S_p^2/2$

S_p = soil sorptivity

F_p = volume/unit area of precipitation infiltrated at ponding

Once ponding time is reached, the infiltration rate is controlled by the soil, and $f_i(t)$ replaces $r_i(t)$ in Equation (2.3). For $t > t_p$ Smith and Parlange (1978), related the accumulated infiltration F and t as follows:

$$Ks'\ (t-t_p) = F - F_p + A_p \exp\left(\frac{-F}{A_p}\right) - A_p\left[\frac{r_i(t_p)-Ks'}{r_i(t_p)}\right] \qquad (2.4)$$

where:

$$A_p = A/Ks'.$$

It should be noted that this not a rainfall excess infiltration model where excess is routed down an impervious basin representation. The model is interactive with rainfall and upslope inflow of surface water. Therefore, infiltration continues after rainfall ceases if upslope inflow is present. El-Kadi (1987) also concluded that the semi-analytic model of Smith and Parlange (1978) is well suited to the study of variability of infiltration under uncertainty in unsaturated zone parameters. Variability studies using the Smith and Parlange model agreed very well with numerical stochastic simulations when the effects of cross-correlation of the parameters are neglected. Channel infiltration is also treated in an interactive manner and will be described in more detail in Chapter 4.

The soil parameters Ks' and A in Equations (2.3) and (2.4) are typically assumed to be uniformly distributed over an entire overland flow plane but can vary from plane to plane. Field evidence indicates that a lognormal distribution can be used to describe the small-scale sampling (within plane) variability of Ks' (Nielsen et al., 1973; Grah et al., 1983; Merzougui, 1982; Rogowski, 1972; Sharma et al., 1980). To more realistically represent Ks' variability, Woolhiser and Goodrich (1988) also assumed Ks' was distributed lognormally and transformed Ks' into a normally distributed random variable z ($z = \ln(Ks')$) with mean $\bar{z}$ and variance S_z^2. With a geometric mean Ks' and coefficient of variation C_v, they split each overland flow

plane into five equal area parallel strips and assigned Ks' values from the midpoint of five equal probability classes. Figure 2.1 illustrates the plane partition and assignment of Ks' values from the cumulative Ks' distribution.

2.3.2 Review of Early Results

The behavior of this model representation of infiltration variability was compared to uniform cases using both the geometric and arithmetic means of Ks'. Using either mean, instead of the spatially variable Ks', produced significantly different responses. The behavior of the spatially variable model was then assessed over a range of soils and storm sizes for various values of C_v. Three storms from a set of 30 from Walnut Gulch raingage #5 were selected to cover a wide range of storm sizes as measured by the time weighted mean rainfall intensity. Soil parameters for the overland flow plane were selected to cover a wide range of soil conditions as measured by a dimensionless infiltration ratio F_p*, defined as follows:

$$F_p^* = \frac{F_p}{\frac{1}{m}\sum_{i-1}^{m} P_i} = \frac{F_p}{\overline{P}} \qquad (2.5)$$

where:

F_p = the total rainfall infiltrated at ponding for the mean rainfall rate of the

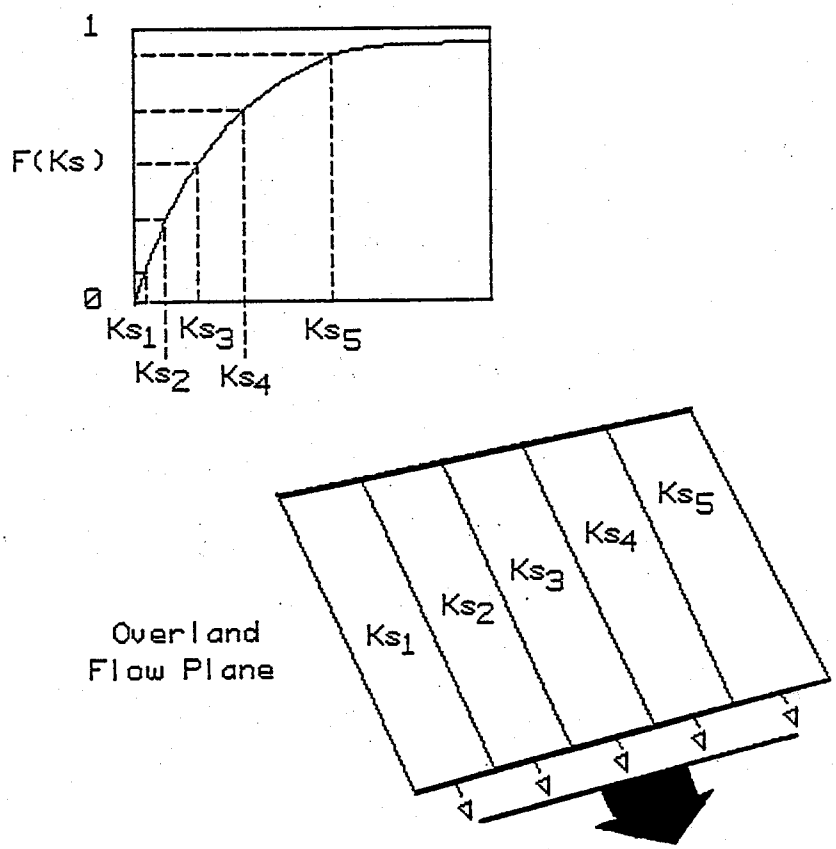

Figure 2.1. Interplane Assignment of Ks'

storm set, $\bar{q}$

$$\bar{q} = \frac{1}{m} \sum_{i-1}^{m} \frac{P_i}{D_i} \tag{2.6}$$

P_i = total precipitation for the ith storm

D_i = total duration for the ith storm

m = 30

The total rainfall infiltrated at ponding (F_p) can be computed from an expression given by Smith and Parlange (1978) as:

$$F_p = A_p \ln \left[\frac{\bar{q}}{\bar{q} - Ks'} \right] \tag{2.7}$$

Figure 12 from Woolhiser and Goodrich is reproduced below (Figure 2.2). In this figure, the runoff response is plotted by storm size versus F_p* for C_v = 0.0, 0.4, and 0.8. The response exhibits an interesting climate-soils interaction. Note that for storm 1 (weighted mean rainfall intensity equal to 33.6 mm/hr) and F_p* = 0.104, the uniform plane (C_v = 0.0) case produces the largest runoff volume and peak rate. For the same storm, when F_p* = 0.574, the largest volume and peak runoff rate are produced when C_v = 0.8. The reversal in hydrograph response from uniform to

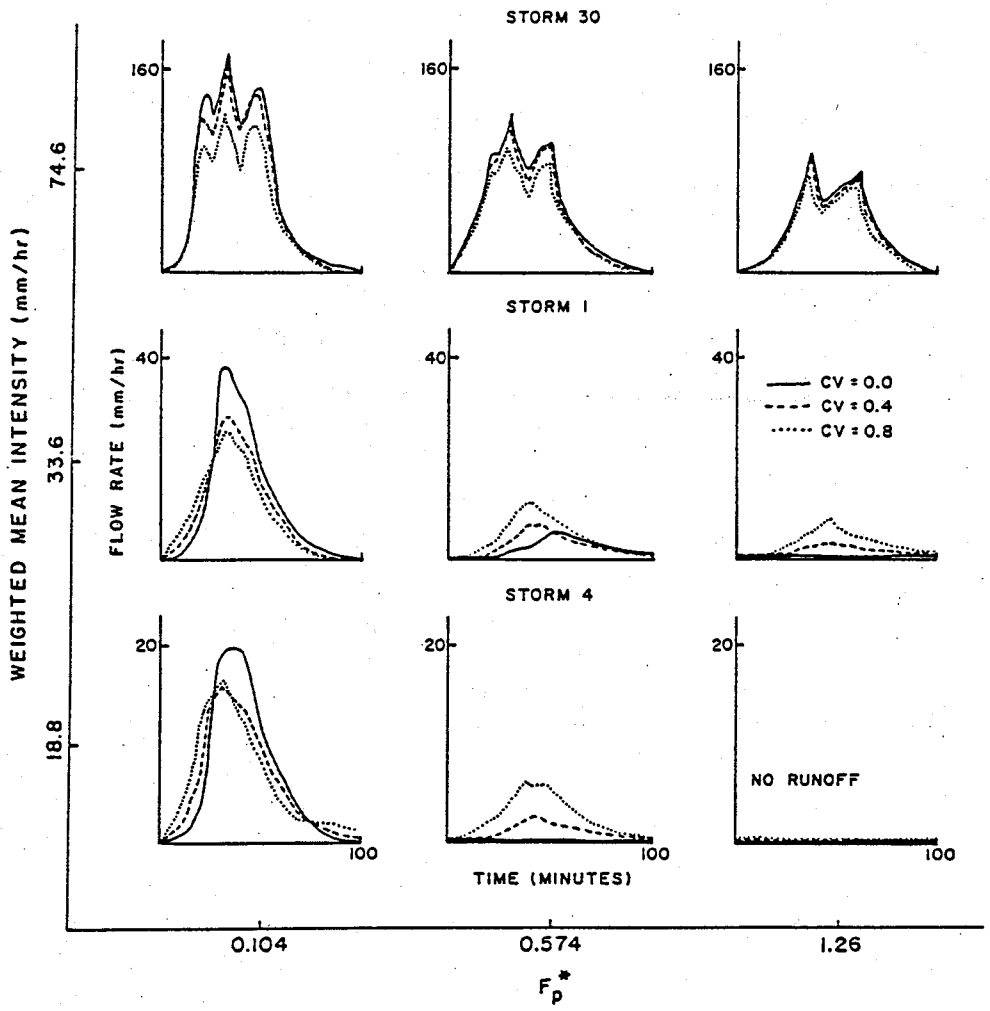

Figure 2.2. Impacts of Climate, Degree of Spatially Variable Infiltration (C_v), and F_p. on the Hydrographs (from Woolhiser and Goodrich, 1988)

spatially variable cases illustrated in Figure 2.2 is explained in the original research as follows " . . . consider a constant intensity rainfall below the geometric mean of Ks', but above the lowest Ks' of the five plane segments for the spatially variable plane. In this case, the uniform plane will produce no runoff, but the spatially varying plane will. As the constant intensity level increases, the spatially variable plane will continue to produce more runoff than the uniform plane until the intensity reaches a certain level. Beyond this level (high intensity storms), the plane segments with high Ks' will dominate the abstraction of rainfall from the spatially variable plane, and the uniform plane with geometric mean Ks' will produce more runoff. Thus, the uniform plane will give higher peaks for low infiltration rates, or for large storms ($F_p^* = 0.104$, or storm 30 in Figure 2.2); while the spatially variable plane will produce larger peaks for higher geometric mean infiltration rates during low to medium intensity rainfall events." (Woolhiser and Goodrich, 1988).

In their original work, only five parallel strips (segments) were used, the sorptivity term A was held constant, and C_v was defined in log transformed terms. To more thoroughly examine this methodology, the work of Woolhiser and Goodrich (1988) is extended to address the following issues:

1. Reformulate the model:

    a. to use mean Ks' and C_v statistics as typically estimated from field measurements

    b. to allow a variable number of strips

    c. to estimate the effective net capillary drive (suction), and the

relative soil saturation at -0.33 and -15 bars tension from textual estimates of Ks'.

2. Compare the model to:

   a. a composite (non-interactive) representation of spatially variable infiltration as well as a uniform representation

   b. an interactive runoff-runon model (Smith, Goodrich, and Woolhiser, 1990).

3. Perform analysis over a range of storm sizes and soil types to determine the number of strips required to replicate the response of a near continuous representation of the lognormal Ks' distribution to within a specified level of accuracy in terms of percent difference in runoff volume.

2.4 Model Reformulation and Improvements

2.4.1 Using Ks' and C_v from Field Estimates

The initial findings of Woolhiser and Goodrich (1988) assumed that Ks' was lognormally distributed and that the statistical characteristics of Ks' were specified by the geometric mean and the coefficient of variation C_v defined in log transformed terms as:

$$C_v = S_z / \bar{z} \tag{2.8}$$

where:

$\bar{z}$ = mean of log transformed Ks' (z = ln Ks')

S_z = standard deviation of z.

Further review of the literature (EPRI Report EA-4228, 1985) demonstrated that most investigators report mean Ks' and C_v values in untransformed terms as they might be derived directly from field data as:

$$C_v = S_{K's} / m_{K's} \tag{2.9}$$

where:

$m_{Ks'}$ = arithmetic mean of Ks'

$S_{Ks'}$ = standard deviation of Ks'

To utilize the mean and coefficient of variation as defined in Equation (2.9) for computing cumulative lognormal densities, the following transforms are required to obtain the median of the untransformed Ks' distribution and the standard deviation of the transformed values:

$$\sigma_{lnK's} = \left[\ln(C_v^2 + 1)\right]^{1/2} \tag{2.10}$$

$$\breve{m}_{K's} = m_{K's} \exp\left(-\frac{1}{2}\,\sigma^2_{lnK's}\right) \tag{2.11}$$

where: $\breve{m}_{Ks'}$ = median of Ks' distribution

$\sigma^2_{lnKs'}$ = variance of the log transformed Ks' distribution

With these values, the pdf and CDF of the lognormal Ks' distribution can be formed as follows:

$$f_{K's}(x) = \frac{1}{\sqrt{2\pi}\;\sigma_{lnK's}\;x} \exp\left[-\frac{1}{2}\left(\frac{lnx - \ln\breve{m}_{K's}}{\sigma_{lnK's}}\right)\right] \tag{2.12}$$

$$F_{K's}(x) = \int_{-\infty}^{x} f_{K's}(x)dx \tag{2.13}$$

Equation (2.12) can be numerically integrated to generalize the model to allow a variable number of parallel strips. This procedure is discussed in the following section.

2.4.2 Variable Strip Formulation

A model formulation that allows a variable number of strips and the

automatic computation of Ks' values derived from equal probability classes is desired. Such a model will allow ready analysis to assess the number of strips required to reproduce runoff response from a near continuous representation of the Ks' distribution. The Ks' for the equal probability classes corresponds to the mean Ks' in that particular class. For example, if ten strips are desired, the overland flow plane will have ten different Ks' values used in the simulation. A single Ks' value will be assigned to ten percent of the area covered by the plane (or 1/(number of strips)). The first Ks' value in this example is the mean of the pdf integrated from 0 to 0.1. The second Ks' corresponds to the mean of the pdf integrated from 0.1 to 0.2 and so on.

Because log transformed values (ln(Ks') is distributed normally) were used in the original work by Woolhiser and Goodrich (1988), the Ks' value corresponding to the midpoint of the equal probability classes were used. When dealing directly with the pdf for the lognormal distribution in Equation (2.12), for a variable number of segments, the first moment of the probability class must be computed numerically. To accomplish this the following computations must be performed.

Let N be the number of parallel strips desired. 1/N is the probability assigned to each class. The first probability class will, of course, have a lower bound or break equal to 0, and the last class will have an upper bound equal to one. The interior breaks defined in terms of the accumulated probability ($F_{Ks'}(x)$) are used in setting the boundaries for the equal probability classes. They can be computed as:

$$B_i = i\left[\frac{1}{N}\right] \qquad i = 1,2,\ldots,N-1 \tag{2.14}$$

where:

N = number of strips

B_i = probability class break.

Although the breaks are easily defined, the integration limits for the cumulative distribution are not easily obtained. The problem is to find the upper integration limit for each probability class. For the first class, this means finding b_1 such that the integrated pdf of Equation (2.12) equals 1/N as shown below:

$$\frac{1}{N} = \int_{a_i}^{b_i} f_{K's}(x)\, dx \qquad i = 1,2,\ldots,N \tag{2.15}$$

where:

a_i = 0 for the first class i = 1

b_N = infinity for the last class i = N

Because the lognormal function cannot be solved analytically, numerical integration is required. The routines to perform the integration were obtained from Press et al. (1986). These routines return the integrated value of the pdf for a specified lower

and upper limit. The integrated value should equal 1/N for equal probability classes. A bisection-type algorithm was developed to find b_1 in Equation (2.15) for i = 1 such that the integral equals 1/N to a prespecified tolerance. For the second equal probability class, b_1 becomes the lower limit of integration (a_2), and the bisection and integrations are repeated to find b_2, and so on for each probability class.

With the upper and lower limits defined for each probability class, the mean of each class can be defined as follows:

$$\overline{K's}_i = \frac{\int_{a_i}^{b_i} K's\, f_{K's}\,(K's)\, dK's}{\int_{ai}^{b_i} f_{K's}\,(K's)\, dK's} \qquad i = 1,2,\ldots,N \qquad (2.16)$$

This procedure and algorithm can then be used to automatically derive mean Ks' values for equal probability classes for a variable number of overland flow plane segments. The ability to define a variable number of flow strips allows an assessment of the number of strips required for modeling studies over a range of storm and soil sizes. This assessment is discussed in Section 2.5.

2.4.3 Estimation of the Required Soil Parameters from Textural Estimates of Ks

Use of the variable strip formulation implies that a wide range of Ks' values will be used for runoff generation computations on a single overland flow plane.

Several other soil-related parameters are required by KINEROSR to carry out these computations. They are the effective net capillary drive (suction) G and the relative soil saturation at -0.33 bar tension (field capacity, SFC) and -15 bar tension (residual, SR). [See pages 5-11 of Woolhiser, Smith, and Goodrich (1990) for a detailed explanation of the use of these parameters]. Formulation of simple regression relations between Ks' and these three parameters is the focus of this subsection.

Field data collected over a wide range of soil types indicate significant correlation between Ks' and these parameters (Rawls et al., 1982). These parameters are difficult to measure in the field so initial estimates of Ks' will be obtained from soil texture. Because these are rough estimates and it is desirable to reduce the number of parameters requiring estimation by way of optimization, the correlation between Ks' and G, SFC, and SR is exploited. Relationships between G, SFC, and SR from Ks' will enable their automatic computation in the variable strip formulation.

Data to estimate each relationship were taken from Table 2 of Woolhiser et al. (1990). The data listed in this table were derived from the large set of field data presented in Rawls et al. (1982). Mean values of Ks' and the three parameters for each textural class were used for regression purposes. Table 2.1 summarizes the regression relationships that were obtained.

The regression relationship between the mean effective net capillary drive (suction) and mean saturated hydraulic conductivity agrees very well with results from Ahuja et al. (1989). From a theoretical analysis of parallel capillary stream tube

Table 2.1. Summary of Regressions Relating Ks', to Soil Parameters G, SR, SFC

Regression	Form	Estimated Coefficients	R^2	Stan. Error of Est.	Range of Independent Variable
G* vs. Ks'	$G = a(1/Ks')^b$	a = 4.83 b = 0.326	0.99	1.56	1.8-16.0
SR vs. Ks'	$SR = a + b\log_{10}Ks$	a = 0.081 b = -0.055	0.65	0.055	0.045-0.19
SFC vs. Ks'	$SFC = a + b\log_{10}Ks$	a = 0.452 b = -0.254	0.98	0.042	0.21-0.83

* The geometric mean of G was used in the regression.

bundles, they showed that the exponent should lie between the extremes of 0.5 for a constant porosity similar media and 0.25 for a constant number of pores per unit bulk area. Exponents obtained from regressions between G and Ks (0.32 to 0.42) of field data they examined (five soil types and numerous horizons) were also within the range noted above. The data they examined had significantly more scatter and the r^2 for the regressions ranged from 0.68 to 0.50 for different soil groups. The high r^2 between suction and Ks obtained in this study is no doubt the result of using mean values as derived from the data in Rawls et al. (1982). Ahuja et al. (1989) noted a strong relationship between suction and Ks and highly significant nonzero exponents. However, because of the scatter of the data, the fraction of total variation not due to regression ($1 - r^2$) indicates a greater independence in the suction Ks relationship than dependence.

The large data scatter in the data set used by both Ahuja et al. (1989) and Rawls et al. (1982) is expected as the data were obtained from widely separated locations. Ahuja et al. (1989) pointed out that a single-suction Ks relationship for comparable soils across a watershed may be permissible with preliminary assessment. Textural sampling of soils within Walnut Gulch shows that the majority of soils fall within the sandy loam grouping; therefore, using the single regression relationship derived above should not be a major shortcoming.

The regression relating Ks and SR was only fair. This should not pose a major problem due to the restricted range of SR and the fact that this value is used only during soil moisture deficit recovery in a rainfall hiatus. Small variations in SR

are not critical in this computation because the relative saturation deficit is the primary driving term in subsequent infiltration. A high degree of correlation exists between Ks and SFC. The relationships and the estimated coefficients described in Table 2.1 were implemented in KINEROSR. With this implementation, the additional comparisons and testing outlined above can be carried out.

2.5 Comparison with Other Model Representations of Infiltration Variability

To assess whether the proposed parallel strip model will adequately represent small-scale variability of infiltration, comparisons with several other model formulations are warranted. A known shortcoming of the parallel strip method is that it does not simulate runoff-runon interactions downslope. The comparisons presented are meant to illustrate the degree of inadequacy imposed by this formulation. Several models in addition to the uniform case are briefly discussed, and comparative simulations are carried out. Much of the material discussed in this section is discussed in greater detail in Smith, Goodrich, and Woolhiser (1990, in press).

The first model representing infiltration variability was compared to the parallel strip model from earlier work done in conjunction with Smith (1987). The model employs a single area composite equivalent rain rate-scaled infiltration rate (f_*) defined as:

$$f_* = \frac{f-Ke}{r-Ke} \tag{2.17}$$

where:

f = infiltration flux (Smith and Parlange, 1978)

r = temporally uniform rainfall rate

K_e = expected value of Ks' over an area with ponded and unponded area.

The scaled infiltration flux, f_*, can be related to the coefficient of variability, C_v, as defined in Equation (2.9). A plot of f_* versus the infiltrated depth F is shown in Figure 2.3. It illustrates that, for the uniform (point) case, infiltration will be rain rate controlled until a certain depth of water is infiltrated. After that point, the infiltration rate is soil controlled. However, as soon as C_v becomes greater than zero, some small percentage of the area will have a small Ks' and will pond nearly instantaneously. The average behavior of the area will exhibit soil-controlled infiltration behavior from near the beginning of rainfall as illustrated in the figure. This model, deemed the "Composite" model, produced results comparable to those of Sivapalan and Wood (1986) using variable soils and temporally uniform rainfall.

The Composite model, like the parallel strip (Woolhiser-Goodrich, W-G) model, does not simulate runoff-runon interactions. Initial test runs between the two models showed very good agreement for temporally uniform rainfall rates. As soon as variable rainfall rates were introduced, results from the two models diverged. The

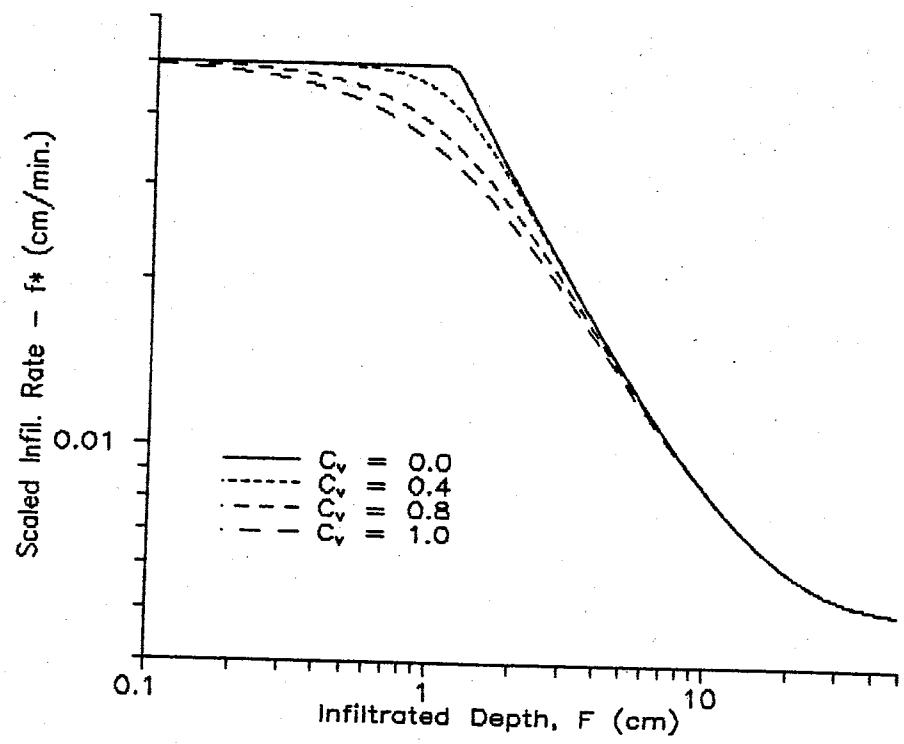

Figure 2.3. Composite Infiltration Curves with Lognormally Distributed Ks as a Function of C_v

divergence can be explained by examining the time history of infiltration in the parallel strip case for variable rainfall rates.

Figure 2.4 illustrates this point for a case where the overland flow area is represented by eight parallel strips, each with different Ks, G, SR, and SFC. At time (t) for a given rainfall rate (r), one-eighth of the relative area is not producing runoff. At time (t + delta t), the rainfall rate drops, and three-eighths of the relative area is now in recession. At the advance time, the infiltration capacity has also decreased in a non-uniform manner across the relative area. The fluctuation of the rainfall rate in relation to the infiltration capacity for each strip causes a unique time and area-dependent infiltration history. The Composite model is incapable of treating this kind of behavior. The W-G strip model is, therefore, more appealing.

Both the Composite and W-G strips models do not incorporate downslope runoff-runon interactions. To examine the impact of this assumption, KINEROSR was modified by Smith et al. (1990) to allow a lognormal variation of Ks down the flow path as well as the across slope variation. The geometric interpretation of this model is that of a series of uniform width rectangular patches each having the same slope and roughness but variable Ks. This model, like the others, does not embody flow concentration downslope. The downslope variation was introduced by randomly sampling from the lognormal Ks distribution. This is deemed the "Interactive" model.

To assess the variation due to random sampling, ten simulations were carried out using different random seeds with 20 strips and 30 downslope Ks values. These simulations were performed on the same overland flow plane (geometry and soils)

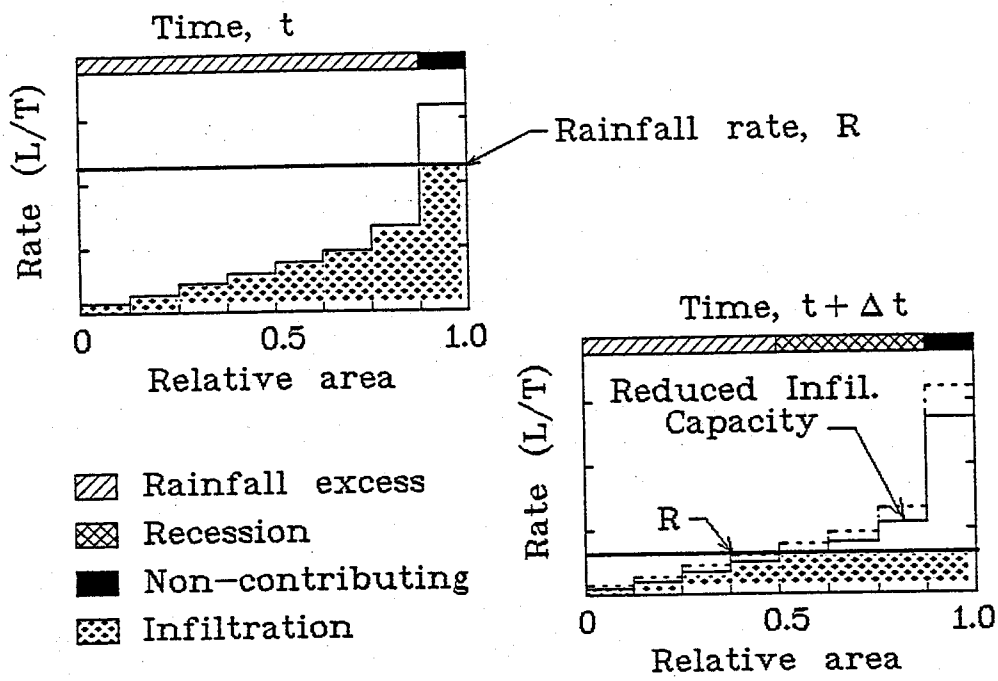

Figure 2.4. Evolution of Time and Area-Dependent Infiltration Capacity (First Presented by Goodrich, Woolhiser, and Sorooshian, 1989)

as were used for central bottom case shown in Figure 2.2 (Storm 4, $F_p^* = 0.574$). Simulations for the same condition for the other models, including a uniform case ($C_v = 0.0$), were also conducted. However, for these runs, ten parallel strips were used in the W-G model with $C_v = 1.0$ after minor improvement of the infiltration algorithm. Also note that, for comparative purposes, G, SR, and SFC did not vary with Ks,' but were set to equal to the constants used in the prior analysis. Figure 2.5 depicts the results of the simulation.

The shaded area in Figure 2.5 shows the range of sampling variation in the Interactive model for the ten runs with different random seeds. Both the Composite and Uniform models are highly biased if one treats the Interactive model as the best overall model representation. The W-G model is also biased high as it accentuates the nonlinear infiltration behavior. Downslope variation in the Interactive model has the tendency to further damp rainfall variability (Freeze, 1980), as indicated in the plot. However, it is interesting to note that the W-G model result does fall largely within the variation bands of the Interactive model.

The case shown in Figure 2.5 is an extreme condition where runoff is a very small percentage of total rainfall. Model comparisons were also performed for the storm 1, $F_p^* = 0.104$ case, for the Interactive, Uniform, and W-G models were run. Plots of these simulations are shown in Figure 2.6. For this case, a much greater percentage of the rainfall is transformed to runoff. The response from the three models is virtually identical with the maximum difference in runoff volume and peak rate of 4.6 and 6.6 percent, respectively. The bias of the W-G model as compared

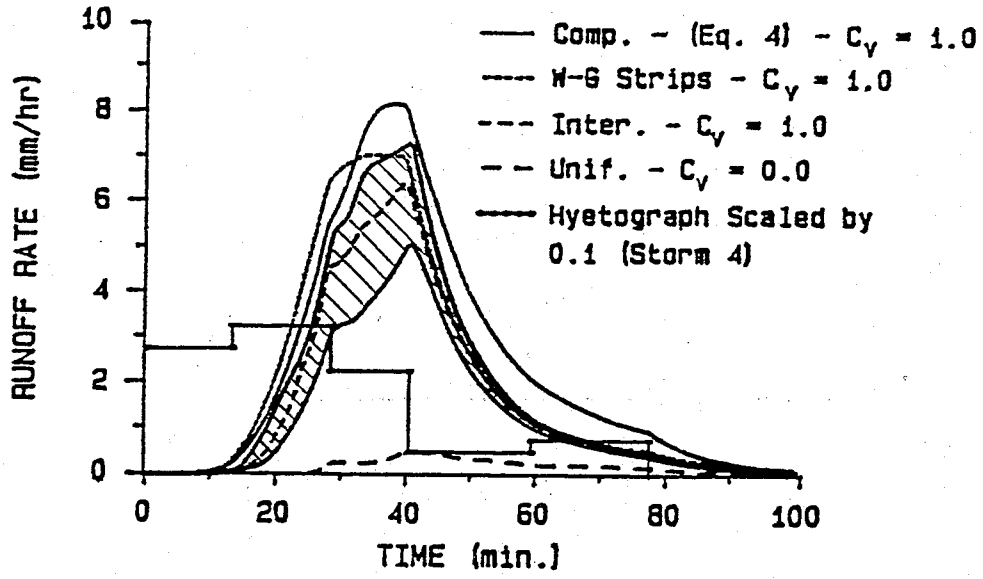

Figure 2.5. Comparison of Methods to Treat Spatially Variable Infiltration in Surface Runoff: Small Runoff/Rainfall Ratio Case (from Smith, Goodrich, and Woolhiser, 1990)

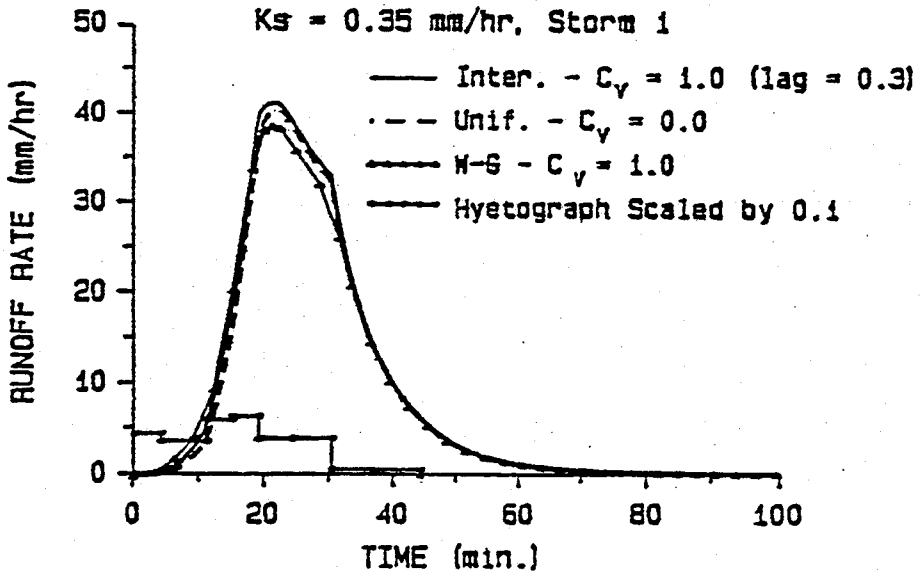

Figure 2.6. Comparison of Methods to Treat Spatially Variable Infiltration in Surface Runoff: Large Runoff/Rainfall Ratio Case (from Smith, Goodrich, and Woolhiser, 1990)

to the Interactive model decreases as runoff becomes a higher percentage of rainfall (larger storms or smaller F_p*). The nonlinearities of infiltration dominate for small runoff events, and a more complex representation of spatially variable infiltration is required if this type of event is of interest.

The plots in Figures 2.5 and 2.6 directly address hypotheses 1B and 1C of Chapter 1 as they apply to infiltration parameters. These hypotheses are repeated below:

HYP (1B): Above a certain soils-climatic scale, positions will not be important to modeling runoff but spatial variability must be considered.

HYP (1C): Above a certain basin-climatic scale, simple property or parameter averages of overland flow will be sufficient to model runoff.

If position is not important but considering spatial variability is, hypothesis 1B implies that the W-G model should reproduce the Interactive model runoff response to within a specified tolerance. If the differences in runoff response shown in Figure 2.5 are acceptable, then hypothesis 1B cannot be false and must be accepted. If the range of variability in runoff response from the Interactive model from sampling is considered, hypothesis 1B can be accepted more easily. For the high percentage runoff case illustrated in Figure 2.6, hypothesis 1B is much more easily accepted. Acceptance of hypothesis 1B implies that the W-G model, with its added complexity,

is acceptable and the Uniform model may or may not be acceptable. For the case shown in Figure 2.5, the Uniform model is clearly not acceptable.

Runoff response from the Uniform versus the Interactive model is used to test hypothesis 1C. As stated above, for the low percentage runoff case shown in Figure 2.5, it would be difficult to accept hypothesis 1C. However, for the case shown in Figure 2.6, the Uniform model nearly reproduces the response of the Interactive model. If hypothesis 1C is accepted for the climate (storm) and soil combinations represented by the case in Figure 2.6, the Uniform model can be used to simulate runoff response. This would result in far less model complexity and would significantly decrease computational requirements.

The cases discussed above demonstrate the dependence of acceptable infiltration model structure on the climatic/soils combinations of interest. Thus, acceptance of hypotheses 1B or 1C depends on the modeling objective. If flood studies are of primary concern, the uniform model may provide sufficient accuracy, but it is unlikely that it will for water yield studies where infiltration losses are a substantial portion of the rainfall volume. Blanket acceptance of the either hypothesis for all basin-climatic combinations is, therefore, unlikely.

As discussed above (Woolhiser and Goodrich, 1988), the interactive model did not exhibit the cross-over effect observed in the W-G model. Using ten strips and the improved infiltration formulation, the cross-over was still observed but was greatly reduced. Bias or errors resulting from ignoring the runoff-runon condition in the W-G model will be reduced by sediment transport and the occurrence of flow

concentration (rilling). This can be expected because if a region consistently produces greater runoff than adjoining regions (intercanopy area vs. under canopy area), sediment will be transported downslope from the runoff production areas to areas with higher infiltration rates which will tend to seal areas further downslope, thus negating further downslope infiltration. The formation of rills downslope from runoff-producing areas will reduce the wetted area available for subsequent infiltration, providing the same effect. The Interactive model assumes no flow concentration which may be a fair assumption for a certain distance from the ridge but, in the Walnut Gulch watershed where the model will be applied, significant rilling takes place in length scales of tens of meters.

The W-G model also ignores Ks correlation structure across the slope. Freeze (1980) concluded that ignoring correlation structure imparted minor effects as compared to including the variability of Ks itself. El-kadi (1987) found that if correlation structure is neglected, mean infiltration rates are underestimated. The correlation issue is moot if one considers the typical range of correlation of Ks for the environment being modeled. A number of investigators (Russo and Bresler, 1981; Grah et al., 1983; Loague, 1986) reported correlation ranges of 10-20m for uncultivated soil. In rangeland soils more closely associated with those in Walnut Gulch, Merzougui (1982) collected field data in which the correlation range was less than 2m. With these short ranges, ignoring the correlation structure of Ks should not present a serious simplification.

From the foregoing analysis, further use of the W-G model in overall watershed modeling efforts is warranted. By using this model, the small-scale variability of infiltration is implemented in the model in a straightforward fashion. The W-G model representation of variability embodies much of the complex behavior shown by the Interactive model with only minor bias. It is parameterized by only two parameters (mean Ks and C_v) and does not require a random seed, thus avoiding the sampling variability problem. In the previous analysis, simulation results were shown to be a function of the number of strips used in the W-G model. Before watershed application, the question of the number of strips required for acceptable simulation must to be addressed.

2.6 Determination of the Number of Parallel Strips for the W-G Model

The important interaction between storm size and soil characteristics demonstrated earlier in this chapter can not be ignored in determining the number of strips for modeling. The analysis is performed over a range of storm sizes and soil types to replicate the response of a near continuous representation of the lognormal Ks' distribution to within a specified level of accuracy. This accuracy level is arbitrarily set at a ten percent difference in runoff volume from the near continuous simulation.

To cover a range of storm sizes and soil types, the same three storms from Walnut Gulch raingage #5 and soils used to generate the hydrographs shown in

Figure 2.2 have been used. A unit width overland plane geometry 91.4m long with a slope of 0.03 and a Manning's roughness of 0.07 was used for all the simulations. The dimensionless measure F_p* (Equation 2.5) was used to characterize the soils selected in the prior analysis. This measure was computed on the basis of a selected set of 30 large storms. To avoid dependence on this selected storm set, F_p*' is computed based on the individual storm under consideration. It is computed as follows:

$$F_p{*}' = \left[\frac{G \cdot \phi \, (S_m - S_I) \, (1 - V_r) \, \ln \left(\frac{\bar{I}}{\bar{I} - K's} \right)}{D} \right] \qquad (2.18)$$

where:

G = effective net capillary drive (suction)

ϕ = soil porosity

S_m = maximum relative soil saturation

S_I = initial relative soil saturation

V_r = volumetric rock content

$\bar{I}$ = weighted mean storm intensity

D = total storm depth

Tables 2.2 and 2.3 contain the storm and soils characteristics used. Table 2.4 contains the matrix of computed $F_p^{*'}$ values for the three storms and the three soils listed in the prior two tables. At each one of the nine locations in the storm/soil matrix in Table 2.4, simulations with decreasing numbers of parallel plane segments (strips) were carried out to assess how runoff volume and peak flow rate are preserved. Simulations with 50, 20, 10, 7, and 5 strips were run. It is assumed that the 50-strip case nearly approximates the continuous lognormal distribution of Ks.

Due to the compression of $F_p^{*'}$ for large events, an additional case of a loamy sand soil (Ks = 61.0 mm/hr, G = 92.2 mm, ϕ = 0.5) with storm 30 ($F_p^{*'}$ = 0.92) was added to the analysis. The change in peak rate and runoff volume as the number of strips decrease is listed in Table 2.5 for storm 30 and soil 2 ($F_p^{*'}$ = 0.07). In this case, seven (7) strips would maintain the runoff volume to within ten percent of the volume resulting from the 50-strip case.

In Figure 2.7, the runoff response for the simulations for the 50 and 7 segment cases in Table 2.5 are shown. In general, as the number of strips decrease, the runoff volume and peak runoff rate also decrease. The exception is the added sandy loam case were the trend is reversed. Closer examination of the simulations for this case reveals that the upper portion of the lognormal Ks distribution controls runoff generation to a greater degree. The variable strips simulations in the weighted storm intensity ($\bar{I}$,$F_p^{*'}$) space outlined above were completed to determine the number of strips required to maintain the volume of the 50-strip case to within ten percent. The number of strips required for ten percent volume preservation at the ($\bar{I}$,$F_p^{*'}$)

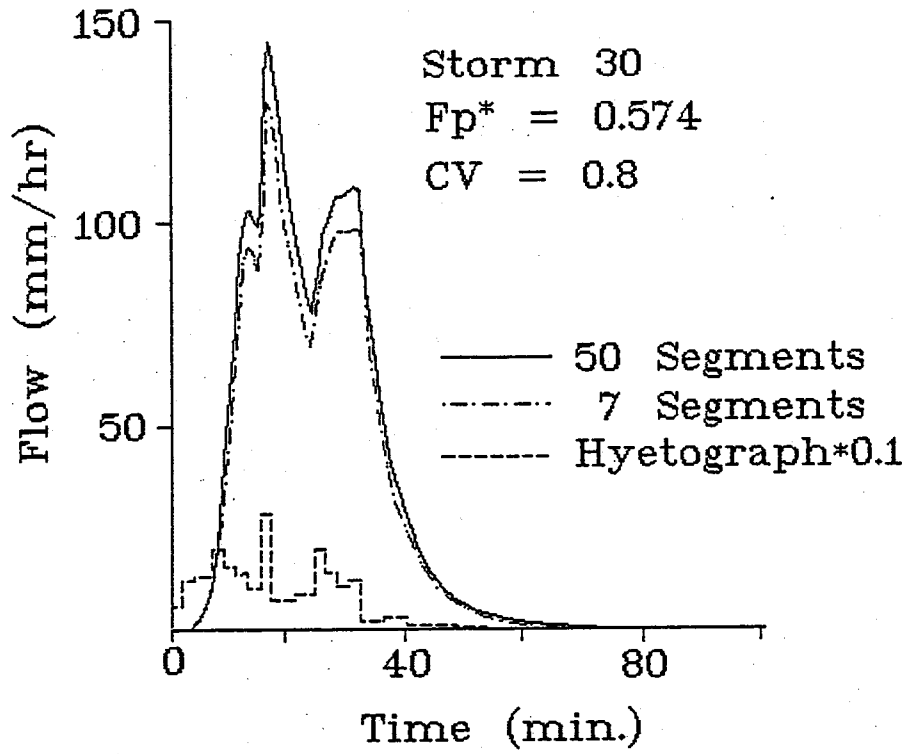

Figure 2.7. Runoff Response as a Function of the Number of Parallel Strips (Storm 30, Soil 2)

Table 2.2 Test Storm Characteristics

Storm	Total Depth (mm)	Weighted Mean Intensity (mm/hr)
4	24.1	18.8
1	24.6	33.5
30	75.9	74.9

Table 2.3 Test Soil Characteristics

Soil	Ks'(mm/hr)	G (mm)*	S_i	S_m	V_r	C_v
1	0.35	495.0	0.0	0.9	0.0	0.8
2	3.40	236.0	0.0	0.9	0.0	0.8
3	10.9	199.0	0.0	0.9	0.0	0.8

* G obtained from regression relationship in Table 2.1.

Table 2.4 F_p^* for ($\bar{I}$ - Soils) Combinations

Storm	$\bar{I}$ mm/hr	Soil 1	Soil 2	Soil 3
4	18.8	0.17	0.88	3.23
1	33.5	0.10	0.46	1.43
30	74.9	0.04	0.07	0.19

Table 2.5. Runoff Volume and Peak Rate Change as a Function of the Number of Parallel Strips

Number of Strips	Volume (mm)	% Difference Volume from 50 Strips	Q_p (mm/hr)	% Difference in Q_p from 50 Strips	Time to Q_p (minutes)
50	50.7	---	147	---	16.8
20	49.7	1.9	143	2.4	16.8
10	47.8	5.8	137	6.6	16.8
7	45.9	9.4	131	10.4	16.8
5	43.3	14.6	124	15.6	16.8

coordinate locations listed in Table 2.4 are shown in Figure 2.8. For the majority of the simulation space, it appears as if five to nine strips are required. As a preliminary decision, eight strips were selected.

The number of strips used to represent infiltration variability affects computational time as routing and infiltration calculations must be made for each strip for the entire storm. Therefore, a smaller number of strips is desired as long as the associated deviation from the 50-strip case is tolerable. To acquire further confidence in the number strips selected, several additional simulations for typical modeling conditions were undertaken.

For the Lucky Hills 106 watershed, six (6) textural soil estimates of infiltration parameters were obtained (see Appendix A). Out of these six estimates, the minimum and maximum Ks' values were selected. Four storms from the closest raingage (# 384), including the largest storm of record, were selected for further analysis. For each of these storms and the minimum and maximum Ks', values the corresponding $F_p{}^{*\prime}$ values were computed. These points are also plotted in Figure 2.8. For each of the four storms at the minimum and maximum Ks' values, simulations were conducted with 50 and eight strips to assess the degradation in results. The results are presented in Table 2.6.

The results presented in Table 2.6 indicate that by using eight parallel strips, the ten percent runoff volume criteria will be easily achieved for the extremes of soil conditions and a wide range of storms on one of the watersheds being used in subsequent research.

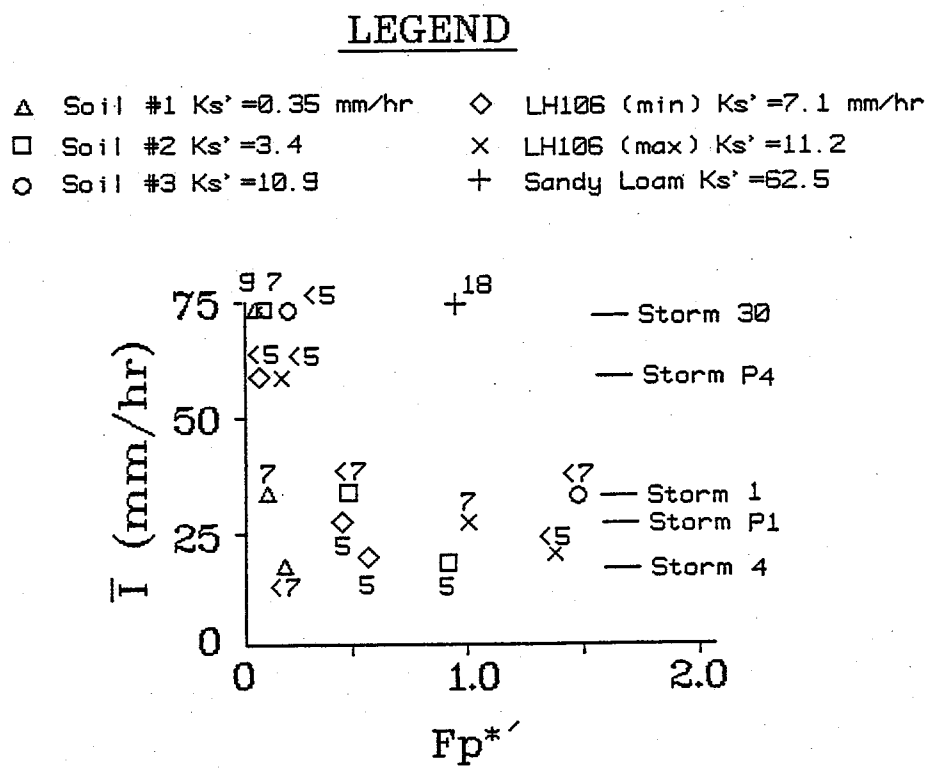

Figure 2.8. Number of Strips Required to Maintain Volume to Within 10 Percent of the 50-Strip Case

Table 2.6 Runoff Volume Error from 50-Strip Case to 8 Strips for Lucky Hills Storms and Minimum and Maximum Ks'

Storm	Weighted Mean Storm Int. (mm/hr)	Minimum Ks' Case		Maximum Ks' Case	
		$F_p^{*'}$	% Volume Difference	$F_p^{*'}$	% Volume Difference
P1	25.7	0.41	4.0	0.97	0.3
P2	7.0	7.14	2.2	10.7	2.2
P3	19.2	0.53	2.3	1.32	0.0
P4*	58.4	0.18	2.5	0.39	0.3

* Storm P4 caused the largest event of record for watersheds LH102, LH104, and LH106.

2.7 Summary and Conclusions

The importance of small-scale infiltration variability has been clearly demonstrated here and by the numerous investigators cited. The methodology of Woolhiser and Goodrich (1988) to model this variability without resorting to further discretization has been generalized and compared to other methods with reasonable success. The estimation of soil suction (G) as well as the residual (SR) and field capacity (SFC) relative soil saturation is automatically computed as Ks' varies using regression relationships. Numerical techniques have been incorporated into the algorithms to automatically compute the mean Ks' of up to 50 equal probability classes. An objective procedure was then used to establish the number of parallel strips required to model infiltration variability over a range of storm and soils conditions that will be encountered in subsequent research.

The methodology developed assumed an equal partition of the relative overland flow area (equal probability classes). A more efficient implementation, using fewer strips, might be achieved if an unequal partition were used. This is indicated by the sandy loam case examined where the primary rainfall/soils infiltration interactions occurred in the upper portion of the Ks' distribution. Implementing an unequal partition methodology would require additional analysis. An automatic procedure would have to be developed to sense which regions of the Ks' distribution would interact with a given storm. The equal area partition methodology avoids this issue at the expense of additioned computational time. Not including a representation of infiltration variability, using equal or unequal area

partitions may not be a bad assumption if very large events (floods) are being studied. In these cases, the uniform results appear to converge to variable cases (HYP 1B and 1C). The large storm size appears to dominate the rainfall-runoff transformation and overwhelm the nonlinearity of infiltration and its variability. However, if model optimization for parameter estimation is to be carried out over a wide range of runoff events, a bias in parameter estimates will likely result by ignoring variability as it is critical in small events. This issue will be discussed in greater detail in Chapter 5.

The analysis presented in this chapter was carried out on a single flow plane. The variability of infiltration will also show up at larger scales where spatial rainfall variability becomes important. At these scales, the watershed regions directly under the high intensity regions of a thunderstorm will produce runoff with a high probability. However, as intensities decrease, away from the storm center, there will be large spatial regions or bands where lower rainfall intensity will significantly interact with spatially variable soils.

Before moving to watershed scales where a large degree of spatial rainfall variability is important, examination of channel routing processes and their impact on the rainfall to runoff transformation must be undertaken. This is the topic addressed in the following chapter.

CHAPTER 3

CHANNEL ATTENUATION EFFECTS ON SEVERAL PRECIPITATION DISAGGREGATION SCHEMES

3.1 Introduction

In Chapter 2, the importance of considering the small-scale spatial variability of infiltration simultaneously with climate was clearly demonstrated. This analysis was carried out on a single overland flow plane. For larger-scale systems where significant flow concentration occurs, the importance of channel processes in the rainfall-runoff transformation must be considered. The primary objective of this chapter is to assess the attenuating impacts of a first order channel on rainfall in comparison to the effects of overland flow and infiltration attenuating impacts. The effects of channel processes will be considered over a range of climatic scales in a manner cosistent with the infiltration analysis presented in Chapter 2. In addition to the size of storm events, their temporal representation will be considered by employing several precipitation disaggregation schemes. This will provide an indirect measure of channel attenuating effects. If the temporal rainfall distribution is significantly attenuated by the channel, in addition to overland flow, a simple, disaggregated, rainfall input representation may provide the same results as a more complex representation.

Given the highly damped nature of hydrologic systems, the question of "how much descriptive precipitation detail is actually required?" must be addressed. This question brings up the issue of time and space scales relevant to modeling a

catchment in a given climatic regime. At this stage of the study, only spatially uniform rainfall will be considered. The damping influence of the channel on temporal precipitation features is be examined in this chapter by employing several intrastorm disaggregation schemes through a simple catchment geometry described below.

The precipitation sequence in each intrastorm disaggregation scheme was derived by holding the total duration and total rainfall amount constant. The durations and amounts were obtained from a set of the 30 largest storms measured at raingage #5 in the USDA-ARS Walnut Gulch Experimental Watershed near Tombstone, Arizona. A constant (CP), triangular (TP), and "Woolhiser-Osborn" (WO) (Woolhiser and Osborn, 1985) disaggregation were obtained from the durations and amounts of the storm set. The actual and disaggregated storms were used as input to "KINEROSR" (Woolhiser et al., 1990) as described in the prior chapter.

For the purposes of this study, a simple geometry of two planes feeding a channel as used by Iwagaki and Takasao (1956), Ishihara and Takasao (1963), and Wooding (1965a) was employed. The plane and channel characteristics were varied to assess their impact on the disaggregation schemes. The impacts of variations in plane characteristics alone were examined by Woolhiser and Osborn (1986). They introduced several dimensionless parameters to characterize the system and a Kolmogoroff-Smirnoff (K-S) statistic to evaluate the performance of the disaggregation schemes against the actual storms on the cumulative distributions of

derived peak runoff rates. A similar approach is employed here and, in addition, channel effects are examined through the use of another dimensionless parameter. At this juncture, a review of prior relevant work is warranted.

3.2 Background Review

Woolhiser, Osborn, and Hershenhorn (1984) described a point interstorm disaggregation scheme to partition daily rainfall amounts into individual storm amount, duration, and time of occurrence. Woolhiser and Osborn (1985) developed methods to perform intrastorm point disaggregation to break up storms into shorter period rainfall amounts and examined seasonal and regional effects on the disaggregation methodologies (Woolhiser and Osborn, 1986). They also investigated the effects of the disaggregation scheme on storm runoff volume and peak runoff rates from an overland flow plane. The geometry and infiltration characteristics of the overland flow plane were varied to assess their relative influence on the observed storm set and the set obtained from the disaggregation schemes. Two dimensionless ratios were introduced to represent the numerous parameters affecting the runoff response timing to rainfall and infiltration properties of the plane. The first is a characteristic time ratio T_* defined as the kinematic time to equilibrium (t_e, [s]) on a plane at a rainfall excess rate ($\bar{q}$ [ft/s]) equal to the mean intensity of a set of m storms divided by the mean storm duration, D.

$$T_* = \frac{t_e}{\overline{D}} \tag{3.1}$$

where:

$$t_e = \left[\frac{nL_o}{1.49\ S^{1/2}\ (\bar{q})^{2/3}} \right]^{3/5} \tag{3.2}$$

n = Manning's roughness coefficient

L_o = length of the plane (ft)

S = slope of the plane

and

$$\bar{q} = \frac{1}{m} \sum_{i-1}^{m} \frac{P_i}{D_i} \tag{3.3}$$

P_i = total precipitation for the ith storm

D_i = duration of the ith storm

The dimensionless infiltration ratio F_p*, defined in Equations (2.5) through (2.7), was used as a measure characterizing soil infiltration capacity in relation to the storm set used.

The watershed and infiltration parameters were varied within realistic ranges to obtain various combinations of the above two dimensionless parameters. Each of the various geometric and infiltration combinations was used as input to KINEROS. Precipitation input from each of the 30 storms was applied to each watershed/infiltration case. For each run, the total runoff volume (V), the time to peak (t_p), and peak runoff rate (Q_p) were tabulated. From these tabulations, empirical distribution functions were formulated for the actual storm. These distributions were used as a basis to compare distributions obtained from the disaggregated storm sets.

The effects of infiltration and runoff time response were assessed by computing the K-S D* statistic between the actual and derived cumulative distributions obtained from the disaggregation schemes. The study of Woolhiser and Osborn (1986) is extended to investigate channel effects on rainfall intensity patterns.

Wooding (1965a) analyzed the same type of geometry employed in this study. He nondimensionalized many of the variables and was able to derive analytic solutions for several types of rainfall patterns. The cases studied were:

(a) known rainfall intensity

(b) known total storm depth

(c) known storm duration

To investigate the effects of channel length, slope, and roughness on response time, Wooding introduced the dimensionless parameter lambda, which is the ratio of equilibrium time in the channel to the equilibrium time of the plane. The study also considered infiltration using a Φ-index approach. Wooding found that, for the case

where total storm depth is known, lambda = 0.5 "separates two regions of fundamentally different properties." For lambda < 0.5, the catchment strongly controls the peak runoff rate.

Golany and Larson (1971) also studied the effects of channel characteristics on the response time of small, second to fourth order watersheds to excess rainfall. Only first-order stream segments received lateral inflow from overland flow planes. Time characteristics of the first-order elementary watersheds were computed using kinematic theory. Time characteristics of the remaining channel segments comprised the thrust of Golany and Larson's (1971) investigation. They recognized that larger watersheds do not typically reach kinematic equilibrium because storms do not have sufficient duration. To circumvent this problem, they defined the time to virtual equilibrium T_{ve}, which can be computed from drainage basin characteristics for a given supply rate. Qualitative results indicate that, as the drainage area increases, the effects of the elementary watershed (changes in slope and roughness) on the time to virtual equilibrium decrease. Backwater effects also become significant as drainage area increases. Increases in channel roughness produced a more gradual rise in the hydrograph and increased T_{ve}.

Hjelmfelt (1981) compared dimensionless peak rates of overland flow for constant intensity rainfall and for an average thunderstorm rainfall hyetograph obtained from the U.S. Weather Bureau records. The study concluded that the constant intensity approximation is valid for storm durations that are roughly equal to, or less than, the kinematic time to equilibrium at the average constant intensity.

Hager (1985) also examined the watershed geometry used in this study. He nondimensionalized various response parameters in a slightly different fashion than did Wooding (1965a). His conclusions are based on a nondimensional length parameter and are not significantly different from those of Wooding.

3.3 Approach

Using the continuity equation and kinematic depth-discharge relations for overland and channel flow, a relation can be derived between the dimensionless parameter lambda and plane, channel, and supply rate characteristics. Figure 3.1 illustrates the variables used to characterize the simple catchment geometry.

To derive the relation for lambda, note that at steady-state, the discharge from the downstream outlet of the catchment is:

$$Q_s = 2\, L_p\, L_c\, \bar{q} \tag{3.4}$$

where:

Q_s = the system steady state discharge

L_p = the length of the plane

L_c = the length of the channel

$\bar{q}$ = the uniform precipitation rate

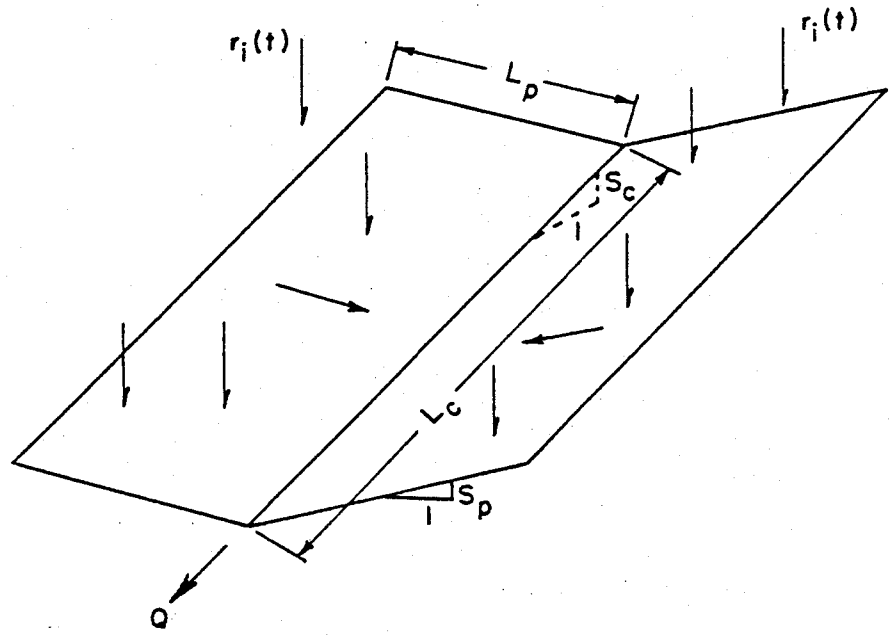

Figure 3.1 Simple Catchment Geometry

The simplified equation of motion also provides a formulation of discharge as a power function of cross-sectional area (A) as:

$$Q = \alpha_c A^m \tag{3.5}$$

where α_c and m are coefficients determined by the channel slope and roughness as well as the cross sectional shape. Using this equation and the continuity equation, the method of characteristics is used to obtain the following relation for the time to kinematic equilibrium in the channel (t_{sc}):

$$t_{sc} = \left[\frac{L_c}{\alpha_c}\right]^{1/m} \left[\, 2\,\bar{q}\, L_p \,\right]^{(1-m)/m} \tag{3.6}$$

Because lambda is defined as the ratio of equilibrium times for the channel and plane, Equation (3.6) can be used to obtain:

$$\lambda = \frac{1}{t_{sp}} \left[\frac{L_c}{\alpha_c}\right]^{1/m} \left[\, 2\,\bar{q}\, L_p \,\right]^{(1-m)/m} \tag{3.7}$$

where:

t_{sp} = time to equilibrium on the plane Equation (3.2)

Variables α_c and m are obtained by assuming that Manning's equation applies for uniform flow in a rectangular channel which implies:

$$Q_s = \frac{1.49}{n_c} (S_c)^{1/2} h^{5/3} w_c \tag{3.8}$$

where:

n_c = Manning's roughness coefficient for the channel

S_c = channel slope

h = normal flow depth (ft)

w_c = rectangular channel width (ft)

It is also assumed that $w_c >> h$ so the $h \approx$ hydraulic radius. To satisfy Equation (3.5), using Manning's formula in Equation (3.8), α_c and m must become:

$$\alpha_c = \frac{1.49}{n_c} S_c^{1/2} w_c^{-2/3} \tag{3.9}$$

$$m = 5/3 \tag{3.10}$$

With the above relationships and the plane parameters specified by Woolhiser and Osborn (1986), various combinations of channel variables were selected to maintain specified levels of lambda. This was accomplished by fixing the plane and supply rate parameters and varying the channel slope and roughness parameters over physically realistic ranges (Chow 1959) for various levels of lambda. With these variables fixed, Equation (3.7) can be solved for the channel length (L_c) that will have a response time such that lambda equals the desired values at channel equilibrium. After rearranging Equation (3.7) to solve for L_c and substituting in Equation (3.1) for the time to plane equilibrium, L_c equates to:

$$L_c = \frac{S_c^{1/2}\, n_p\, (\lambda L_p)^{5/3}}{S_p^{1/2}\, n_c} \left(\frac{2}{w_c}\right)^{2/3} \tag{3.11}$$

Once L_c is computed, the steady-state discharge can be computed using Equation (3.4). With this value, the steady-state velocity, flow depth, and width were computed using an assumed rectangular cross section in which the flow depth is specified to be

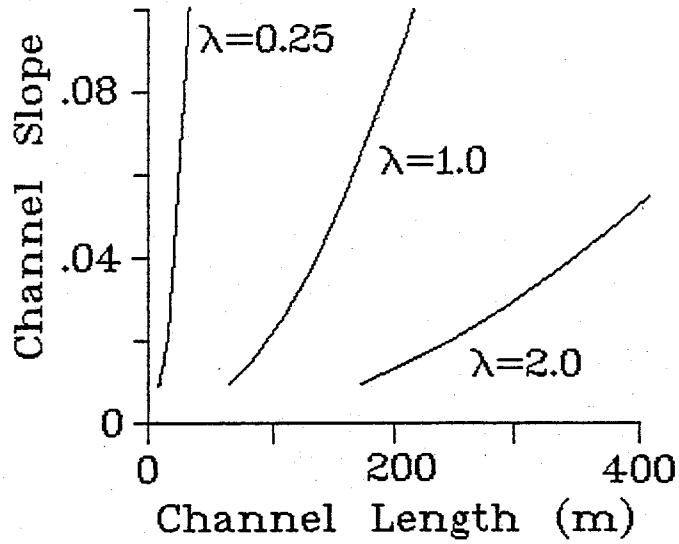

Figure 3.2. Channel Slope Versus Length for Varying Lambda, Fixed n_c = 0.02, L_p = 30.5m, S_p = 0.1, and n_p = 0.01

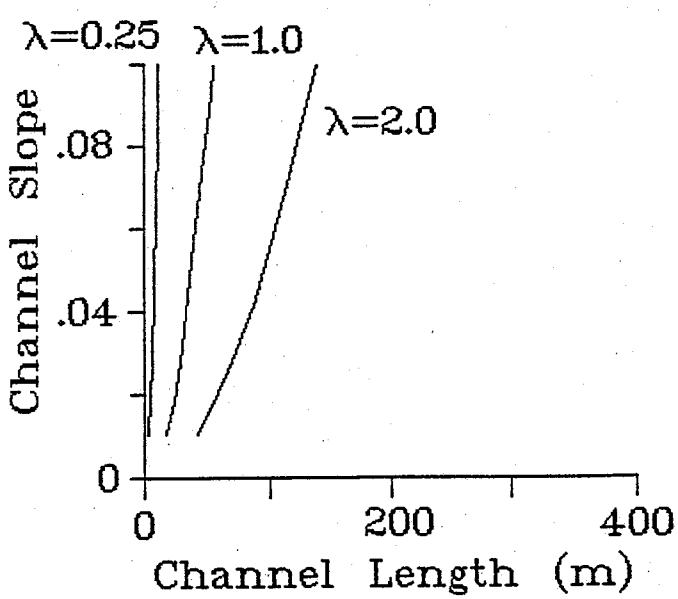

Figure 3.3. Channel Slope Versus Length for Varying Lambda, Fixed n_c = 0.08, L_p = 30.5m, S_p = 0.1, and n_p = 0.01

90% of the hydraulic radius. This approximates the wide channel condition in which flow depth approximates the hydraulic radius and facilitates computations. The Froude number and the kinematic flow number (Liggett and Woolhiser, 1967) were also computed to verify that the particular combination of variables selected did not violate the kinematic assumption. Contributing flow planes of 30.5, 91.4, and 152.4 meters were selected with various slope and roughness combinations.

For an elementary watershed with contributing plane lengths of 30.5 meters, slope of 0.1, and Manning's n of 0.01, plots of channel length versus channel slope for lambda ranging from 0.25 to 2.0, for n_c = 0.02 and for n_c = 0.08 are presented in Figures 3.2 and 3.3. The plane characteristics for the figures are L_p = 30.5 meters, S_p = 0.1, and n_p = 0.01.

To address whether lambda adequately captures the influence of channel slope, roughness, and length on response time, several combinations of L_c, n_c, and S_c that resulted in the same lambda were selected for further examination. For each case, the catchment geometries were set up in KINEROSR, and two rainfall impulses were applied to impervious planes. The rectangular channel was approximated in KINEROSR by an impervious trapezoidal channel with steep side slopes (5:1). Justification for this approximation comes from Golany and Larson (1971). They expressed basin travel time for uniform flow as a power function of supply rate, roughness, and slope. Little variation in the exponents of this power function was observed with changes in cross-sectional shape.

The first rainfall impulse used to test how well lambda captures the channel influence had a duration equal to the time of equilibrium on the planes, and the second impulse had a duration sufficiently long to drive the channel system to equilibrium. An intensity equal to the mean storm intensity (Equation 3.3) of the storm set was used. Figure 3.4 illustrates an example of hydrograph plots for partial equilibrium for equal lambda but unequal channel attributes. The figure demonstrates that lambda is, in fact, a good parameter to capture various combinations of L_c, n_c, and S_c.

3.4 Simulations to Assess Channel Attenuating Effects on Precipitation Distribution

To examine the effect of a channel on runoff response to varying rainfall inputs, an identical plane and a channel component were added to the cases examined by Woolhiser and Osborn (1986) to form the open-book geometry illustrated in Figure 3.1. The channel lengths, slopes, and roughnesses were chosen to give values of lambda = 0.0 (no channel), 0.5, 1.0, and 1.5. The dimensionless parameters T_* and F_p^* were varied by changing properties of the overland flow planes. The cases simulated are shown Table 3.1. Spatially varied infiltration on the overland flow planes was not considered in these simulations so that channel effects could be more easily isolated.

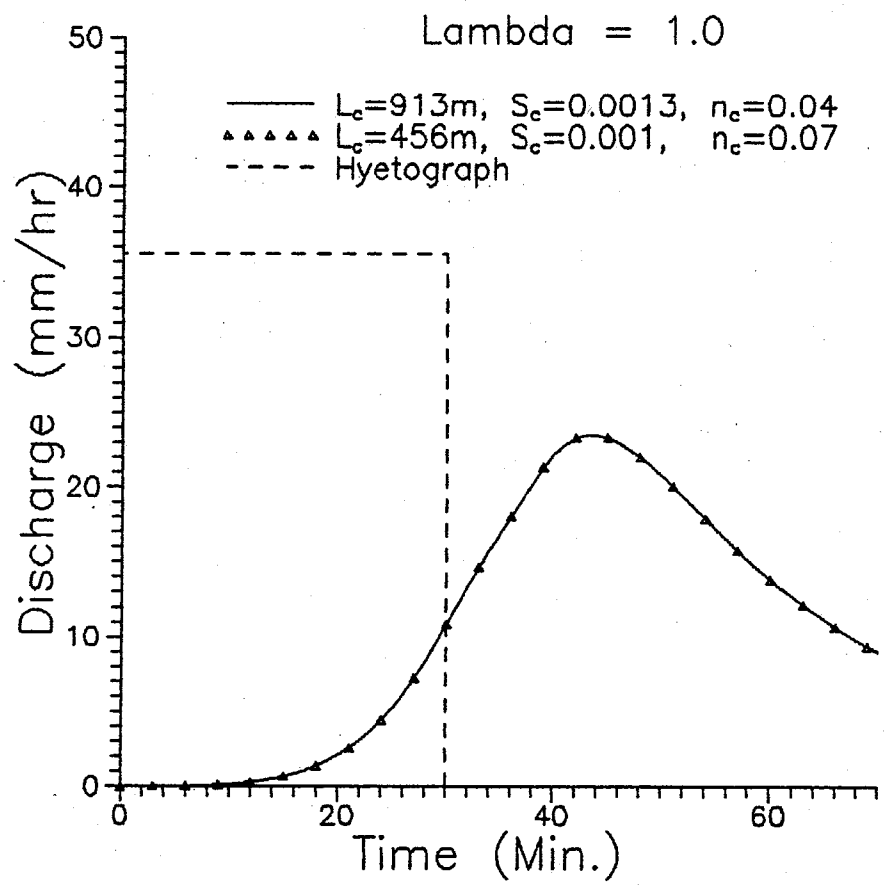

Figure 3.4. Hydrograph from Pulsed Input for Two Different Catchments with Equal Lambda

Table 3.1 Selected Plane and Channel Model Parameters

Case	Length of Plane (m)	S_p	n_p	t_e (min)	T_*	F_{p*}	Lambda
1-4	30.5	0.10	0.01	1.63	.345	0.0	0.0,0.5,1.0,1.5
5-8	152.4	0.005	0.05	27.67	.585	0.0	0.0,0.5,1.0,1.5
9-12	30.5	0.10	0.01	1.63	.0345	0.104	0.0,0.5,1.0,1.5
13-16	30.5	0.10	0.01	1.63	.0345	1.15	0.0,0.5,1.0,1.5
17-20	30.5	0.10	0.01	1.63	.0345	0.290	0.0,0.5,1.0,1.5
21-24	152.4	0.005	0.05	27.67	.585	0.104	0.0,0.5,1.0,1.5
25-28	152.4	0.005	0.05	27.67	.585	0.290	0.0,0.5,1.0,1.5
29-32	152.4	0.005	0.05	27.67	.585	1.15	0.0,0.5,1.0,1.5
33-36	152.4	0.005	0.05	27.67	.585	0.590	0.0,0.5,1.0,1.5
37-40	91.4	0.03	0.07	14.56	.308	0.0	0.0,0.5,1.0,1.5
41-44	91.4	0.03	0.07	14.56	.308	1.26	0.0,0.5,1.0,1.5
45-48	91.4	0.03	0.07	14.56	.308	0.574	0.0,0.5,1.0,1.5

Actual data for each of the 30 storms were input to KINEROSR. For each storm, the total runoff volume[1], peak flow rate, and time to peak were stored and used to formulate an empirical cumulative distribution function.

[1] Total runoff volume was computed as the accumulated runoff plus the remaining storage on the elements at the computed time to dryness on the plane.

When the actual storms were input, the total depth and duration for each was also stored and used as a basis for the following three types of precipitation disaggregation:

(1) Constant Intensity Precipitation (CP)

(2) Precipitation Intensity distributed as an isosceles triangle (TP)

(3) Woolhiser-Osborn (1985) disaggregation model (summer Walnut Gulch parameters (WO).

The WO disaggregation method requires a random seed to generate a sequence of rainfall intensity patterns given the sequence of storm depths and durations. For all cases in Table 3.1, the precipitation realization resulting from the arbitrary random seed of 100 was used. The random variability introduced by this disaggregation method is discussed in a later section.

3.5 Results

The distribution functions for peak rate at the extreme low end of the range of dimensionless plane response parameters (T_* and F_p*) for lambda equal to 0.0, 0.5, 1.0, and 1.5 are shown in Figure 3.5. This set of dimensionless parameters represents the most rapid plane response examined. As lambda is increased to 1.5, the channel length, slope, and roughness characteristics increase the equilibrium time of the channel. Although the peak rates are reduced by the increase in channel

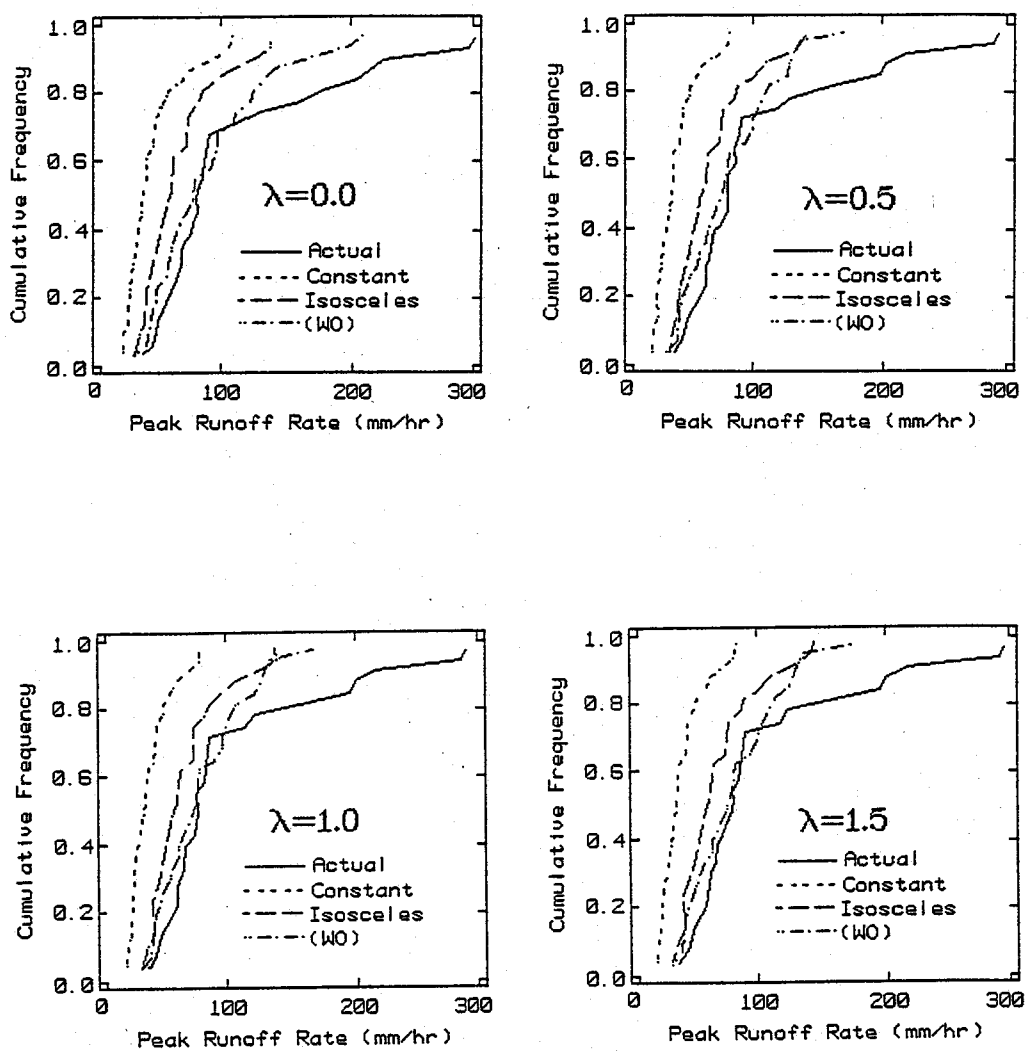

Figure 3.5. Empirical Distributions Functions of Peak Discharge for a 30.5m Impervious Plane (Cases 1-4, $T_* = 0.0345$, $F_{p*} = 0.0$)

equilibrium time, the relative difference between the distributions remains largely unchanged. Woolhiser and Osborn (1986) explained this by noting that the time resolution of the disaggregated and real storms is greater than the equilibrium time of both the plane (1.67 min.) and channel (2.50 min. @ lambda = 1.5). Therefore, the distributions shown in Figure 3.5 are essentially distributions of the peak rainfall rates. These figures show that the Woolhiser-Osborn disaggregation clearly does a better job of explaining the variability of the actual rainfall.

As the dimensionless parameters increase, indicating an increased damping effect, the superiority of the WO disaggregation method is no longer apparent. This is illustrated in Figures 3.6 through 3.8. Figure 3.6 presents the distributions of peak rates from a 91.4m plane with a dry silt loam soil. Figures 3.7 and 3.8 show the distributions resulting from 152.4m planes that are impervious and for planes with a dry sandy loam soil, respectively. For the 91.4m plane, the time to equilibrium is 14.6 minutes. This time is well beyond the time resolution of the storm set. This increase in plane equilibrium time and the resulting increase in T_* causes a pronounced collapse of the difference between the distributions.

Cases 45-48 illustrated in Figure 3.6 also incorporate infiltration. This adds to the collapse of the difference between the distributions. The difference between Figure 3.5 and Figure 3.7 illustrates the convergence of the distributions as a function of T_*. Woolhiser and Osborn (1986) pointed out that Hjelmfelt (1981) demonstrated how the distributions will converge as T_* increases for an impervious plane.

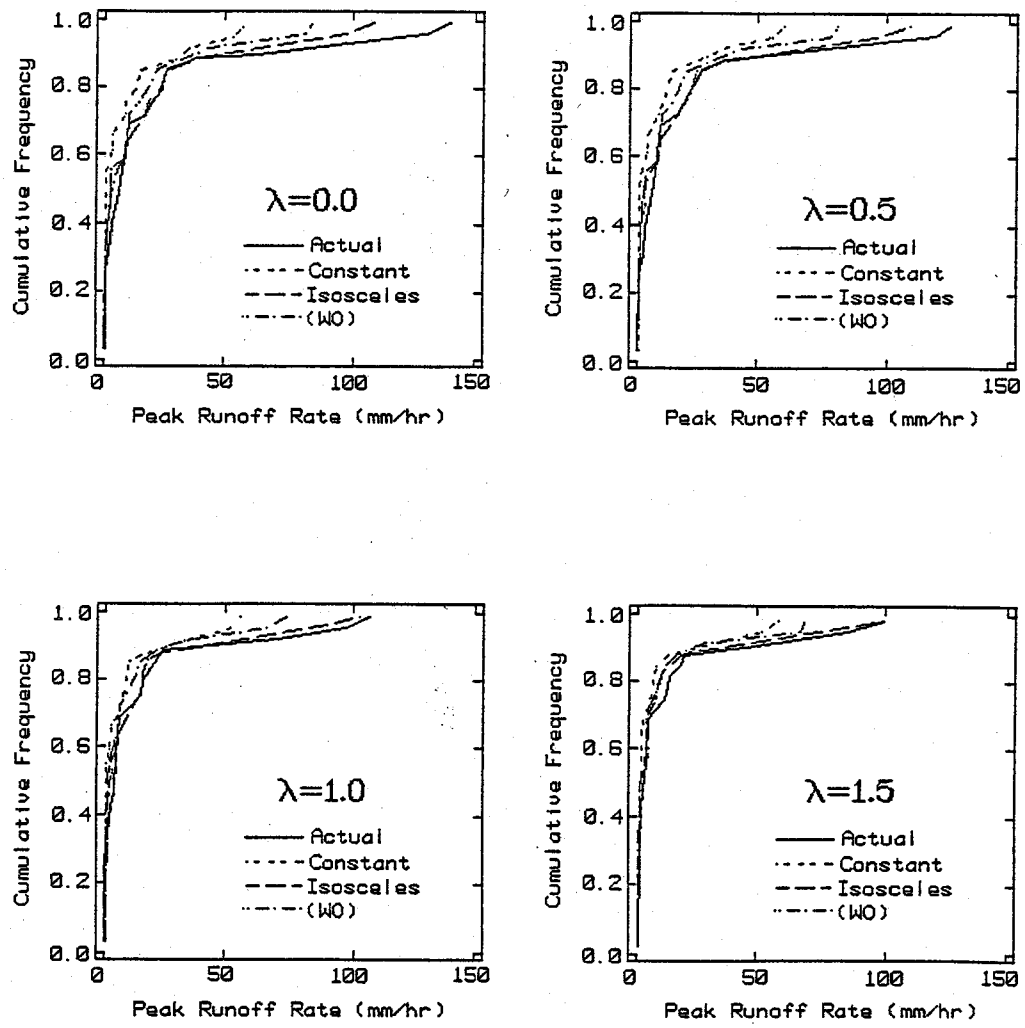

Figure 3.6. Empirical Distributions Functions of Peak Discharge for a 91.4m Infiltrating Plane (Cases 45-48, $T_* = 0.308$, $F_{p*} = 0.574$)

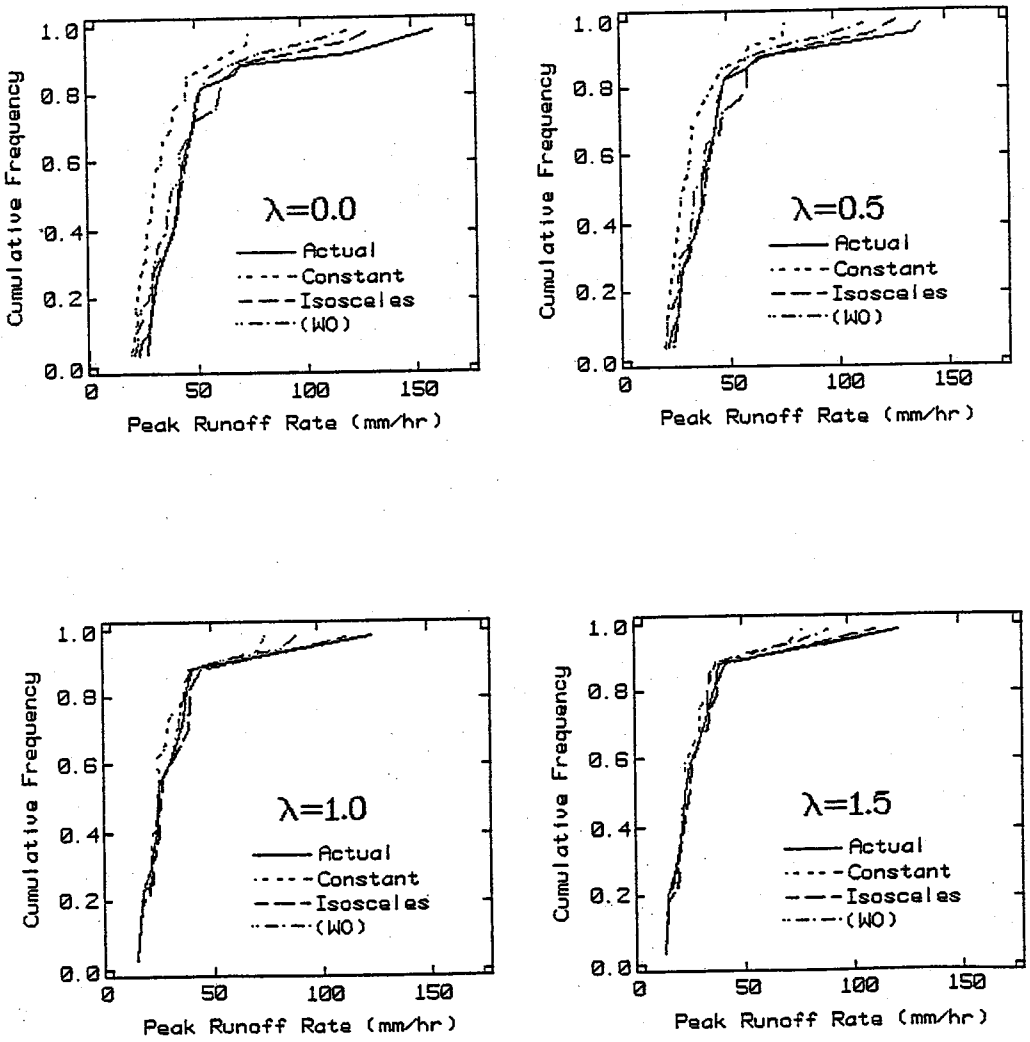

Figure 3.7. Empirical Distributions Functions of Peak Discharge for a 152.4m Impervious Plane (Cases 5-8, $T_* = 0.585$, $F_{p*} = 0.0$)

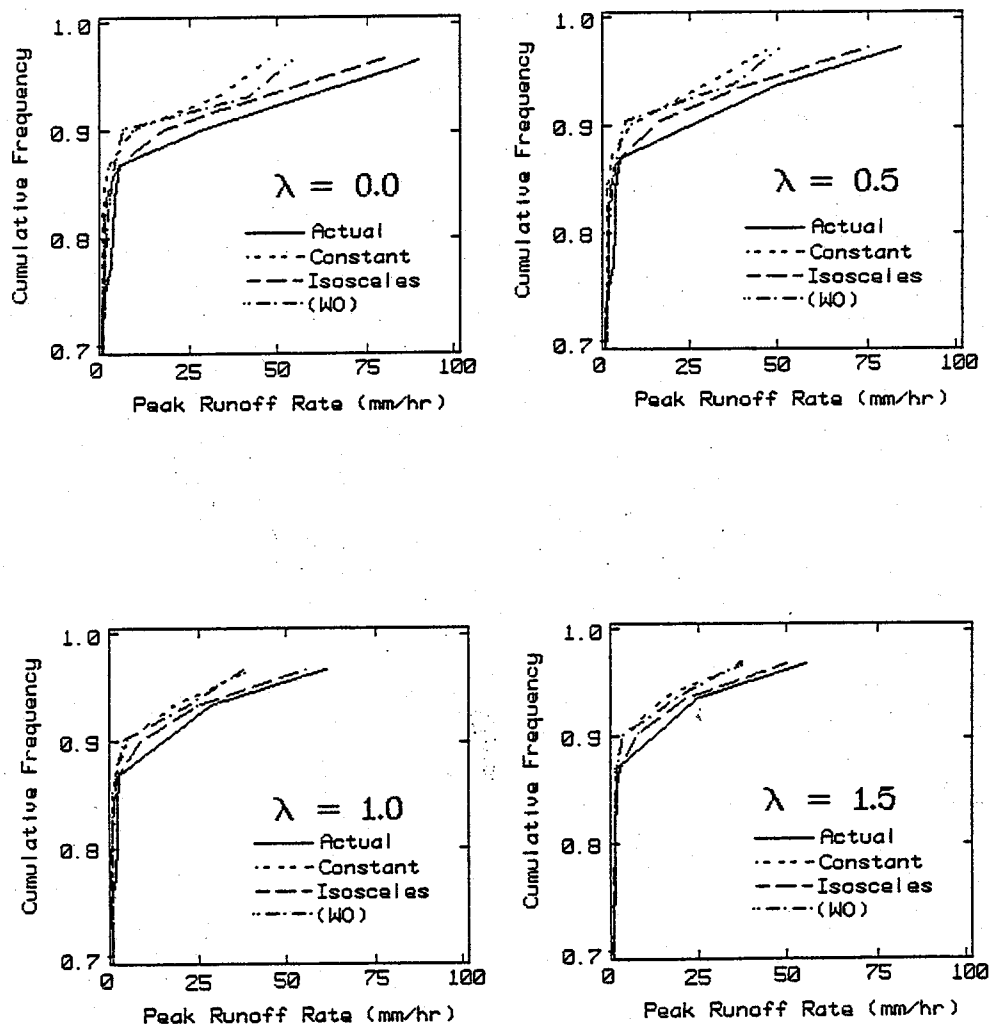

Figure 3.8. Empirical Distributions Functions of Peak Discharge for a 152.4m Infiltrating Plane (Cases 29-32, $T_* = 0.585$, $F_{p*} = 1.15$)

Figure 3.8 presents the upper extreme values of T_* and F_p* simulated in the study for the four levels of lambda. Note that with large F_p* (1.15), many of the 30 storms do not produce runoff; therefore, in Figure 3.8 the cumulative frequency range is 0.7 to 1.0. For the purposes of this study, an event was considered to produce zero runoff if the total runoff volume in depth over the basin was less then one half the measuring resolution of the raingages (0.15 mm).

In all cases, the increase of the channel effect (increasing lambda) causes a decrease in the peak rate and a general tightening of the distributions, as would be expected. In Figures 3.7 and 3.8, an apparent jump in the degree of distribution convergence occurs between lambda equal to 0.5 and lambda equal to 1.0. The effect is disproportionate to the relative changes observed in the transition of lambda from 0.0 to 0.5 and from 1.0 to 1.5. This "jump" is also apparent in Figure 3.9a. This illustration contains the outflow hydrographs for each level of lambda. These hydrographs result from the largest of the 30 storms with the same catchment used to generate the distributions shown in Figure 3.8. The disproportionate change in runoff rate for the transition of lambda from 0.5 to 1.0 agrees with the observations by Wooding (1965a). He concluded that a fundamental difference in catchment response occurs when lambda is above or below 0.5. By passing through lambda equal to 0.5, a transition in dominance of overland flow on the planes to a dominance of channel flow may be indicated. The transition does not appear to be present in all cases, as shown in Figure 3.9b. In this case, the largest storm was applied to 91.4m impervious plane. Even though the "jump" in peak rates is not

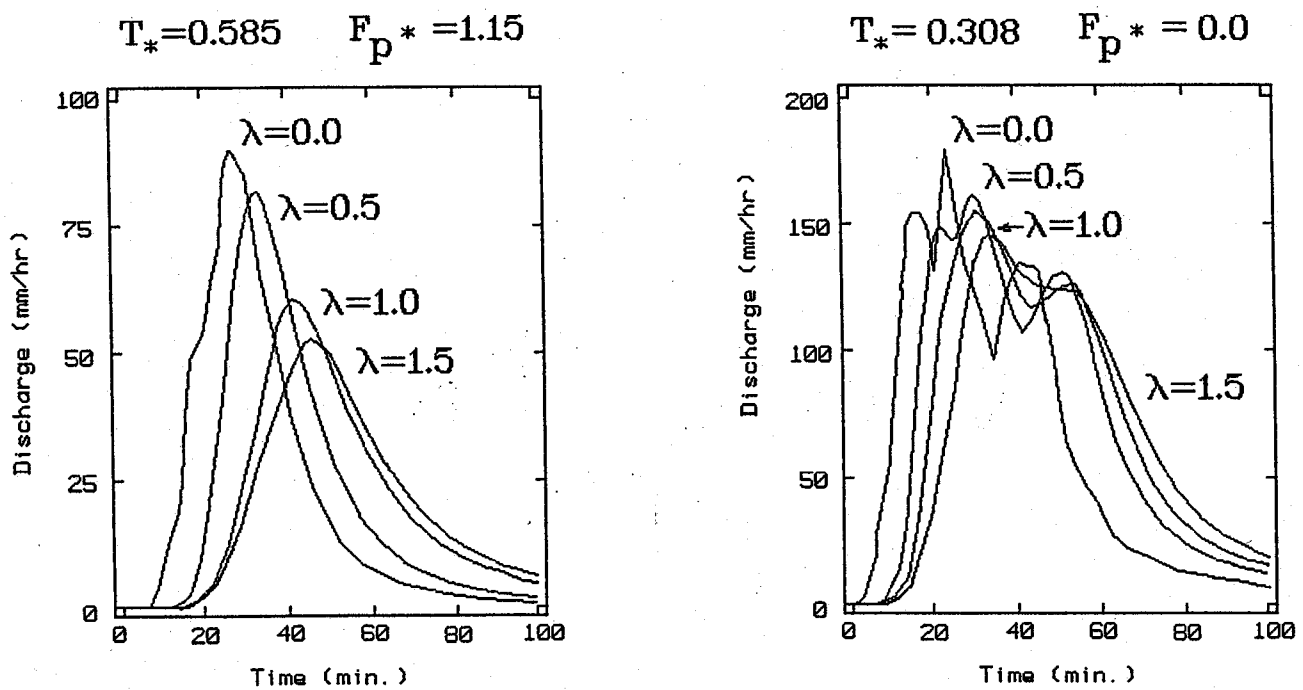

Figure 3.9. (a) Largest Storm Hyetograph and Resulting Hydrographs for All Lambda with 152.4m Infiltrating Planes ($T_* = 0.585, F_{p*} = 1.15$);

(b) Largest Storm Hyetograph and Resulting Hydrographs for All Lambda with 90.4m Impervious Planes ($T_* = 0.308, F_{p*} = 0.0$)

apparent, closer examination reveals a much greater degree of smoothing in the transition of lambda from 0.5 to 1.0.

In an attempt to quantify the effect of changes in the three dimensionless parameters on the derived peak flow distributions, the Kolomogorov-Smirnov (K-S) D* statistic was computed for each of the simulation cases:

$$D* = \max [\, | F(\tilde{q}_p) - F_i(q_p) | \,]; \quad i = 1,2,3 \qquad (3.12)$$

where:

$F(\tilde{q}_p)$ = the Cumulative empirical distribution of peak runoff rate from actual rainfall data

$F_i(q_p)$ = the Cumulative empirical distribution of peak runoff rate from the three disaggregated storms.

In a strict statistical sense, D* cannot be used to test hypotheses concerning these empirical distributions. It was selected for this study as a convenient measure for relative comparison of the various derived distributions. Statements made concerning hypothesis acceptance or rejection and critical levels are made only to give a feel for possible differentiation of the distributions. A problem in interpretation of D* also arises when a large number of zero events occur because of infiltration (large F_p*). Cursory examination of the literature did not reveal possible solutions to this

problem. Its impact on the sample size and statistical interpretations was not studied.

Contour plots of D* versus T_* and F_p* for each level of lambda for the constant disaggregation scheme are presented in Figures 3.10a-d. Similar plots for the TP and WO methods (Summer Walnut Gulch) are presented, respectively, in Figures 3.11a-d and 3.12a-d. For a two-sample K-S test, the null hypothesis that the peak flow distributions from the disaggregated storms came from the same population as the one obtained from the actual storm cannot be rejected for a significance level of $\alpha = 0.1$ (Type I error) if D* is less than 0.22 for a sample size of 30. Using this level as a guideline, we see that constant intensity (CP) disaggregation does not produce peak flow distributions similar to those obtained from the actual storms for any level of T_*, F_p*, and lambda used in the study. The increase in lambda from Figure 3.10a-d has little apparent effect in lowering the level of D*. For the TP disaggregation (Figures 3.11a-d) a large region of the T_*, F_p* space will pass the null hypothesis stated above. As with the CP disaggregation plots, this sequence of plots demonstrate a minor decrease of the D* level as lambda is increased.

The reduced sensitivity of D* to increases in T_* is apparent in this sequence of plots (Fig. 3.11a-d). This implies that the TP method does a better job of representing the time variability of the actual data. This effect is even more pronounced in the sequence of plots for the WO method (Figures 3.12a-d). The D* values fall below the critical level for nearly the entire T_*, F_p* region in this sequence

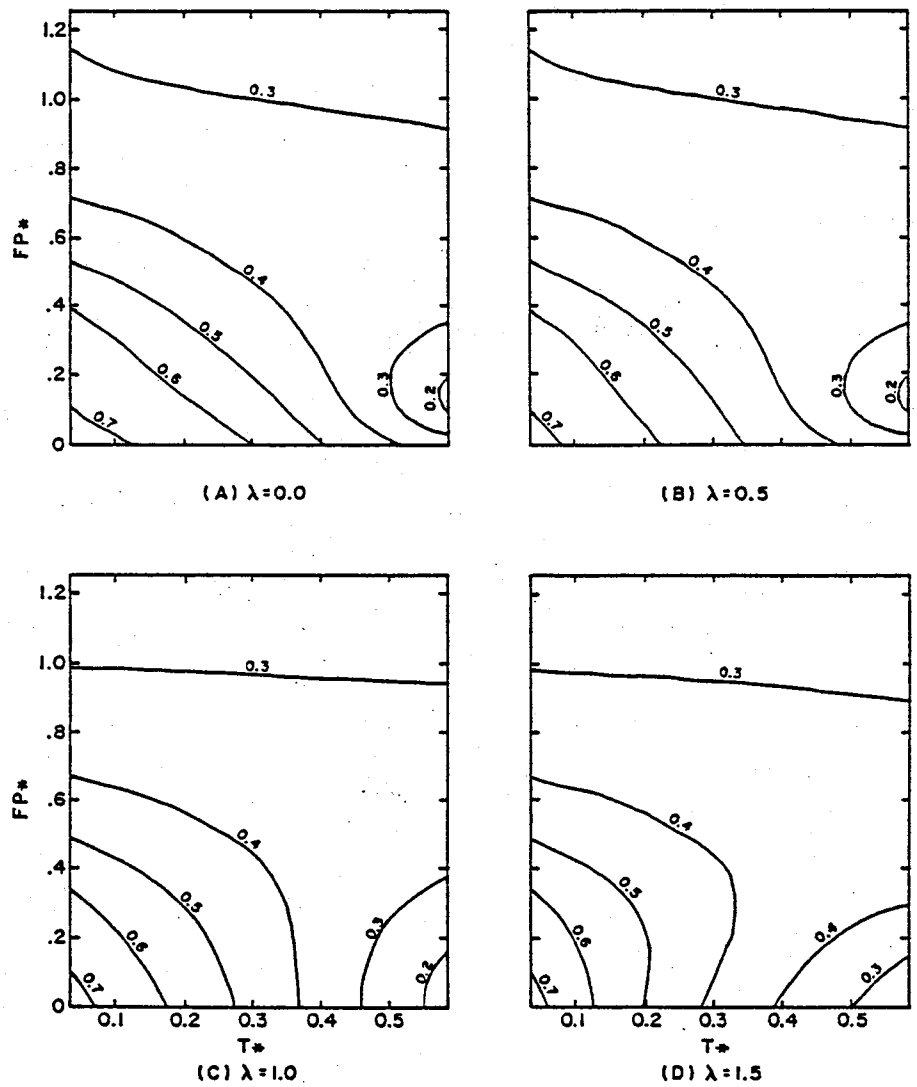

Figure 3.10 (a-d) K-S D* Contour Plots for = 0, 0.5, 1.0, 1.5 Using Constant Storm Disaggregation

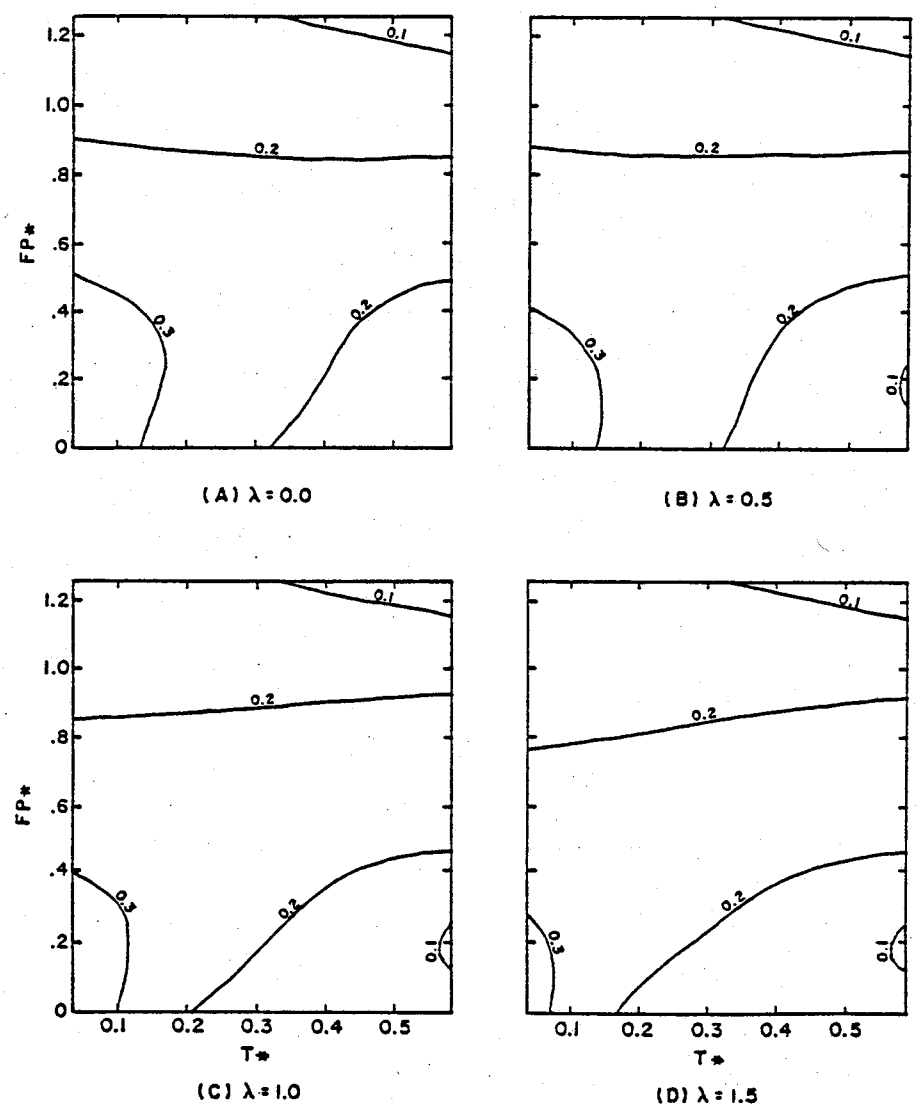

Figure 3.11 (a-d) K-S D* Contour Plots for = 0, 0.5, 1.0, 1.5 Using Isosceles Storm Disaggregation

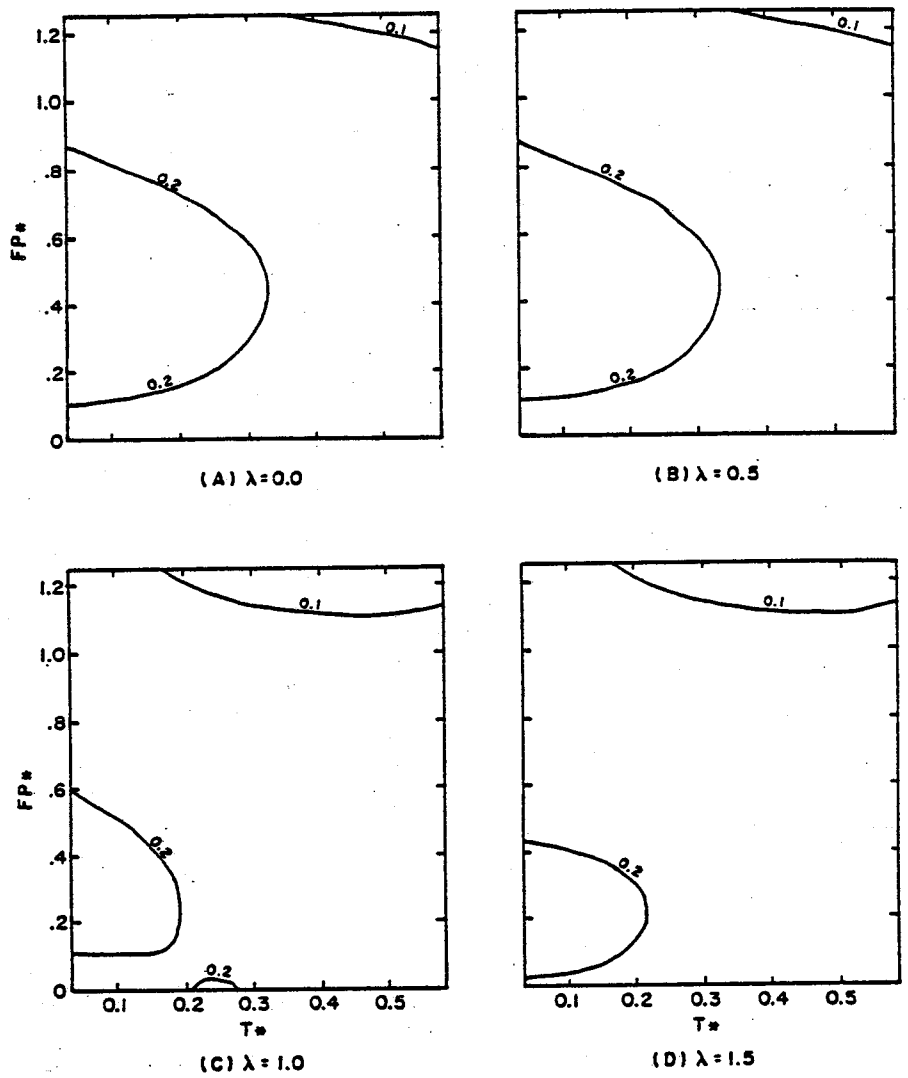

Figure 3.12 (a-d) K-S D* Contour Plots for = 0, 0.5, 1.0, 1.5 Using Woolhiser-Osborn Storm Disaggregation

of plots. As before, only minor reduction of D* through the T_*, F_p* region is observed as lambda is increased. Closer examination of the TP and WO plots reveals a visible "jump" in the reduction of D* when the transition of lambda from 0.5 to 1.0 takes place. This correlates well with the observations related to Figures 3.7-3.9.

In the Woolhiser-Osborn method (Summer W.G.) sequence of plots (Figures 3.12a-d), an increased level of D* is observed as F_p* increases from zero to approximately 0.5. This effect appears to be counter intuitive as one would expect a decrease in D* as damping is induced by increased infiltration. As mentioned earlier, this sequence of plots ultimately resulted from a single realization of storms generated by the WO disaggregation method.

If this realization of storms had peak rainfall intensities biased late in time versus those of the actual storms, the above effect could be explained. For a moderate initial infiltration rate, the early low intensities of the storm would infiltrate and wet the soil, decreasing soil sorptivity, while producing little or no runoff. When the high intensities in the latter portion of the storm hit the catchment, a relatively large peak rate would result because the infiltration rate would be greatly reduced from the earlier storm rainfall. At very high F_p* (> 0.5), enough damping may be induced by infiltration such that the storm timing no longer affects D*, thus lowering the level of this statistic. To verify this effect, D* contour plots would have to be produced for other disaggregated storm realizations.

Increasing the channel effect appears to have little effect on the level of D* for peak flow rate distribution. This is, of course, a function of the measure D* selected for the study. Visual examination of the distribution plots for increasing lambda (Figures 3.6-3.8) indicates a more pronounced effect as lambda is increased. Further inspection reveals that the maximum difference between the cumulative distributions (D*) is often obtained at very low peak runoff rates. In this region, the cumulative frequency is rapidly rising and the distributions are nearly parallel. If extreme events were of interest and storms producing lower peak rates were excluded from the analysis, a greater sensitivity of D* to lambda may result.

The discussion to this point has been concerned with the distributions of peak rate. Relative rankings of the three disaggregation methods using the D* statistic were also made based on the time to peak distributions, the total runoff volume distributions, and reproduction of the number of nonzero events. Compilation of the rankings was carried out. The rankings indicate that the WO disaggregation method is always equal to or better than the other methods for replicating the number of nonzero events. For the peak rate distributions, the WO method is superior except for cases of moderate infiltration (F_p* from 0.1 to 0.3) and large T_*. For the time to peak distributions, the WO method is almost always the best of the three. For the peak volume distributions, the isosceles method is superior in moderate ranges of infiltration and the 30.5 and 152.4m overland flow plane cases.

Study of the summary statistics also reveals a decrease of the range of means and standard deviations between the distributions as lambda is increased for a given

plane geometry. Scatter plots of simulated peak flow rate versus simulated total runoff volume using observed storm breakpoint data also illustrate the impacts of plane, infiltration, and channel changes.

The impacts of changes in plane geometry are shown in Figure 3.13a-c as T_* increases for 30.5, 91.4, and 152.4m impervious planes. Levels of lambda equal to 0.0 and 1.5 are shown on the plot. The highly dispersed points in Figure 3.13a for $T_* = 0.0345$ and $F_p^* = 0.0$ indicate very sharply peaked hydrographs. These hydrographs closely reflect the highly variable nature of the rainfall intensities as little or no damping takes place for this case. When T_* is increased (Figure 13b and 13c), the correlation between total volume and peak rate improves. When the channel effect is strengthened by increasing lambda, the correlation is further improved.

Figures 3.14a-c illustrate the effect of increasing infiltration for a constant T_* at lambda equal to 0.0 and 1.5. The increase in F_p^* has a much more pronounced effect on reducing the volume versus peak rate variability then does an increase in T_*. For the catchment scale studied, this demonstrates the importance of explicitly incorporating physically-based infiltration models unless only large floods are considered. The results of many studies that only consider excess precipitation may no longer be valid if interactive infiltration is incorporated.

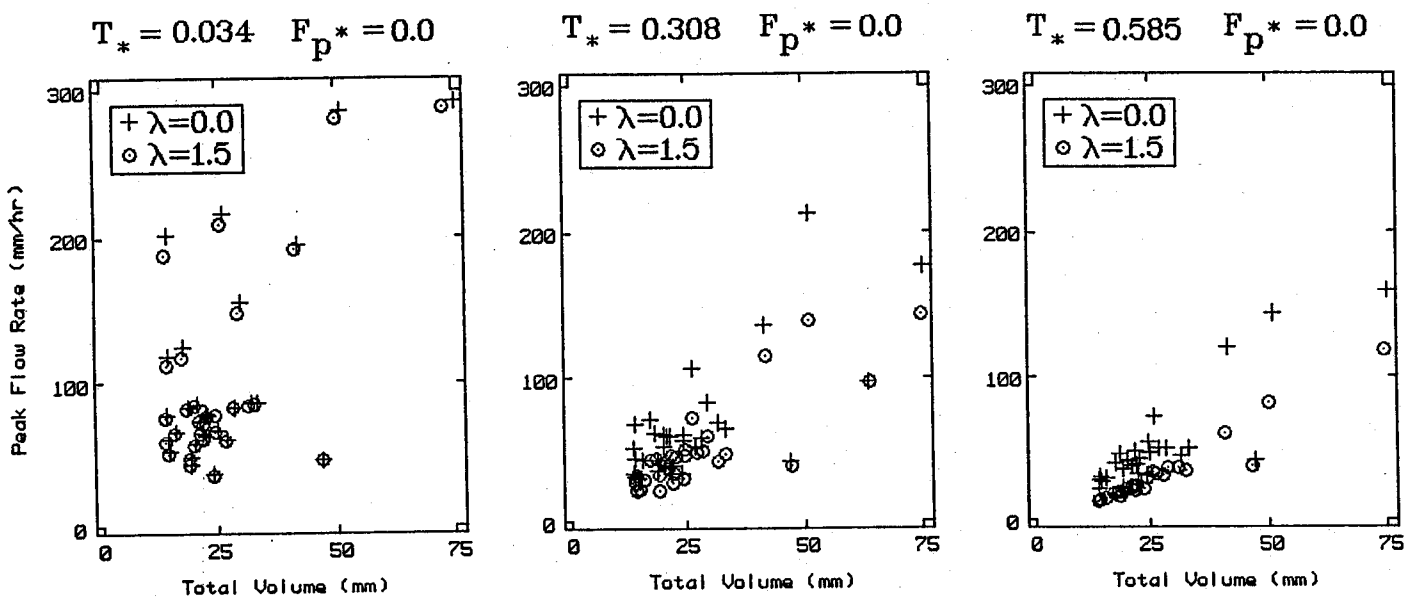

Figure 3.13 (a-c) Scatter Plots of Runoff Volume Versus Peak Rate for Fixed F_{p*} and Increasing T_*.

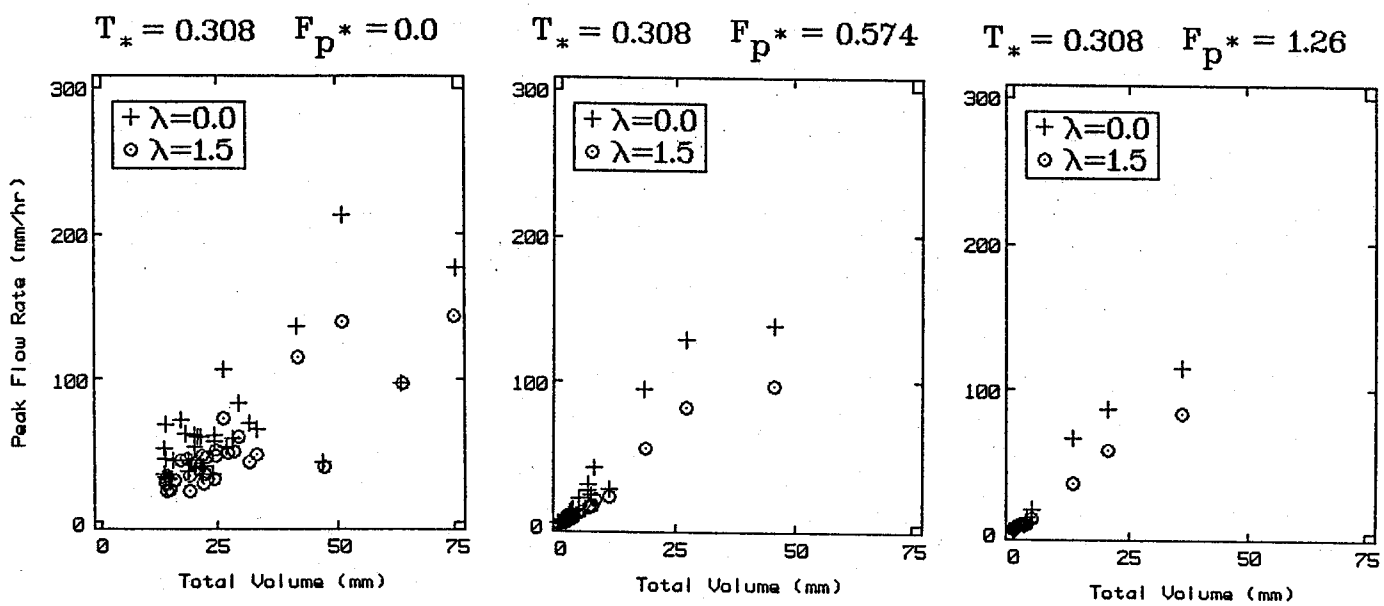

Figure 3.14 (a-c) Scatter Plots of Runoff Volume Versus Peak Rate for Fixed T_* and Increasing F_p*.

3.6 Random Storm Variation in the Woolhiser-Osborn Disaggregation Method

The Woolhiser-Osborn (WO) method of storm disaggregation requires a random seed to generate a storm intensity realization. A random seed of 100 was used for the (WO) disaggregation for all of the simulation cases listed in Table 1. This section investigates how the results of those simulations are affected by random variation.

Case 4 ($T_* = 0.0345$, $F_p^* = 0.0$, and lambda = 1.5) and case 8 ($T_* = 0.585$, $F_p^* = 0.0$, and lambda = 1.5) were selected for the random variability analysis. For each of the two cases, the actual storm amounts and durations were disaggregated by the WO method using ten different random seeds. The empirical peak rate distribution was formed for each realization, and basic statistics for each of the distribution realizations were compiled.

Plots of all ten peak rate distribution realizations for each of the two cases are shown in Figures 3.15a and 3.15c. Histograms for the sample containing all ten realizations (n = 300) are presented in Figures 3.15b and 3.15d. The distributions shown in Figure 3.15a vary highly when the peak rate exceeds five inches per hour. Because of the short response time ($T_* = 0.0345$), these distributions actually represent rainfall intensity pattern variations. The largest peak rate for each of the realizations ranges from 6.45 to 26.6 inches per hour. The high peak rate is unrealistic, and an upper limit should be placed on this (Woolhiser, 1988, personal communication). The histogram shows that the high positive skew of 3.68 and the

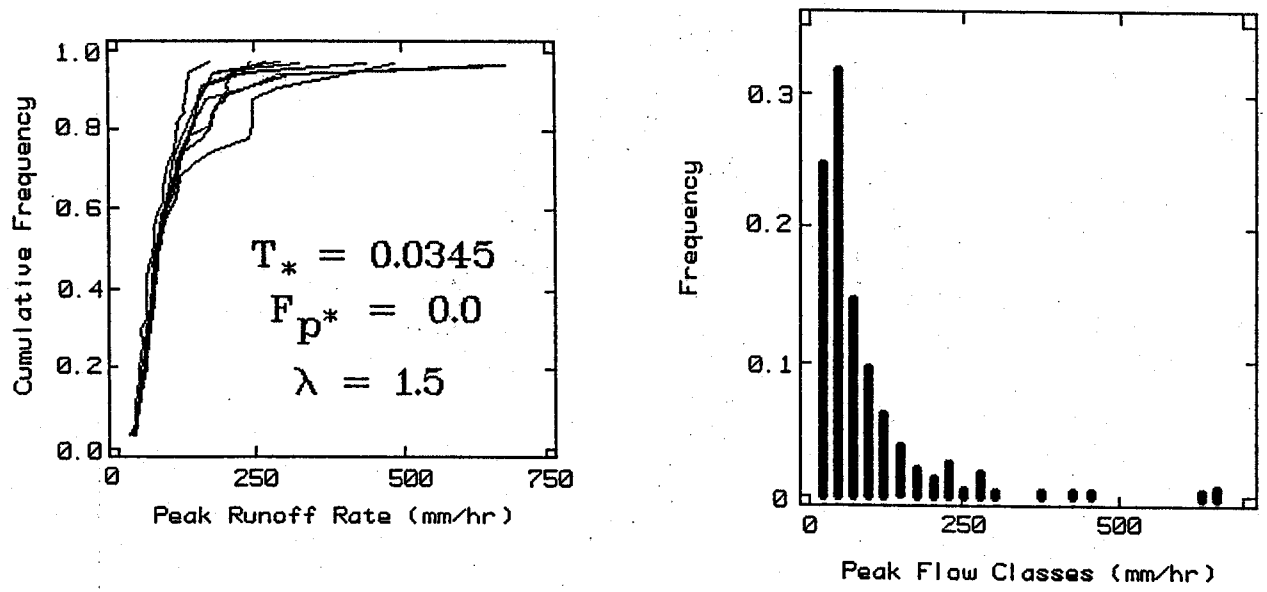

Figure 3.15 (a) Ten Realizations of Empirical Distribution Functions of Peak Rate for a Fast Responding Catchment ($T_* = 0.0345$).

(b) Histogram for All Ten Realizations of Empirical Distribution Functions of Peak Rate for a Fast Responding Catchment ($T_* = 0.0345$).

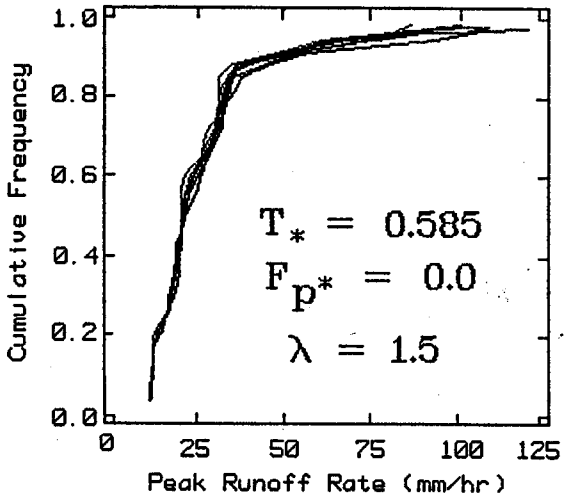

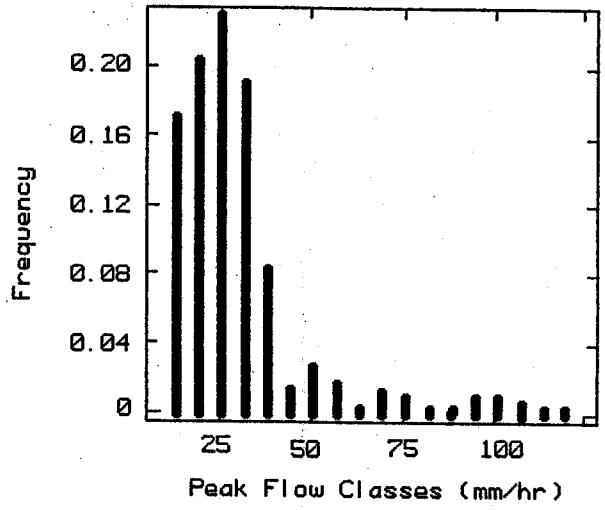

Figure 3.15 (c) Ten Realizations of Empirical Distribution Functions of Peak Rate for a Slowly Responding Catchment ($T_* = 0.585$).

(d) Histogram for All Ten Realizations of Empirical Distribution Functions of Peak Rate for a Slowly Responding Catchment ($T_* = 0.585$).

coefficient of variation of the lumped sample of 300 is 89%. In the second case where $T_* = 0.585$, the peak rates and the overall variability is greatly reduced. The skew of the lumped sample of all the distribution realizations is reduced to 2.53, and the coefficient of variation is reduced to 70%.

Ultimately, the impact of this random variation on the results stated earlier for a single realization is desired. To assess this impact, the D* statistic was computed for each of the distribution realizations. For the fast response case in Figure 3.15a, the computed D* values ranged from 0.133 to 0.267, with a mean and standard deviation of 0.173 and 0.041, respectively. For the slower responding case in Figure 3.15c, the computed D* values ranged from 0.100 to 0.133 with a mean and standard deviation of 0.101 and 0.016. For the realization used in the overall study, with a random seed of 100, the D* for the fast- and slow-responding cases was 0.167 and 0.100, respectively. In the mean, for the small number of realizations tested, it appears as if the conclusions reached earlier would not have been significantly affected by random variation in the disaggregation scheme. A greater degree of truth is wrought into this statement as the damping effect of the catchment increases by increasing the dimensionless parameters. The small effect on D* for even the fastest responding catchments may result from the fact that the maximum difference in the distributions (D*) is typically found in a range of low peak rates.

3.7 Conclusions

The following conclusions can be reasonably drawn from this portion of the study:

(1) As a measure of channel effects on catchment response, lambda adequately embodies the influence of channel slope, length, and roughness.

(2) Increases in the channel effect decrease the differences in empirical distribution functions of peak flow rate for catchment response times that are greater than the time resolution of precipitation intensities.

(3) For lambda < 0.5, overland flow plane characteristics have a greater influence on catchment response. For lambda ≥ 0.5, channel characteristics have a greater influence.

(4) For cases where $F_p^* > 0.4$, $T_* > 0.1$, and lambda > 1.5, the isosceles disaggregation scheme will perform as well as the Woolhiser-Osborn scheme.

(5) Random variation of the Woolhiser-Osborn disaggregation scheme imparted a negligible effect on the computed K-S D* statistic for empirical peak rate distribution functions.

(6) The range for which channel effects were studied does not significantly decrease K-S D*.

(7) For the ranges of dimensionless parameters examined, changes in T_* and F_p^* have a much more pronounced effect in decreasing the difference between empirical and actual peak flow distributions than do changes in lambda (channel effects). This indicates persistent dominance of overland flow on catchment response even for lambda > 0.5.

(8) Infiltration characteristics appear to play a more important role in catchment response than an increase in overland catchment response time (increasing T_*).

The final three conclusions (6-8) highlight the persistent dominance of infiltration and overland flow processes for the various cases of the elementary watersheds examined. In the semi-arid Southwest, at basin and hillslope scales that are even smaller than the open-book geometries considered here, significant rilling and flow concentration takes place. Yet in many models, very good results are obtained by using a sheet flow representation. In other words, the flow concentration processes are incorporated into the overland flow plane without discernible degradation in model accuracy. This is often accomplished by way of optimized adjustments of the hydraulic roughness parameters. Instead of an optimized adjustment which requires the subjective selection of an objective function, is there a systematic procedure to incorporate channel flow within an equivalent overland

flow plane? This topic will be explored in the following chapter. In this manner, the central hypothesis concerning the level of channel representation (geometric complexity) required to model the overall rainfall to runoff transformation can be addressed.

CHAPTER 4

A METHOD FOR GEOMETRIC MODEL SIMPLIFICATION

4.1 Introduction

The primary objective of this chapter is the development and testing of an objective, reproducible, procedure to simplify a complex geometric watershed representation into a simpler one. The important relationship between geometric model complexity and map scale was alluded to earlier. The stream network on a map is typically used to delineate overland flow and channel model elements. This implies a fundamental distinction between the subprocesses of overland and channel flow. The primary distinction between the two is due to the modelers' perceived reality of the watershed as interpreted through the map. The channel network derived from the map is, of course, a function of the map scale. Figure 4.1 illustrates this point. Although it is a schematic diagram, the correlation of decreasing drainage density with decreasing map scale is readily apparent on actual maps. Maps covering the Lucky Hills subwatersheds of Walnut Gulch at three different map scales clearly show this trend.

The relationship of decreasing drainage density with decreasing map scale is shown in Figure 4.1. This relationship is typically apparent on both contour and planimetric maps. Avoidance of the drainage density/map scale relationship cannot be accomplished by using stream networks generated from Digital Elevation Models (DEM) data. The geometric model delineation between channel and overland flow must be made if stream networks are derived from DEM data. Theoretically,

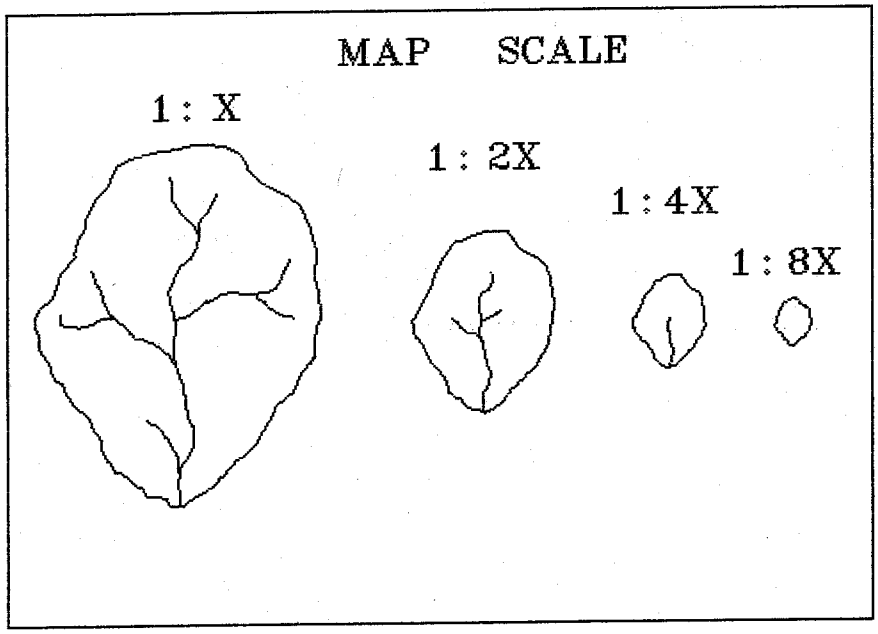

Figure 4.1. Basin Representation as a Function of Map Scale

network generation algorithms can define first-order channels all the way to the watershed boundary or ridge (to within the DEM data resolution). To avoid this case, an a priori definition of the support area at the head of a first-order channel must be made. This effectively fixes a drainage density and again partitions overland flow and channel processes.

Map scale impacts on design flood procedures used in Australia were noted by Pilgrim (1986), and scale-related equations were proposed to make adjustments. Geomorphologists have long noted the dependence of channel head locations on map scale. Kirkby (1988) emphasized this point by stating "there is no unambiguous method for determining the exact position of channel heads. . . A satisfactory hillslope hydrological model must, therefore, be insensitive to the exact density of channels chosen." If a generalized, drainage density insensitive, hillslope model cannot be defined, the range of scales over which the model is applicable should be quantified.

Even at extremely small length scales, flow concentration occurs. The commonly used kinematic overland flow equations, where a sheet flow analogy is assumed, do not explicitly treat flow concentration. However, if the relationship between discharge (flux) and depth (storage per unit area) used in kinematic equations is viewed in a statistical sense, this model implicitly treats flow concentration. Rills or areas of flow concentration with greater runoff depth are less impacted by microtopographic roughness. Therefore, effective roughness in these areas is smaller. The sheet flow approximation has been experimentally verified

(Bell et al., 1989; Wheater et al., 1989) and works very well up to a certain point (length scale). Beyond this scale, the sheet flow approximation with an effective roughness breaks down, and channel flow must be treated directly.

4.1.1 Channel and Overland Contributing Area Representation of Watershed

Consider a given base map covering the watershed of interest with a fixed contour interval and scale. The map may have a channel network as drawn by the map maker or one may be derived from contours or DEM data. With this information, the basic delineation between overland flow planes and channels is derived. A large-scale base map of the Lucky Hills 106 (LH-106) watershed and the basin subdivision into planes and channels is shown in Figure 4.2. The segmentation of the basin into channels and overland flow areas is accomplished by tracing the flow paths from heads of channel and channel junctions to internal basin divides or the watershed boundary. Cascades of overland flow areas may be introduced if there is a significant difference in slope, soil type, or land use (roughness).

The first step in deriving the overland flow planes from the basin contributing area segmentation (shown on the right in Figure 4.2) is to measure their area. A mean flow length for each overland segment is also measured. This length becomes the length of the overland flow plane. By dividing the area by the flow length, the width of the plane is obtained. During the flow length digitization, the slope of the flow element is also determined using Gray's method (1961). In his method, the plane slope is the slope of the hypotenuse of the right triangle that has the same base

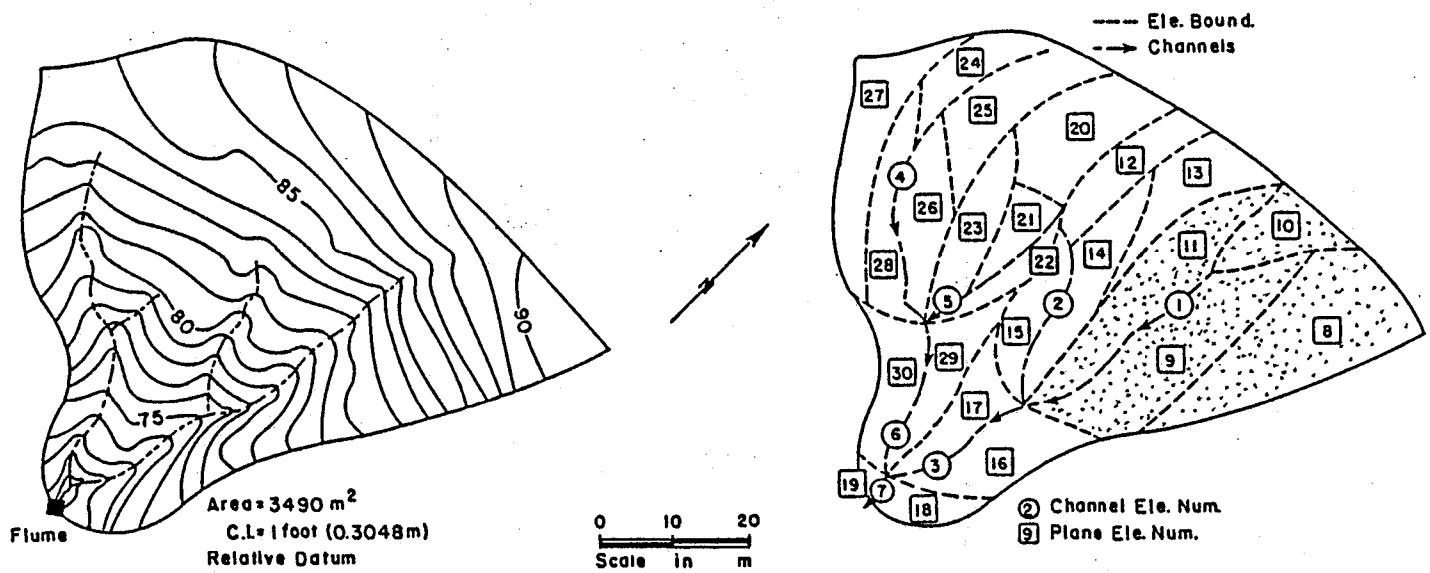

Figure 4.2. Lucky Hills-106 Watershed: Base Map and Basin Segmentation

length and area as the area under the overland flow profile. Channel slope and length are obtained in the same manner. For this study, trapezoidal channel geometry was measured in the field. Hydraulic roughness estimates were also field estimated, and soil samples were obtained to determine textural properties.

Consider the first-order watershed of LH-106 with channel number 1 and contributing planes 8, 9, 10, and 11 (shaded region in Figure 4.2). The basis for this segmentation hinges on the map including the first-order channel (#1). What would happen if the base map for LH-106 was a smaller scale such as the 1:2X map in Figure 4.1, where the first-order channels are no longer apparent? In this case, channel 1 and its four contributing planes could be represented as a single plane contributing to the head of channel 3 (see Figure 4.2). Scale-related interpretations of the elementary watershed for a different base map are diagrammed in Figure 4.3a.

4.1.2 Evidence to Support a Simplified Slope Representation

If the simple single plane from the smaller scale base map is used, several implicit modeling assumptions are made. In the simple system, no channel or concentrated flow processes are implied. For this case an overland sheet flow analogy for the entire area is assumed. A greater degree of spatial averaging of soils, geometric and hydraulic parameters will also result by using the simple system. For example, in using the complex model depiction, the continuous distribution of topographic slope is approximated by four plane slopes and a channel slope. When using the simple model, the slope distribution is approximated by a probability mass

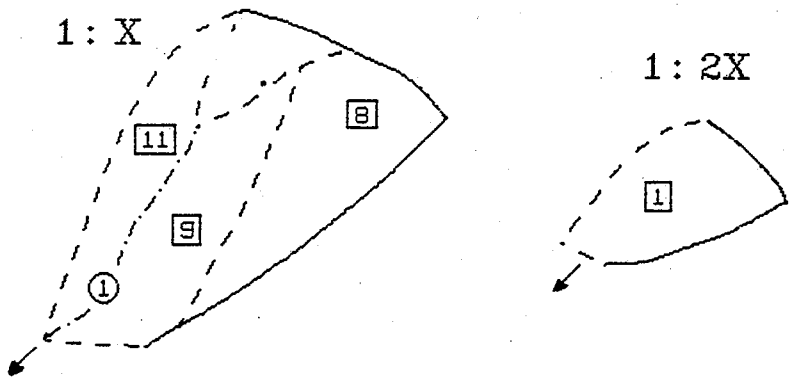

(a) Elementary Watershed Base Map Representation.

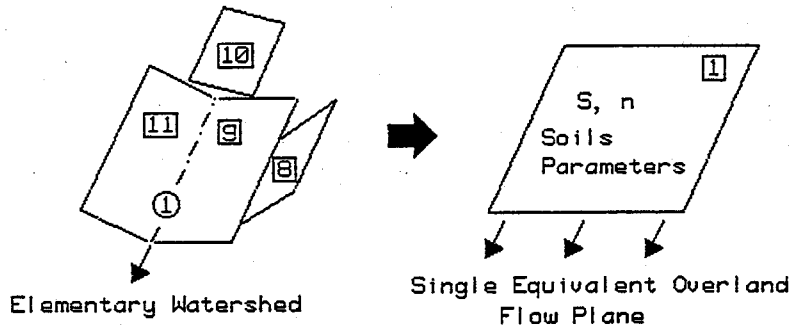

(b) Model Representation.

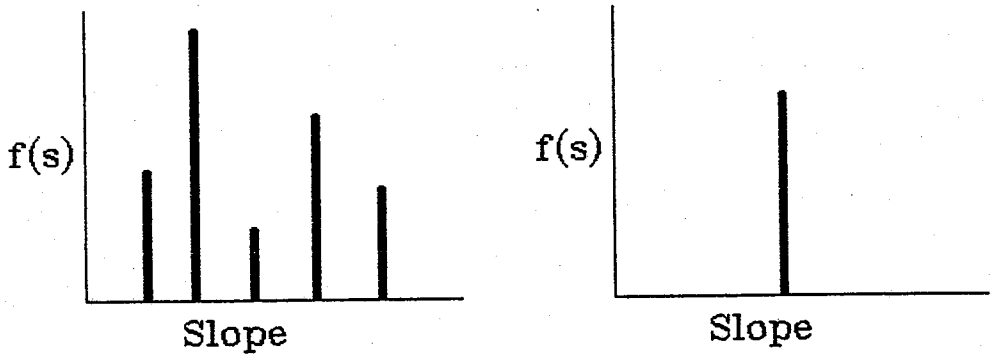

(c) Model Slope Distribution.

Figure 4.3. Model Representation as a Function of Map Scale

of one, associated with a single slope as assigned to the individual flow plane as shown in Figure 4.3.

Collapsing the slope distribution by using a geometrically simpler model may not greatly impact modeling results, as long as the essential features of the distribution are captured. Slope distributions derived from 30 X 30 meter DEM data for Walnut Gulch for all of its major subwatersheds display surprisingly similar features over a large range of basin scales. Empirical slope density functions are presented in Figure 4.4 for three of the Walnut Gulch watersheds covering a large range of scales. A persistent trimodal distribution with peaks at roughly 2, 5, and 7 percent slope is apparent for the watersheds used in Figure 4.4 as well as all of the primary Walnut Gulch watersheds. Although the frequency at each mode varies, the distribution shapes are remarkably similar. If the discrete slope distribution of the simplified geometric model approximates the trimodal distributions in Figure 4.4, much of the essential topographic character of the watershed may be captured.

4.2 Rules for Geometric Model Simplification

It is postulated that, as the map scale is incrementally reduced, or analogously, the viewing point is moved farther away from the watershed, the basin channel order will decrease incrementally. In other words, the first-order channels are no longer observed at the smaller map scale; therefore, what were elementary watersheds are now represented by single overland flow planes. If the map scale is reduced another

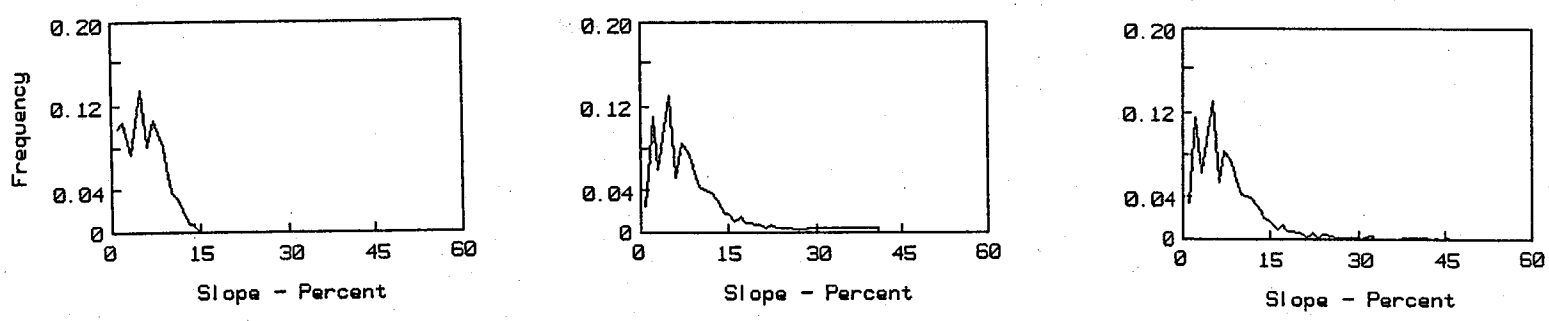

Subwatershed 4:

Area = 2.28 km^2

Subwatershed 6:

Area = 95.1 km^2

Walnut Gulch

Area = 149 km^2

Figure 4.4. Slope Distributions as a Function of Basin Scale

increment, the second-order channels on the original base map are essentially clipped off, further reducing drainage density and model complexity.

As the drainage density is reduced, channels or model areas of flow concentration are replaced by overland flow model elements. The model replacement of channel by overland flow elements can theoretically continue until the entire basin is modeled as a single overland flow plane. In doing so, the topographic distortion and misrepresentation of channel flow may have significant impacts on rainfall-runoff modeling results. The degree of allowable geometric model simplification, measured in terms of some specified level of model simulation error, is hypothesized to be a function of basin scale (Hypothesis 1, Chapter 1). In a small watershed, aggregation of model elements to sizes greater than hundreds of meters is likely to cause significant model impacts. In a very large watershed, aggregation (or geometric model simplification) on this scale will likely cause minor impacts. Investigation of this hypothesis is a central theme of this study.

Starting with a complex basin representation and simplifying the model structure by successively replacing first-order watersheds with overland flow planes has several advantages. As the geometric complexity is reduced, it is possible to measure the decrease in model performance and relate this loss to the increase in averaging resulting from simplification. To systematically assess changes in model performance during simplification, objective, reproducible rules are required.

Consider the model representation of the first-order watershed and its relationship to model representation of the same area at a smaller map scale. At

this scale, the model depicts the area as a single overland flow plane (Figure 4.3). Each model representation (complex and simple) attempts to simulate the same rainfall-runoff process. To establish rules for geometric watershed simplification, an attempt is made to maintain model equivalence between these two watershed representations. Thus, given the hydraulic, soil, and geometric parameters for the distributed complex case, comparable parameters must be derived for the simple uniform single plane representation. The rules used in this study to obtain these parameters are as follows:

1. Maintain subwatershed area
2. Maintain the mean overland flow length
3. Compute slope and soil parameters using area weighted averages
4. Maintain a characteristic response time by requiring the equilibrium storage from uniform rainfall to be equal on both the complex and simple system.

Using Rules 1 and 2, the width (W) and length (L) of the equivalent single plane are determined. To maintain the mean overland flow length (L), the following relation is used:

$$L = \frac{AR}{L_c} \tag{4.1}$$

where:

AR = area of the elementary watershed

L_c = length of the channel being replaced

With the length of the plane defined, the width (W) is simply found by dividing the area by the flow length (L). The slope (S) and the soil-related parameters of the single equivalent plane are defined by using the complex element (including the channel) area weighted averages of the comparable parameters. The research version of KINEROSR was modified to explicitly treat rainfall on channels. The area of the channel is defined as (L_c * BW), where BW is the trapezoidal channel bottom width. This is the area over which rainfall is counted in volume balance computations. Channel infiltration is assumed to occur over the trapezoidal wetted perimeter. These modifications allow channel area and channel attributes to be properly accounted for in the model simplification (aggregation) process. This is especially critical in basins with large sandy channels. The only remaining parameter to be defined for the equivalent plane is the hydraulic roughness (Manning's "n"). The roughness of the simple (single plane) case is adjusted to maintain the same equilibrium storage obtained on the complex (multiplane and channel) case. The

concept of equilibrium storage, its use in adjusting roughness, and its importance is explained more fully in the next section.

4.3 The Importance of Equilibrium Storage

4.3.1 Background

Watershed storage plays a significant role in the transformation of rainfall to runoff. Equilibrium storage is defined as volume of water stored on the surface of an impervious watershed under spatially and temporally uniform rainfall when kinematic equilibrium is achieved. Changes in storage primarily impact the time to peak and the peak runoff rate. On an infiltrating basin, runoff volume can also be affected as infiltration opportunity times are increased. Lane et al. (1975) noted that storage represents the overall system performance at equilibrium. Zaghloul (1981; 1983) stressed the importance of maintaining storage between complex and simple watershed representations.

Wu et al. (1978) were the first to use the notion of maintaining equilibrium storage to establish an equivalence between a complex and uniform runoff system. In their work, the complex system consisted of a surface or watershed with spatially variable roughness. Equivalent uniform roughness was computed so that equilibrium storage was maintained on the complex and simple systems. In applications to outdoor laboratory and natural catchments, they found that the simple system with the equivalent uniform roughness reproduced runoff response very well.

Wu et al.'s (1978) approach was used to produce a uniform equivalent roughness from a spatially variable case, but was not used in geometric simplification as is the case in this study. During geometric simplification, regions of flow concentration are replaced by an equivalent overland flow area. The equivalence is defined by the geometric rules above and by distortion of the roughness to preserve equilibrium storage. The interpretation of roughness distortion in this investigation follows the ideas of the computational roughness actually being a statistical average as discussed above. As more and more concentrated flow is incorporated or simplified into a single plane, the mean roughness will typically decrease.

The equilibrium storage is a very efficient measure of basin response behavior. The storage integrates the effects of slope, flow convergence, and spatially distributed hydraulic roughness. Using equilibrium storage, a characteristic time (T_{ch}) of the basin can be objectively defined as:

$$T_{ch} = \frac{ST_{eq} / AR}{q} \tag{4.2}$$

where:

ST_{eq} = equilibrium storage

AR = basin area

q = uniform rainfall rate

The characteristic time defined above is superior to a typical basin time to equilibrium for gauging catchment response behavior. It can be computed in a straightforward manner from a specified basin geometry. The time to equilibrium is often very difficult to objectively define due to its sensitive dependence on numerical procedures. Theoretically, the time to equilibrium is infinite, and Golany and Larson (1971) had to define a time to virtual equilibrium to avoid these problems. Calculation of a time to equilibrium in all but extremely small natural watersheds is very difficult using actual events because of the nonuniformity of rainfall in both time and space.

4.3.2 Storage Computations and Determination of Equivalent Roughness

The storage at kinematic equilibrium is computed for a unit width overland flow plane as follows. First recall the kinematic equations for overland flow (Equation 2.1). In Equation (2.1), let $r_i(t)$ equal q as defined in Equation (4.2) and for an impervious case ($f_i(x,t) = 0$), the following ordinary differential characteristic equations can be derived:

$$\frac{dx}{dt} = \alpha m h^{m-1} \tag{4.3}$$

$$\frac{dh}{dt} = q \tag{4.4}$$

By dividing Equation (4.4) by Equation (4.3), a relation between the flow depth and distance down the plane is obtained:

$$\frac{dh}{dx} = \frac{q}{\alpha m h^{m-1}} \tag{4.5}$$

For steady but nonuniform flow with a zero depth upper boundary condition, Equation (4.5) is integrated to define h as a function of x:

$$h(x) = \left(\frac{qx}{\alpha}\right)^{1/m} \tag{4.6}$$

The volumetric storage per unit width is found by integrating Equation (4.6) for the length of the plane:

$$ST_{eq} = \int_o^L \left(\frac{qx}{\alpha}\right)^{1/m} dx = \frac{m}{m+1}\left(\frac{q}{\alpha}\right)^{1/m} L^{(m+1)/m} \tag{4.7}$$

The equilibrium storage can be equivalently expressed as the mean depth of the flow strip by dividing Equation (4.7) by L. For simple geometry, such as the overland flow plane used above, the storage can be easily computed. For more complex geometries involving branching channel and trapezoidal channel geometry, simple analytical solutions cannot be obtained. The storage for such complex cases can be easily computed numerically, and KINEROSR has been modified to do so.

Using aggregation rules 1-3 with the given complex elementary watershed and its associated parameters, all of the parameters for the single equivalent plane can be determined with the exception of the hydraulic roughness. To solve for the roughness, the complex impervious basin is driven to equilibrium with rainfall rate q and its storage (ST_{eq}) is saved. Equation (4.7) can then be solved for the roughness n if $(1.49\ S^{1/2})/n$ is substituted for α:

$$n = \frac{1.49\sqrt{S}}{q}\left[\frac{m+1}{m}\right]^{m}\left[\frac{ST_{eq}}{W}\right]^{m}\left[\frac{1}{L}\right]^{m+1} \tag{4.8}$$

where W, L, and S for the equivalent plane are obtained from rules 1-3. Thus, all of the parameters for the equivalent plane have been defined in a repeatable and objective manner. With the equivalent parameters defined, the question of runoff response equivalence between the simple and complex model representation can be addressed. The assessment of equivalence is presented in Section 4.4. Before doing

so, the relationship between the basin characteristic time and the kinematic time to equilibrium on an overland flow plane is examined in the following section. This section is presented to further illustrate the generality of the equivalence rules.

4.3.3 The Basin Characteristic and Kinematic Equilibrium Time Relationship

The time to kinematic equilibrium is defined as the time required for the characteristic originating from the top of the plane (x = 0) to reach the end of the plane (x = L) with constant lateral inflow q. By integrating Equation (4.3) the time to kinematic equilibrium (T_{eq}) is obtained:

$$T_{eq} = \left[\frac{L}{\alpha q^{m-1}}\right]^{1/m} \tag{4.9}$$

Due to the nonlinear dependence of both the characteristic and kinematic equilibrium time on the rainfall rate q, it was anticipated that the equivalence relationships would have to be established over a range of rainfall rates. However, if the characteristic and kinematic equilibrium times are related, the rainfall rate cancels out of the relationship. To demonstrate this, consider the dimensionless form of the kinematic overland flow equation (Equation 2.1). The dimensionless form is obtained by making the following substitutions:

$$x' = x/L, \quad h' = h/h_{eq}, \quad t' = t/t_{eq}, \quad q' = q/q_o \tag{4.10}$$

where:

h_{eq} = Equilibrium depth at x = L

q_o = Equilibrium discharge per unit area at x = L

x',h',t',q' = dimensionless distance, depth, time, and rainfall rate, respectively.

When these substitutions are made, with uniform rainfall, the depth-discharge coefficient α, the scaled time to equilibrium T_{eq}, the scaled length L, and the scaled rainfall rate all equal unity. If these values are substituted into Equations (4.2) and (4.7), the characteristic basin time and the equilibrium storage become:

$$T_{ch} = ST_{eq} = \frac{m}{m+1} \tag{4.11}$$

because the scaled area/unit width is also equal to one. Assume that the time to kinematic equilibrium and the characteristic basin response time are related as follows:

$$T_{eq} = C\ T_{ch} \tag{4.12}$$

For the dimensionless equations, $T_{eq} = 1$ and $T_{ch} = m/(m+1)$. Therefore, C must equal $(m+1)/m$ resulting in:

$$T_{eq} = \frac{m+1}{m} T_{ch} \tag{4.13}$$

The importance of Equation (4.13) cannot be overemphasized. Because the relationship is independent of the rainfall rate, a greater degree of generality for application can be expected. Unlike the procedure presented above, the geometric simplification schemes of Lyngfelt's (1985) and Zaghloul (1981; 1983) are dependent on rainfall intensity. This presented both investigators with the need for further optimization using the simplified model geometry and thus results in a loss of generality for their methodologies.

To numerically verify the independence of the T_{eq}-T_{ch} relationship and to test the numerical estimation of storage by KINEROSR, an elementary watershed and its equivalent single plane were considered. The watershed consisted of four planes, two in a cascade, feeding the head and sides of a channel. The parameters of the equivalent plane were computed using the rules described above for a uniform rainfall rate of 12.7 mm/hr. Then rainfall rates of 25.4 and 50.8 mm/hr were used to drive the elementary watershed to equilibrium and obtain an equilibrium storage. For this example, the Chezy roughness relations were used where $\alpha = C/S$ and the depth-discharge exponent $m = 3/2$. The roughness for the equivalent plane was then

computed using Equation (4.8). The results of the tests are shown in Table 4.1. The results illustrate that the T_{eq}-T_{ch} relationship is virtually invariant with changing uniform rainfall rate, and storage computations in KINEROSR are carried out with sufficient accuracy.

The results shown in Table 4.1 are very encouraging, but additional testing of the simplification (aggregation) methodology over a larger range of conditions is required. The material discussed in the next section summarizes these tests.

4.4 Testing of the Simplification Procedure

To assess the behavior of the aggregated system, rainfall runoff simulations were conducted on both the complex and aggregated models. Simple uniform rainfall patterns were used to drive an impervious basin to equilibrium and partial equilibrium. Additional simulations employed a measured rainfall event as input for both an impervious and infiltrating condition. The five-element case and its equivalent single plane used in the simulations in Table 4.1 were used for these tests. Hydrographs for the complex and simple watershed representation for the cases outlined above are shown in Figures 4.5 through 4.8.

The runoff response is preserved very well for all but the partial equilibrium case (Figure 4.6). The removal of the channel and the delay it induces result in a flat-topped hydrograph for this case. However, the numerical simulation for the single plane compares favorably to the analytic solution. The flat-topped response of the partial equilibrium case may present problems in the simplification process

Table 4.1 Equivalent Roughness Values for Various Rainfall Rates

q (mm/hr)	T_{ch} (min)	T_{eq} (min)	α	c	Percent Difference
12.7	7.28	12.14	3.960	13.199	..
25.4	5.79	9.64	3.952	13.173	0.20
50.8	4.60	7.69	3.942	13.139	0.46

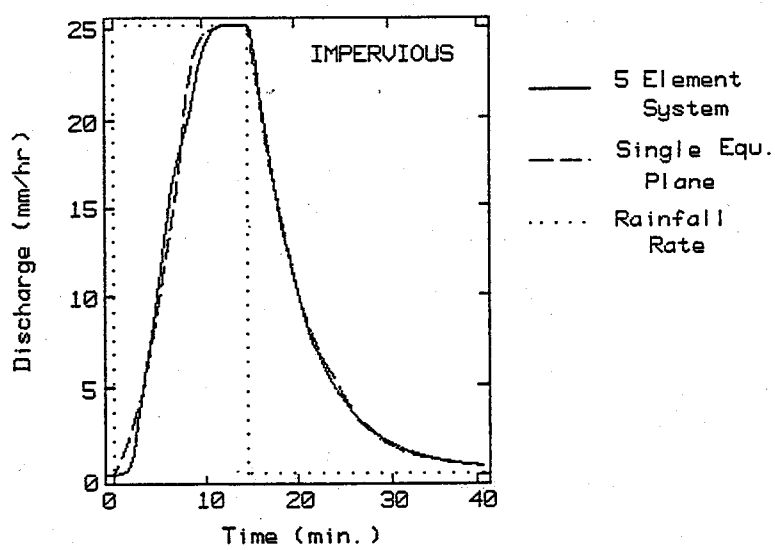

Figure 4.5. Five Element Versus Single Equivalent Plane: Equilibrium Simulation

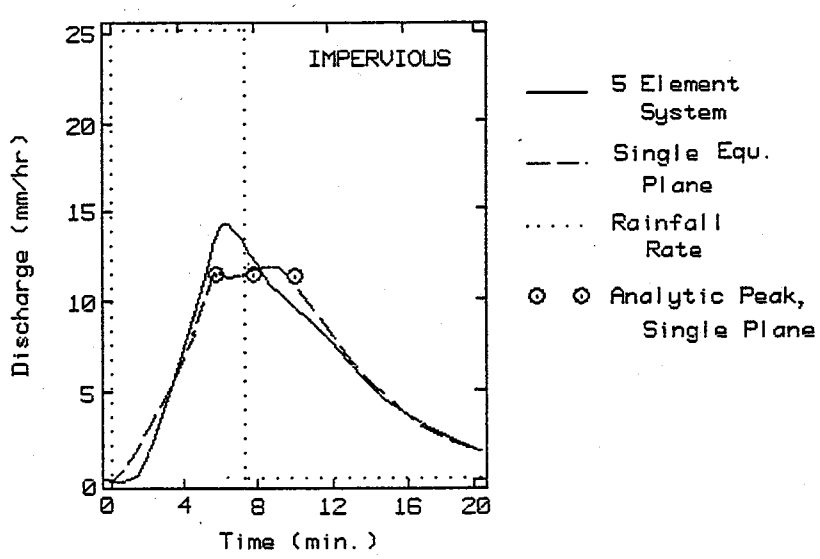

Figure 4.6. Five Element Versus Single Equivalent Plane: Partial Equilibrium Simulation

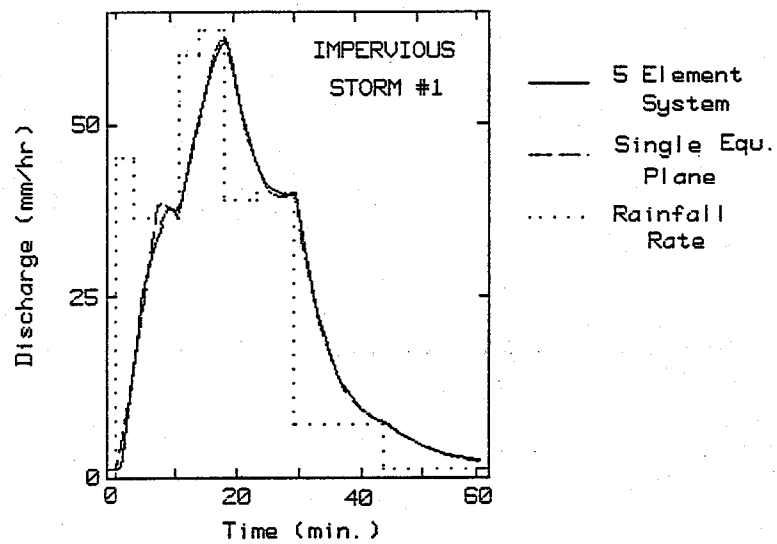

Figure 4.7. Five Element Versus Single Equivalent Plane: Measured Rainfall Event (Impervious)

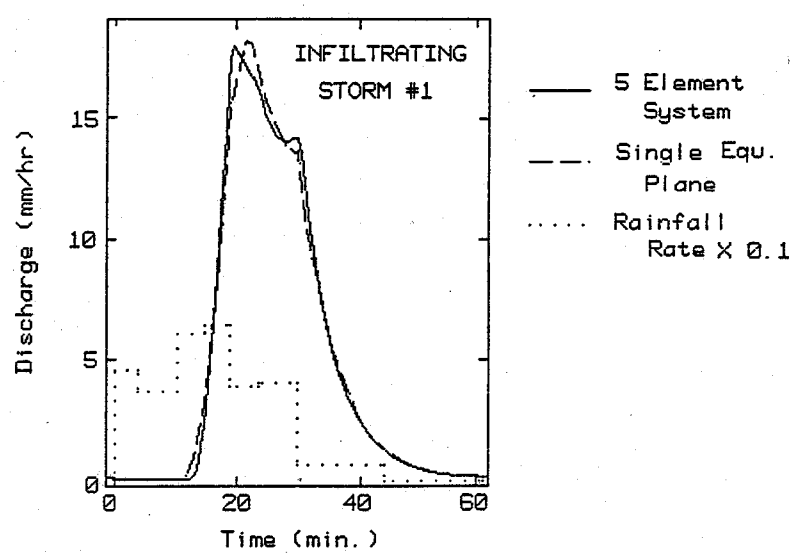

Figure 4.8. Five Element Versus Single Equivalent Plane: Measured Rainfall Event (Infiltrating)

when an entire watershed is replaced by a single equivalent plane. However, will significant make differences at the outlet of a much larger watershed where only the first-order watersheds are replaced by planes? The partial equilibrium problem in the process of simplification is further mitigated when infiltration is introduced as shown in Figure 4.9.

The examples above compare an elementary watershed model representation to its single equivalent overland flow plane. To evaluate the simplification procedure in a watershed situation where higher order channels exist, the Lucky Hills-106 (LH-106) basin shown in Figure 4.2 is used. The results presented below are an elaboration of the work initially presented by Goodrich et al. (1988). For this study, assumed spatially uniform rainfall rates were obtained from a raingage roughly 180 m from the centroid of the watershed. In Chapter 2, the importance of storm size was demonstrated. Therefore, small, medium, and large storms were selected. Rainfall event information is shown in Table 4.2. More information about the watershed and field estimation of model parameters is presented in Appendix A. For the simulations presented in this chapter, Ks values were estimated from textural classes of Rawls et al. (1982). Because the purpose of the present evaluation is assessment of simplification, none of the field estimated parameters were adjusted in an attempt to match observed runoff measurements.

Using the simplification rules, aggregation of channel and overland flow elements is performed by sequentially clipping off the lowest order channels and their contributing planes and replacing them with single equivalent planes. At each level,

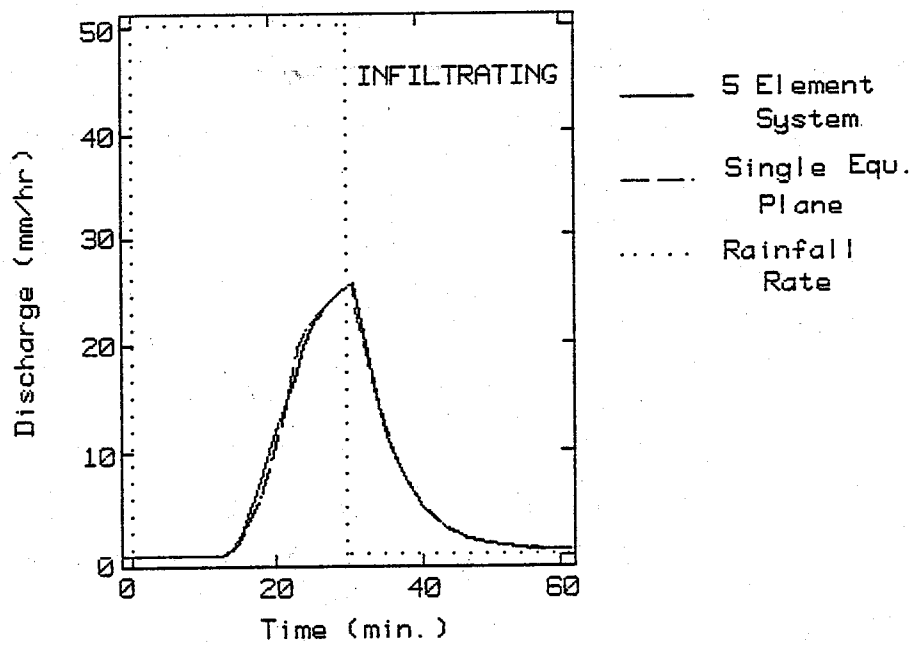

Figure 4.9. Five Element Versus Single Equivalent Plane: Partial Equilibrium Simulation (Infiltrating)

Table 4.2. Storm Characteristics for Test Events

Event	Date	Duration (min)	Total Depth (mm)	Peak Int. (mm/hr)	Weighted Mean Int. (mm/hr)	Return Period (years)*	Relative Size
1	8/10/71	64	27.4	133.4	25.7	~2.8	Large
2	8/31/66	133	16.5	50.8	7.0	<1.0	Small
3	8/23/82	96	30.7	68.6	19.2	~2.0	Medium

* Osborn and Renard (1988)

a simpler system is obtained until the entire watershed is replaced by a single equivalent overland flow plane. LH-106 is a very small watershed and would only be a portion of a single flow plane for the model representation of much larger basins containing LH-106. In reference to the map scale analogy discussed at the beginning of the chapter, on 7 1/2 minute, 1:24,000 scale USGS topographic maps, there are no channels shown in LH-106.

Four successive levels of aggregation of the Lucky Hills 106 watershed are schematically diagrammed in Figure 4.10. For each level of aggregation, simulations with the three rainfall events listed in Table 4.2 were conducted with and without infiltration variability (C_v = 0.0 and C_v = 0.8; see Chapter 2). Peak runoff rates and runoff volumes from the simulations at each level of aggregation were compared to the most complex watershed model representation (30 elements). The results, as well as VAX 11/750 CPU simulation times, are summarized in Table 4.3 and are graphically presented in Figure 4.11.

Table 4.3 illustrates that, for the largest of the three storms (event 1), the impacts of simplification are minor through the entire range of aggregation from 30 to 1 element. This storm appears to be large enough to overwhelm the variability of both the distributed infiltration and geometric model parameters in the complex 30 element system. In other words, the storm, not the basin, controls the runoff dynamics. When the storm is the dominant factor, extensive aggregation can be accomplished. The importance of storm characteristics in the Lucky Hills watersheds

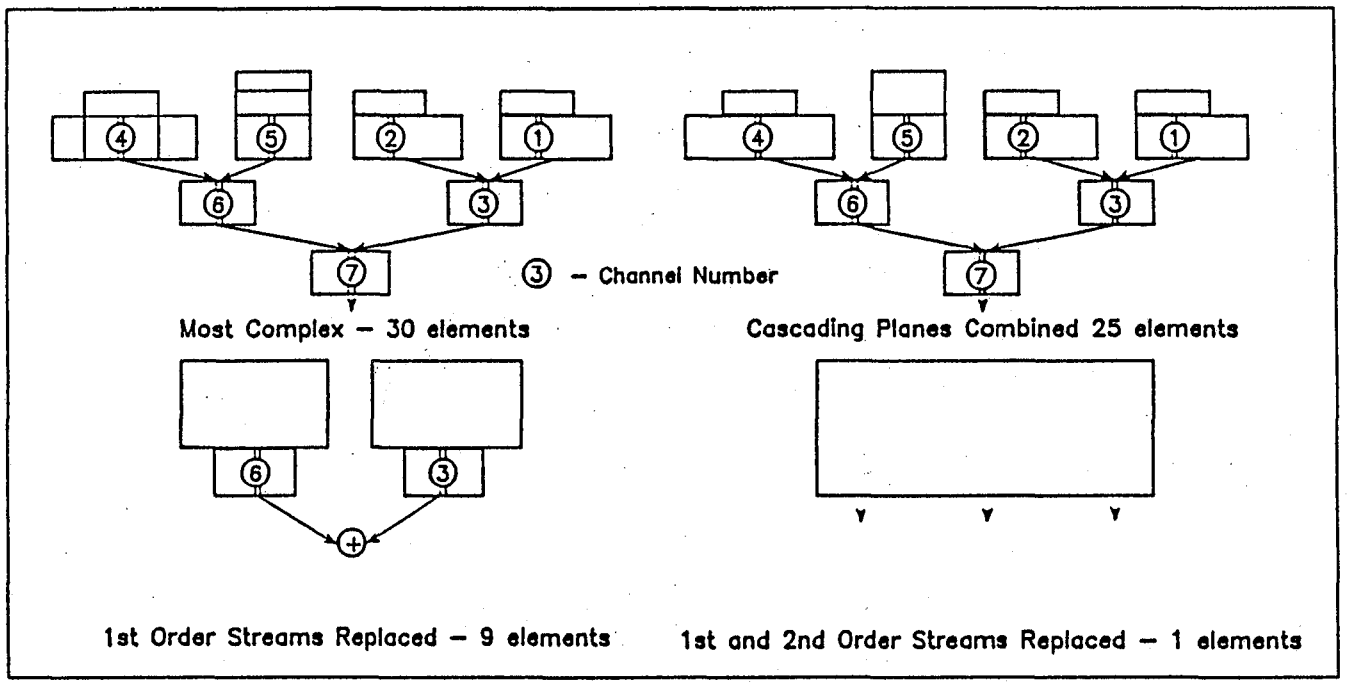

Figure 4.10 LH-106: Four Levels of Model Aggregation

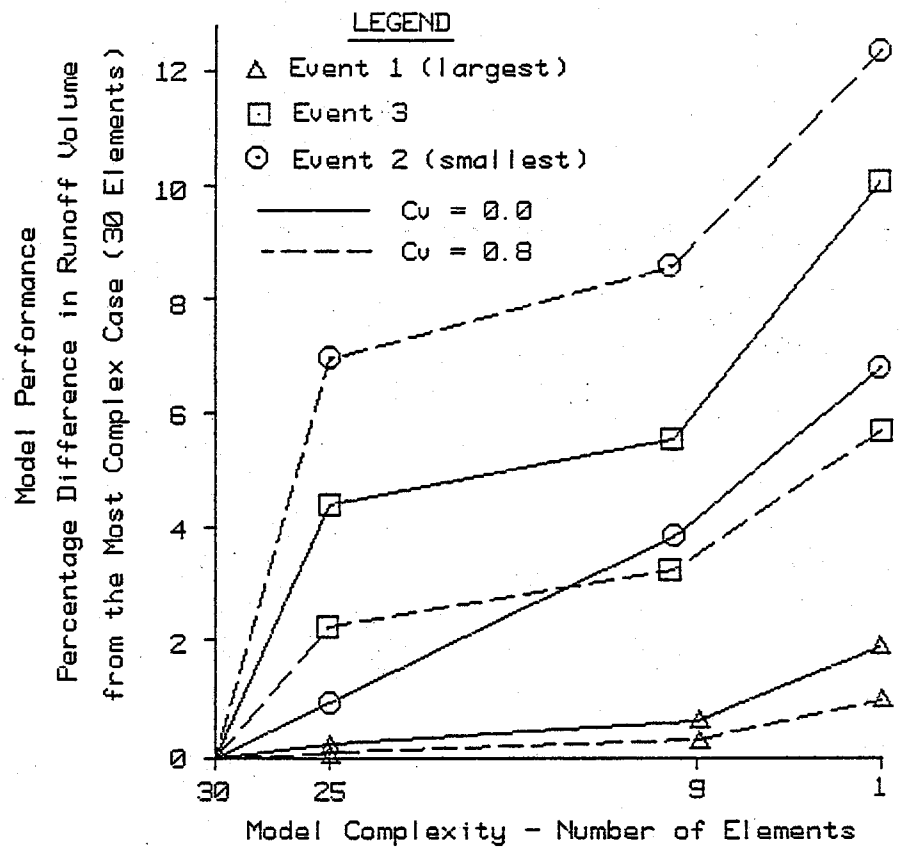

Figure 4.11 Model Performance Versus Model Complexity

Table 4.3. Summary of Simplification Impacts

Event	CV	Num. Ele.	Qp (mm/hr)	% Diff.	Total Vol. (mm)	% Diff.	Observed Qp	Observed Vol.	CPU Time (min:sec)
1	0.0	30	90.4		10.13		106.9	17.2	1:22.4
		25	91.2	-0.88	10.11	0.20			1:18.4
		9	92.2	-1.99	10.07	0.59			0:31.3
		1	92.7	-2.54	9.93	1.97			0:12.2
1	0.8	30	90.4		11.01				8:24.8
		25	90.7	-0.33	11.00	0.09			7:08.2
		9	91.7	-1.44	10.97	0.36			2:25.6
		1	91.9	-1.66	10.90	1.00			0:58.6
2	0.0	30	12.6		1.03		16.1	2.34	1:20.9
		25	12.5	0.79	1.02	0.97			1:15.1
		9	11.6	7.94	0.99	3.88			0:27.9
		1	10.3	18.30	0.96	6.80			0:12.3
2	0.8	30	16.5		1.86				9:13.9
		25	15.8	4.24	1.73	6.99			7:45.2
		9	15.6	5.45	1.70	8.60			2:31.2
		1	15.3	7.27	1.63	12.4			0:52.5
3	0.0	30	15.3		3.58		20.8	9.47	2:21.6
		25	15.3	0.0	3.42	4.47			2:12.8
		9	14.9	2.61	3.38	5.59			0:48.2
		1	14.2	7.19	3.22	10.1			0:17.2
3	0.8	30	18.0	5.24					13:56.2
		25	17.9	0.55	5.12	2.29			11:52.4
		9	17.8	1.11	5.07	3.24			3:51.7
		1	17.7	1.67	4.94	5.73			1:28.2

was noted by both Osborn and Lane (1969) and Osborn et al. (1971). They found thatrainfall completely dominated rainfall-runoff regressions relationships.

Event 1 is the largest of the three events selected but, as the data in Table 4.2 indicate, it is still relatively small from a flood frequency viewpoint. The aggregation results, therefore, imply that for flood design work with return periods of more than several years, significant geometric model simplification can be made without sacrificing model accuracy. For very large floods, process model simplification (nonlinear to linear) might also be accomplished. The success of unit hydrograph theory, applied to large floods, attests to this observation.

Watershed simplification effects are much more apparent for the small and medium sized events (#2 and #3). For these events, the basin controls runoff response to a greater degree. The nonlinearities associated with infiltration thresholds are more important for small events where the runoff to rainfall ratio is small, as was demonstrated in Chapter 2. The same degree of geometric model simplification cannot be accomplished for the small storms as compared to the largest event. This points out the dependence of allowable geometric model aggregation on modeling application objectives. Water yield studies will require a greater level of model complexity than will flood studies.

The above analysis directly addresses Hypothesis 1A, which is restated below:

HYP (1A): The degree of allowable geometric model simplification is a function of storm size.

It is assumed that the preservation of runoff volume from the most complex model representation is the desired goal. If the degree of allowable geometric model simplification, assessed in terms of volume preservation, is not a function of storm size, then the same level of aggregation should be possible regardless of storm size. Storm, or runoff event size, could be measured with any number of variables, some of which are presented in Table 4.2. For considering this hypothesis, the estimated return period of the storm is used.

Now consider the percent difference in runoff volume for the single element model representation (number of elements = 1) for the three events with C_v = 0.0. The percentage differences for events 1, 2, and 3 are 1.97, 6.80, and 10.1 percent, respectively (see Table 4.3). (For peak rates, the differences caused by aggregation to 1 element for events 1, 2, and 3 are -2.54, 18.3, and 7.19 percent, respectively. If an error in stage of two times the measuring resolution of runoff charts (3.0 mm) is assumed, the percentage difference in peak rate caused by this measurement error is 1.45, 3.15, and 3.05 percent for events 1 through 3, respectively. Thus, a substantial portion of the aggregation error falls within the stage measuring error at peak runoff rates). If Hypothesis 1A were false, the percentage differences should be nearly equal. From another viewpoint, if an acceptable percentage difference in volume is specified, the level of allowable geometric simplification could be determined. If a 5 percent volume difference is set for the case above, the model could be simplified to 1, 9, and 25 elements for events 1, 2 and 3, respectively, again demonstrating that Hypothesis 1A should be accepted.

Although the criteria for acceptance of this hypothesis are quite subjective and are only tested with three events, a strong indication exists that it should be accepted. A more thorough examination of Hypothesis 1A with a greater number of runoff events is carried out in Chapter 6.

If small-scale variability of infiltration is considered in the simulations (C_v = 0.8), the aggregation results are improved for events 1 and 3. Event 2 does not behave in the same manner, but examination of several hydrographs from the event 2 simulations (Figure 4.12) shows that runoff from the spatially variable case more closely resembles observed runoff. For the C_v = 0.0 case, no runoff results from the first burst of rainfall for any level of aggregation. Therefore, no error in runoff volume occurs in this portion of the hydrograph, which accounts for the opposite trends of improved aggregation results with C_v = 0.8 as compared to events 1 and 3.

During the aggregation procedure, lumping, or averaging, of the soil properties takes place. The simplification rules objectively distort the roughness to maintain equilibrium storage on an impervious model geometry. On impervious geometries for all the events, the peak rates on the 1 element LH-106 representation were preserved to within one percent of the 30-element representation. The test events included both equilibrium and partial equilibrium cases on an impervious basin surface. This illustrates that the hydraulic characteristics are adequately maintained by the aggregation rules. When these rules are applied to infiltrating cases, one would expect a deviation of simulations with aggregation for infiltrating cases.

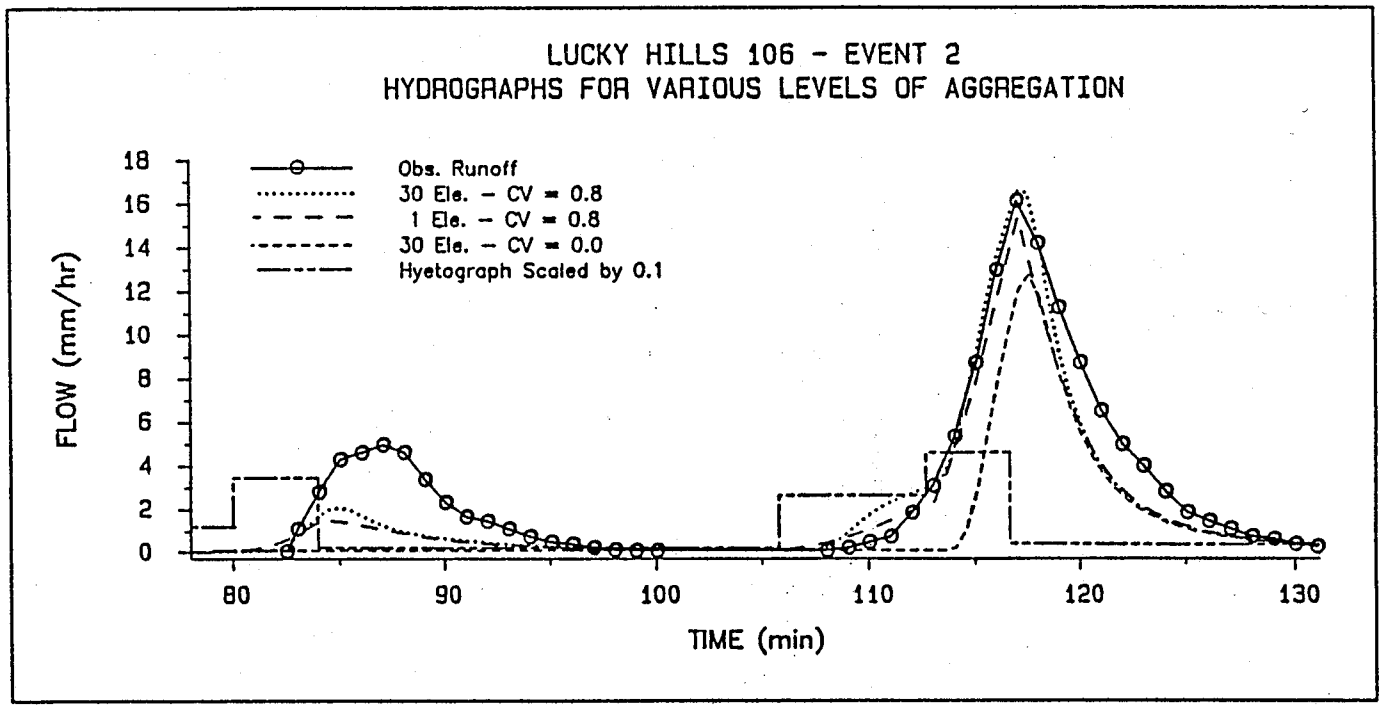

Figure 4.12. Event 2 Hydrographs

Area weighted averaging of soil properties does not preserve basin infiltration characteristics during simplification. This deviation is mitigated by including small-scale infiltration variability as described in Chapter 2. By incorporating this variability, the variability lost during the simplification due to averaging is partially compensated for. For example, when simulations for the 30 element geometry with $C_v = 0.0$ are compared to simulations with the simple 1 element representation with $C_v = 0.75$, runoff volumes are maintained to within 5 percent. Increasing C_v, therefore, compensates for the loss of variability due to averaging during aggregation.

Besides averaging of soil properties during aggregation, the computational distances are also distorted. The simplification procedure also hinges on distortion of the roughness value. Sensitivity of the aggregation procedure to these factors is explored in the next section.

4.5 Sensitivity of the Simplification Procedure to Computational Length and Initial Roughness

4.5.1 Sensitivity to Computational Length

Within KINEROSR, a strategy has been adopted to conserve computational time by automatically adjusting the number of spatial computational nodes as the length of a plane or channel elements vary. For a given basin, the characteristic length (CLEN) is defined as the longest cascade of planes or the longest channel length. For elements with length greater or equal to CLEN, 15 computational nodes

are used. For element lengths (XL) less than CLEN, the number of nodes is equal to 15 * (XL/CLEN) (to the nearest integer) with a minimum of five nodes.

As geometric simplification proceeds, longer equivalent overland flow planes usually replace elementary subwatersheds. This will eventually force the remaining longer planes to have 15 computational nodes. However, the overall number of nodes in the basin will decrease as fewer elements are used to model the watershed after each level of aggregation. The characteristic length for LH-106 is 45.1 meters (m) for the most complex basin description. After the aggregation is carried out, the length of the equivalent plane for the watershed is 69.6 m.

To assess the sensitivity of the aggregation procedure to CLEN, three characteristic lengths of 15.2, 45.1, and 137.2 m are considered. This provides nearly an order of magnitude change in CLEN. For CLEN = 15.1 m, virtually all of the elements for LH-106 will have 15 nodes for both the 30 and 1 element model. This CLEN provides the most accurate simulation. At CLEN = 137.2 m, all of the elements in the 30-element system will have five nodes, and the final plane will have eight nodes. For these CLEN values, as well as the original CLEN = 45.1 m, simulations for events 1, 2, and 3 (see Table 4.2) using the 30 and 1 elements model geometries were run. The results are shown in Table 4.4.

In this table, the percentage differences in runoff volume and peak rate caused by aggregation from 30 to 1 element for each CLEN are shown in columns 3 and 5. In columns 4 and 6, the delta percentage difference changes for volume and peak rate from the most accurate simulations (CLEN = 15.2m) are shown. It can

Table 4.4. Sensitivity of Aggregation to Computational Length

(1) Event	(2) CLEN (m)	(3) % Diff. Vol. 30 to 1 Element	(4) Delta % Diff.	(5) % Diff. Qp 30 to 1 Element	(6) Delta % Diff.
1	*15.2	1.97		-2.54	
	45.1	1.97	0.0	-2.54	0.0
	137.2	2.03	0.06	-2.25	0.29
2	15.2	7.12		18.3	
	45.1	6.80	0.32	18.3	0.0
	137.2	6.65	0.47	18.2	0.1
3	15.2	10.2		7.13	
	45.1	10.1	0.16	7.19	0.06
	137.2	9.94	0.26	8.80	1.67

* The shortest characteristic length (CLEN) will result in the greatest number of computational nodes and the most accurate solution.

be concluded that the node density change contributes only a minor portion of the aggregation error for volumes (Maximum Delta = 6.6% = 0.47/7.12*100 for event 2). The computational node density has a greater impact on peak rates as would be expected. For event 3, the percentage of aggregation error caused by CLEN change is 23% (= 1.67/7.13*100).

These numbers are conservative, however, because CLEN is held constant during aggregation and the element lengths (XL) become larger. This process more closely resembles the change in CLEN in Table 4.4 from 45.1 m to 15.2 m because a greater number of nodes per element results for both scenarios. If comparisons are restricted to the CLEN = 15.2 m and 45.1 m cases, it can be concluded that the percentage of aggregation error which can be attributed to changes in computational node density is less than one percent for volumes and peak rate. This is true for all three events over the full range of aggregation from 30 to 1 element.

4.5.2 Sensitivity to Initial Roughness

The key to maintaining model equivalence during simplification is the distortion of the hydraulic roughness to maintain equilibrium storage. For the most complex geometry, an assumed or estimated roughness value is selected. For the procedure to be fairly general, it must be able to accommodate a wide range of initial roughness values. To test the ability of the procedure to handle a wider range of initial roughnesses, the Lucky Hill-106 roughness values used in the previous section were multiplied by factors of two and ten. In addition, the storm causing the

largest runoff event of record (event 4) was included in the analysis. This event occurred on 7/17/75, with a duration of 72 minutes, a total depth of 70.1 mm, and a weighted mean intensity of 58.4 mm/hr. For each of the events and each level of roughness (N, 2N, and 10N), the simulations at each level of aggregation for C_v = 0.0 and C_v = 0.8 were run.

The errors caused by model aggregation, as measured by the percentage differences in runoff volume from the most complex case, are presented in Figure 4.13 for the C_v = 0.0 case. In this figure, the percentage volume differences are plotted as functions of the number of model elements by storm and initial roughness level. Before examining the figures, recall that the ordering of storm size from low to high, by weighted mean intensity, is event 2, 3, 1, and 4. Several trends are apparent from the plots.

The greatest aggregation impacts occur for the roughest initial conditions and the smallest storm. These results are analogous to those presented above and in Chapter 2, namely, that the greater the basin influence, by way of high infiltration losses or large attenuation from high roughness, the greater the aggregation errors. The larger the basin influence, or watershed attenuating ability, the less likely that any event will drive the basin to equilibrium. Because the aggregation rules are based on maintaining equilibrium storage, the further from equilibrium, the greater the likelihood that simplification will introduce significant deviation from the complex basin representation. Although the cases which incorporate small scale infiltration variability (C_v = 0.8) are not plotted in Figure 4.13, aggregation errors are generally

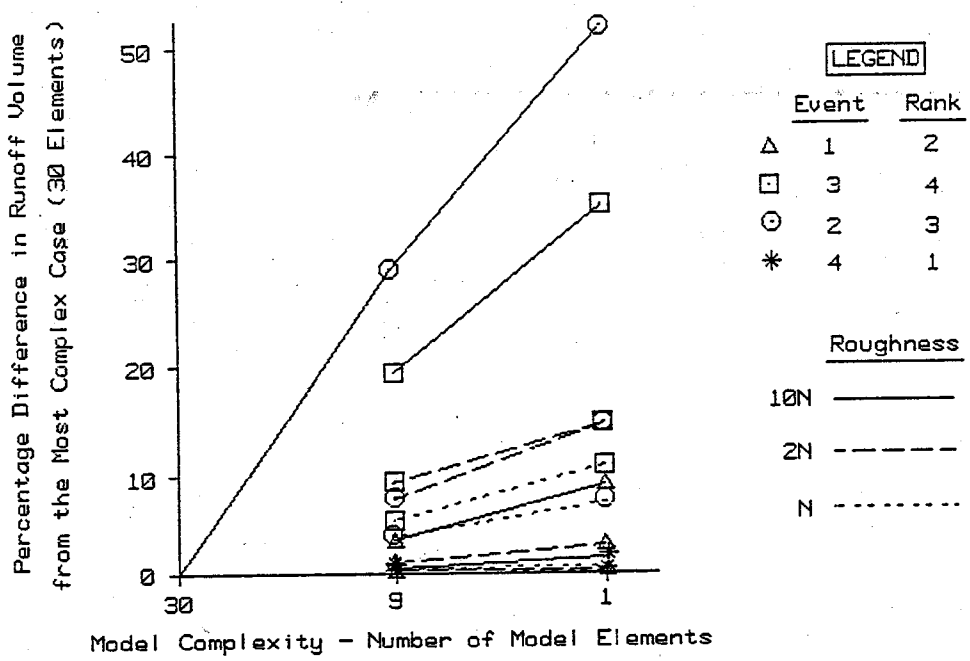

Figure 4.13 Model Aggregation Error Versus Model Complexity for Various Initial Roughness Values (C_v = 0.0)

reduced when C_v = 0.8. Including small- scale variability compensates for variability lost during simplification by averaging.

Before disregarding the simplification methodology for high initial roughness cases, consider the geomorphic consequences of natural basins with extremely high hydraulic roughness values. These basins are typically densely vegetated and have low erosion rates. In such basins, the drainage density and degree of basin dissection by channels are usually much smaller than in low roughness, sparsely vegetated areas such as Lucky Hills. Thus, the initial geometric model representation of a low drainage density basin will be much simpler because fewer channels are present. Indeed, if one examines the heavily grassed USDA-ARS 10 hectare R-5 experimental watershed near Chickasha, Oklahoma by way of an approximately 1:2000 scale base map, only one channel is observed. Therefore, a feedback mechanism likely exists such that the drainage density is directly related to the hydraulic roughness. Sediment transport relations bear this out as transport capacity is inversely related to roughness.

Referring back to Figure 4.13 for cases where the basin influence, by way of infiltration or roughness is large, greater aggregation errors result (events 2 and 3). Consequently, a greater degree of geometric model complexity must be maintained to preserve model accuracy. Significant simplification can be accomplished for very large events (event 4) for a wide range of initial roughness conditions.

These trends suggest a continuum in the influence of basin and climate scales in the transformation of rainfall to runoff. For a given basin, storm sizes (climate scales) above a certain threshold will dominate runoff generation. These storms overwhelm basin dynamics, driving the basin to equilibrium (or close to it) and thus largely control runoff response, allowing substantial geometric aggregation without seriously increasing model error.

Now consider the same basin and apply a treatment that notably increases infiltration and roughness, such as contour plowing. The same class of storms that overwhelmed the untreated basin are not likely to overwhelm the plowed basin (partial equilibrium conditions). Therefore, a greater degree of geometric complexity, describing the disturbed basin, must be maintained to achieve comparable modeling results. However, consider increasing the climate scale (storm size) as applied to the plowed basin. At some new, higher threshold, these storms will again overwhelm the plowed basin, and geometric aggregation will be possible. This continuum could continue until the probable maximum storm scale is reached.

These findings help address the initial question in Chapter 1 regarding the domination of hydrologic subprocesses in runoff generation at various basin-climate scales. Although they pertain only to the small LH-106 catchment, larger basin scales are considered in Chapter 6. For all basin scales, if the climate is considered a hydrologic subprocess, it clearly dominates runoff generation where geometric aggregation can reduce the entire catchment to a single overland flow plane. Remember, the single remaining plane still treats infiltration and routing in a

nonlinear manner as structural model simplification (nonlinear to linear) is not treated in this study. The single plane also contains significant "complex equivalent" information established by way of the simplification rules.

Not having the "complex equivalent" information for a simple model geometry is not considered a detriment to modeling efforts. It is unlikely that the applications modeler will start with a very complex basin representation and simplify. If the modeler is conducting flood studies and decides to use a simple geometry, then a roughness value is all that must be estimated by way of optimization. Soils and topographic parameters would be field estimated using the simpler system with larger elements. The roughness is the only parameter distorted in such a way that it would be difficult to estimate a priori. Given the subjective nature of roughness estimates, roughness calibration is often required regardless of the starting modeling complexity. The point is that larger spatial averages and simplifications to routing will not impart significant uncertainty into the modeling process where the climate is dominant.

4.6 Summary

The relationship between base map scale and initial geometric model complexity has been demonstrated. Changes of map scale will result in different basin model representations with different levels of complexity (i.e., different numbers of plane and channel elements). Objective rules for geometric model simplification, which result in reproducible aggregation procedures, have been defined. A critical aspect of the aggregation procedure is the preservation of

equilibrium storage from complex to simple basin representations. The equilibrium storage is a powerful measure of basin performance as it integrates the effects of slope, flow convergence, and hydraulic roughness.

The simplification methodology was applied to the Lucky Hills-106 watershed, and model performance at several levels of aggregation was tested for three runoff events covering a range of storm size. For the largest storm tested, significant geometric simplification was possible, with only minor effects on model performance.

The sensitivity of the aggregation procedure to initial roughness and numerical computational length was also assessed. Model performance errors due to changes in computational node density constitute a minor percentage of overall aggregation errors. Initial roughness does have a serious impact on the ability to simplify basin representation. Increasing initial roughness and/or decreasing the percentage of rainfall transformed to runoff increases model aggregation error.

These conclusions are reached after examination of the analysis on LH-106. Although this is a very small catchment, it provided a focal point for assessing geometric model complexity requirements. At larger spatial scales, the effects of spatially variable rainfall and channel losses will have a greater impact on the ability to aggregate watershed elements. Chapter 6 addresses model simplification over a range of watershed scales.

The analysis of LH-106 presented in this chapter used a combination of assumed or roughly estimated model input parameters. To ensure that conclusions regarding the model and the aggregation procedure provide insight into actual

watershed process behavior, confidence in the model must be established. To accomplish this task, model calibration and verification using observed rainfall-runoff data must be undertaken. This phase of the investigation in presented in the following chapter.

CHAPTER 5

MODEL SENSITIVITY, CALIBRATION, AND VERIFICATION

5.1 Introduction and Background

The geometric model simplification procedures introduced in the last chapter were tested on a small watershed, the parameters of which were estimated from field measures. A reasonable level of confidence exists in the definition of geometric (topographic) parameters given the availability of large-scale maps and the ability to directly measure channel geometries. A much lower degree of confidence exists in the hydraulic roughness and soil hydraulic parameter estimates as they were not directly measured nor can they be easily measured. Therefore, model calibration to better estimate these highly uncertain parameters is required.

To acquire greater confidence in the model, the simplification procedure and subsequent interpretations regarding basin dynamics, verification, in addition to calibration, with observed data is required. Without verification using observed data, study conclusions must be confined to the realm of the computer and its simulations. If model confidence can be acquired with rainfall-runoff data, a degree of realism can be attached to the conclusions of this study and valid insights into actual watershed process behavior can be obtained. Beven (1989) pointed out that great care must taken in making interpretations regarding distributed hydrologic model predictions. The primary objective of this chapter is to demonstrate model realism and to ensure that realistic interpretations can be made.

Calibration and verification of distributed rainfall-runoff models are made difficult by the very nature of distributed systems. Beck (1987) noted that the intrinsic problem due to aggregation is that the dimension of the input/output observations is much smaller than those of the state and parameter vectors. Aggregation, as implied by Beck, denotes the discretization of space-time domain. Because partial differential problem formulations are by nature, continuous, we cannot track all states and parameters over the entire space-time domain and, therefore, must aggregate to make the problem tractable. Verification of distributed states and parameter vectors would require an observation system so elaborate that it is infeasible. Without adequate data (internal and input/output), identification, and estimation problems result routinely.

The curse of inadequate distributed field data for model calibration and verification was also pointed out by Beven (1988, 1989) and Klemes (1988). Beven concluded that, for modeling continuous flow, more than four or five parameters will result in identifiability problems (Kirkby, 1976; Blackie and Eeles, 1985). More parameters might be allowed with increased field measures of distributed state variables, but such data are rarely available. Warwick (1989) concurred with this conclusion noting that increases in process model complexity will not decrease modeling error unless data sampling is increased. Therefore, due to the paucity of distributed data, only several parameters should be used for model calibration. Parameter estimation problems introduced by overparameterization and poor model

structure are well documented (Sorooshian and Gupta, 1983, 1985; Johnston and Pilgrim, 1976; Jun, 1989).

Beck (1987) equated the lack of parameter identifiability and overparameterization to surplus model content. The crux of the problem is that one would like to know the internal description of a system which is of substantially higher order than what can be observed about the external system description. "The model may contain descriptions either of a type of behavior not actually observed in a sample of data or of multiple types of behavior, the individual components of which cannot be disentangled from observation of their collective effect. The consequences are usually apparent in the absence of a uniquely "best" combination of parameter values that fit the data and result in parameter estimates with high error variances and covariances." (Beck, 1987). Beck also concluded that reducing the number of parameters is equivalent to increasing the number of observed data, and that throwing out the most insensitive parameters is equivalent to discarding the most uncertain parameters.

The primary type of data that will be used to calibrate and verify KINEROSR and the simplification procedure is rainfall-runoff data from the USDA-ARS Walnut Gulch Experimental Watershed. Because these are input/output data, the preceding comments are applicable. However, using the nested Lucky Hills watersheds, some degree of interior model knowledge or confidence can be acquired. The nested basins will allow internal verification of the model. Still, only two internal measures of runoff data are collected within LH-104. Given this constraint, only a small

number of "free" optimization parameters are justified in light of the comments above. Sensitivity of dependent model variables (runoff) to parameter variation offers a method to select those parameters which should be included in model calibration.

5.2 Sensitivity to Selected Optimization Parameters

Because the model will be applied, calibrated, and verified over a wide range of events, the sensitivity analysis of runoff to model parameters will also be conducted over a range of runoff event sizes. To conduct the initial sensitivity analysis, the most complex representation of LH-106 (30 elements) as shown in Figure 4.2 was used. Ten runoff events, covering a range of runoff size and initial conditions, were selected from a set of 30, carefully checked, rainfall-runoff events. Geometric model parameters of plane area, slope, and width were measured on 1:480 scale maps with a 1 foot (0.3048 m) contour interval. Channel geometries were measured in the field. Soil samples were taken at six field locations and were used to estimate rock content and soil hydraulic parameters. A more detailed explanation of the estimation of initial model parameters and runoff event selection is presented in Appendix A. Initial soil moisture estimates were computed by the daily water balance component of CREAMS (Knisel, 1980) independently of KINEROSR. Appendix B contains a more detailed summary of the use of CREAMS.

To ensure that initial parameter estimates provided reasonable runoff estimates, a single event (#53) was selected for model fitting. The size of this event

falls in the middle of the ten selected events, and it is double peaked, providing a more complex test of the model. The roughness and Ks parameters were selected for initial model fitting after discussions with an experienced KINEROSR user (Woolhiser, personal communication, 1988). User experience indicated that these parameters have significant impact on runoff predictions. Adjustments to these two parameters were made by applying a uniform multiplier to the Ks and roughness of each plane and channel model element over the entire watershed. By doing so, relative differences in field parameter estimates are maintained but are scaled in a linear fashion.

Using the observed rainfall from raingage 83, the roughness and Ks multiplers (parameters) were manually adjusted to fit observed runoff. The simulated and observed hydrograph for event 53 for the best set of multipliers is presented in Figure 5.1. The simulated runoff volume, peak runoff rate, and time to peak agree to within 0.15 percent of the respective observed data.

Beven (1989) noted that it is very easy to fit a single rainfall-runoff event. The fitting exercise above proves this and is not meant to serve as a general endorsement of KINEROSR. The exercise of obtaining the manually derived parameter multipliers is only meant to start, or center, the sensitivity analysis around a range of values which will produce reasonably realistic runoff simulations for all ten events. Table A.1 in Appendix A provides observed summary runoff information for these ten events (highlighted by an asterisk in table A.1).

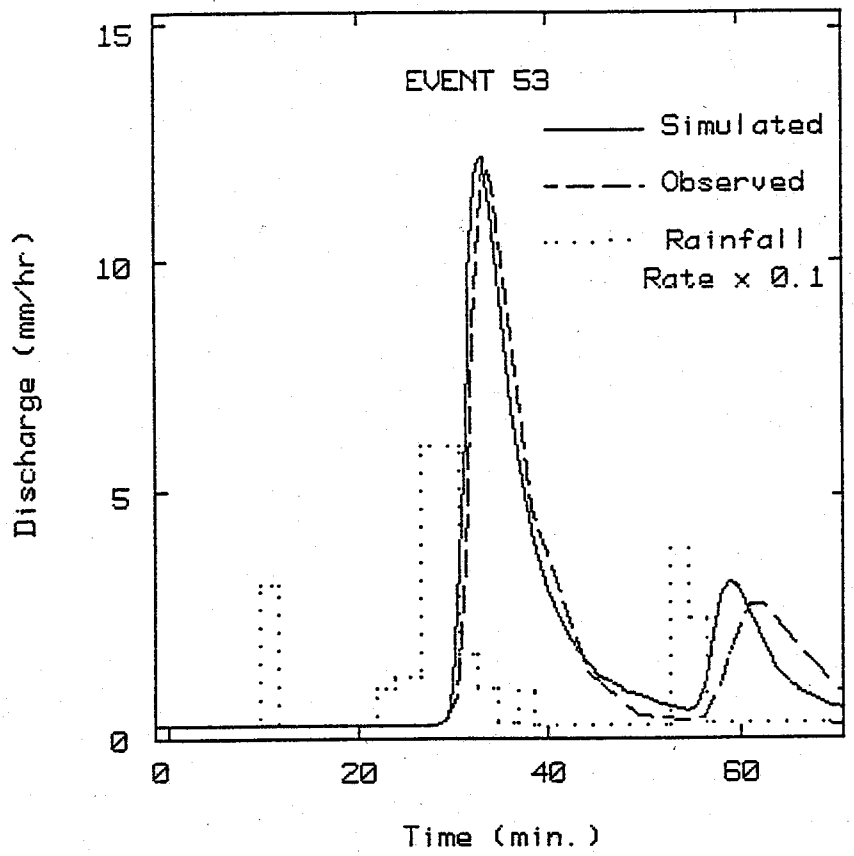

Figure 5.1 Observed Versus Simulated Runoff for Event 53 (Roughness and Ks Parameter Multipliers Manually Adjusted)

Runoff volume, peak runoff rate, and time to peak will be used to assess the sensitivity of runoff characteristics to changes in various parameters. Univariate sensitivity analysis is carried out using the uniform multiplier approach described above. Model sensitivity due to multiple parameter interactions is indirectly addressed later in this chapter when optimization results are discussed. Table 5.1 contains a list of the parameters considered in the sensitivity analysis and a brief description of how they are used in the model.

The parameters selected for the sensitivity analysis are those that cannot be measured directly in the field with a high degree of confidence. Parameters that can be directly and accurately measured are excluded from the analysis. Field measured values for these parameters will be input into the model. It is assumed that they can be determined with sufficient accuracy so that very little uncertainty is introduced into simulated runoff by the uncertainty in these parameters. Also excluded are those parameters which can be determined by repeatable, objective, rules, such as characteristic computational length (CLEN) discussed in the previous chapter.

Uniform multipliers of 0.9 and 1.1, corresponding to a +/- 10% parameter perturbation, were applied to all of the parameters listed in Table 5.1. The roughness and Ks parameters for planes and channels were considered independently to see if some insight into the relative domination of channel or overland flow processes could be acquired. The results are presented graphically in Figure 5.2 to illustrate the effect of the parameter perturbations over the full range of the ten selected events. The effects on the time to peak (Tp), peak runoff rate (Qp), and

Table 5.1. KINEROSR Model Parameters Used in the Sensitivity Analysis

Parameter	Units	Description
C_v	---	Coefficient of variation of Ks
DINTR	L	Interception depth
Ks_p	L/T	Saturated hydraulic conductivity for overland flow planes. Note: If obtained for soil it should be corrected for volume of rock.
Ks_c	L/T	Saturated hydraulic conductivity for channels
POR	---	Soil porosity
$R1_p$	---	Manning's n for overland flow planes
$R1_c$	---	Manning's n channels
RECS	---	Infiltration recession factor
ROC	---	Volumetric rock content of soil
SI	---	Initial relative soil saturation
SMAX	---	Maximum relative saturation under imbibition

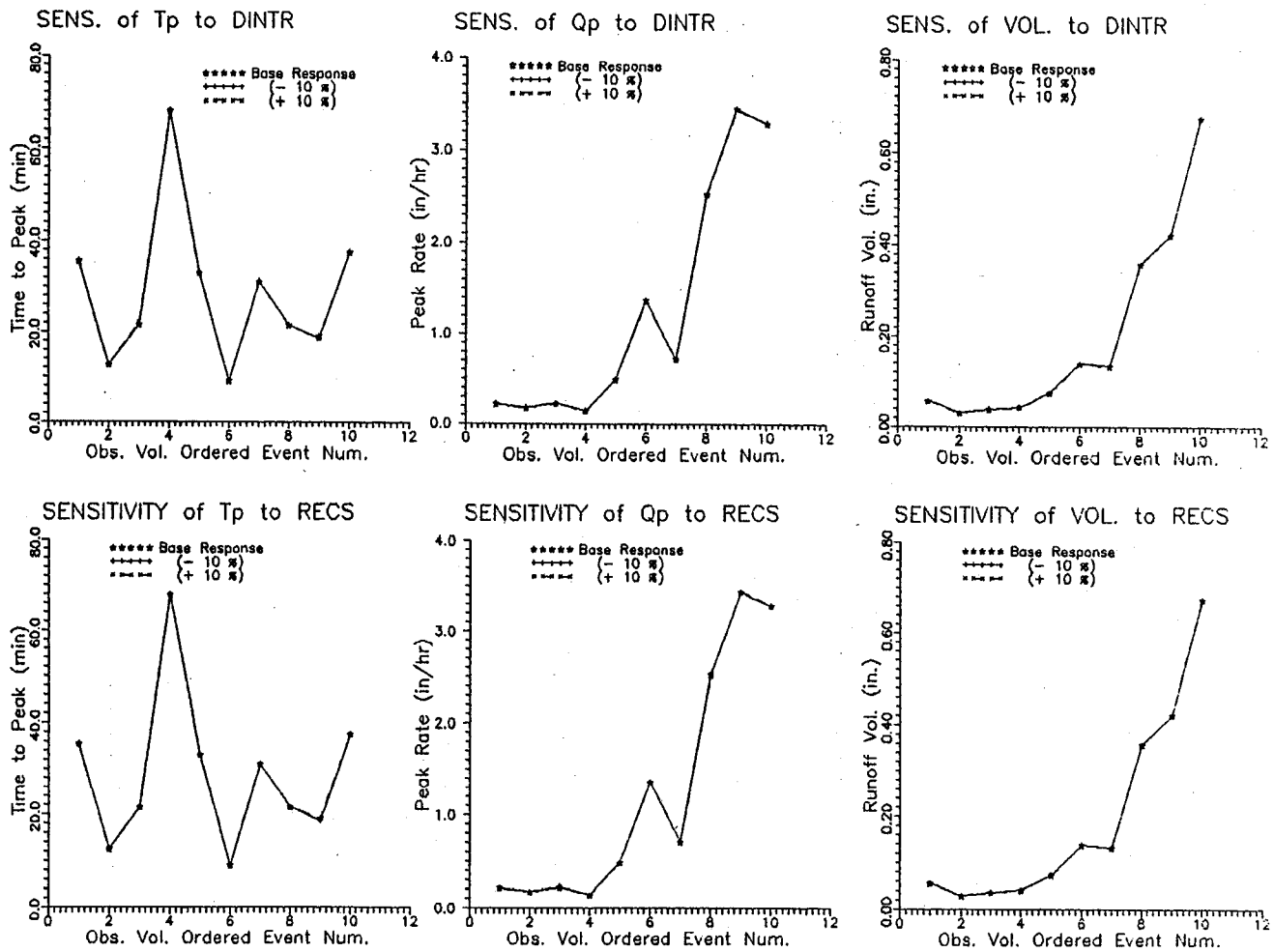

Figure 5.2 Sensitivity of Tp, Qp, and VOL. of Simulated Runoff to a -/+ 10% Perturbation of Selected Model Parameters Over a Range of Ten Events

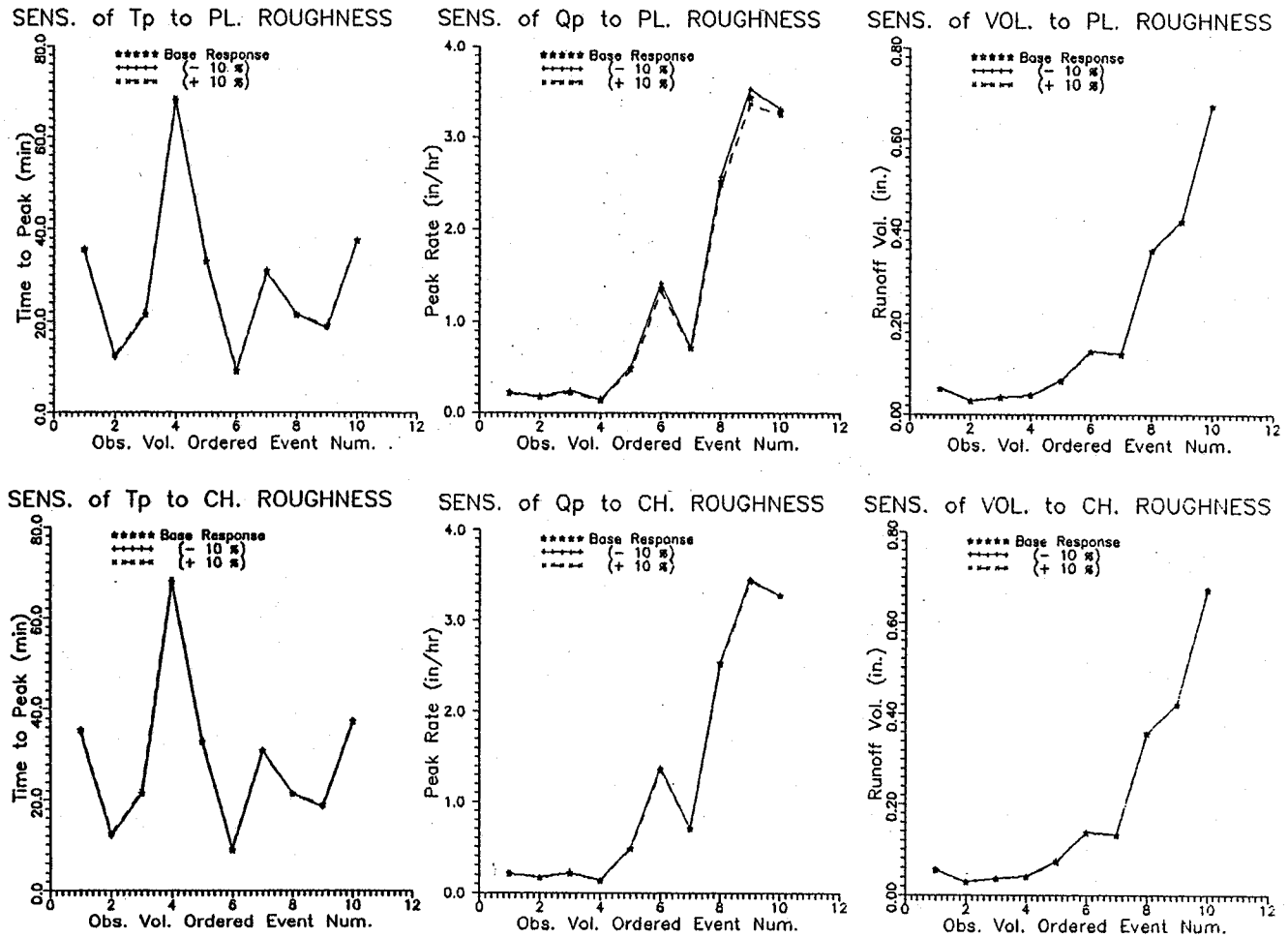

Figure 5.2 Sensitivity of Tp, Qp, and VOL. of Simulated Runoff to a -/+ 10% Perturbation of Selected Model Parameters Over a Range of Ten Events - (Continued)

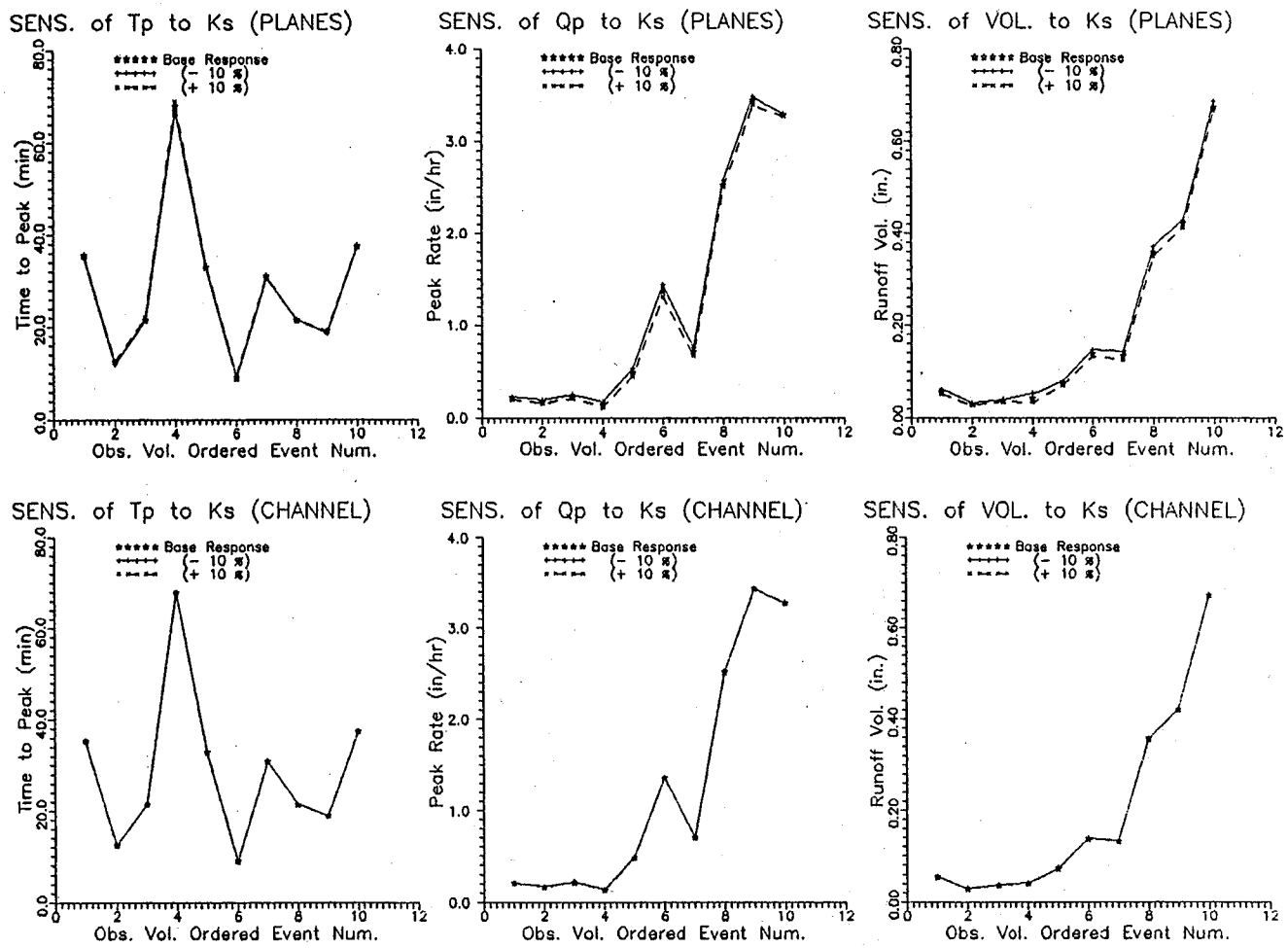

Figure 5.2 Sensitivity of Tp, Qp, and VOL. of Simulated Runoff to a -/+ 10% Perturbation of Selected Model Parameters Over a Range of Ten Events - (Continued)

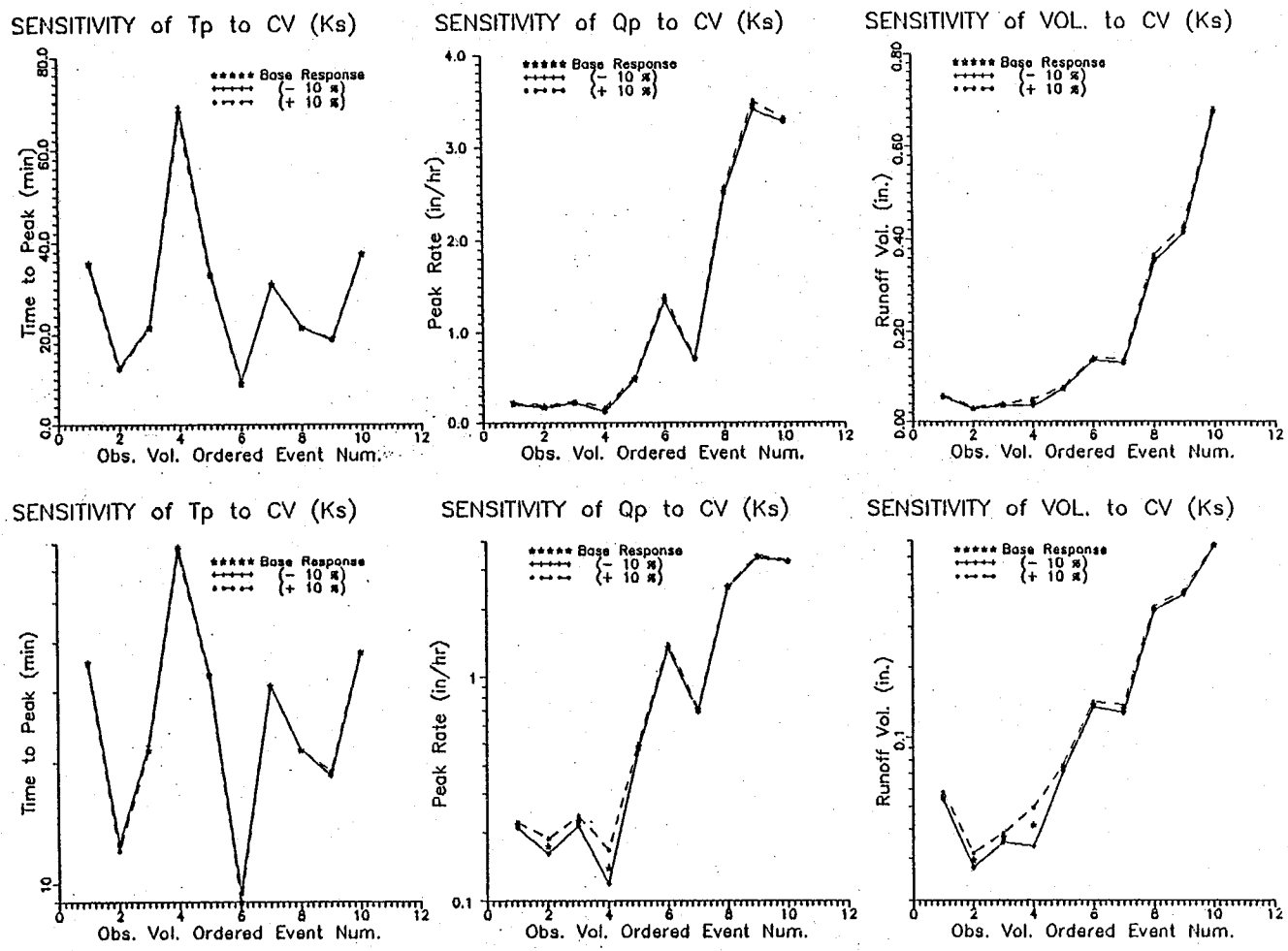

Figure 5.2 Sensitivity of Tp, Qp, and VOL. of Simulated Runoff to a -/+ 10% Perturbation of Selected Model Parameters Over a Range of Ten Events - (Continued)

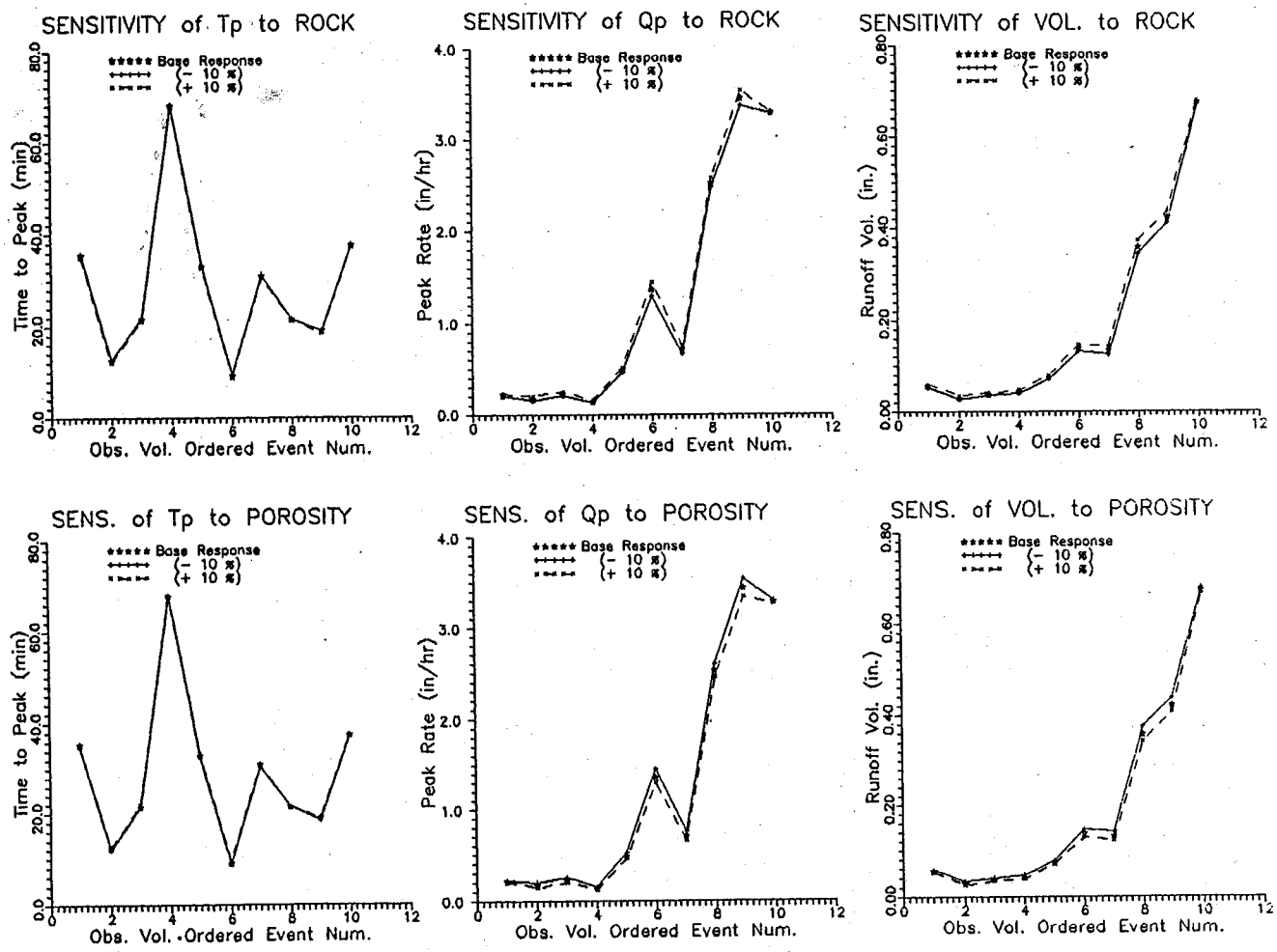

Figure 5.2 Sensitivity of Tp, Qp, and VOL. of Simulated Runoff to a -/+ 10% Perturbation of Selected Model Parameters Over a Range of Ten Events - (Continued)

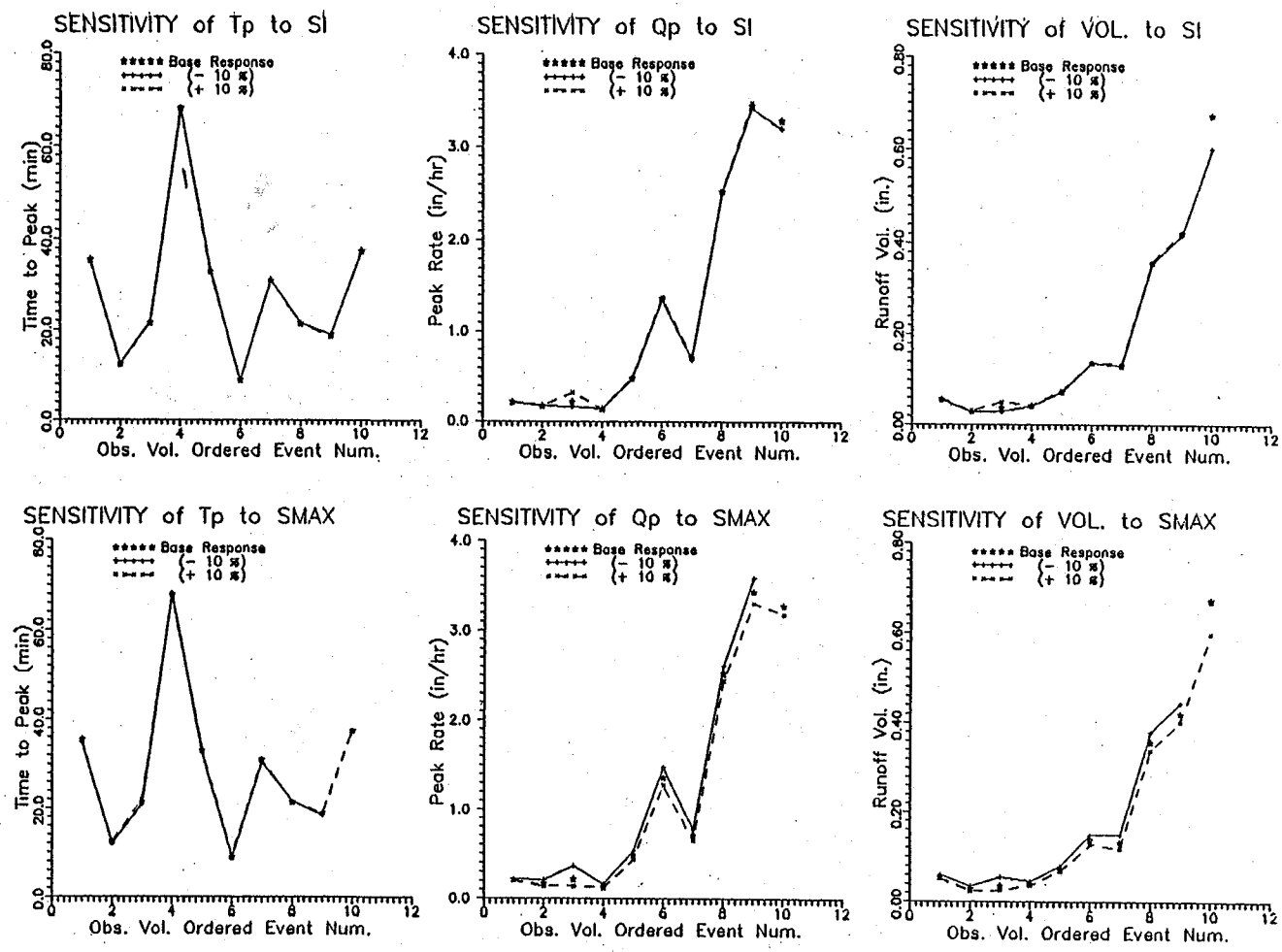

Figure 5.2 Sensitivity of Tp, Qp, and VOL. of Simulated Runoff to a -/+ 10% Perturbation of Selected Model Parameters Over a Range of Ten Events - (Continued)

runoff volume (VOL) are shown. In these figures the base response corresponds to a zero percent parameter perturbation. Solid and dashed lines track the change in runoff response for the -/+ 10% perturbations. The events are ordered from small to large (1-10) based on the runoff volume for each event.

The parameters with negligible impact on the runoff characteristics are the interception (DINTR), the microtopographic roughness term (RECS), as well as channel roughness ($R1_c$) and channel Ks_c. The initial interception values are very small for desert species in LH-106 and, therefore, so are the 10% perturbations. RECS affects the surface area over which infiltration can occur during runoff recession. It is only active on recession when the rainfall rate drops below the infiltration capacity. Because of the way RECS is used in the model, perturbations to it should logically impact runoff volume only. As shown in Figure 5.2, the impact of pertubations of RECS on runoff volume are negligible. Given these results, DINTR and RECS will not be considered for possible calibration parameters. RECS will be set to a value estimated from photogrammetrically measured stereophotos, and DINTR is set to values obtained in the literature for the desert species present (Branson et al., 1981; Tromble, 1983).

The minor effect of channel parameter perturbations results from the small percentage of area that the channels occupy in the basin (less than 2%). Some impact on Tp and Qp by the channel roughness can be detected. It is somewhat surprising that channel roughness changes do not have greater impact, as all of the runoff generated must flow through channel segments to reach the basin outlet.

These findings give an indication of the domination of overland flow processes in runoff generation at this basin scale. This is confirmed by examining the impact on runoff characteristics due to changes to roughness and Ks of overland flow planes ($R1_p$ and Ks_p).

Related to the plane Ks values is the coefficient of variation of Ks_p, (C_v). C_v has significant impact on both Qp and runoff volume (VOL). The sensitivity results for C_v are plotted in both linear and logarithmic scales. The logarithmic plot emphasizes the greater relative impact of C_v on the small runoff events, as was shown in Chapter 2. The other parameters which have significant impact on runoff characteristic are all related to infiltration. The porosity (POR), rock content (ROC), and the initial and maximum relative soil saturation (SI and SMAX) are all used to compute the infiltration capacity of the soil.

The effect of SI and SMAX should be viewed simultaneously as the soil moisture deficit (SMAX-SI) is one of the primary terms defining soil suction. Recall also that the suction term is automatically computed from Ks_p. This was done so that small-scale infiltration variability could be easily treated. By defining the suction term in this way, it can also be removed from consideration as a calibration parameter. In addition, because the suction is highly correlated with Ks_p, including it and Ks_p is likely to lead to identifiability problems.

SI will not be used as a calibration parameter as it will be determined outside of KINEROSR using CREAMS in a repeatable objective manner. The variability of SMAX as determined from textural soils data (Rawls et al., 1982) is relatively

small in comparison to other soil hydraulic properties. Because of this fact, coupled with fact that the moisture deficit (SMAX-SI) is the primary parameter of interest, SMAX will also be excluded from calibration. Considering SMAX for calibration, with SI determined independently, would constitute an inconsistent treatment of the two parameters in calibration.

The remaining two parameters, porosity and rock content, have a relatively large impact on runoff when perturbed, but are closely linked with infiltration computations. It is assumed that treatment of the small-scale variation of infiltration in a distribution sense (Chapter 2) will capture the majority of runoff response variation induced by variations in porosity and rock content. Because of the close association between porosity, rock content, and the infiltration computations, these two parameters will also be excluded from calibration to minimize parameter interaction.

To further reduce the possibility of parameter interaction during calibration, a distinction between channel and overland Ks and roughness will not be made. The calibration parameter space will, therefore, consist of three multipliers (three parameters). They are uniform basin multipliers for Ks, C_v, and hydraulic roughness. The roughness multiplier is kept because of its impact on Tp and Qp and because of the subjective nature of the initial estimation. The Ks multiplier is retained because it has significant impacts on both Qp and runoff volume. It also affects the suction term by way of its regression relationship. Ks is also difficult to measure directly, is highly variable, and has been crudely estimated from soil texture

measures. The C_v multiplier is also kept in the calibration because of its impacts on Qp and volume and because enough data were not available to define this parameter with a good deal of certainty. The resulting small number of calibration parameters should satisfy the concerns regarding overparameterization mentioned above as well as minimize parameter interaction.

To place the parameter sensitivity analysis in perspective, the sensitivity to rainfall input has also been considered. In the analysis above, measured breakpoint rainfall was obtained from raingage 83. This raingage is approximately 180 m from the centroid of LH-106. Another raingage (384) is located roughly 120 m from the basin centroid. For each of the ten events, the rainfall measured from each of these gages was used to simulate runoff. The fixed set of model parameters (zero perturbation) obtained from fitting event 53 was used for both rainfall input sequences. The variation induced in Tp, Qp, and runoff volume by using the two nearby gages individually is shown in Figure 5.3. In this figure, the observed values are plotted as small stars, and the bands represent the range in variation of Tp, Qp, and volume caused by using different raingages for input.

Figure 5.3 shows that by using the measured rainfall from two adjacent raingages independently, significant variations in runoff characteristics are produced. The two raingages are only about 300 m apart. Typically, for such length scales, rainfall is considered spatially uniform. The results presented in Figure 5.3 indicate otherwise. Table 5.2 contains the total rainfall depths measured for raingage 83 and 384 and summary statistics for each of the events considered. The mean and

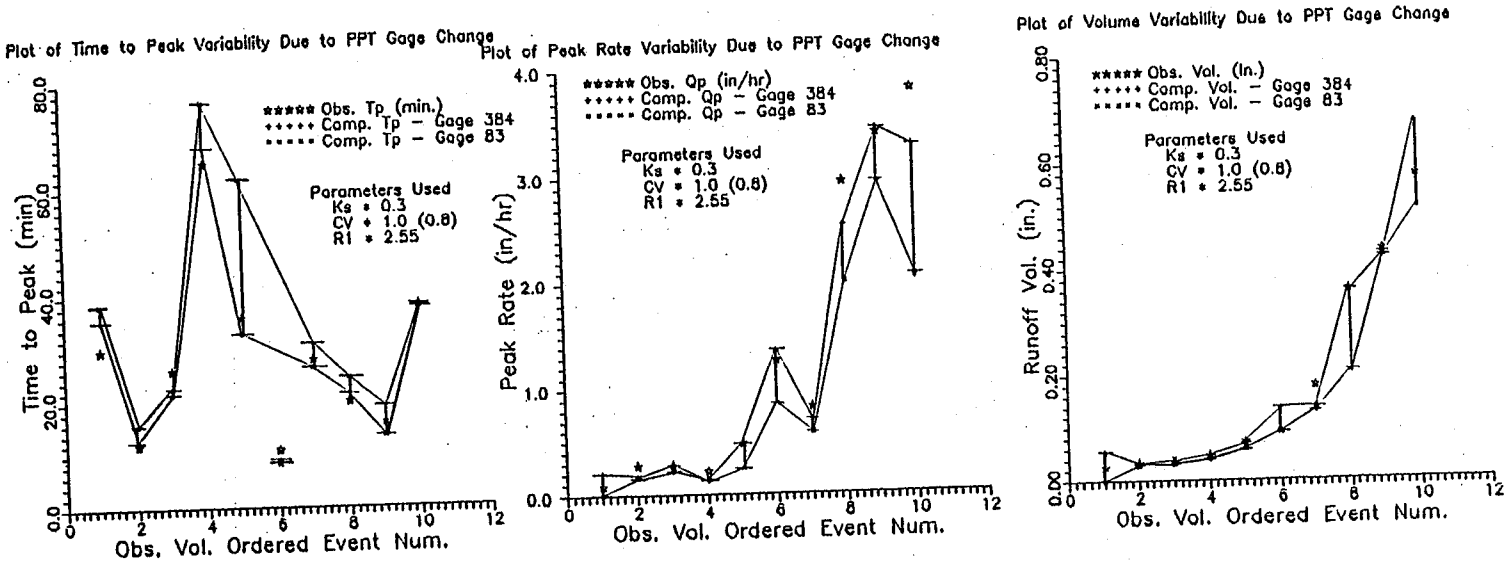

Figure 5.3 Variation in Tp, Qp, and Runoff Volume Caused by Using Rainfall Input from Two Adjacent Raingages (Approximately 300 m Apart)

Table 5.2. Lucky Hills Rainfall Depth Comparisons

Date D/M/Y	Event No.	Total Rainfall (mm) Gage 384	Gage 83
14/ 7/73	48	13.5	15.2
27/ 7/73	49	43.4	39.9
19/ 7/74	50	23.4	26.4
28/ 7/74	51	15.2	18.5
29/ 7/74	52	6.4	7.1
30/ 7/74	53	8.9	12.4
1/ 8/74	54	22.6	27.7
12/10/74	56	8.6	9.7
22/10/74	58	7.9	9.1
29/10/74	59	19.0	20.1
5/ 7/75	60	19.8	18.8
8/ 7/75	61	7.4	7.4
12/ 7/75	62	26.6	27.2
17/ 7/75	63	70.6	72.6
7/ 9/75	64	11.2	13.0
13/ 9/75	64A	17.3	18.5
6/ 9/76	65	24.4	23.6
10/ 9/76	66	9.9	11.4
13/ 7/77	67	10.4	11.4
23/ 7/77	69	8.1	8.9
31/ 7/77	70	12.2	13.5
1/ 8/77	71	10.9	11.7
15/ 8/77	72	26.7	21.6
16/ 8/77	73	12.4	13.7
1/ 9/77	74	27.7	27.7
26/ 9/77	75	26.9	27.9
26/ 9/77	75A	30.2	25.9
	n = 30	Mean = 19.3	20.0
		Stan. Dev. = 13.7	13.2

standard deviations for the rainfall totals are very similar, but percentage differences in individual rainfall totals range as high as 40%. Because interactive infiltration is used in KINEROSR, rainfall intensities rather than rainfall totals are the key input in runoff computations. Greater variation can be expected in intensities due to differencing of accumulated rainfall depths. Differencing is required because the weighing gages used in Walnut Gulch trace total accumulated rainfall on a rotating drum. This trace is digitizied for time and depth coordinates which are then differenced to obtain rainfall intensities. A dramatic illustration of the differences in simulated runoff caused by using the nearby raingages individually is shown in Figure 5.4. This figure shows the measured hyetographs for the two gages and the resulting simulated hydrographs for event 3 used in Chapter 4.

Many factors contribute to spatial variability of rainfall on the scale of 300 m between gages 83 and 384. They include wind effects, slope-aspect effects on gage catch, turbulence caused by the free-standing gage itself, and actual rainfall differences. Several studies have documented these effects in different climatic regimes.

In a Mediterranean climate, Lavee (1986) found differences of 10 to 100% in hydrologic and meteorologic rainfall at the same location. Hydrologic rainfall is measured with a raingage orifice parallel to the ground surface, and meteorologic rainfall is measured with a horizontal raingage orifice (Sharon, 1980). Lima (1989) illustrated the dramatic effect that changes in the incidence angle of rainfall can have

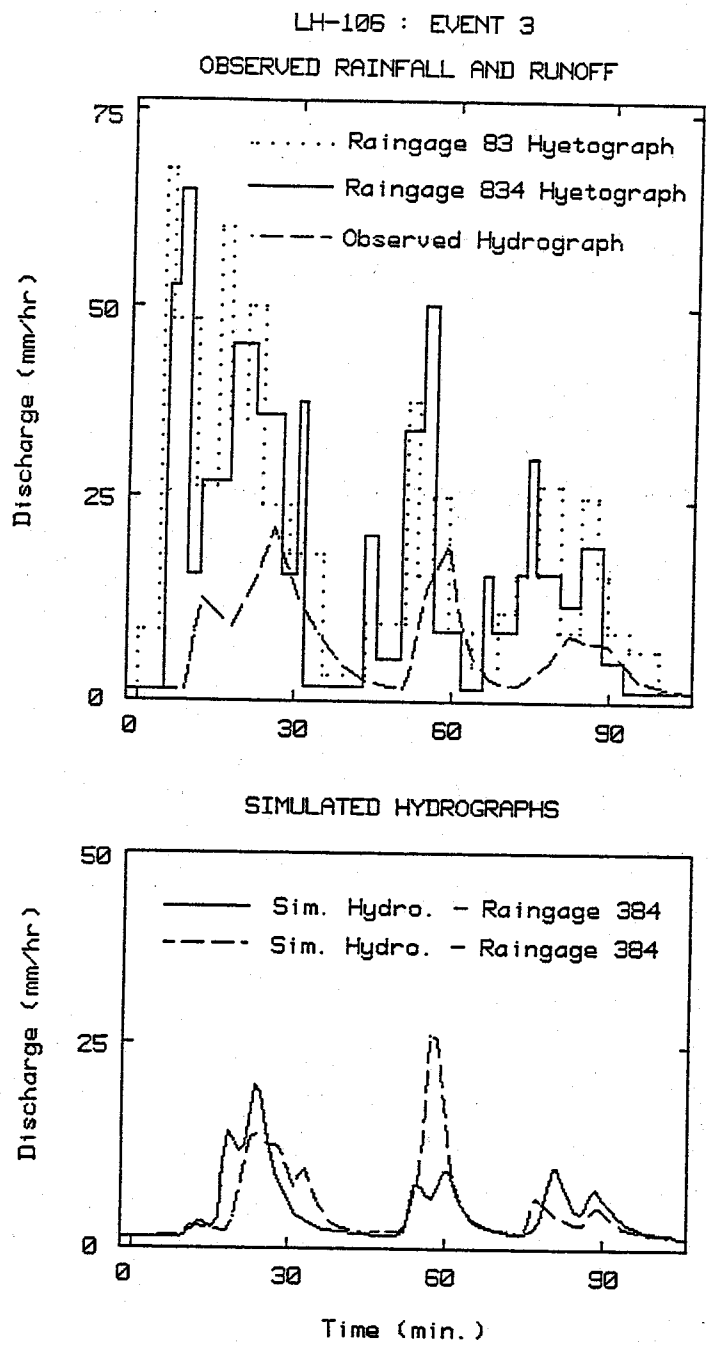

Figure 5.4 Runoff Simulations on LH-106 Using Rainfall from Adjacent Raingages for Event 3 (August 23, 1982)

on overland flow modeling. Lavee (1986) also found that total rainfall varied between 20 and 40% in distances of less than 100 m.

Turbulence effects on rain catch were documented by Neff (1977) and Hanson (1989). Neff used a pit gage adjacent to a normal, above ground, gage installation and found that the above ground gage underestimated total rainfall catch by an average of 15%. The undercatch increased to 30% as wind speed increased. Hanson (1989) found similar results using shielded and unshielded gages. A 15% undercatch in the unshielded gage resulted when surrounding wind speeds were approximately 10 m/s.

In addition to the topographic and meteorologic factors discussed above, mechanical and data reduction errors also contribute to differences in raingage observations. Chery and Beaver (1976) examined Walnut Gulch rainfall data processing and analyzed the measuring accuracy of several data reduction personnel on analog charts of different time and depth scales. For a typical range of storm sizes, they found that the integral squared error (IE) was less than 15% and typically ranged from 5 to 8% where:

$$IE = \frac{\left(\sum_{i-1}^{n} (r_a - r_r)^{1/2} \right)^2}{\sum_{i-1}^{n} r_a} \; x \; 100 : \quad i = 1,2,..,n \qquad (5.1)$$

where:

r_a = actual rainfall rate

r_r = read rainfall rate

This measure shows that overall measurement accuracy is quite good but masks inaccuracies in peak rainfall intensity measurement. Peak rainfall intensities determine peak runoff rate to a large extent in a watershed as small as LH-106. Further analysis of the data in Chery and Beaver (1976) shows that the average percentage difference in measured to actual peak rainfall intensity was 20%, with a coefficient of variation of 0.85 and maximum and minimum differences of 50 and 3%, respectively. Shirley (unpublished) examined the accuracy of rainfall intensities obtained by differencing the analog accumulated depth traces. He found that the accuracy decreases when the time interval used to compute rainfall intensities decreases. For 2-minute intensities, the maximum measurement error can be as large as the theoretically correct rate being measured.

Closer examination of Figure 5.4 suggests that actual spatial differences do exist between the two raingages and are not merely an artifact of data processing or

wind turbulence. The second peak is the result of a high intensity burst of rainfall on gage 384 that would be missed entirely if gage 83 were used alone. In an attempt to capture this additional information from multiple raingages, a space-time rainfall interpolation algorithm was developed.

In this algorithm, centroid coordinates of all plane and channel model elements, as well as raingages coordinates, are measured and input into KINEROSR. During runoff simulation, the intensities from surrounding gages are linearly interpolated to provide an element intensity. Details of the procedure are presented in Appendix C. Initially, it was not envisioned that rainfall interpolation would be used on this small scale; however, it was anticipated that interpolation would be required for modeling larger scale watersheds (Walnut Gulch subwatershed 11). The effects of incorporation of rainfall interpolation on the small Lucky Hills watersheds will be discussed more fully in the following chapter.

The primary point of the lengthy discussion of rainfall uncertainty is to bound the expectations of the calibration and verification exercise. With the uncertainty in rainfall input due to small- and large-scale variability, in addition to data processing errors, it is impossible to calibrate the model with a degree of certainty greater than the certainty of rainfall input data. This has been pointed out by numerous investigators (Hromadka 1987, 1987a; Hughes, 1989; Hughes and Beater, 1989; Bras and Rodriguez-Iturbe, 1976; Troutman, 1983) but not at the scale of 300 m. Comparison of Figures 5.2 and 5.3 also points out that runoff variations induced by rainfall variability far outweigh the 10% perturbations used in the sensitivity analysis.

This further justifies the selection of only three parameters (multipliers) for model calibration. The sensitivity of modeling results as a function of basin scale is discussed in more detail in the following chapter.

5.3 Model Calibration and Verification

5.3.1 Background

The goal of model calibration and verification for the four watersheds used in this investigation is to acquire confidence in the model and in the ability to make physically realistic interpretations regarding the geometric simplification process over a range of basin scales. The goal is not to find an "optimum" set of parameter multipliers, but a set that is reasonably close to optimum. In fact, Beven (1988a) argued that, because of the extremely complex nature of runoff generation, a true optimum solution and an ultimate validation may never be achieved. He argued that we must operate under a concept of "unknowability".

Given the "unknowability" of the spatial and temporal distribution of rainfall and its significant impact on simulated runoff, the points raised by Beven (1988a) must be given further consideration. The undersampling of the rainfall field often leads to a bias in estimated parameters. Troutman (1983, 1985) noted that spatial sampling errors of the precipitation field resulting from the use of a small number of raingages is the dominating factor causing bias in parameter estimates. The resulting bias can be so great that the final parameter estimates bear no resemblance to physically realistic values but are acting as mere fitting parameters. Final

parameters estimates from this investigation will be examined to ensure they are realistic.

5.3.2 Calibration and Verification Data

In keeping with the earlier methodology, a wide range of runoff event sizes and initial conditions will be employed in calibration and verification. There are several reasons for doing so. The first and most obvious reason is to ensure that some degree of generality (at least for basins similar to Walnut Gulch) can be attached to model conclusions and interpretations. Second, every attempt should be made to activate all states of the model so that the resulting parameter estimates used in the model will be unbiased in relation to event size or initial condition (James and Burges, 1982; Sorooshian et al., 1983). The events selected should also include complex, multipeaked hydrographs to more fully test model dynamics as it is relatively simple to fit single-peaked hydrographs (Beven, 1988b).

The calibration and verification events must be independent. In partitioning the events between the two sets, events outside the range of calibration will be held for the verification set. By doing so, the model's predictive capability beyond the calibration range can be assessed (Klemes, 1982). This will test whether the model has more power than regression by embodying causal process knowledge to allow extrapolation.

The importance of obtaining the best possible rainfall and runoff records for selection of the calibration and verification events cannot be overemphasized.

Minimization of observation errors in these records is a must. If significant data errors exist, parameter bias can result in the calibration, just as misrepresentation of rainfall inputs causes bias (Troutman, 1983, 1985). For this investigation, the selected events were chosen from a homogenous time period in which no changes were made to the measuring instrumentation. No major watershed management changes occurred for the period of time selected.

Extremely thorough data checking was conducted for each runoff station and raingage for all of the selected events. If any concerns became apparent during initial data selection from the computer data base, the original analog charts were scrutinized. If further questions persisted, the personnel who collected and processed many of the charts were consulted. It is interesting to note that many of the observation and data processing errors would not have been discovered unless runoff hydrographs and raingage charts from the same storm were examined simultaneously from nearby runoff flumes and raingages. This data redundancy, available in the nested Lucky Hills watersheds, greatly minimized possible observational errors.

A target of obtaining 30 "best possible, minimum error" rainfall-runoff events for each watershed was established. This figure was selected as a compromise between a reasonable number of test events and computational time constraints. The homogenous period of record on Lucky Hills largely constrained the number of useable events as well. Tables containing summary information on all of the rainfall-runoff data events for each of the four watersheds are presented in Appendix A. Frequency histograms of event runoff volume and peak runoff rate for 30 selected

events on LH-106 are presented in Figure 5.5 as a typical example of the data distributions. The histograms illustrate the large percentage of small events in the selected set. A set of 27, 27, and 25 events were selected for LH-106, LH-102, and LH-104, respectively. The set consisted of all events recorded in the homogenous time period that were not rejected due to possible errors and met a minimum runoff criteria. A minimum runoff volume of 0.25 mm over the basin was selected. This depth of runoff over the basin is consistent with the measuring resolution of the raingages. Trying to discern runoff dynamics from smaller events only invites trouble in parameter estimation, as observation error most certainly will dominate the rainfall-runoff simulation.

To satisfy the requirements of full model testing over a range of event sizes and initial conditions, a matrix of relative event size versus dry to wet initial conditions was established to aid in calibration event selection. The initial set of 30 events was ranked by observed runoff volume and split into three sets of ten corresponding to small, medium, and large events. The primary purpose of examining events with different initial conditions is to ensure full exercise of suction-related infiltration dynamics. Another way of exercising this model component is to inspect rainfall hyetographs and select storms which peak early or late. The suction terms will be most important for dry initial conditions and early-peaking storms and least important for wet initial conditions and late-peaking storms. Therefore, both initial relative soil saturation (SI) values obtained from CREAMS and storm patterns were used in selecting events covering a range of conditions for fully activating

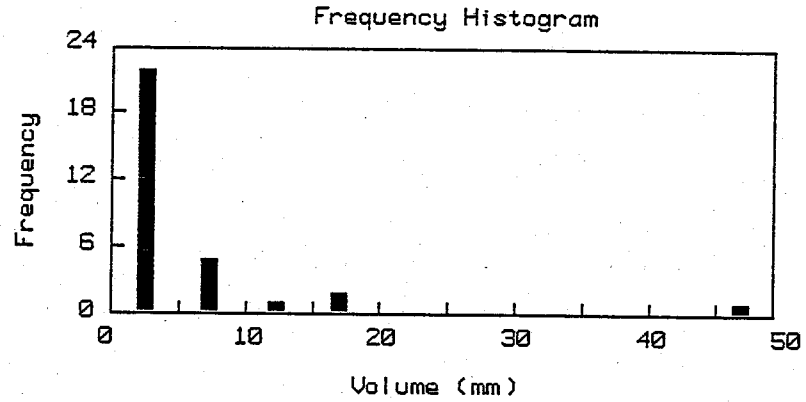

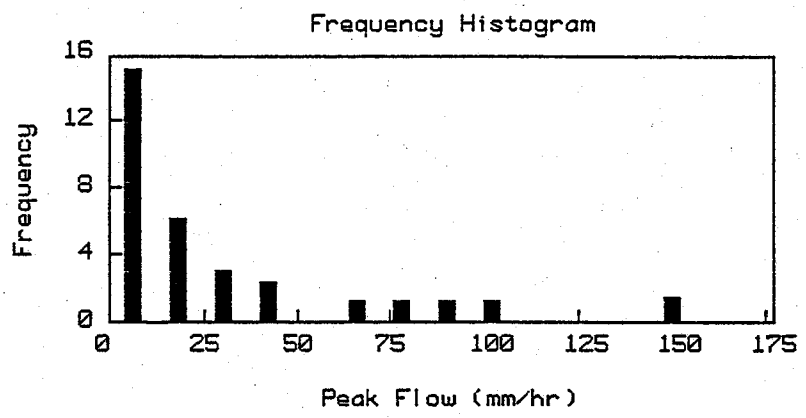

Figure 5.5 Frequency Histograms of Runoff Volume and Peak Runoff Rate for LH-106 for the Selected Calibration and Verification Events

infiltration dynamics. A schematic of the selection matrix with rough storm pattern sketches for LH-106 is shown in Figure 5.6. In addition to the nine calibration conditions depicted in Figure 5.6, event 53 was added at the (medium storm size - wet initial condition) location. Because of the close proximity of LH-102 and LH-104, the same events were selected for calibration in these watersheds. One event was dropped from the LH-104 calibration set after an error was detected and calibration proceeded with nine events. The remaining events were held for independent verification.

The same strategy was employed for calibration event selection for subwatershed 11 (WG11, area = 631 hectares). However, due to the large spatial scales, all of the combinatorics of possible initial conditions and thunderstorm cell locations could not be covered with ten calibration events. The type of conditions found in WG11 that differ from the Lucky Hills watersheds are storm center location (lower or upper portion of the basin) and dry or wet initial channel conditions, as channel losses are very important in WG11. These limitations are recognized, but to allow ready comparison of results across all basins, ten events were used for calibration in WG11 as well.

5.3.3 Measuring Model Performance

Numerous measures have been suggested to gauge model performance. Investigations of various measures have been presented by Aitken (1973), James and Burges (1982), Nash and Sutcliffe (1970), McCuen and Snyder (1975), Willmott

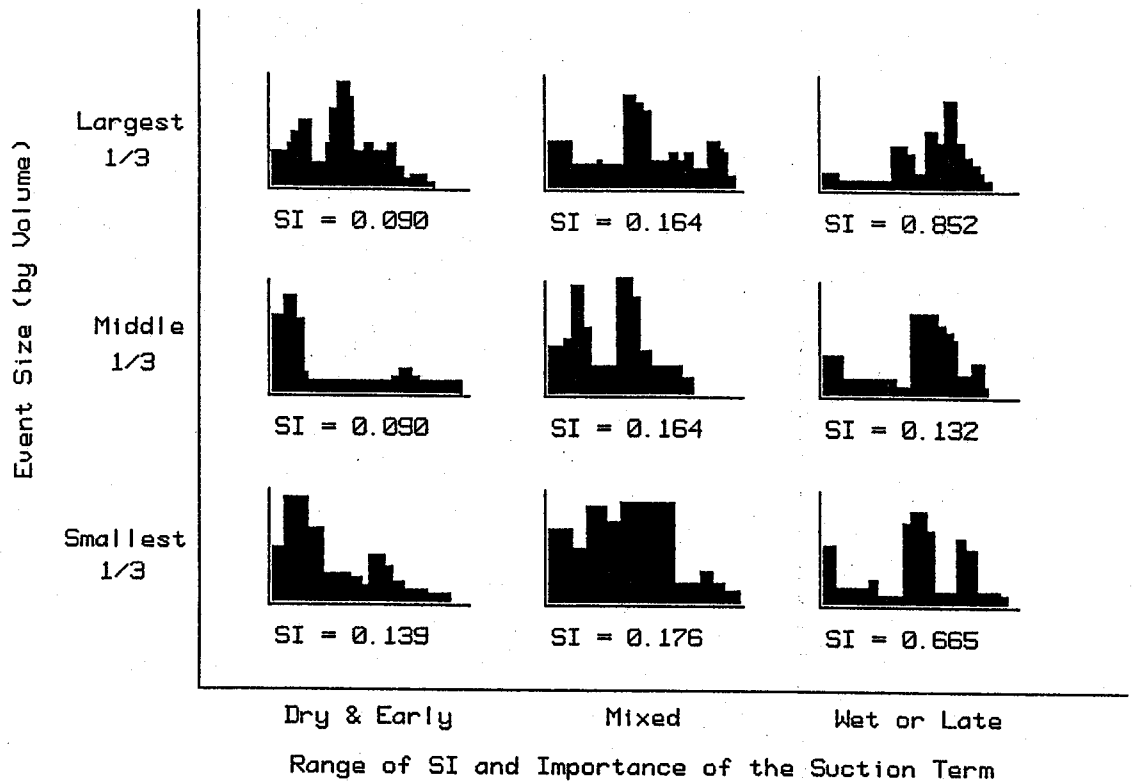

Figure 5.6 Calibration Event Selection Matrix for LH-106

(1982), and Willmott et al. (1985). Although many measures can be used, Martinec and Rango (1989) cautioned that using too many criteria can cause difficulty in assessing model performance. The primary measure selected to assess model performance in this study is the coefficient of efficiency, E, introduced by Nash and Sutcliffe (1970). The coefficient is computed as follows:

$$E = 1 - \left[\frac{\sum_{i=1}^{n} (\hat{Q}_i - Q_i)^2}{\sum_{i=1}^{n} (Q_i - \overline{Q})^2} \right] ; \quad i = 1,2,..,n \qquad (5.2)$$

where:

Q_i = simulated model runoff summary variable

Q_i = observed runoff summary variable

Q = mean of Q_i for all events i = 1 to n.

Q_i can be time varying discharge, event runoff volume, event peak runoff rate, or time to peak rate. For this study only event runoff volume and event peak runoff rate will be used for Q_i in Equation (5.2).

The coefficient of efficiency was selected because it is dimensionless and is easily interpreted. If the model predicts observed runoff with perfection, E = 1. If E < 0, the model's predictive power is worse than simply using the average of

observed values Q_i. For this study, the mean of the runoff summary variable will be computed from the Q_i values separately in the calibration and verification event subsets. Martinec and Rango (1989) stressed that the mean for the period of interest should be used and not a long-term mean (continuous simulation in their case) as this will artifically improve the efficiencies. This measure has also been used by other investigators to assess event model performance on Walnut Gulch (Hughes, 1989; Hughes and Beater, 1989) and other small experimental watersheds (Loague and Freeze, 1985; Loague, 1986; Loague, 1990). Comparison of results from this study with other investigations will be facilitated by using this measure.

In addition to this measure, the usual unweighted squared difference measure was computed for the entire event hydrograph allowing for a time shift between observed and simulated hydrographs. Timing-based measures such as time to peak and differences in observed and simulated runoff without allowing a time shift were not computed for the following reason. The response time of the small Lucky Hills watersheds is on the order of minutes for a high-intensity rainfall event. Because the raingage and runoff clocks are not the same, the error in clock time can be on the order of the response time. The time shift in computing the least squares differences was introduced to minimize the clock timing error, as very large penalties are introduced during a steep hydrograph rise for very small timing differences.

The primary runoff variables used in model calibration and verification are total event runoff volume and peak runoff rate. More weight will be given to runoff volume for determining infiltration related multiplier parameters. Peak runoff rate

will be given more weight in determining the roughness multiplier. For overall consideration, preservation of runoff volume will be given highest priority. For the small watersheds, this should preserve peak rate relatively well, as a high correlation exists between runoff volume (V) and peak rate (Qp). For the selected LH-106 runoff events, whose frequencies of V and Qp are shown in Figure 5.4, a correlation coefficient of 0.9 exists between V and Qp, with a standard error of estimate of 16 mm/hr in the dependent variable Qp. For the ten calibration events on each watershed, the coefficient of efficiency (E) will be computed for both V and Qp. The same statistic is used to assess the model simulations of runoff volumes and peaks of the verification events. For the verification events, the model is assessed for both forecasting efficiencies (E_f) and prediction efficiencies (E_p). Forecasting efficiencies are computed using matched sequences of simulated and observed runoff variables. Prediction efficiencies are computed after the simulated and observed runoff variables are independently ranked. This measure is more useful in assessing the model's ability to reproduce typical runoff distributions for frequency analysis. Forecasting efficiency is the more rigorous of the two tests.

Although the coefficient of efficiency is a widely used measure with easily interpretable properties, it is not without its shortcomings. As Loague (1990) pointed out, large runoff event variables are more heavily weighted, producing better efficiencies if large events are simulated with more accuracy than small events. However, if large events are avoided and a narrow range of event sizes is used, the coefficient can also artificially penalize the user. Imagine a set of events that all

have the same runoff volume. The denominator in Equation (5.2) will vanish, resulting in E = $-\infty$, even if the model simulates runoff almost perfectly. The smaller the observed data variance [a small denominator in Equation (5.2)], the better the model must perform to achieve comparable efficiencies. A slight bias toward better simulation of large events is not considered a major problem because they account for a large percentage of total runoff volume and often pose greater management problems. Therefore, Equation (5.2) will be used to compute E over the range of events selected with the bias toward large events kept in mind. Khan (1989) offered a methodology for model evaluation of bands of runoff ranges, but a great deal of data is required and the method cannot be used easily in calibration.

The mean and standard deviation of simulated V and Qp will also be presented for comparison with the same statistics for the observed data. Formal hypothesis testing for comparing observed and simulated distributions will not be made given the small samples used in this study, the required underlying distribution assumptions, and the arbitrary selection of confidence levels required. The means and standard deviations are presented for qualitative assessment and are only intended to provide additional summary information to the computed efficiency coefficients.

5.3.4 The Search for Acceptable Model Parameters

Efficiency coefficients for V and Qp are used as the objective functions to judge model performance at various parameter locations. To reiterate, the

parameters in this study are the uniform multipliers M_K, M_C, and M_R applied to the distributed, field estimated, values of Ks, C_v, and R1 (roughness), respectively. The parameter space is, therefore, three-dimensional, and the goal is to find a set of parameter multipliers within this space that will acceptably reproduce observed runoff when they are applied to their respective field estimated model parameters.

Numerous algorithms exist to find optimum parameters for a specified objective function. For nondifferentiable functions, often encountered in rainfall-runoff models, a direct search algorithm such as the simplex method presented by Nelder and Mead (1965) is commonly employed. However, these algorithms are not without their problems. The values of final, "optimal" parameters obtained by the algorithm are often a function of the starting location, step size, and stopping criteria. Many times local, instead of, global maxima (for the objective function used here) are obtained. Selection of an inappropriate objective function for the error data structure and poor model structure with significant parameter interactions can also cause great difficulty for many optimization algorithms (Sorooshian and Dracup, 1980; Sorooshian and Gupta, 1983).

Remember that the goal of model calibration in this study is not to find the optimum set of parameter multipliers but to find a near optimum set that will ensure that the model can be used and interpreted with confidence. Beven (1989) argued that an "optimum" model is unlikely given the watershed complexities rarely addressed in either data collection or model structure. Given these difficulties in application of optimization algorithms, an "intelligent" grid search for acceptable

model parameters was undertaken for this study. Intelligent in this situation implies a redefinition of the search space based on results from simulations in a small sample of the parameter space. To examine response surface characteristics, a griding procedure must be conducted anyway. Indeed, Beck (1987) pointed out the failure of many constrained optimization procedures and argued for griding out the entire response surface with the availability of more computing power. Beck goes on to note that there will be relatively few rewards by enhancing algorithmic optimization methods.

The subgrid search was carried out for each of the watersheds to obtain acceptable parameter multipliers M_K, M_C, and M_R. Table 5.3 contains the final multipliers obtained for each watershed. The following section addresses the acceptability of these multipliers. With regard to Troutman's (1983, 1985) concerns, it should be stressed that in all cases when the multipliers are applied to their respective distributed, field-estimated, parameters, realistic parameter estimates are obtained. The resulting Ks values ranged from 2.4 to 19.8 mm/hr for Ks, 0.02 to 0.09 for Manning's roughness, and from 0.8 to 1.0 for C_v. The response surface for M_R = 2.2 of LH-104 calibration efficiencies for V and Qp are show in Figure 5.7. The plots indicate that some interaction between M_K and M_C does exist. It should also be noted that the best combination of M_K and M_C for runoff volume (0.55 and 0.8) does not coincide with the best combination for peak rate. However, the Qp efficiency response surface is very flat and still yields an efficiency of approximately 0.97 for M_K = 0.55 and M_C = 0.8. M_R was selected primarily on the basis of Qp

Table 5.3. Final Multipliers (Calibration Parameters)

Basin	M_K	M_C	M_R
LH-106	0.3	1.0	1.0
LH-102	0.55	1.0	2.2
LH-104	0.55	0.8	2.2
WG11	1.325	1.0	1.25

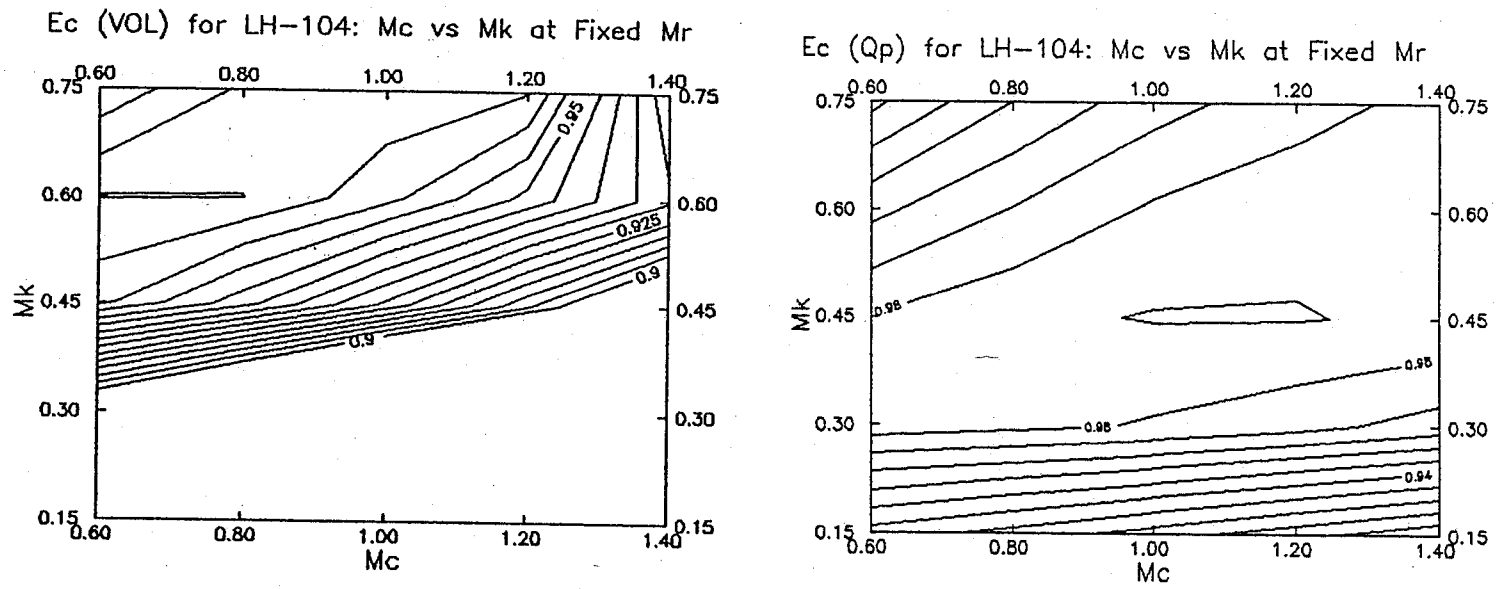

Figure 5.7 Response Surface Plots of Volume and Peak Rate Calibration Efficiency at Fixed M_R for LH-104

efficiencies. Figure 5.8 shows the variation in volume and peak rate efficiency as a function of the roughness multiplier M_R for fixed M_K and M_C. The figure illustrates that M_R has very little effect of runoff volume as was shown in the sensitivity analysis.

Figures comparable to 5.7 and 5.8 were examined for the other watersheds to aid in the selection of final multipliers. A more detailed examination of these figures is carried out in the following chapter when watershed response as a function of basin scale is discussed. By examination of the efficiencies over a range of the multiplier parameter space, a set of multipliers for each watershed has been selected. The question of acceptability of these parameter remains. Does the model reproduce observed runoff behavior when the final multipliers are applied to the distributed field estimated model parameters?

5.3.5 Verification of Model Acceptability

Calibration and verification efficiencies for observed and simulated runoff volumes and peak rates are shown in Table 5.4 for each of the watersheds. Efficiency coefficients for both forecasting and prediction are included. Table 5.5 contains summary statistics and average sum of squared differences (allowing for a time shift) for the watersheds. Examination of the tables supports the conclusion that the model performed very well for the Lucky Hills watersheds and marginally well for WG11 for independent verification event sets.

Note that the calibration efficiencies for WG11 are quite good. Possible reasons for the degradation of model results during WG11 verification were alluded

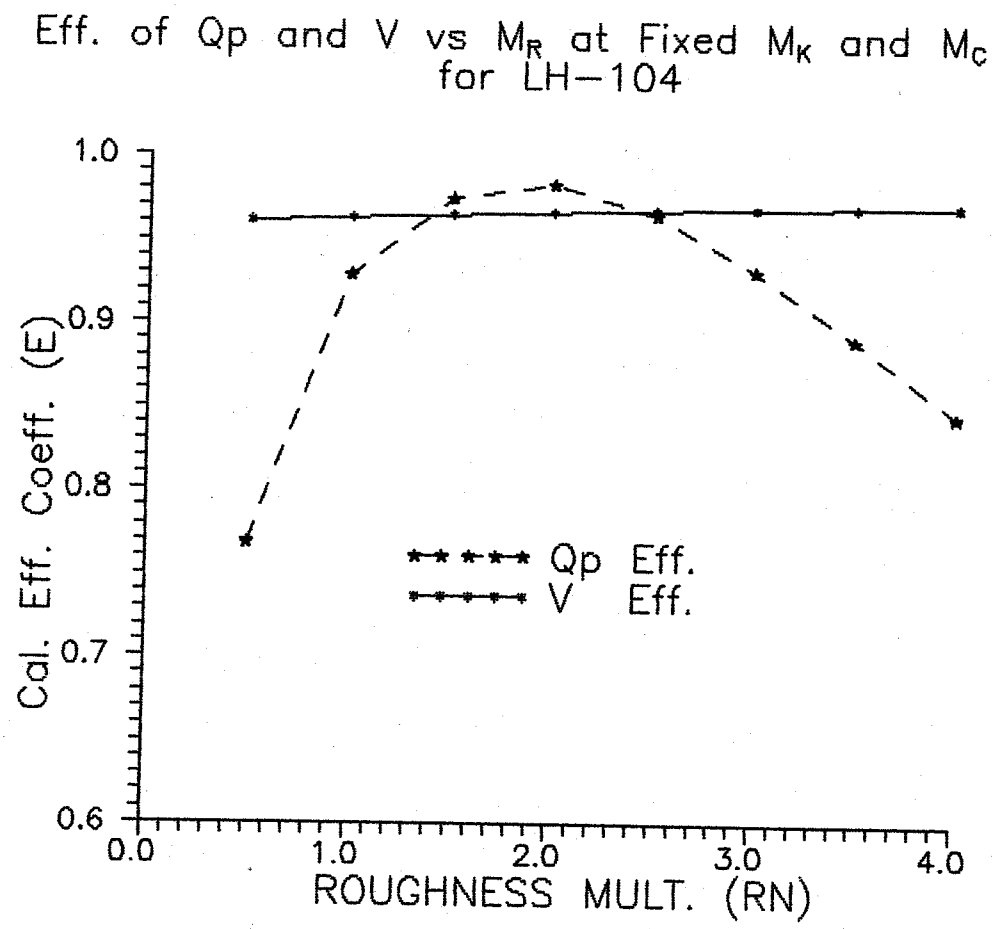

Figure 5.8 Response of Volume and Peak Rate Calibration Efficiency to M_R for Fixed M_K and M_C for LH-104

Table 5.4. Calibration and Verification Forecasting and Prediction Efficiencies for Runoff Volume and Peak Rate for All Study Basins

		Calibration Efficiencies				Verification Efficiencies			
		E_f		E_p		E_f		E_p	
Basin	Area (ha)	V	Qp	V	Qp	V	Qp	V	Qp
LH-106 n_c = 10 n_v = 17	0.36	0.98	0.95	0.98	0.98	0.98	0.79	0.98	0.83
LH-102 n_c = 10 n_v = 17	1.46	0.97	0.97	0.97	0.97	0.93	0.93	0.94	0.95
LH-104 n_c = 9 n_v = 16	4.40	0.97	0.98	0.97	0.98	0.99	0.96	0.99	0.97
WG11 n_c = 10 n_v = 20	631	0.86	0.84	0.96	0.90	0.49	0.16	0.70	0.25

n_c = number of calibration events
n_v = Number of verification events

Table 5.5. Mean and Standard Deviation for Volume and Peak Rates and Average Sum of Squared Deviations for Calibration and Verification Events Sets for All Study Basins

Basin	Area (ha)	Event Set	Type	Num. of Events	V (mm) Mean	V (mm) S.D.	Qp(mm/hr) Mean	Qp(mm/hr) S.D.	Average Sum of Sq. Dev. $(mm/hr)^2$
LH-102	0.36	Calib.	Obs.	10	4.74	5.03	34.2	36.8	
			Sim.	10	4.78	4.98	35.6	36.8	520
		Verif.	Obs.	17	6.22	11.4	27.1	36.7	
			Sim.	17	6.96	12.1	33.3	38.5	1170
LH-102	1.46	Calib.	Obs.	10	4.57	4.48	27.6	27.8	
			Sim.	10	4.36	4.61	26.5	27.7	258
		Verif.	Obs.	17	6.01	9.88	24.6	26.6	
			Sim.	17	6.76	12.1	25.3	31.1	688
LH-104	4.40	Calib.	Obs.	9	4.27	4.49	28.0	30.1	
			Sim.	9	4.44	4.99	24.8	29.3	343
		Verif.	Obs.	16	6.37	11.9	26.3	34.6	
			Sim.	16	6.76	12.3	23.0	30.2	897
WG11	631	Calib.	Obs.	10	2.54	1.88	4.37	4.25	
			Sim.	10	2.39	2.03	4.04	3.72	75
		Verif.	Obs.	20	2.16	1.78	4.30	3.25	
			Sim.	20	1.89	2.62	3.78	5.52	110

to earlier. In WG11, significant large-scale rainfall variability is present in most rainfall events and channel losses are much more important. With a small calibration set of ten events, many of the combinations of storm pattern and channel initial conditions as well as storm size and basin initial conditions could not be covered. Thus, the calibrated parameters may not have captured sufficient information to allow modeling of events in the verification set that are distinctly different from those in the calibration set. It should also be noted that the level of field data collection in WG11 was not as intensive as in the Lucky Hills watersheds due to manpower constraints. This, of course, leads to greater uncertainty in the initial parameter estimates. Additional discussion of model performance as a function of basin scale in presented in Chapter 6.

The modeling results presented here are also compared to other modeling efforts using a distributed kinematic wave type model on another USDA Agricultural Research Watershed and on Walnut Gulch with a conceptual model. Loague and Freeze (1985), Loague (1986), and Loague (1990) did extensive work on the R-5 watershed (area = 0.1 km^2) near Chickasha, Oklahoma. Their best forecasting efficiencies for volume and peak rate were 0.25 and 0.71, respectively, when calibration with Ks adjustments were done. The calibration in this study used three parameters which would help improve efficiencies. However, by examining the final parameter multipliers used for LH-106 (Table 5.3), it is apparent that only one parameter (M_K) was adjusted in the calibration, yet E_f of 0.98 was obtained for verification volumes in this study. Loague (1990) obtained slightly improved results

when additional soils information was incorporated and no calibration was done. R-5 is significantly different from Walnut Gulch, and some data problems were encountered by Loague (1990); therefore, comparisons to the present study's results may not be entirely fair.

More comparable results can be found in Hughes and Beater (1989), who used data from six Walnut Gulch watersheds (43 large events), with a lumped and semidistributed conceptual model. Their best forecast efficiencies were -0.02 and 0.01 for the lumped and semidistributed version of their more complex model that did not allow parameter adjustment for verification events. Using model parameters predicted by basin and climate measures while still allowing calibration, Hughes (1989) obtained a calibration and verification efficiency of 0.07 and 0.03, respectively, for Walnut Gulch runoff data. It is not clear how Hughes and Beater (1989) and Hughes (1989) computed efficiencies, but due to the dimensionless nature of the measure, it still provides a fair indication of their modeling results on Walnut Gulch watersheds.

The summary statistics above demonstrate that the model simulations are, by and large, very good for the Lucky Hills watersheds and relatively good (in comparison to other studies) for WG11. The efficiencies and statistics presented in Tables 5.4 and 5.5 embody a great deal of information for the entire calibration and verification event sets. To more fully evaluate model performance, visual presentation of individual events is offered. Visual analysis, although subjective, is still a valuable tool for model evaluation Willmott et al. (1985).

Figures 5.9 to 5.12 contain scatter plots of observed versus simulated runoff volumes and peak rates for the calibration and verification event sets. The figures are arranged from small (Figure 5.9) to large (Figure 5.12) basin size. These figures further confirm the conclusions drawn above regarding model performance for the Lucky Hills and WG11 watersheds. It should also be noted that the largest runoff event on record for Lucky Hills (Event 63), which is included in the verification set, is well predicted for all the Lucky Hills watersheds. For these basin scales, the model has extrapolation capability as it simulates runoff from events well outside the calibration range. The scatter plots for the WG11 verification set show a trend of underprediction for small events and over prediction for large events. However, the WG11 simulations cannot be dismissed outright as being unacceptable.

For yet a more detailed model assessment, individual hydrographs for the worst and best (near best in some cases) events in the calibration event set are presented. For all of the Lucky Hills watersheds, the worst simulation occurred for event 73. This is also the smallest event, by observed runoff volume, included in the calibration set. The worst and best simulations on WG11 occurred on July 24, 1986 and on August 4, 1980, respectively. The worst simulation on WG11 also corresponded to the smallest event of the calibration set. A single best event on all of the Lucky Hills watersheds could not be selected; therefore, event 62 was selected as a "near best" event for the three Lucky Hills watersheds. A single "near best" event is desired in order that comparisons of the hydrographs can be made across a range of basin scales in Lucky Hills. In addition, for the LH-106 and LH-102 worst and best

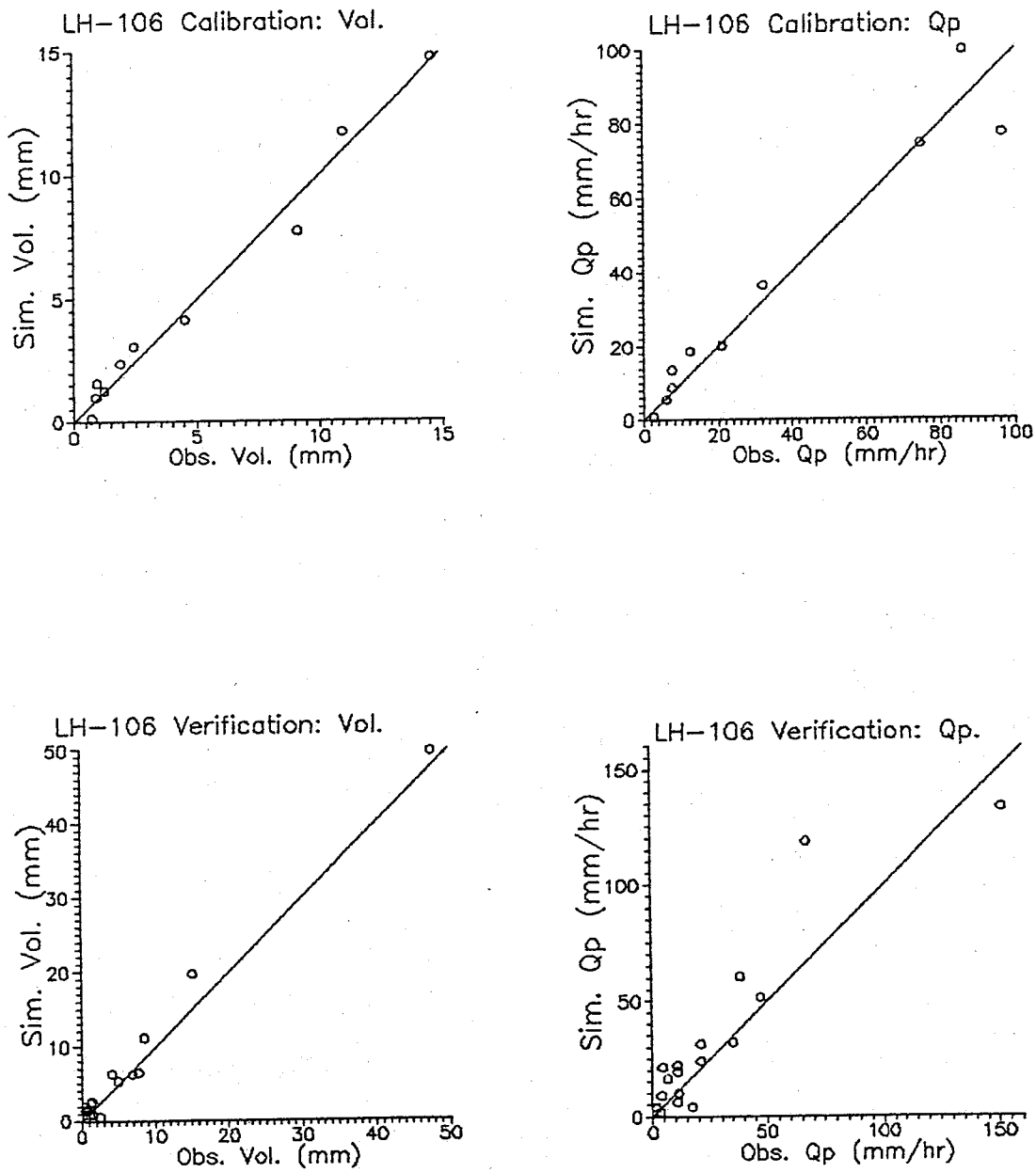

Figure 5.9 LH-106: Observed Versus Simulated Volumes and Peak Rates for Calibration and Verification Event Sets

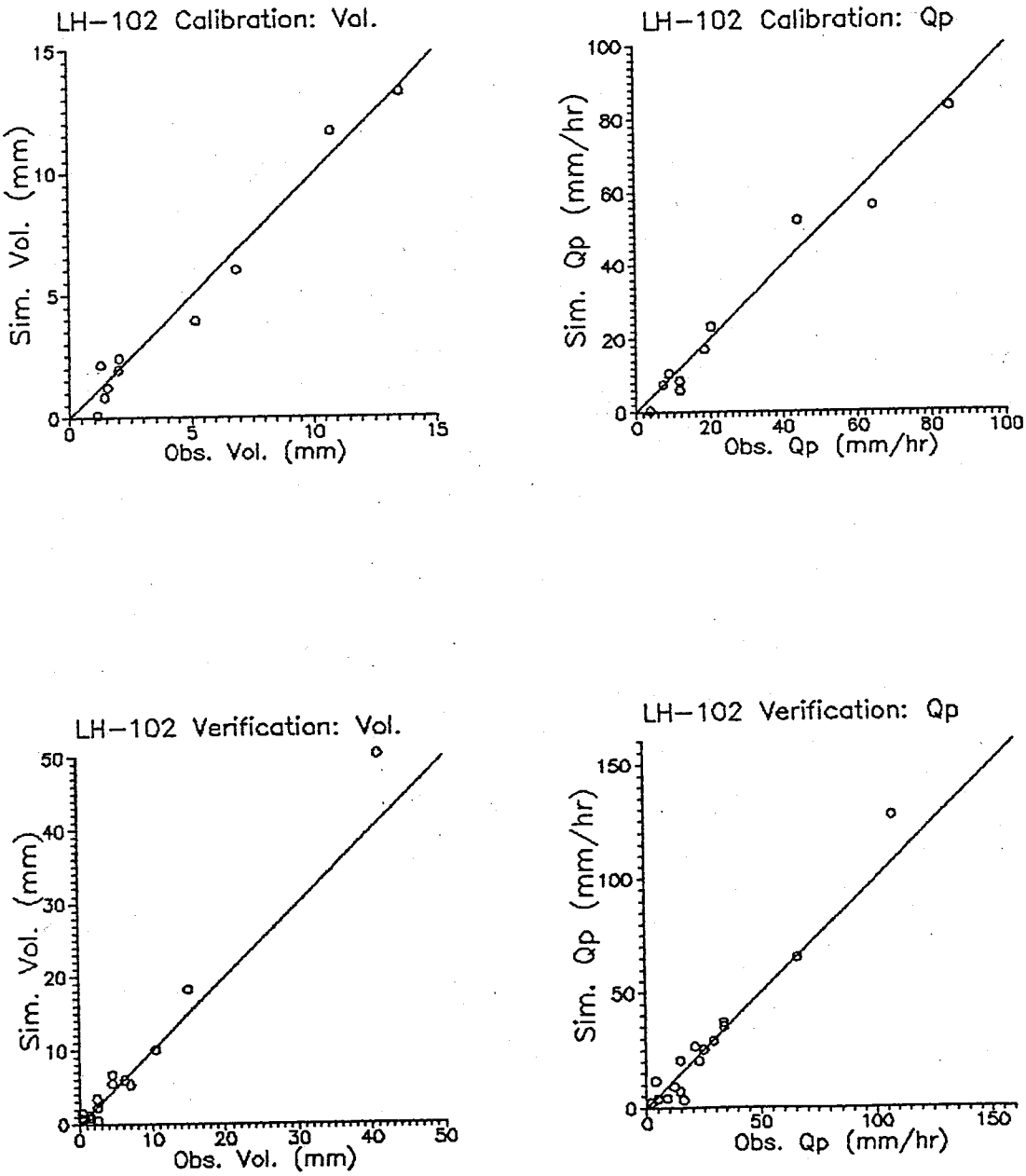

Figure 5.10 LH-102: Observed Versus Simulated Volumes and Peak Rates for Calibration and Verification Event Sets

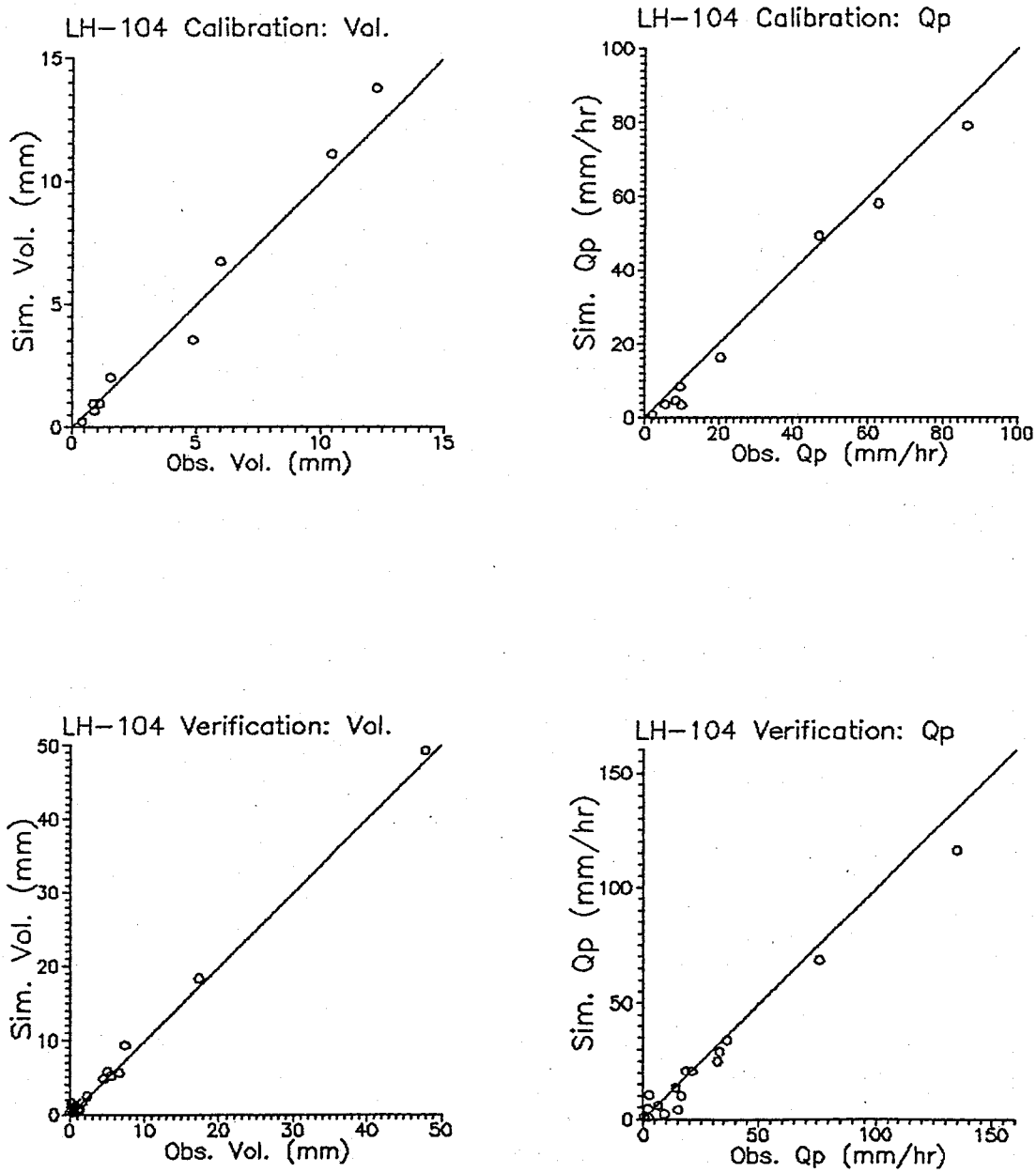

Figure 5.11 LH-104: Observed Versus Simulated Volumes and Peak Rates for Calibration and Verification Event Sets

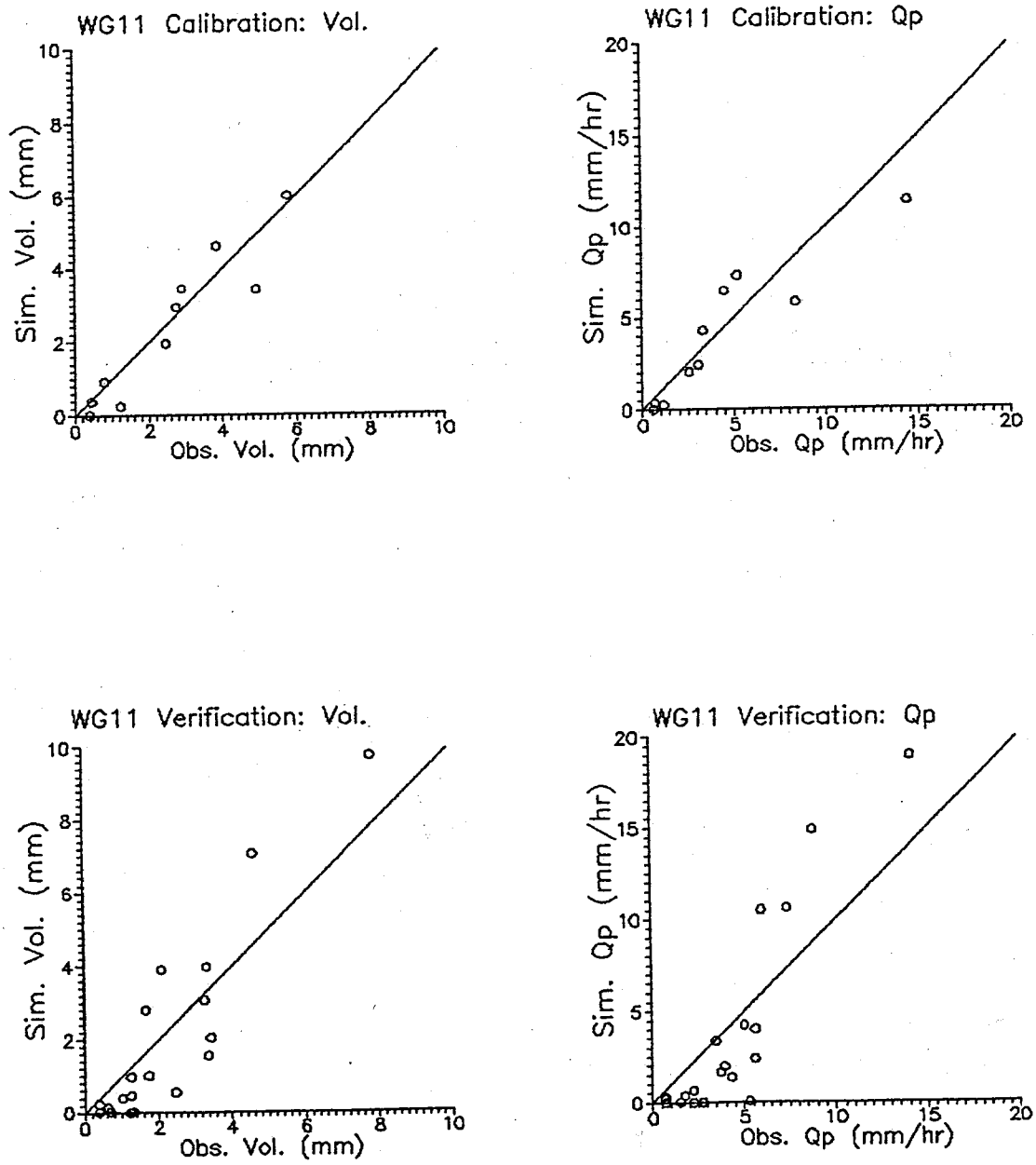

Figure 5.12 WG11: Observed Versus Simulated Volumes and Peak Rates for Calibration and Verification Event Sets

plots, the corresponding model simulations using the final parameter multipliers from LH-104 are presented. Because LH-106 and LH-102 are subbasins of LH-104, this will allow visual assessment of internal model consistency.

The best and worst calibration simulation hydrographs for all the basins, in ascending basin drainage area, are shown in Figures 5.13 to 5.16. Timing errors of approximately eight to ten minutes or less are irrelevant in the Lucky Hills watershed, as clock error could easily be this large. The best or near best simulations occur for the larger events for all of the watersheds, and the worst simulations occur for the smallest calibration event for all basins. These small events have observed runoff volumes and peak rates that are smaller by more than a factor of ten than any of the largest three events in the calibration set. For events of this size, the uncertainty associated with measurement error can become a large percentage of the observed runoff. The nonlinearities in the infiltration process will also tend to dominate the rainfall-runoff transformation for such small events as was illustrated in Chapter 2.

The important issue of internal model accuracy can be partially addressed by examining the third best simulations in LH-106 and LH-102 shown in Figures 5.13 and 5.14. In these figures, the hydrographs obtained from using the final LH-104 multipliers on the internal LH-106 and LH-102 basins are illustrated. For the larger event (#62), very good internal simulations were obtained using the overall, larger LH-104, basin parameter multipliers. The same cannot be said for the small event (#73), as simulations were very poor for this event even when using parameter

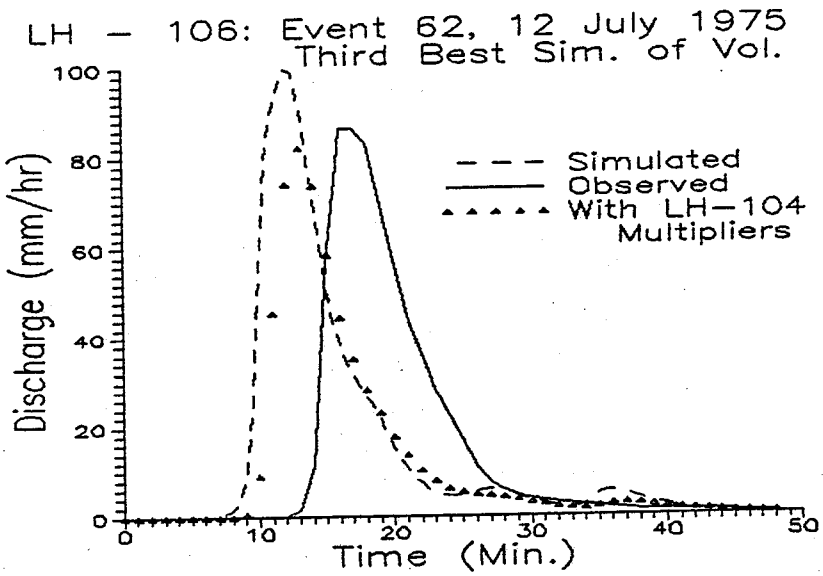

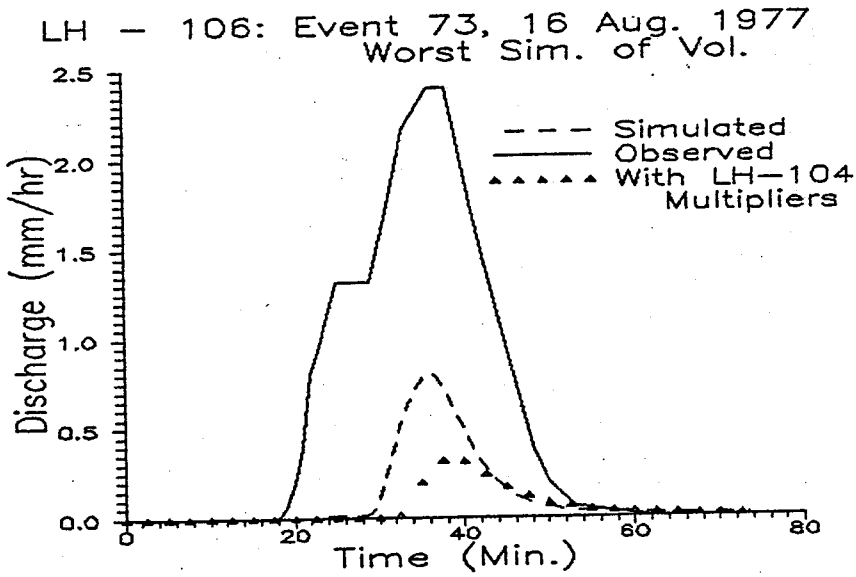

Figure 5.13 LH-106: Third Best and Worst Calibration Hydrographs Based on Volume and Comparable LH-104 Model Hydrographs Using LH-104 Multipliers

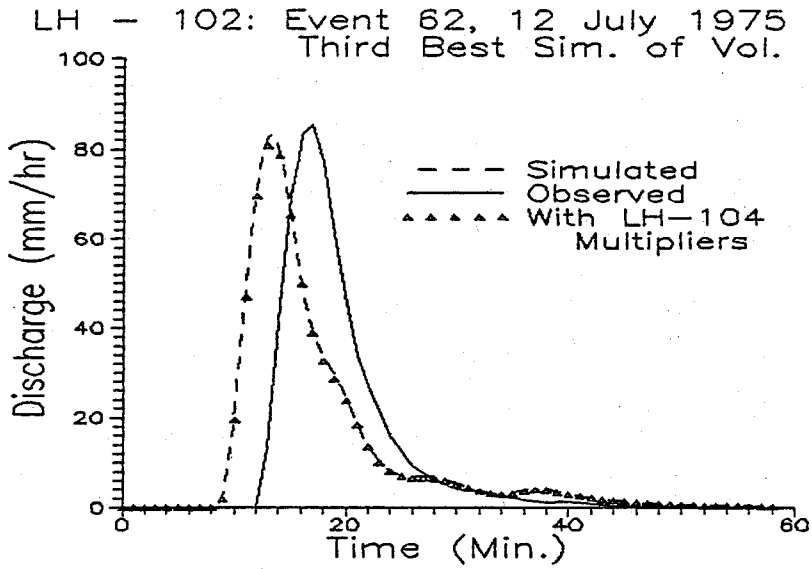

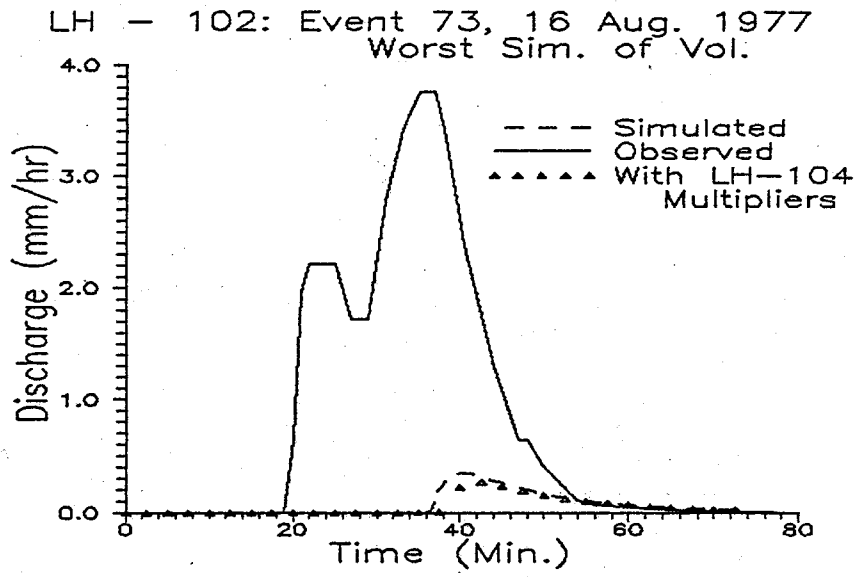

Figure 5.14 LH-102: Third Best and Worst Calibration Hydrographs Based on Volume and Comparable LH-104 Model Hydrographs Using LH-104 Multipliers

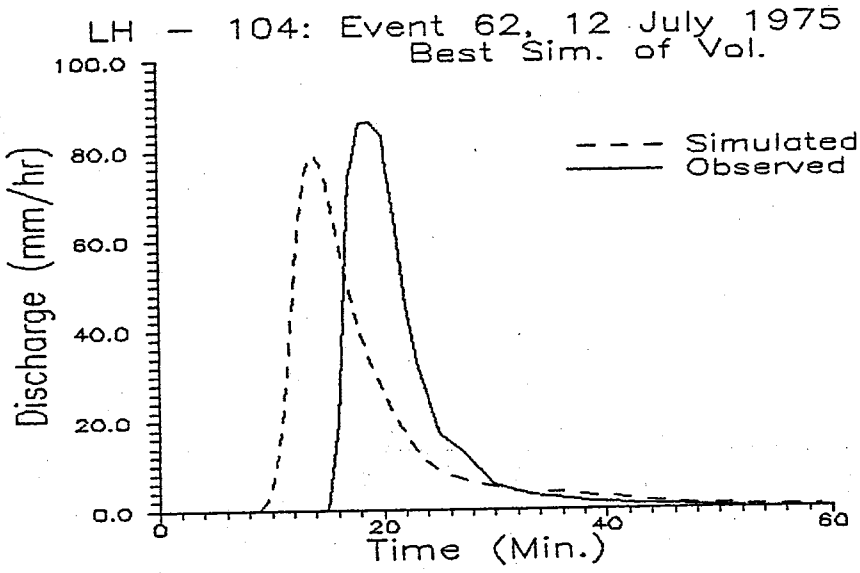

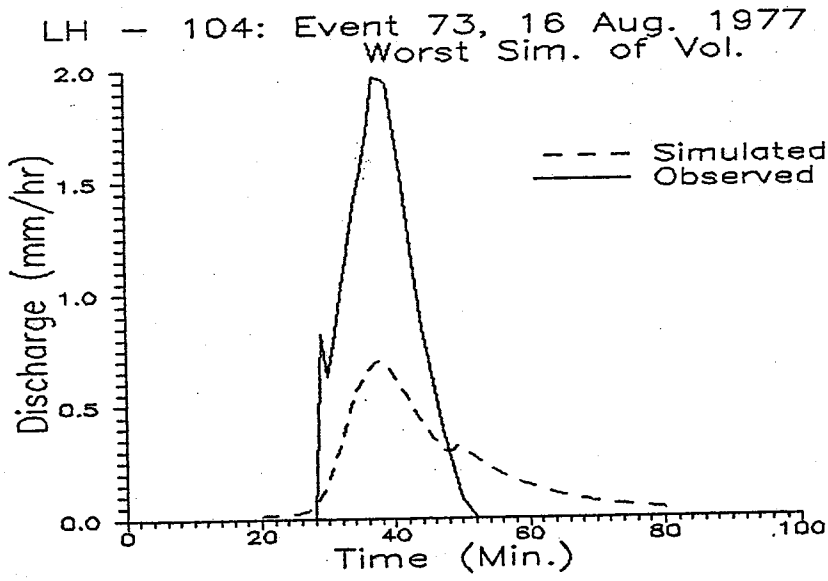

Figure 5.15 LH-104: Best and Worst Calibration Hydrographs Based on Volume

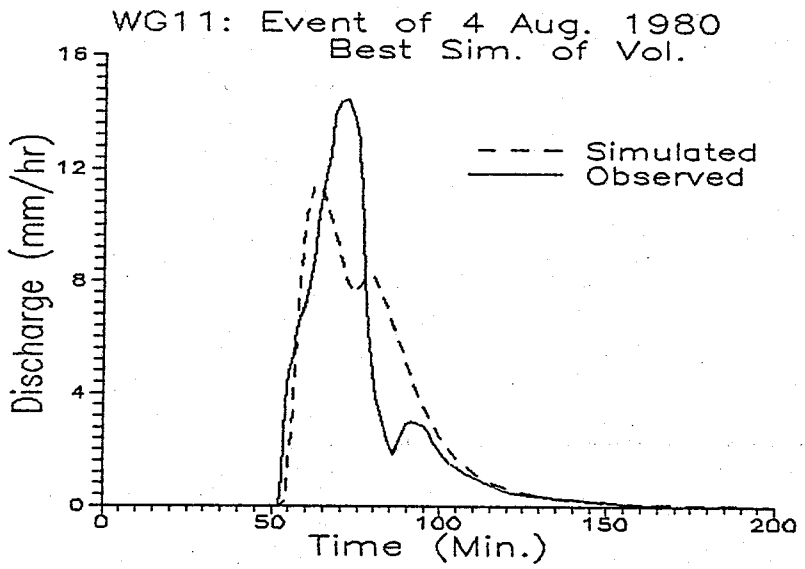

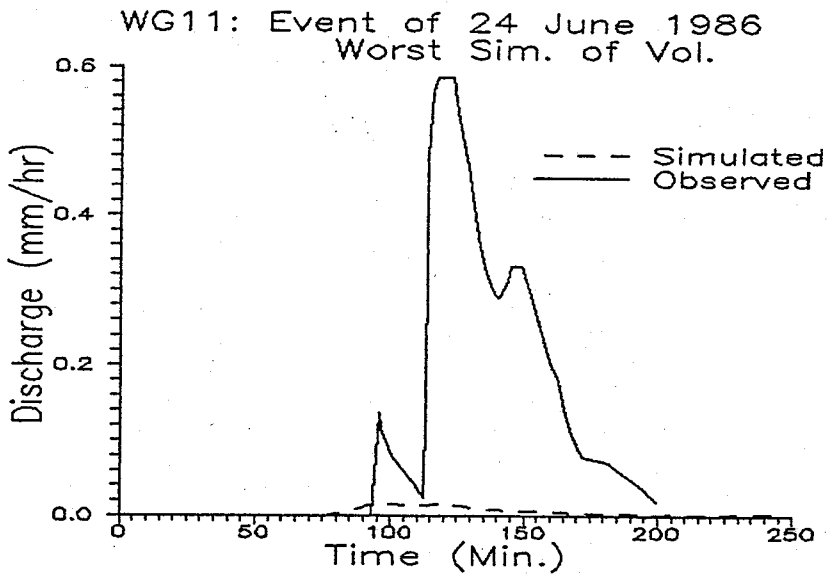

Figure 5.16 WG11: Best and Worst Calibration Hydrographs Based on Volume

multipliers obtained for the individual internal watersheds. An overall assessment of internal model accuracy is obtained by recomputing E_f for LH-106 and LH-102 when the parameter multipliers for LH-104 are used in the internal catchment simulations. For LH-106, using LH-104 multipliers, the calibration forecast efficiency (E_f) is 0.91 and 0.86 for runoff volume and peak rate, respectively. Comparable efficiencies for LH-102 are 0.96 and 0.97. Therefore, using the LH-104 multipliers caused virtually no change in the LH-102 efficiencies and about a ten percent decrease in the efficiencies for LH-106 (see Table 5.4). The coefficient of efficiency is influenced to a greater extent by the larger events in the set of interest. The good efficiencies obtained by using LH-104 multipliers for the internal basin suggest a good deal of internal model accuracy for medium to large events.

5.4 Conclusions

Sensitivity analysis was carried out on the smallest watershed analyzed (LH-106) to identify parameters to be used in model calibration. Parsimony of parameters was obtained by using parameter multipliers which scale, distributed, field estimated parameters linearly. The sensitivity analysis justified the selection of three overall watershed parameter multipliers. The three multipliers were M_K, M_C, and M_R, which are applied to the distributed model parameters Ks, C_v, and R1 (roughness), respectively.

Model performance was measured primarily by the coefficient of efficiency (E: Nash and Sutcliffe, 1970) for runoff volume and secondarily for peak runoff rate.

Using E as an objective function, a search through the three-dimensional calibration space defined by the three multipliers was carried out to find acceptable, near optimum multipliers. Loague (1990) and Beven (1989) argued that if any model calibration is done, our so-called "physically-based" models reduce to merely black-box conceptual models. This study argues that because it is impossible to perfectly measure initial model parameters in the field, some calibration is justified. Because hydraulic roughness values are subjectively estimated and soil textural properties were used to crudely estimate infiltration-related soil parameters, the initial uncertainty in these parameters is high. Therefore, calibration to obtain refinements to these estimates is justified.

After calibration, model performance was verified using an independent set of rainfall-runoff events. Results indicate that the model performs very well for all of the Lucky Hills watersheds. Model performance falls off for WG11, but is still very good when compared to related studies. In all basins, the model performance was much better for larger events. Small events were not simulated well, as infiltration nonlinearities, and measurement uncertainties tend to dominate runoff generation in these cases.

In addition, internal model accuracy was shown to exist for medium and large events in the Lucky Hill catchments. This is very important, as it helps verify distributed model dynamics and allows a degree of realism to be attached to model-based interpretations regarding actual basin dynamics. Overall, the results are very positive and instill a good sense of confidence in the model for prediction of medium

to large rainfall-runoff events. Performance of medium to large events is well reflected in the coefficient of efficiency. Given these results, it is concluded that the model can be used with confidence to examine watershed response and to assess the effects of geometric model simplification over a range of basin scales.

CHAPTER 6

SENSITIVITY AND GEOMETRIC MODEL COMPLEXITY AS A FUNCTION OF BASIN SCALE

6.1 Introduction

Results from Chapter 5 indicate good model performance for all study basins for all but the very small events. The model performed especially well in the Lucky Hills watersheds. With model confidence established by results in the previous chapter, the analysis proceeds to the primary objective of this chapter; namely the consideration of the issues of model performance, sensitivity, and geometric simplification (aggregation) as function of basin scale. The analysis of these topics was restricted primarily to the calibration event set for each watershed. The restriction to this event set is not viewed as a problem because both the sensitivity and aggregation results will be judged on deviations from the calibration event set results. The calibration event set results will be regarded as "true", error-free results so that the impacts of aggregation and process sensitivity can be isolated. The Nash-Sutcliffe (1970) coefficient of efficiency for runoff volumes and peaks was used often as a measure to indicate how model results change as a function of basin scale. Using this measure gives less weight to very small events and, therefore, will avoid misleading interpretations clouded by the large, relative uncertainties in measurement for very small events. However, when instructive, results of individual events and results over the entire range of the calibration event set are presented.

Model performance as a function of basin scale is the first issue addressed in this chapter. It summarizes the results presented in the last chapter graphically and in the context of increasing basin size. Model sensitivity is examined next with two major subissues treated. The first explores model sensitivity to the calibration parameter multipliers over the range of study watershed scales. The second subissue explores the sensitivity of the model to specific model parameters related to hydrologic subprocesses over a range of basin scales. Through this analysis, insight into the issues of hydrologic subprocess domination as a function of basin scale is acquired. Finally, geometric model simplification as a function of both storm and basin scale is treated. Prudent selection of various simulation scenarios during model aggregation allows the isolation of effects due to routing, infiltration, and rainfall representation during simplification.

6.2 Model Performance as a Function of Basin Scale

In Chapter 5, model performance and evaluation were discussed for each watershed. In this chapter, model performance is discussed for the entire range of study catchment scales. Ready comparison over the range of scales of the Lucky Hills watersheds is facilitated by the fact that a common set of rainfall-runoff events was used for this set of watersheds. A number of factors did not allow the same set of events to be selected for WG11. The large increase in watershed area from Lucky Hills to WG11 (4.40 to 631 ha) and the large spatial translation (6 km), combined with station specific runoff data collection histories, prevented a common storm set.

Nevertheless it is useful to combine model performance, measured in terms of coefficient of efficiencies (see Table 5.4), across the range of basin scales considered. This examination sets the stage for a number of interpretations made later in this chapter.

In Figure 6.1, the forecast efficiencies for runoff volume and peak rate for both the calibration and verification event sets are plotted against basin drainage area. The figure more clearly illustrates some of the conclusions reached in the last chapter, namely, the decrease in model performance for the verification event set as basin scale increases. Calibration efficiencies for both peaks and volumes are very good over the entire range of scales considered. The reducted verification model performance for WG11 is hypothesized to result from the inability of the small number of calibration events (10) to capture the majority of runoff-generating situations in the larger watershed due to greater spatial variability of rainfall and the greater importance of channel losses. Other factors affecting model performance at the larger scale are more clearly demonstrated in Figures 6.2 and 6.3.

In Figures 6.2 and 6.3, observed and simulated calibration and verification event set means and standards deviations are plotted as a function of basin area (data in Table 5.5). The figures show that both statistics are reasonably well maintained by the model. A slight tendency for the model to overestimate runoff volume (V) and peak rate (Qp) variance is indicated by the illustrations. However, the figures clearly confirm the decrease in V and Qp per unit area as watershed size increases, as is so characteristic of semiarid watersheds (Renard, 1970). This

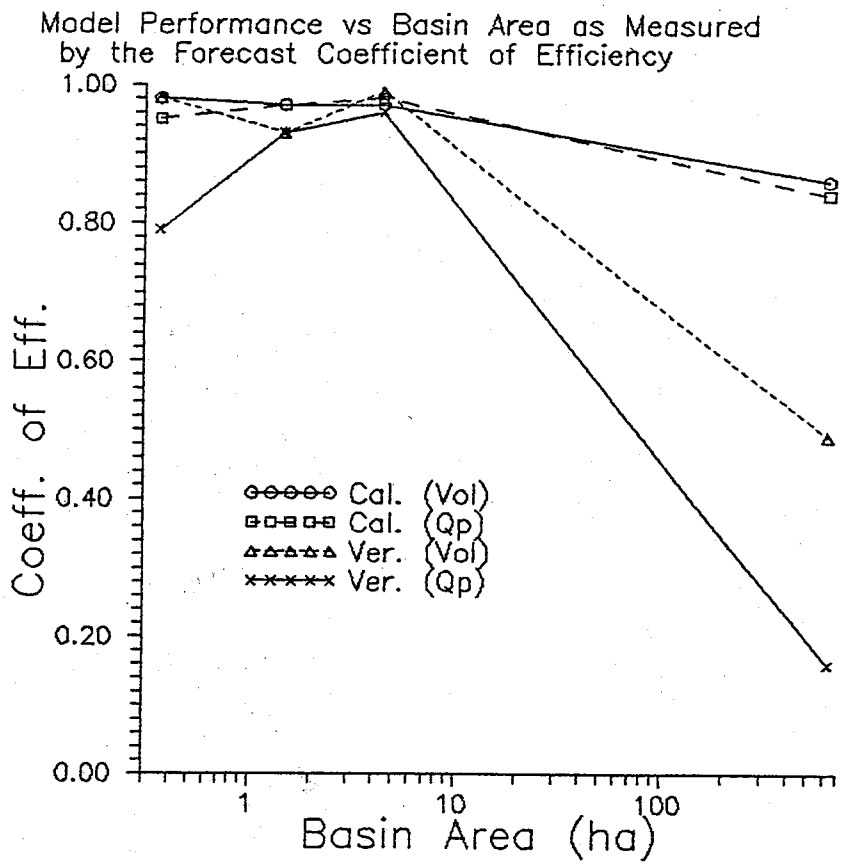

Figure 6.1 Model Performance Versus Basin Area as Measured by the Forecast Coefficient of Efficiency

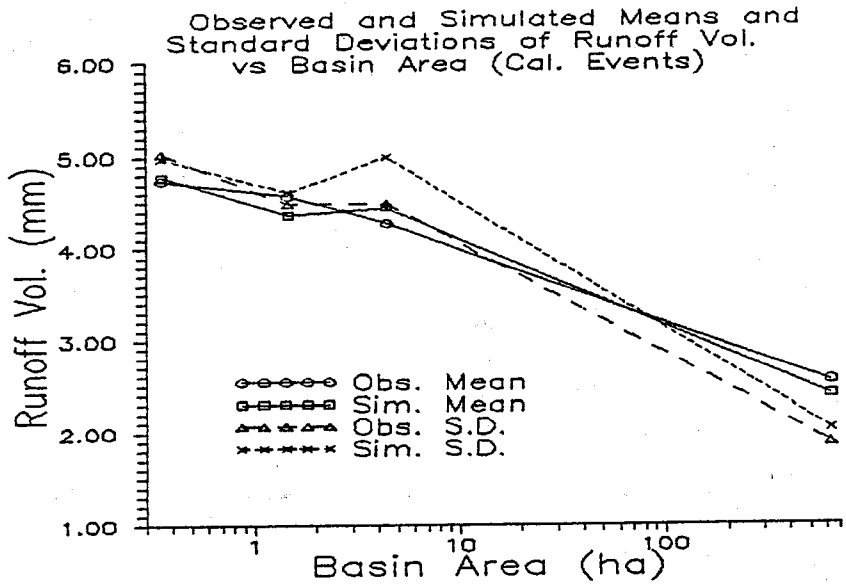

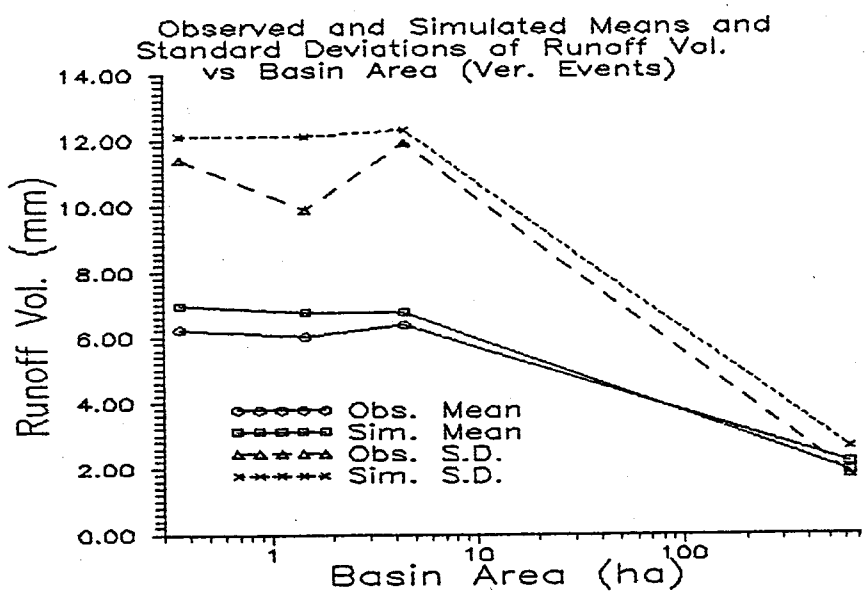

Figure 6.2 Observed and Simulated Means and Standard Deviations of Runoff Volume Versus Basin Area for the Calibration and Verification Event Set

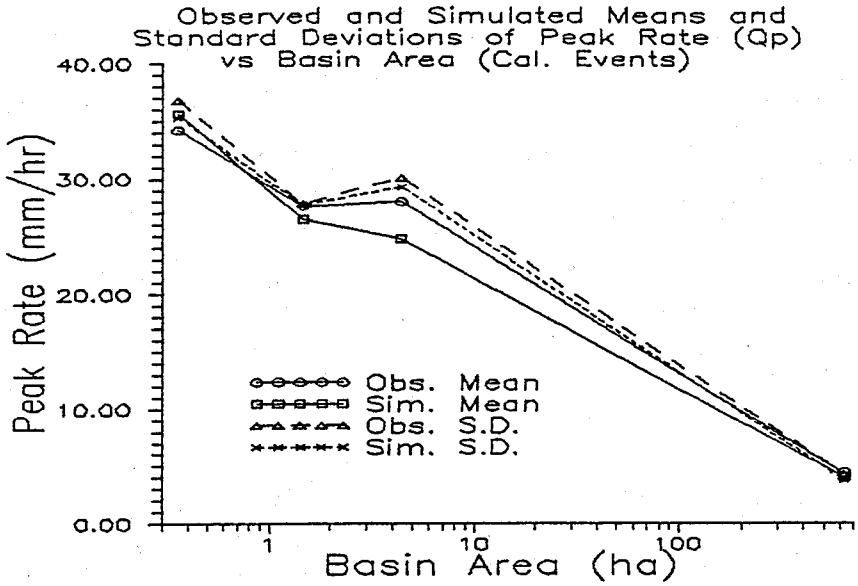

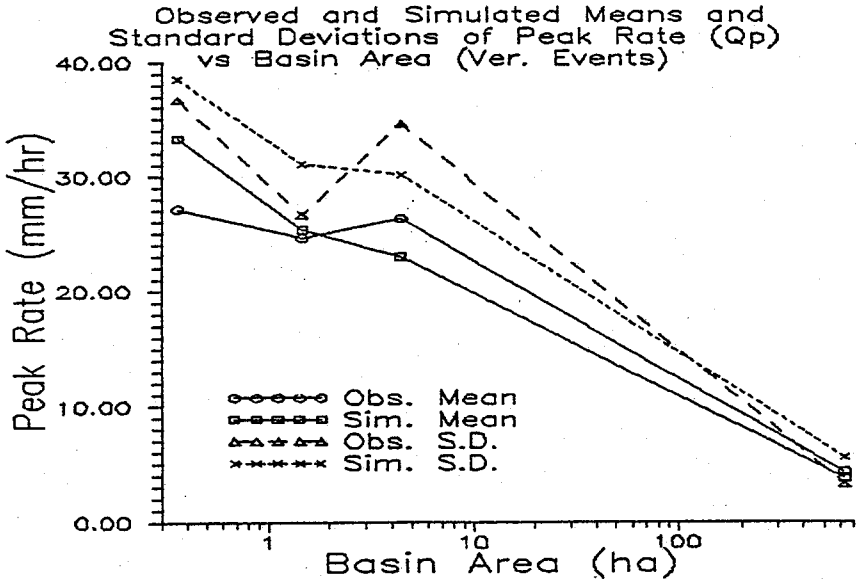

Figure 6.3 Observed and Simulated Means and Standard Deviations of Peak Runoff Rate Versus Basin Area for the Calibration and Verification Event Set

decrease in unit area runoff for increasing watershed size also helps explain the decrease in model performance with larger basin area shown in Figure 6.1.

Because of the limited spatial extent of the majority of runoff producing thunderstorms in Walnut Gulch (Osborn et al., 1979; Osborn et al., 1980; Osborn and Simanton, 1981; Osborn, 1982), the probability of approaching equilibrium or near equilibrium runoff conditions decreases with increasing areal extent. Therefore, rainfall inputs become less dominant with increasing watershed area. The nonlinearities associated with infiltration become more important as basin size increases and storm domination decreases. At the same time, the storm runoff volumes per unit area approach the measuring resolution of raingages. Both the nonlinear nature of runoff generation and the relative amount of input uncertainty increase with increasing watershed area.

This runs counter to observations and analysis made by several investigators (Anderson et al., 1981; Dooge, 1981; Beven et al., 1988; Wang et al., 1981). They stated that rainfall-runoff response typically becomes more linear as basin size increases. This may be largely due to the fact that effluent streams (runoff per unit area increases with increasing basin size; gaining watersheds) are much more widely studied. These watersheds also often have large, highly damped, base and throughflow runoff components that are not observed in Walnut Gulch. Results of this study covering a portion of Walnut Gulch do not imply that beyond some scale, larger than that studied here, linearity with increasing basin size does not occur.

Exploration of the increasingly nonlinear nature of runoff response in the study areas as basin size increases is also addressed directly in the following section.

6.3 Model Sensitivity as a Function of Basin Scale

6.3.1 Sensitivity of the Objective Function to Basin Scale for Calibration Multipliers

The sensitivity results presented in this subsection and the following subsection (6.3.2) were obtained using the most geometrically complex watershed representation for each basin. These basin representations were obtained from the large-scale base maps by way of the procedures described in Chapter 4. By exploring the behavior of the coefficient of efficiency for V and Qp for various combinations of calibration multipliers, further insight into model behavior as a function of watershed scale is acquired. In Figure 6.4, the response surface of forecast efficiencies for the calibration event set (Ec) for runoff volume is plotted as a function of multipliers M_K and M_R for each of the Lucky Hills watersheds. To make these plots comparable, the area weighted mean Ks for each watershed was computed. The range of multiplier M_K was then selected so that each watershed maintained the same range of area weighted average Ks. This adjustment cannot completely account for spatially distributed differences in Ks among the watersheds, but it will enable general interwatershed response comparisons. Computing limitations did not allow a comparable plot to be generated for watershed WG11.

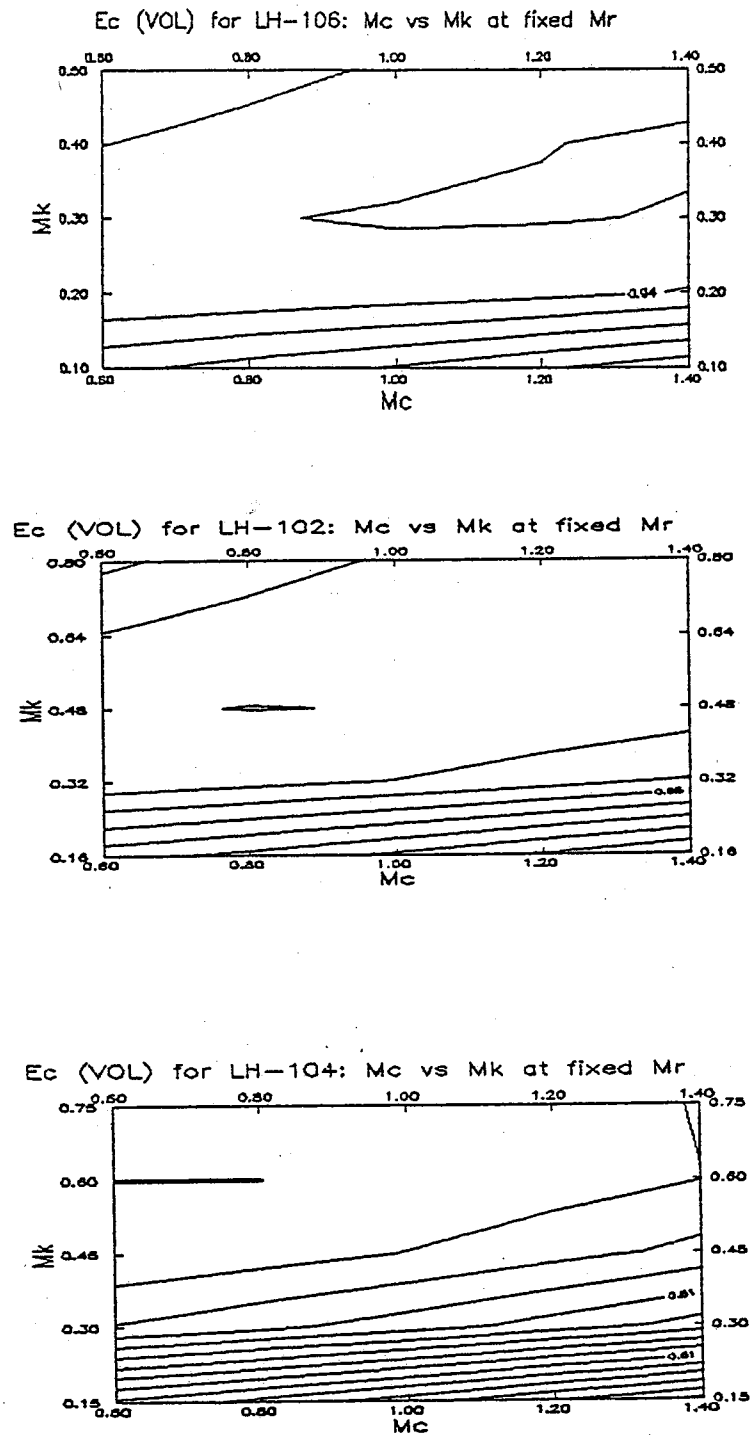

Figure 6.4 Ec Response Surface for Runoff Volume as M_K and M_C Vary with Fixed M_R for the Lucky Hills Watersheds

Several conclusions can be drawn from Figure 6.4. The sensitivity of Ec to M_C is slight for all of the Lucky Hills watersheds. This occurs because effects of small-scale infiltration variability ($C_v > 0.0$) primarily impact small events (Chapter 2 and 5). The runoff characteristics of small events are not well captured by Ec and, therefore, little sensitivity to M_C is observed. A general steepening of the response surface to change in M_K is also observed as basin scale increases. This indicates a greater sensitivity of infiltration conditions as watershed area increases, supporting the conclusions above regarding the increase in infiltration nonlinearities as basin size increases. The greater importance of infiltration, or decreasing storm influence, with increasing watershed scale in also apparent in Figure 6.5.

The change in Ec for Qp and V as a function of M_R for fixed M_K and M_C for each watershed is shown in Figure 6.5. Note the very flat response of both Ec for Qp and V for LH-106. This implies that, from a routing standpoint, embodied in M_R, the basin has very little influence on runoff characteristics. LH-106 is the smallest of the watersheds (0.36 ha) and, therefore, responds very quickly. As watershed scale increases, the curvature of the Ec-Qp versus M_R curve increases, indicating greater basin control of peak runoff rate.

A possible explanation of this behavior again relates to the relative scale of storms to infiltration abstractions. Because of the quick response of LH-106, the watershed is more likely to be near, or in, equilibrium for the larger events which more strongly control Ec. In an equilibrium condition, Qp depends on the rainfall

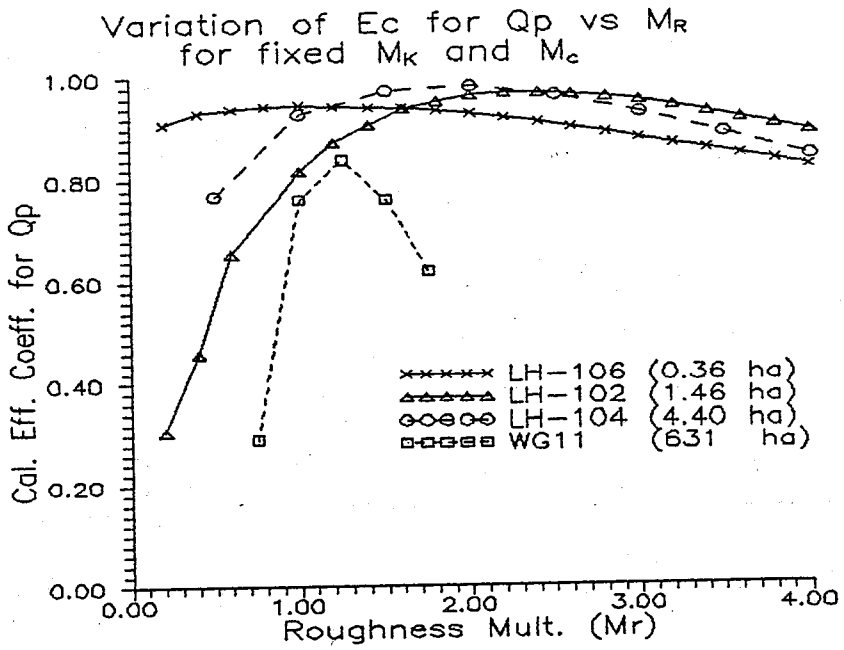

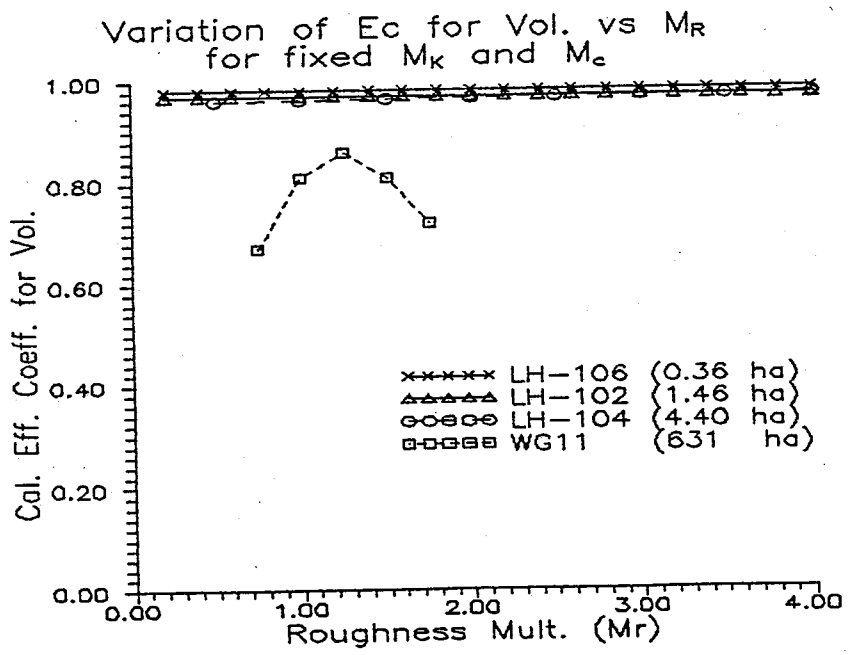

Figure 6.5 Ec for Qp as a Function of M_R for All Study Basins

rate and is independent of changes in roughness. If equilibrium is not reached, Qp is dependent on the flow depth which is directly influenced by both changes in roughness and rainfall rate. Therefore, in partial equilibrium, a greater sensitivity of Qp to roughness is expected. The top portion of Figure 6.5 would suggest that a transition in peak runoff generation from storm to basin domination occurs between basin areas corresponding LH-106 (0.36 ha) and LH-102 (1.46 ha). This conclusion is, of course, dependent on the calibration storm set and Ec.

Another transition related to runoff volume generation appears to occur between LH-104 (4.40 ha) and WG11 (631 ha). Virtually no dependence exists between Ec-V and M_R on the Lucky Hills watersheds. This drastically changes when WG11 is treated. The cause of this dependence is due to the interactive infiltration algorithm and increased channel losses. As roughness increases, response is slowed, and greater opportunity time exists for infiltration to occur. A runoff model using an excess routing methodology will not exhibit this behavior. Another factor affecting Ec-V with changes in M_R is an increase in storage left on the basin at the end of simulation. This storage will either run off or infiltrate if a longer simulation time is allowed. (Note: The retention of storage on the basin for long simulation times also suggests a change in the minimum infiltrating channel bottom width from zero to some small finite value, say 5% of the field measured bottom width. The variable infiltrating bottom width function is described in Woolhiser et al., 1990.) This factor was discovered and the simulation times were increased so that changes

in infiltration accounted for more than 80 percent of the runoff volume change for all events when M_R was varied near the final multiplier.

The watershed response as a function of the calibration multipliers does not allow changes in response to be assigned to channel or overland flow processes as the multipliers are applied over the entire watershed. To further distinguish how hydrologic subprocess domination (overland flow routing, channel routing, channel infiltration, etc.) may change over a range of watershed scales, process specific model parameter multipliers are employed. This procedure is discussed in the following section.

6.3.2 Hydrologic Subprocess Sensitivity as a Function of Scale

To examine this issue, the sensitivity research version of KINEROSR described in section 5.B. was employed. This program allows selection of hydrologic subprocess specific multipliers. These multipliers are applied to all field-estimated model parameters associated with that multiplier. For example, if a multiplier for channel roughness is selected, all channel roughness values in the input model parameter file are multiplied. To assess the impact of model sensitivity change, it is assumed that model output for the calibration event set, with the final M_R, M_K and M_C multipliers applied, is true and error-free (base model output). The change in model output due to process multipliers being applied is judged against the base model output. The model sensitivity gauged in this fashion is used to gain insight into hydrologic subprocess domination as a function of basin scale.

The parameter multipliers were primarily selected to investigate the differences in overland and channel flow. Multipliers for both the hydraulic roughness and saturated hydraulic conductivity of overland flow planes and channels were selected to highlight these differences. In addition, the coefficient of variation (C_v) of the Ks multiplier (M_C) on the overland flow planes and sensitivity to input precipitation is examined. The initial sensitivity work conducted on LH-106 presented in Chapter 5 showed small perturbations in runoff characteristics for a 10 percent change in the parameter multiplier values. Therefore a +30 percent change in each multiplier was used here with the exception of the rainfall multiplier.

For the rainfall multiplier, a +/- 15 percent change in the associated multiplier has been selected. This is consistent with typical raingage catch errors reported by Neff (1977) and Hanson (1989). Note that the algorithm that is used to scale the rainfall, scales the intensities of each raingage before spatial interpolation. By doing so, the precipitation scaling multiplier is applied in both time and space throughout the rainfall event.

The percentage runoff volume difference for a +30 percent change in saturated hydraulic conductivity (Ks) for planes and channels for each of the calibration events for each watershed is shown in Figure 6.6. The abscissa of each graph is the base model runoff volume per unit area obtained for the unperturbed case which represents a relative measure of event size. The upper portion of Figure 6.6 illustrates approximately equal sensitivity of runoff volume over the range of study basin scales to changes in Ks of the overland flow planes. This is not surprising as

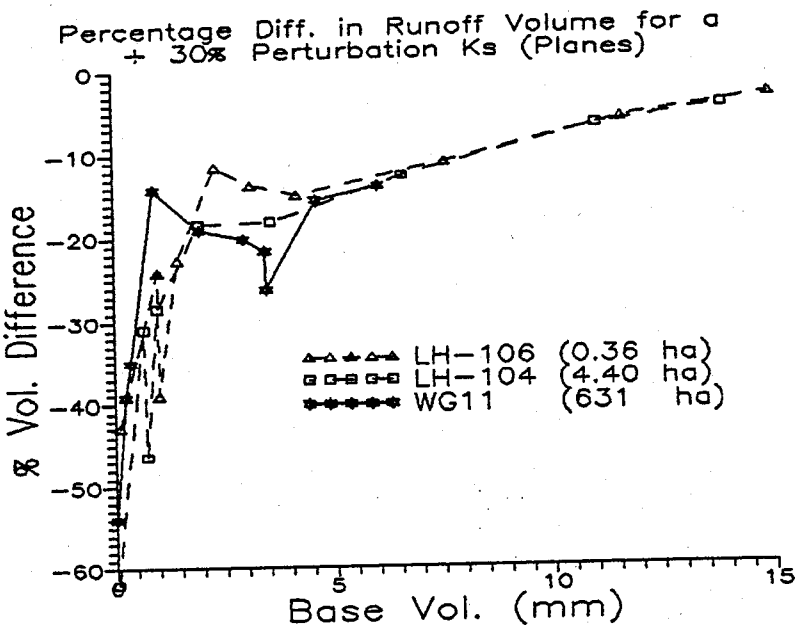

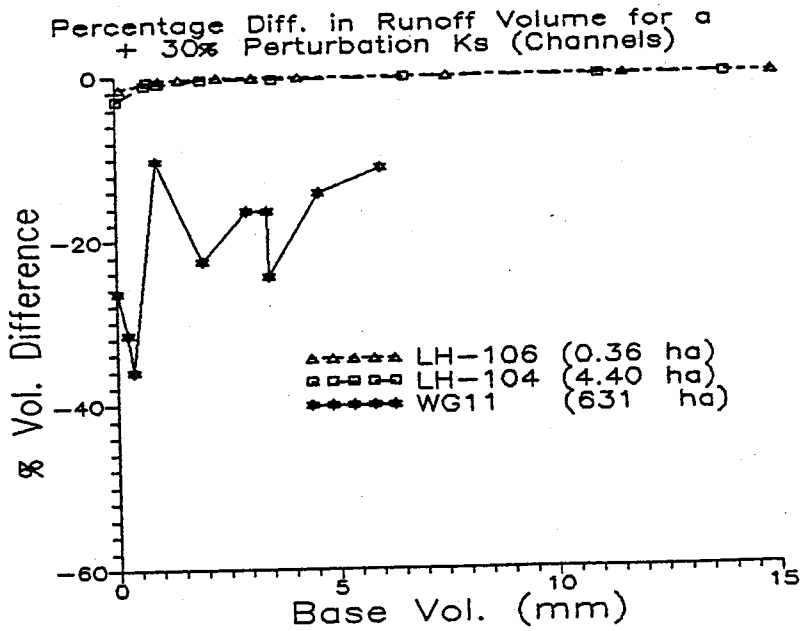

Figure 6.6 Sensitivity of Runoff Response to Perturbations of Ks (Planes) and Ks (Channels) over a Range of Basin Scales

the percentage basin area covered by overland flow planes is large for all the watersheds and runoff production mechanisms are modeled in a similar manner for each watershed.

The sensitivity of basin outflow to a change in Ks of the channels shows a distinct difference between the small Lucky Hills basins and WG11 (lower portion of Figure 6.6). This illustrates the importance of channel infiltration processes in the larger watershed. Also note that sensitivity decreases as event size increases. This reinforces the conclusion that as storm size increases, the nonlinear attenuating effects of the basin decrease. The differences in channel losses for separate events for LH-104 and WG11 are shown in Figures 6.7a and 6.7b. In these figures the watershed integrated plane and channel infiltration rates per unit area are plotted as a function of time in addition to the basin hyetograph and hydrograph. The ratio of the peak of channel infiltration to the peak runoff rate is approximately 0.7 for the WG11 event and only 0.02 for the LH-104 event, clearly illustrating the increasing dominance of channel processes with basin scale.

The differential sensitivity of hydraulic roughness on overland flow planes and channels for a range of basin scales is shown in Figure 6.8. In this case the percentage change in peak runoff rates (Qp) is used to illustrate the roughness sensitivity. A more distinct, but somewhat noisy, ordering of increasing sensitivity to roughness with increasing basin scale is apparent. Greater separation of event set sensitivity for channel roughness is also apparent.

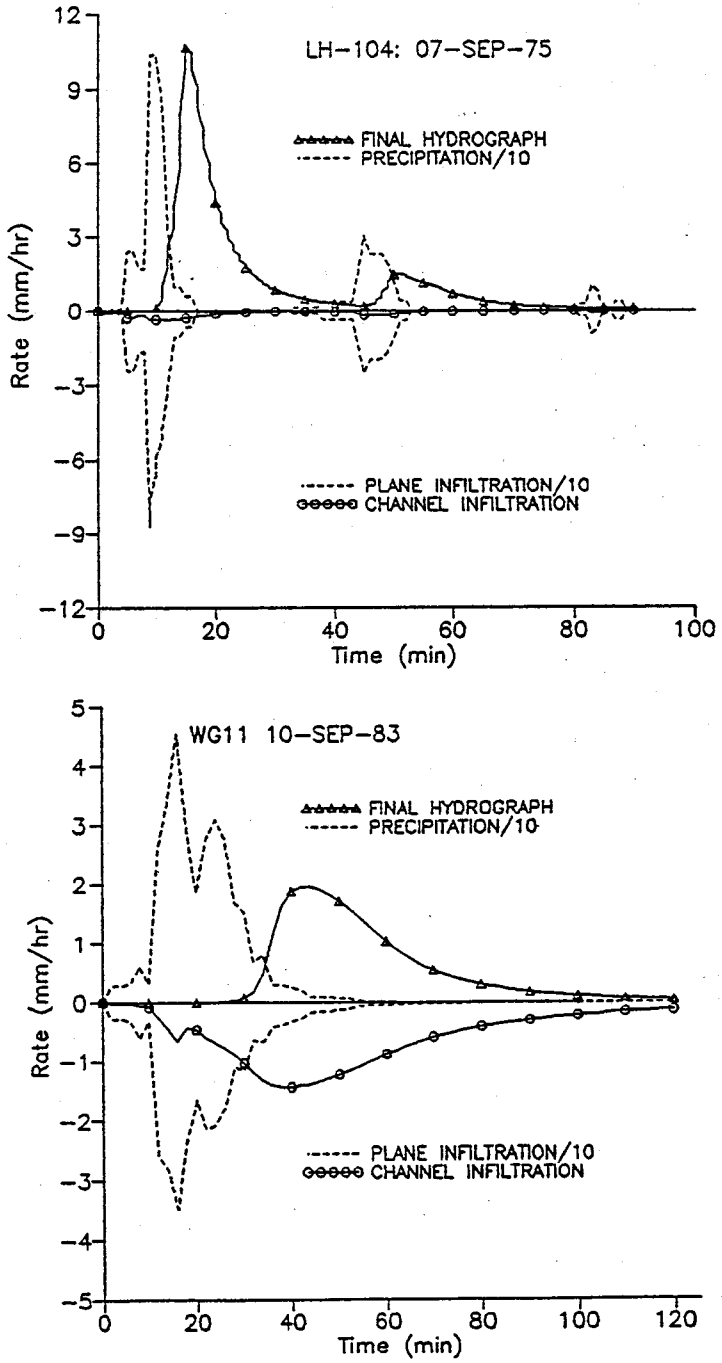

Figure 6.7 Illustration of the Importance of Channel Infiltration Losses on
(a) LH-104
(b) WG11

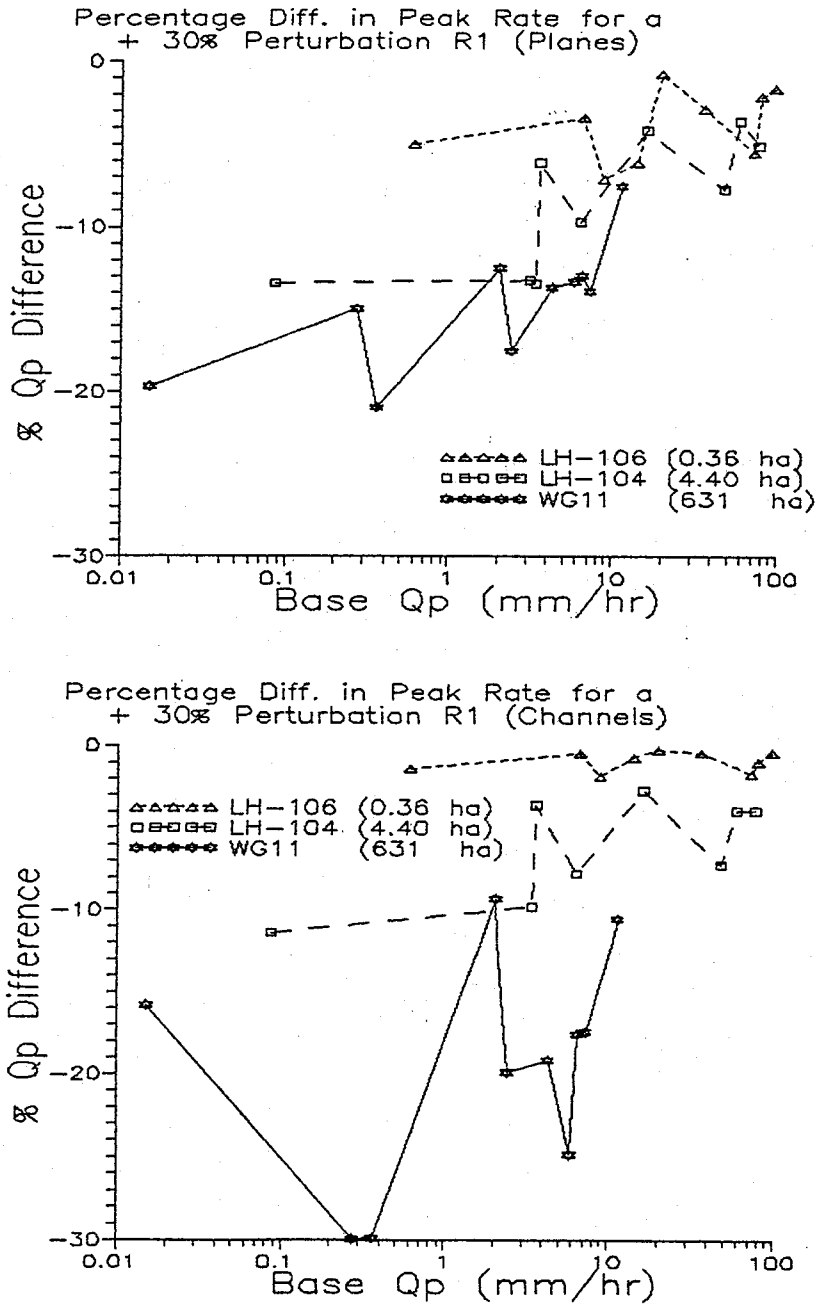

Figure 6.8 Sensitivity of Runoff Response to Perturbations of Roughness (Planes) and Roughness (Channels) over a Range of Basin Scales

Incorporation of small scale infiltration variability ($C_v > 0.0$) was shown to be important for small runoff events in Chapter 2 on a simple overland flow plane. The sensitivity of runoff volume to C_v over a range of basin size shown in Figure 6.9 confirms the same tendency. The upper portion of the plot is for a + 30% perturbation to C_v and in the lower portion the percentage change in runoff response when small scale infiltration variability is not modeled by setting $C_v = 0.0$ is shown. A small, but discernable, increase in sensitivity to C_v for increasing basin scale is apparent for medium to large events (greater than 2 mm). A great separation of C_v sensitivity with basin scale is not apparent in Figure 6.9 but when the sensitivity is measured in terms of the coefficient of efficiency of the calibration event set (Ec) the separation between large and small basins is readily apparent (Figure 6.10). The change in Ec of Qp and Ec of V for changing M_C (C_v) in shown in Figure 6.10.

The different degree of apparent sensitivity to C_v shown by changes in runoff volume per unit area (Figure 6.9) and by changes in E (Figure 6.10) can be clarified as follows. Normalizing by calculating the runoff volume per unit area does facilitate comparison between watersheds. However, in a losing, semiarid environment with influent streams where runoff per unit area decreases with increasing basin size, much larger storms are required to produce the same volume of runoff per unit area for larger basins. This fact can be more easily seen if statistics associated with the runoff ratio are examined (see Table 6.1). The mean runoff ratio of the calibration event set for WG11 is smaller than that of LH-106 by nearly a factor of three. Once again, these statistics support the conclusion that basin attenuating influence via

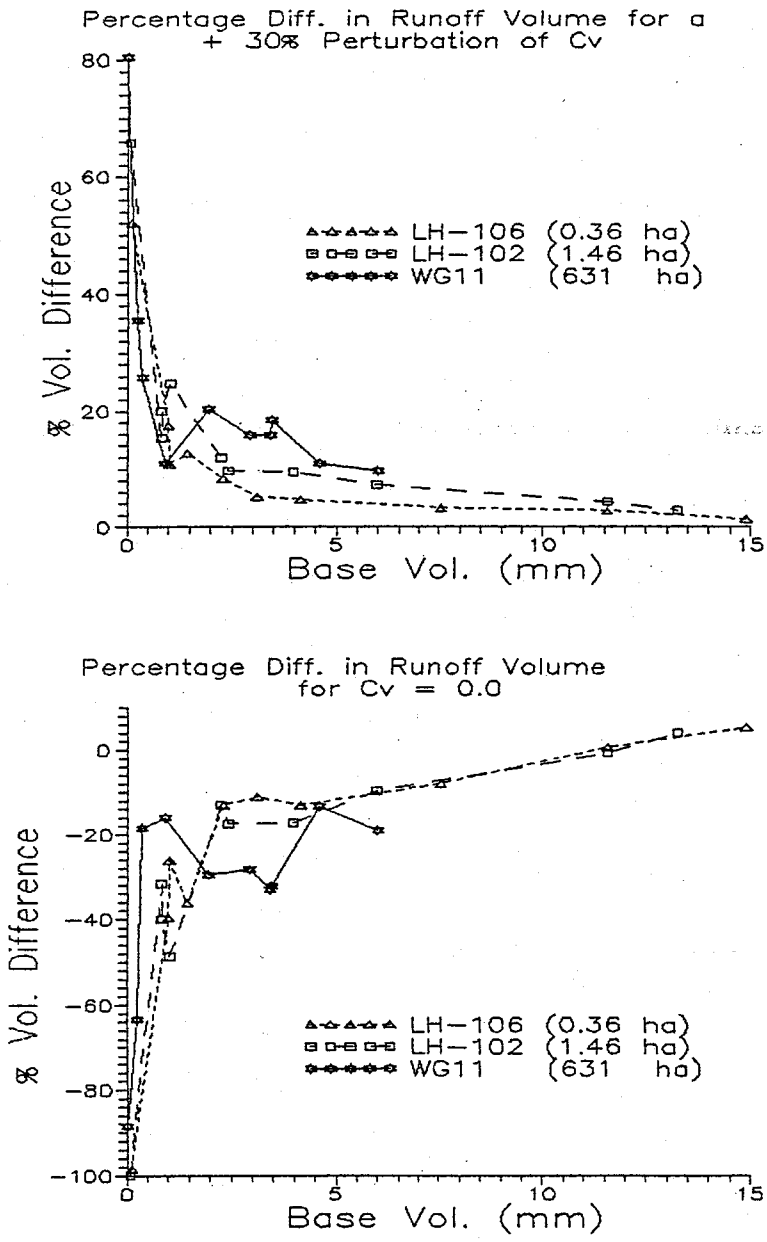

Figure 6.9 Sensitivity of Runoff Response to Perturbations of C_v over a Range of Basin Scales

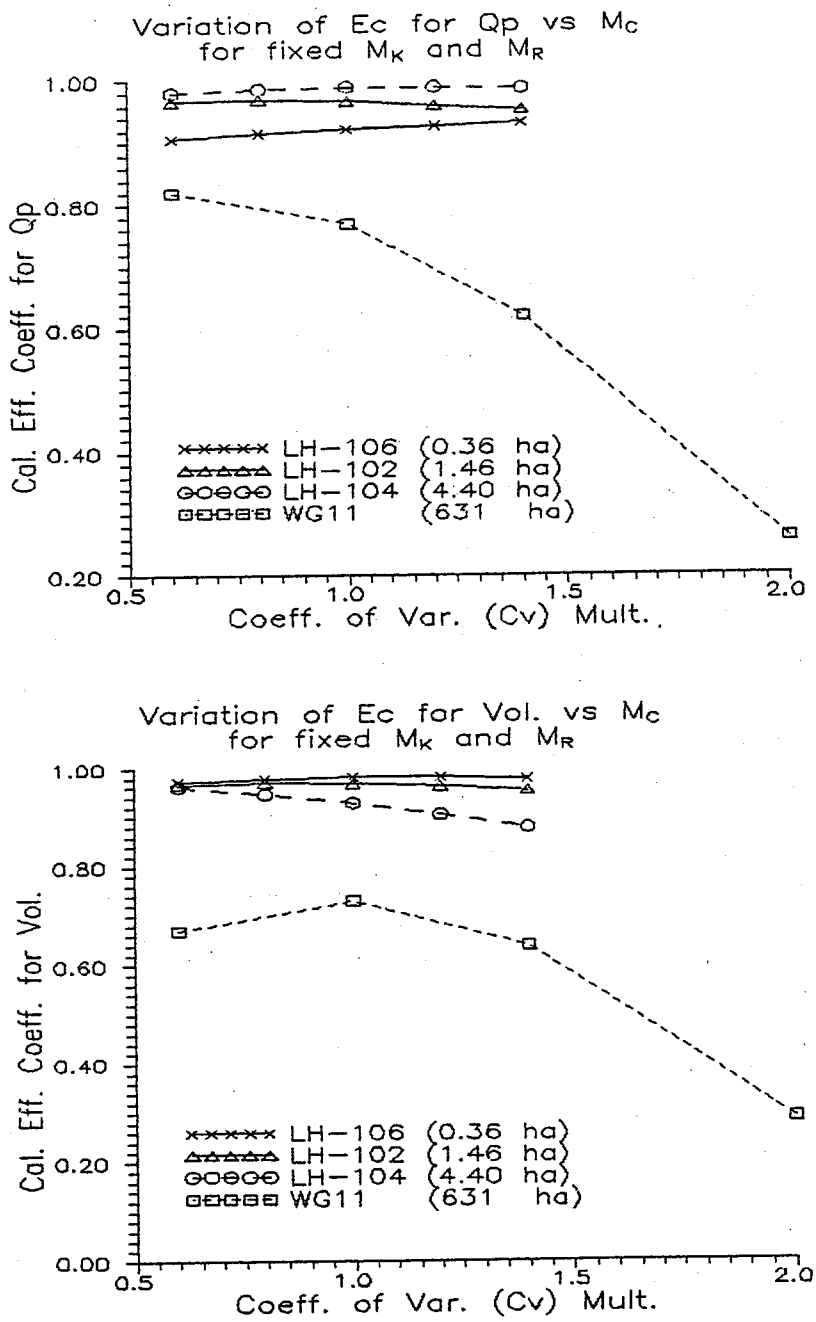

Figure 6.10 Ec for Qp and V as a Function of M_C for all Study Basins

Table 6.1. Calibration Set Runoff Ratio Statistics

Basin	Area (ha)	Mean	S.D.	Range
LH-106	0.36	0.25	0.17	0.013 - 0.61
LH-102	1.46	0.22	0.17	0.010 - 0.58
LH-104	4.40	0.21	0.18	0.004 - 0.58
WG11	631	0.09	0.06	.0013 - 0.19

infiltration and routing increases with basin scale in relation to climatic influence. C_v also becomes more important at larger basin scales. At these scales the watershed regions directly centered under the high intensity regions of a thunderstorm will produce runoff with a high probability. But as intensities decrease, away from the storm center, there will be large spatial regions or bands where lower rainfall intensity will significantly interact with spatially variable soils. This interaction with increasing basin attenuating influence supports the idea of increasing nonlinearity with basin scale.

The type of nonlinearity referred to is not the classic notion of nonlinearity in runoff response (Minshall, 1960). It deals with the threshold nonlinearities of infiltration which in turn must include the spatial and temporal variability of precipitation. To address the classical definition of input-output linearity or nonlinearity by proportionality and superposition the model sensitivity to perturbations in rainfall is assessed. To do so the input rainfall distribution is scaled by +/- 15% for each basin's calibration event set. The precipitation interpolation algorithm preserves spatial rainfall patterns after this scaling. The perturbed input was used to simulate runoff on each of the watersheds using the calibration multipliers for Ks, C_v, and roughness (R1). This represents a more realistic assessment of model response than an excess approach with uniform rainfall.

If runoff response becomes more linear with increasing watershed scale the runoff perturbations should approach +/- 15% perturbations in volumes that would be expected in a truly linear model. The runoff perturbations in terms of percentage

volume change are plotted in Figure 6.11. Examination of the figure reveals the linearity in runoff response does not increase with increasing basin scale. In fact it could be argued that response becomes more nonlinear with increasing watershed scale. Increasing nonlinearity in response also occurs for decreasing event size; again, pointing out the emerging domination of basin routing and infiltration nonlinearities as climatic scale (storm size) decreases or basin scale increases. Also note that runoff sensitivity to rainfall for a 15% perturbation is much larger than for 30% perturbations to the other parameters. Again, this stresses the need to accurately define rainfall.

These trends in nonlinearity are further illustrated in Figure 6.12. This figure shows the change of peak runoff rate as a function of the precipitation multiplier for a selected small and large event (intermediate on the Lucky Hills watersheds) on each of the basins. The events were selected to have comparable total runoff per unit area. If linearity holds, the change in Qp with increasing rainfall should plot as a straight line. Approximate linearity is apparent for the intermediate event on the small watersheds for rainfall multipliers of one and above. This apparent linearity immediately disappears when the larger basin (WG11) or the smaller event is considered. Increasing curvature (nonlinearity) occurs as basin scale increases for the small event on the Lucky Hills catchments. The curvature does not increase as we go to watershed WG11 but this is an artifact of normalizing the peak runoff rate to a unit area measure (recall the runoff ratio statistics in Table 6.1).

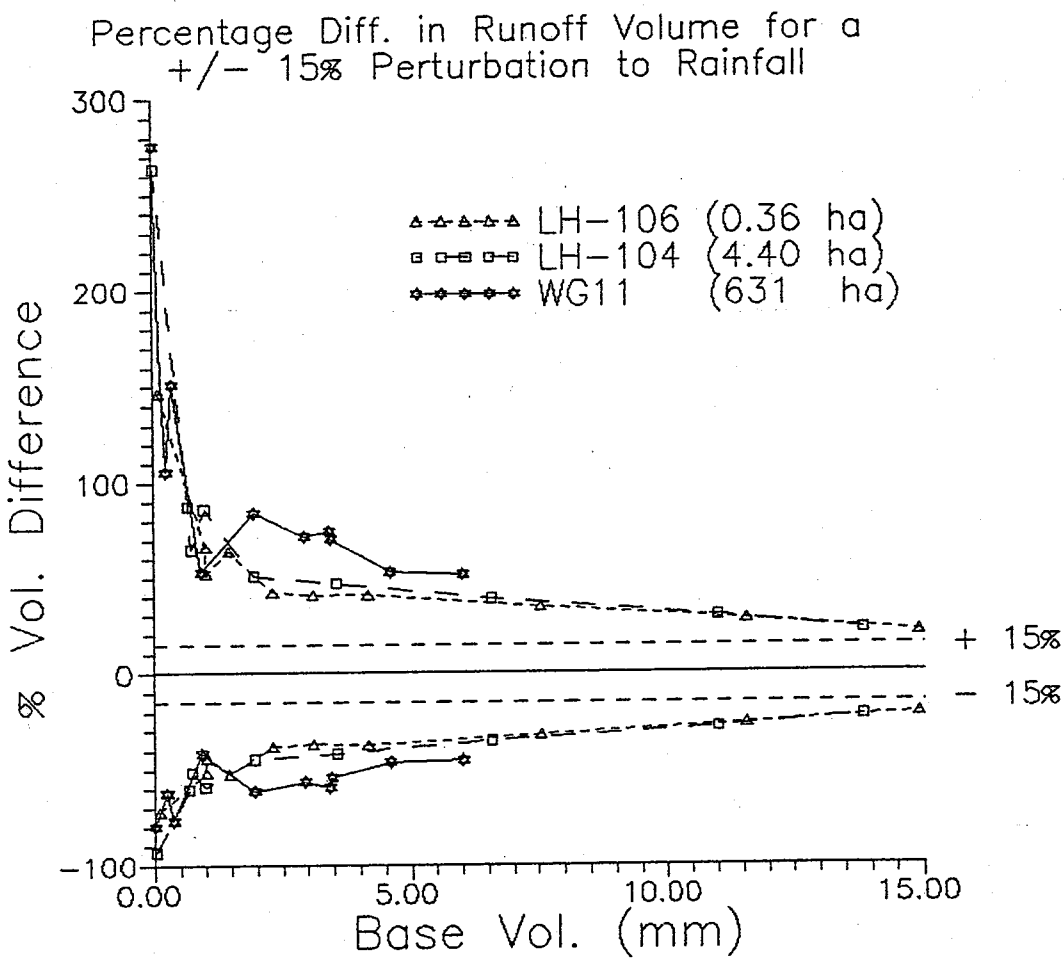

Figure 6.11 Sensitivity of Runoff Response to +/-(15%) Perturbations of Rainfall over a Range of Basin Scales

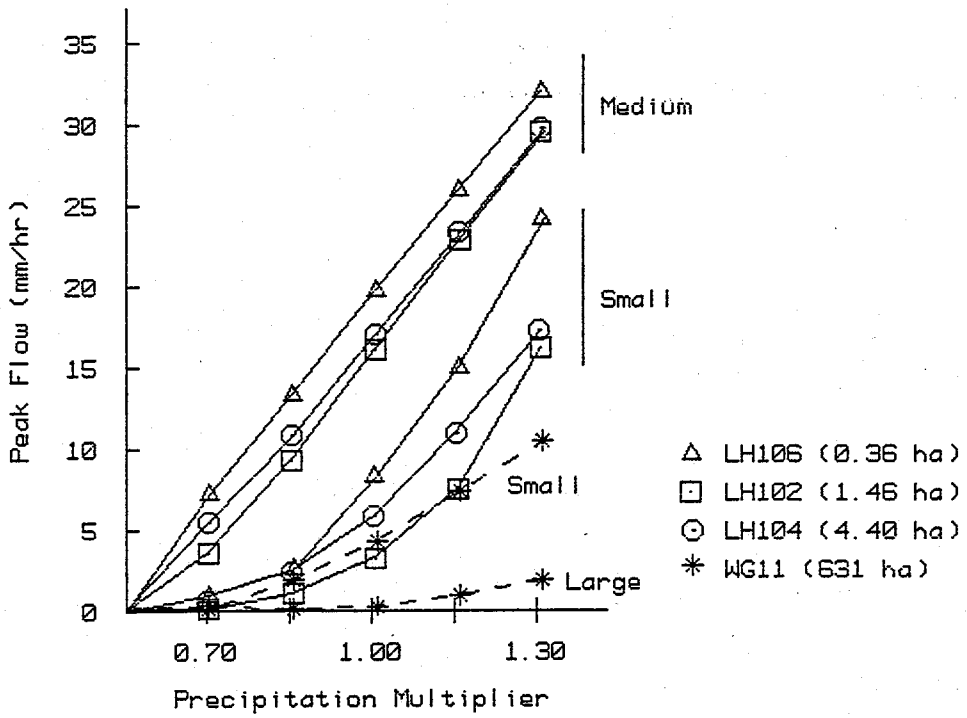

Figure 6.12 Sensitivity of Peak Runoff Rate for Several Events to Perturbations of Rainfall over a Range of Basin Scales

Much larger runoff events on WG11 are chosen by selecting events with comparable total runoff per unit area between the Lucky Hills and WG11. A more realistic comparison could be made by selecting events with equal runoff ratios. If runoff ratios continue to decrease with increasing basin scale the area normalized runoff will approach the measuring resolution of available instrumentation. Measurement error will become a larger proportion of overall modeling error in this case and model performance is expected to deteriorate.

The findings presented in the section indicate that the application of unit hydrograph (UH) analysis is semiarid regions may be wholly inappropriate. The limited spatial uniformity of rainfall in semiarid regions combined with increasing nonlinearities associated with channel losses would limit applications of UH to small watersheds. However, the inappropriateness of UH concepts on small watersheds has been clearly demonstrated by Minshall (1960) due to nonlinear runoff response behavior. Thus small basin response starts out responding in a highly nonlinear manner and becomes more nonlinear as basin scales increase for semiarid regions represented by Walnut Gulch over the range of basin scales studied. Formal application of UH concepts to the study basins to assess the appropriateness of UH concepts will be undertaken in a future study.

Increasing nonlinearity with basin size will make it more difficult to formulate response relationships at the catchment scale (Dooge, 1986) and to employ the concept of a representative elementary area (REA) proposed by (Wood et al., 1987). These conclusions are, of course restricted to the basin/climatic environment

representative of Walnut Gulch over the range of scale studied. Linearity may appear at larger scale but it is doubtful in a losing environment with influent streams. Domination of response by channel flow is often cited as the reason for increasing linearity with basin scale (Wang et al., 1981; Gupta et al., 1980; Diskin, 1973). Domination of channel processes with increasing scale is also shown in this study via process related sensitivity analysis. But the domination of channel processes in this study is largely the result of nonlinear channel infiltration losses. Regardless of channel effects the findings indicate the importance of accurate knowledge of the spatial rainfall pattern.

The sensitivity analysis discussed in this section employed the most complex model representations of the respective watersheds. Analysis of model performance at varying levels of geometric model complexity over a range of catchment scales is required to determine the proper level of basin discretization to capture the nonlinearities demonstrated in this section.

6.4. Geometric Model Simplification as a Function of Basin Scale and Storm Size

6.4.1. Geometric Model Simplification as a Function of Basin Scale

Hypothesis 1 is addressed in this section by assessing model performance at different levels of basin discretization over the range of study basin scales. The hypothesis is restated at this point for convenience:

HYP (1): At a certain basin scale, represented by a base map of a given scale, in the climatic regime specified above, a maximum allowable size of overland flow elements will exist so that elements below this size will adequately model basin runoff and elements above this size will not.

To concentrate strictly on model performance as a function of basin discretization level it is assumed that the simulated runoff for the most complex basin model representation is true and error free. The most complex basin model representation of each watershed employed 30, 68, 235, and 243 modeling elements for LH-106, LH-104, LH-106, and WG11 respectively. Basin discretization was carried out according to the procedures outlined in Chapter 4 with the largest scale base maps available for each watershed.

Using the simplification rules presented in Chapter 4 successive levels of geometric model simplification were then carried out on each watershed by reducing the stream order by one at each level of model aggregation. In doing so the elementary watersheds consisting of a first order channel and contributing overland flow planes are replaced by a single equivalent overland plane. Therefore as simplification proceeds overland flow elements increase in size.

At each level of geometric model simplification runoff simulations were performed using the calibration event set. Model degradation using the simplified model geometry is measured by computing the forecast coefficient of efficiency (E_f)

of the simplified runoff simulation set against the "true", most complex, runoff simulation set. Because the most complex runoff simulations are assumed to be true and error free, deviations of E_f from 1.0 represent a measure of model error due to geometric simplification (greater spatial averaging and routing simplification). If no error results from simplification the computed efficiencies should remain at one.

As each watershed is simplified a number of factors contribute to the overall simplification error. The three primary components of the overall simplification error can be attributed to the following factors:

1. Simplification of routing
2. Area weighted averaging of soil parameters
3. Simplified representation of spatial rainfall variability

Routing simplification occurs as concentrated flow in channels is replaced by overland flow. But the routing simplification rule maintains equilibrium storage throughout aggregation by distorting the hydraulic roughness using the rules in Chapter 4. This distortion in roughness also compensates for the topographic distortion of the slope distribution as the effects of slope and roughness cannot be separated in the coefficient (α) of the kinematic depth-discharge relation ($Q = \alpha h^m$: Lane et al., 1975). Thus a great deal of "characteristic" routing information is preserved by this procedure.

The preservation of routing characteristics contrasts greatly with the error imparted by simple area weighted averaging of soil parameters and decreased

sampling density of the spatial rainfall pattern. Analysis presented in Chapter 2, as well as in Woolhiser and Goodrich (1988) and in Binley, et al. (1989), demonstrated that equivalent soil hydraulic conductivity parameters cannot be obtained by simple averaging. Thus a more "intelligent" equivalence in the simple model representation for routing is established by the simplification rules then is established for soils or rainfall.

In addition to the three components of simplification error discussed above, numerical error due to changes in computational node density is experienced. Analysis presented in section 4.5.1. demonstrated this component of the overall simplification error is small in comparison to the other components outlined above. Maintenance of the equilibrium storage at each level of simplification is another indication that numerical error is not a significant component of the overall simplification error. In all of the study basins, at all levels of geometric model simplification, the equilibrium storage deviated less than one percent from the storage on the complex system.

The components of the simplification error can be separated by judicious selection of various simulation scenarios. The routing simplification is inherent in all simulations if simple and complex geometric representations are being compared as channel routing has been replaced by overland flow routing. However, the simplification error due to routing alone, can be isolated if simulations are done with a single raingage on an impervious watershed for both the complex and aggregated watershed representation. In this case the runoff generated from the simple system

is used to compute forecast efficiency coefficients (E_R; forecast routing efficiency) for Qp and V assuming the complex impervious system is true and error free. It is assumed that the error due to routing alone equals the difference in the coefficient of efficiency for this case ($DE_R = 1.0 - E_R$). The total simplification error is obtained by making complex and simple model simulations with infiltration and multiple raingages ($DE_T = DE_R + DE_I + DE_P$; where DE_I is the simplification error due to averaged soil parameters affecting infiltration and DE_P is the simplification error due to simplified spatial rainfall interpolation). The simplification error due to routing and simplified interpolation of the rainfall field is obtained by comparing simple to complex impervious simulations with two raingages in the case of the Lucky Hills Watersheds to obtain (DE_{R+P}). It is assumed $DE_P = DE_{R+P} - DE_R$ where DE_R was obtained from the prior impervious single raingage simulations. DE_I is also isolated in a similar manner where a simulation run with infiltration and a single raingage is used to obtain DE_{R+I}.

The various components of simplification error for two levels of geometric model simplification are shown in Table 6.2 for LH-102. The impacts of simplification are much greater for Qp than V as measured through the change in the coefficient of efficiency. It is also clear that the simplification error related to infiltration from averaging of soils parameters is the principal component of the overall simplification error. Also included in Table 6.2 are the changes in efficiencies for Qp and V caused by using raingage 384 or 83 independently as compared to "true" case using both raingages with the interpolation algorithm. These simulations

Table 6.2. LH-102 Simplification Error Components

Simp. Error Component	Stream[1,2] Order Replaced	DE (Qp) for Given Component	Percent of Total Simplification Error DE_T for Qp	DE (V) for Given Conponent	Percent of Total Simplification Error DE_T for V
Total (DE_T)	1st	.0035	---	.0015	---
	2nd	.0732	---	.0086	---
Routing (DE_R)	1st	.0002	5.7	0	0.0
	2nd	.0108	14.8	.00003	0.3
Ppt. Avg. (DE_P)	1st	.0001	2.8	0	0
	2nd	.0116	15.8	0	0
Infil.Avg. (DE_I)	1st	.0032	91.4	.0015	100.
	2nd	.0508	69.4	.0086	97.7
Changing Input Raingage	(Most Complex Model)				
Gage 83[3]	None	.0032	41.3	.0748	870.
Gage 384	None	.2182	298.0	.1704	1980.

[1]The most complex model for LH-102 has 68 elements.
After 1st order channel replacement LH-102 has 16 elements.
After 2nd order channel replacement LH-102 has 1 element.

[2]When an order of stream is replaced the stream and overland flow planes contributing to the stream are replaced by a single overland flow plane.

[3]Gage 83 is closest to LH-102.

were done with the most complex model representation (68 elements). Note that the change in efficiencies due a raingage change is far greater than the total simplification error for volume and is a substantial portion of the simplification error in Qp.

Recall that raingages 384 and 83 are less than 300 meters apart. The large errors caused by using the raingages independently, highlights the importance of small scale rainfall variability when the basin scale is commensurate with raingage density. Many of the reasons for the small scale rainfall variability were discussed in more detail in Chapter 5. The magnitude of the error caused by rainfall variability further justifies a great deal of geometric model simplification.

Simplification effects on individual events are presented in Tables 6.3 and 6.4. The impervious, single gage simulations comparing the simple (1 model element) system to the complex (68 model element) system is shown in Table 6.3. In this table the differences in Qp and V for each event of the LH-102 calibration event set measure the routing simplification error. The individual event errors representing total simplification error (routing, infiltration and rainfall averaging) are contained in Table 6.4. For both simulation scenarios the impacts of geometric model simplification are greater for small runoff events. The larger the event, the smaller the simplification error. This trend reflects the relative importance of the climate/basin influence on the rainfall-runoff transformation discussed earlier. The larger the storm, the smaller the relative attenuating influence of the basin. Because the basin in not as important for these events, significant geometric model simplification can accomplished with minor impacts on simulation results.

Table 6.3. Routing Simplification Error on LH102 (68 to 1 Element)

	Relative Percent Error		Peaks (mm/hr)		Volumes (mm)	
Event	Peak	Volume	68 Ele.	1 Ele.	68 Ele.	1 Ele.
1	-10.49	-0.72	16.85	15.08	7.40	7.35
2	- 9.46	-0.43	51.72	46.82	9.46	9.42
3	-16.19	-0.19	36.99	31.00	5.74	5.73
4	1.22	-0.23	31.27	31.65	11.39	11.36
5	-19.48	-0.27	47.91	38.57	8.50	8.48
6	1.14	-0.44	97.11	98.11	12.81	12.76
7	0.11	-0.33	45.60	45.65	16.80	16.74
8	- 0.43	-0.24	105.68	105.23	26.14	26.08
9	- 2.66	-0.10	146.08	142.19	25.77	25.74
10	0.33	-0.24	99.60	99.93	25.70	25.63
Mean =	- 5.59	-0.32	67.88	65.43	14.97	14.93
S.D. =	7.74	0.17	41.45	42.25	8.11	8.10

Table 6.4. Total Simplification Error on LH102 (68 to 1 Element)

	Relative Percent Error		Peaks (mm/hr)		Volumes (mm)	
Event	Peak	Volume	68 Ele.	1 Ele.	68 Ele.	1 Ele.
1	-58.95	-22.37	0.35	0.14	0.09	0.07
2	-61.06	-28.13	5.90	2.30	0.83	0.60
3	-56.45	-18.97	8.52	3.71	1.24	1.00
4	-39.72	-31.80	7.52	4.53	1.94	1.32
5	-36.47	-22.93	10.52	6.68	2.15	1.66
6	-40.79	- 9.46	23.34	13.82	2.42	2.19
7	- 4.73	- 7.85	17.16	16.34	3.96	3.65
8	-34.96	-11.72	52.35	34.05	5.99	5.29
9	- 5.03	- 3.84	83.22	79.04	11.68	11.23
10	- 2.56	- 1.90	56.23	54.79	13.28	13.02
Mean =	-34.07	-15.90	26.51	21.54	4.36	4.00
S.D. =	22.68	10.37	27.72	26.48	4.61	4.56

The total simplification error and simplification errors for routing, infiltration averaging and rainfall averaging were developed for each of the Lucky Hill watersheds. Because 10 raingages were used in the WG11 simulations separation of the individual simplification error components was not readily accomplished. However, the routing error can be isolated by performing calibration event set simulations on an impervious watershed with a single central raingage (gage #88). To display this information as a function of basin scale (area), the average support area for the head of all channels for each stream order was computed.

As the watersheds are simplified the support area to the head of the remaining elementary channel segments increases. The average support area for each order of the stream therefore represents a geometric measure of the degree of model simplification and an average size of overland flow elements used to represent the watershed. For the Lucky Hills catchments the components and total simplification error in terms of Ec of Qp are plotted as a function of mean stream order support area in the upper portion of Figure 6.13. Total simplification error versus area for Qp and V for WG11 is shown in the upper portion of Figure 6.14. The simplification error due to routing in WG11 is shown in middle portion of Figure 6.14.

Figure 6.13 and 6.14 can be used to determine the level of geometric model complexity required to maintain a specified level of the coefficient of efficiency. For example, if an efficiency of 0.97 for Qp is selected, LH-106 could be simplified to a single overland flow element by removing all first and second order channels. To

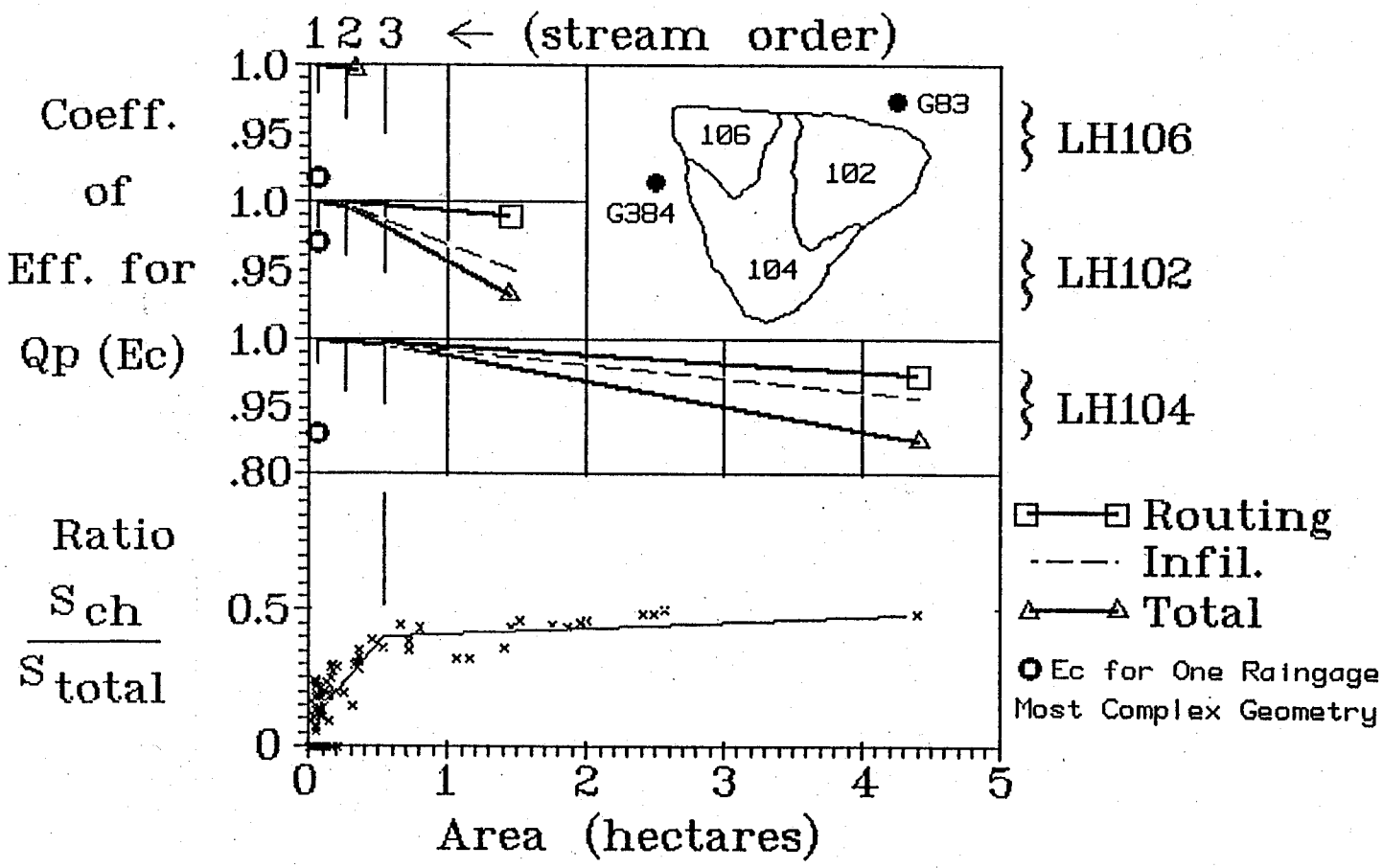

Figure 6.13 Model Performance for Various Levels of Geometric Model Simplification for the Lucky Hill Watersheds

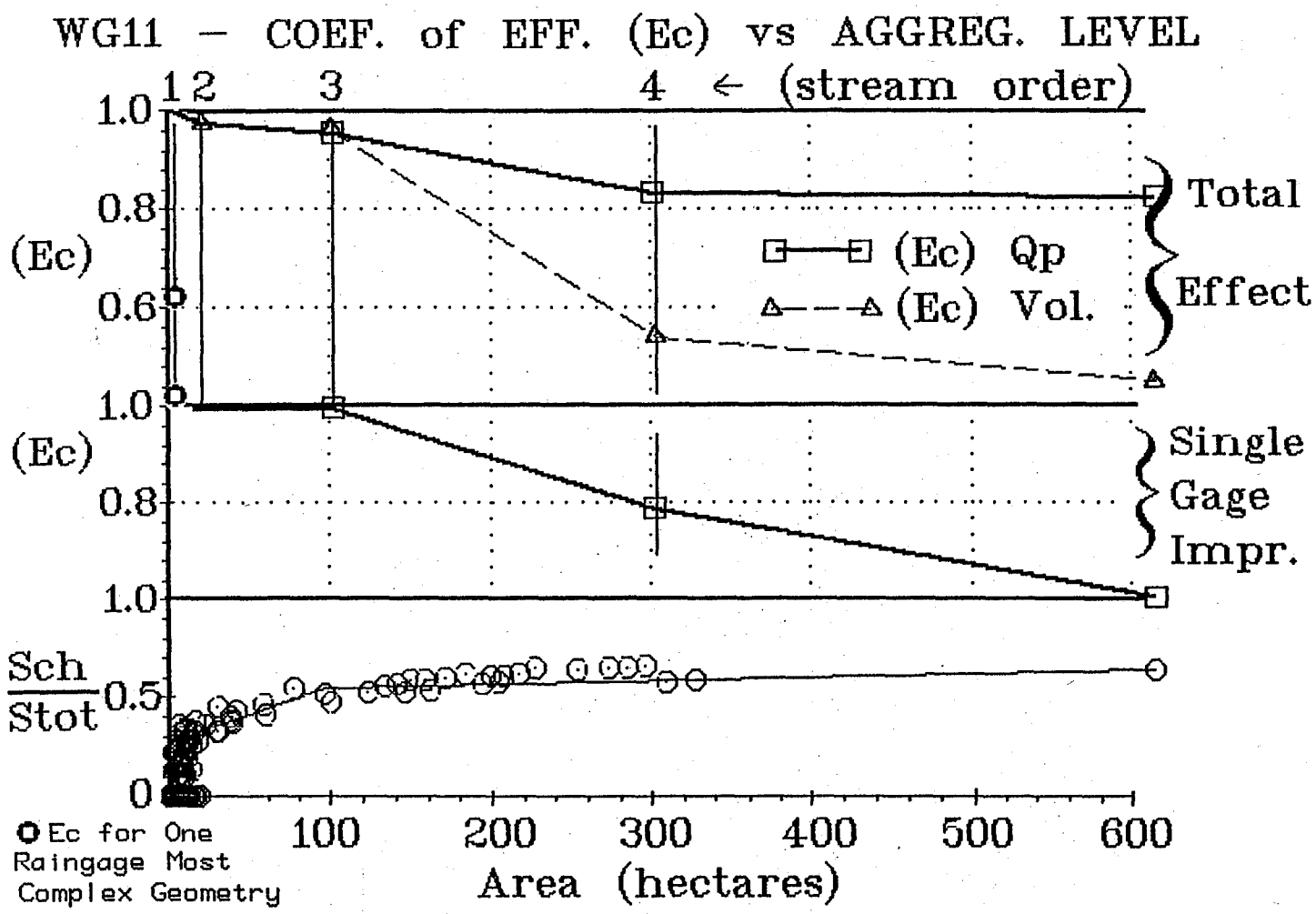

Figure 6.14 Model Performance for Various Levels of Geometric Model Simplification for WG11

address hypothesis (1) an arbitrary level of acceptable geometric simplification error must be established. If the level of simplification error is expressed in terms of a coefficient of efficiency Figures 6.13 and 6.14 can be used to establish the allowable size of overland flow elements that support a channel head that will adequately model basin runoff. Overland flow elements greater than this size will not adequately model runoff. The acceptable support area will define the stream order from the base maps used to initially discretize the watershed. Thus for a given basin scale with the climatic scale defined by the calibration event set and a specific model performance level hypothesis (1) can be accepted or rejected using Figures 6.13 and 6.14

Alternatively, simplification could be carried out until a significant change in model performance is detected with the next level of simplification. Using this criteria LH-106 could still be simplified to a single overland flow element. In LH-102 the first order channels could be removed leaving 16 model elements. In LH-104 the first and second order channels could be removed leaving 12 model elements. For WG11 the first and second order channels could also be removed (16 remaining model elements) without introducing significant simulation errors caused by geometric model simplification. Using these levels of model complexity, the average support area, the percentage of the average support area to total basin area and the resulting drainage density are computed for each watershed (see Table 6.5).

The values in Table 6.5 are useful in defining the required level of geometric model complexity a priori without beginning at a very complex level and simplifying

Table 6.5. Suggested Levels of Geometric Model Complexity to Maintain Model Performance (Ec > 0.9)

Basin	Area (ha)	Number of Model Elements	Percent Average Support Area		Average Support Area (ha)	Drainage Density (m)
LH-106	0.36	1	100		0.36	0.0
LH-102	1.46	15	16	(6)	0.23	1.52×10^{-3}
LH-104	4.40	11	12	(6)	0.53	0.65×10^{-3}
WG11	6.31	17	16	(.01)	101	1.32×10^{-3}

Numbers in parenthesis denote the standard deviation in percent

as was carried out in this study. For basins as small as LH-106 the attenuating influence of the basin itself is very small in relation to the climatic scales (supported by Figure 6.5) and therefore the basins can be entirely simplified to a single element. At a threshold between the basin area scales of LH-106 and LH-102 significant basin attenuation occurs for the climatic scales represented by the calibration event set. This conclusion is supported by Figure 6.5 showing sensitivity to roughness and Figure 6.13 which shows that total basin geometric simplification imparts significant impacts on model performance for basin scales equal to or greater than those of LH-102 (1.46 ha).

The reason for significant degradation in model performance for large degrees of geometric model simplification for LH-102 and the larger basins was mentioned previously in Chapter 4. After significant simplification is carried out substantial concentrated flow from channels has been replaced by overland flow processes. If overland flow no longer dominates the runoff measured at the basin outlet this degree of simplification cannot be made without serious model impacts. The transition from overland to channel dominated flow is an important threshold to define for both geometric simplification and hydrologic subprocess studies. The equilibrium storage provides a key indicator to define this transition.

The equilibrium storage integrates the effects of topography, hydraulic roughness and slope convergence on model performance. When significant flow concentration occurs the equilibrium storage in the channels in relation the total basin equilibrium storage will be large. The ratio of the equilibrium channel storage

to total subbasin storage (ST_c/ST_t) at the downstream outlet of every model element is plotted as a function of the contributing area to each element in the bottom portion of Figures 6.13 and 6.14. In each plot the general trend of the (ST_c/ST_t) ratio increases rapidly and then stabilizes. The break in the slope of this trend corresponds to the allowable stream order reduction by simplification for watersheds LH-104 and WG11. The allowable level of simplification for LH-102 is in the vicinity of the break but does not correspond as well as the two larger watersheds. The stabilization of the (ST_c/ST_t) ratio appears to provide good measure of the transition from overland to channel dominated flow for the topography and channel morphology of the Walnut Gulch study basins.

The level of allowable geometric simplification for LH-102 and the larger basins is well defined by both the percentage of the average support to total basin area and the drainage density (Table 6.5). Both measures are relatively stable across the large range of basin scale studied here. These measures and the (ST_c/ST_t) ratio provide a basis for defining an acceptable level of basin discretization (geometric model complexity). However, the level of complexity must also be examined in relation to the available rainfall data. Also plotted on Figures 6.13 and 6.14 are the efficiencies computed from simulations using with most complex model geometry with a single raingage. They are plotted as large circles at the area corresponding to the support area for the first order channels. For the all the watersheds the efficiencies are from the simulations using the closest raingage to the watershed centroid.

In all but LH-102 the error imparted by using a single raingage is greater than the total simplification error from reducing the watersheds to a single overland flow plane. Thus the geometric model complexity must be commensurate with spatial rainfall data availability. Some of the error caused by using a single raingage would probably be compensated for if the single gage were also used in calibration to adjust parameter multipliers. This was tested on LH-106 and some decrease in simplification error was noted but calibration results using two raingages could not be matched with a single gage. This illustrates that incorporating rainfall variability on the small scale of hundreds of meters does provide valuable input information when used with the model rainfall interpolation algorithm. The precipitation interpolation algorithm does compute simple spatially variable rainfall patterns with as few as two raingages. This justifies the use of more modeling elements than the number of available raingages. Determination of the proper number of model elements for a given number and pattern of raingages was not pursued in this investigation. But a large number of elements for a small number of raingages is not justified unless strikingly different soils and land use patterns exist in the watershed. This relates to the degree of allowable spatial averaging of overland flow element parameters.

The question of averaging was raised in hypothesis (1C) and can be examined by evaluating model performance at various levels of geometric model aggregation. This hypothesis was stated in Chapter 1 as:

HYP (1C): Above a certain basin-climatic scale simple property or parameter averages of overland flow will be sufficient to model runoff.

The simplification procedure performs simple area weighted averaging for soils parameters but roughness is distorted to maintain equilibrium storage. From the simplification results presented above it is apparent the HYP (1C) can only be accepted at very small basin scales (LH-106). When this hypothesis was originally conceived, review of the literature suggested that as basin scale increases, runoff response characteristics will become more linear and small scale variability will be averaged out (Wood et al., 1987, Dooge, 1981; Beven et al., 1988; Wang et al., 1981). The sensitivity results in section 6.3.2 counter this notion and therefore force the rejection of HYP (1C) for increasing basin scales. However, simple averages can be used if the climatic scale is large enough as the nonlinearities associated with infiltration are overwhelmed by very high rainfall intensities.

For the case where storms dominate soils abstractions (large runoff to rainfall ratios), simple soil parameter averages model runoff response nearly as well as distributed parameters (see Figure 2.6, section 4.4. and the following section). The results presented in this study suggest that simple overland flow element parameter averages can only be used in modeling runoff for large storms in small catchments. Therefore the ability to use simple averages is inversely related to increasing basin scales and directly related to increasing climatic scales. The ability to use simple averages also implies that a greatly simplified geometric model representation will

be adequate for runoff simulations. The dependence of geometric model simplification on climatic scale (storm size) is investigated in the following section.

6.4.2. Geometric Model Simplification as a Function of Storm Size

This section more formally addresses hypothesis 1A which was informally addressed in Chapter 4. The hypothesis is restated at this point:

> HYP (1A): The degree of allowable geometric model simplification is a function of storm size.

To concentrate only on the change in model performance it is assumed that the simulated runoff for the most complex basin model representation is true and error free. To test this hypothesis over a greater number of events and a larger range of storm sizes the calibration and verification event sets for each watershed are combined. For each basin the most complex geometric model parameter file is completely simplified to 1 overland flow plane using the rules presented in Chapter 4. The calibration and verification rainfall events are then used as input with the simplified model geometry to produce runoff. The simplification error is defined as the simulated runoff volume from the simple model (Vs) minus the runoff volume from the complex model (Vc). The percentage simplification error then is defined as (Vs - Vc)/Vc * 100.

In Figures 6.15 through 6.18, the simplification and percentage simplification error versus the log transformed runoff volume from the complex (true) model for each study basin are plotted. The linear regression of the simplification and percentage simplification errors versus the log transformed volumes with the 95% confidence intervals about the regression line are also included in these figures. To test hypothesis 1A more precisely using the data presented in Figures 6.15 through 6.18, the following null hypotheses are offered:

HYP (1A-1): The slope of the regression line of simplification error versus log transformed complex model runoff volume equals zero.

HYP (1A-2): The slope of the regression line of <u>percentage</u> simplification error versus log transformed complex model runoff volume equals zero.

If these null hypotheses are accepted, it implies that the simplification error (HYP 1A-1) and percentage simplification error (HYP 1A-2) are independent of event runoff size. Note that event runoff size is used as a surrogate measure of storm size which was used in the phrasing of hypothesis 1A.

In all cases where the simplification error is used (top portion of Figures 6.15 to 6.18), HYP (1A-1) must be accepted at a 95% confidence level as a line with zero slope lies within the confidence bands. However, if the <u>percent</u> simplification error

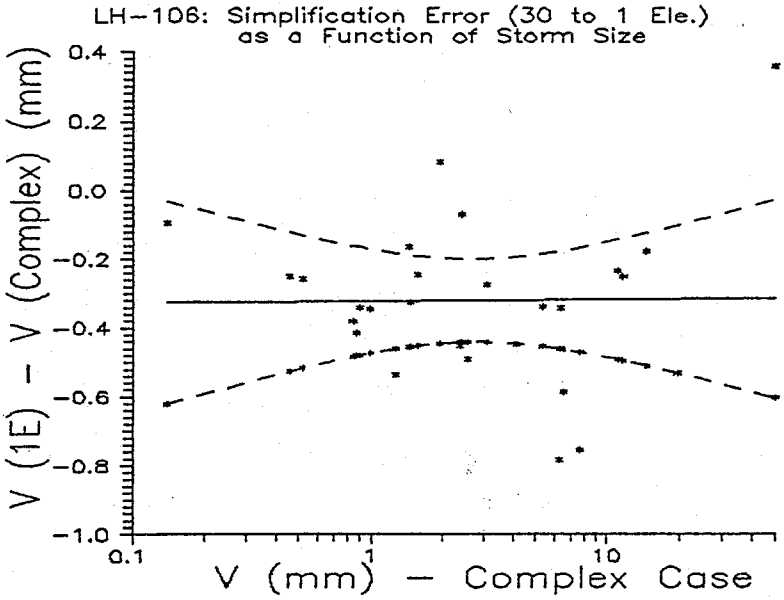

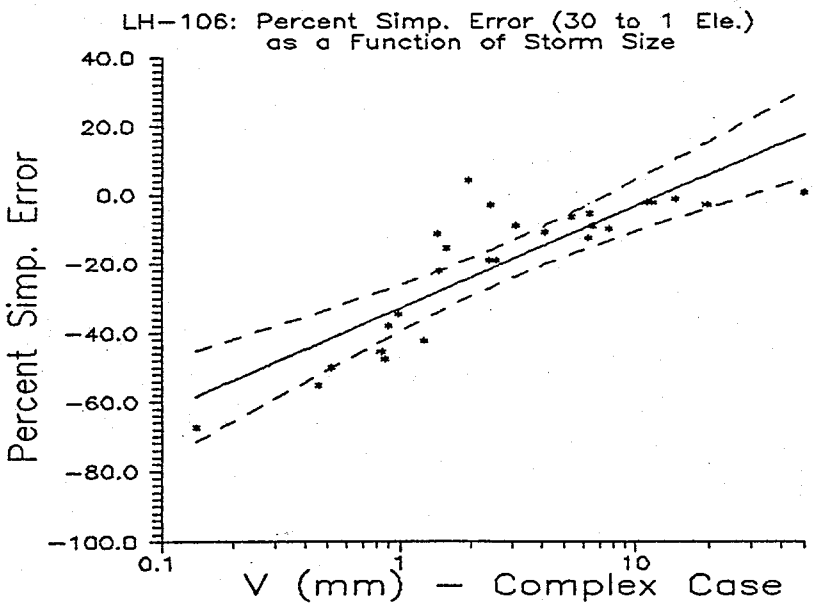

Figure 6.15 Simplification and Percentage Simplification Error (30 to 1 Ele.) Versus Runoff Volume for LH-106

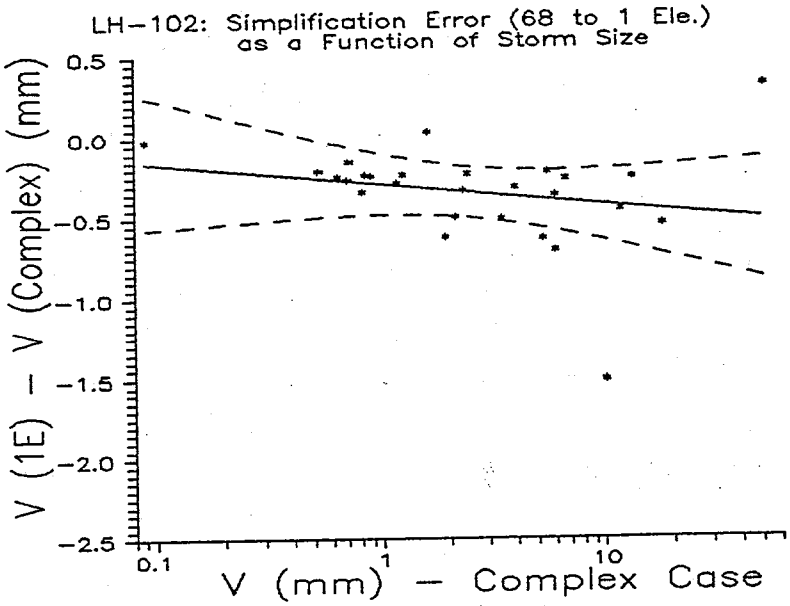

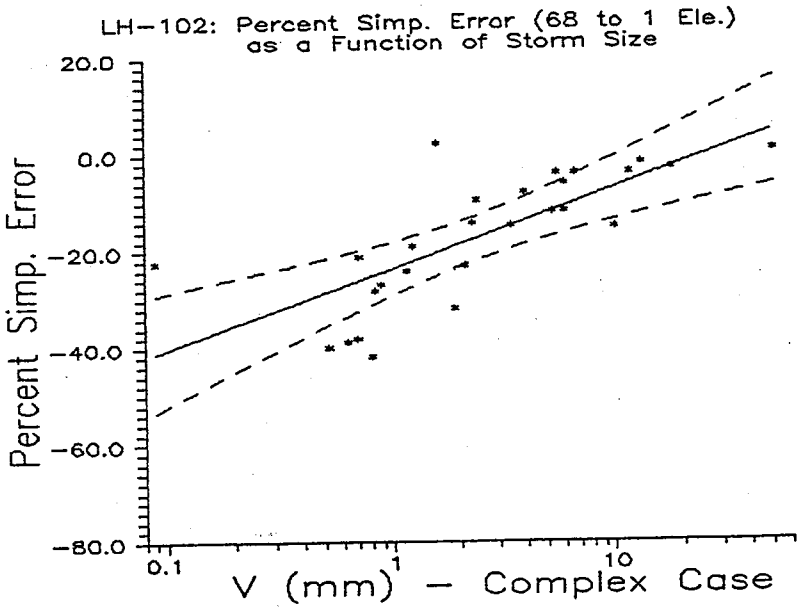

Figure 6.16 Simplification and Percentage Simplification Error (68 to 1 Ele.) Versus Runoff Volume for LH-102

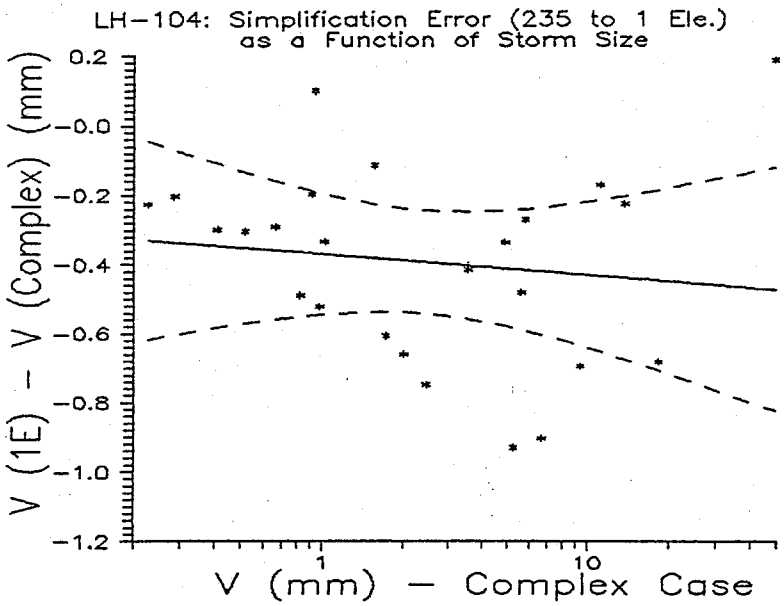

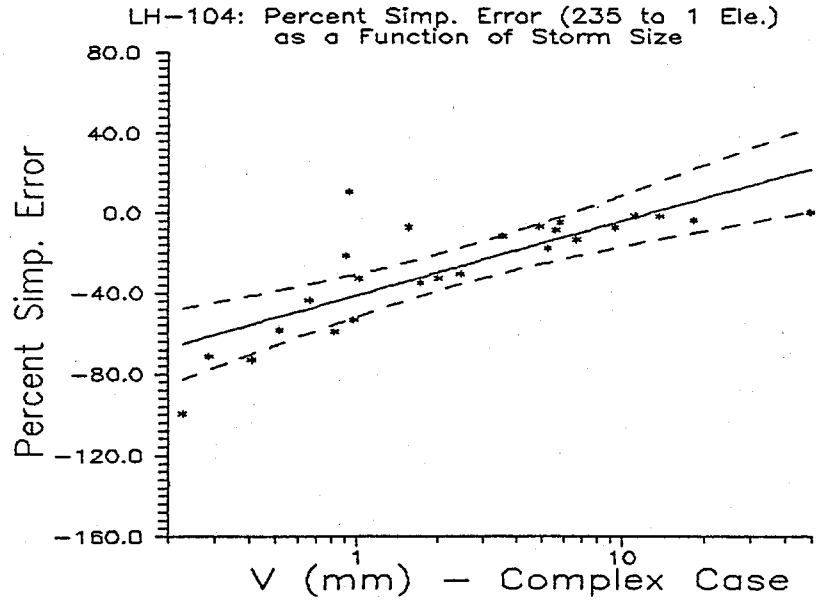

Figure 6.17 Simplification and Percentage Simplification Error (235 to 1 Ele.) Versus Runoff Volume for LH-104

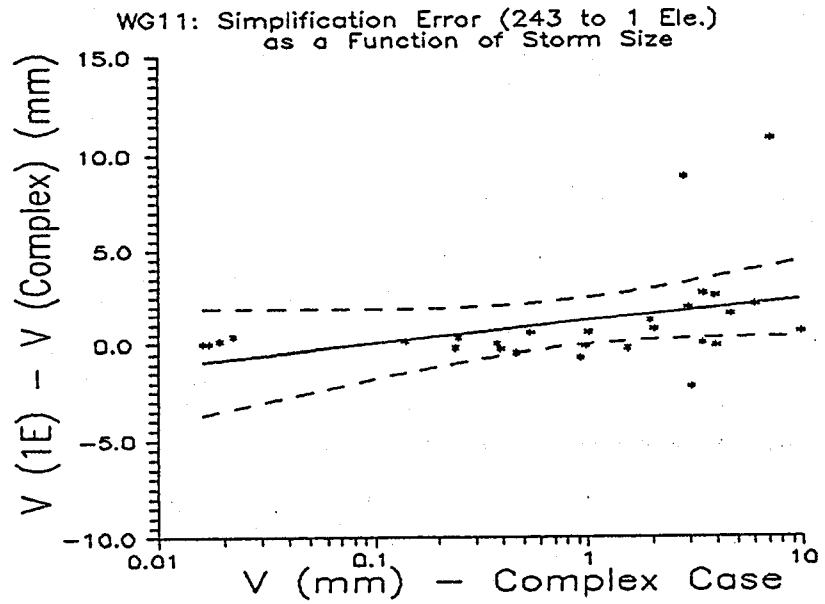

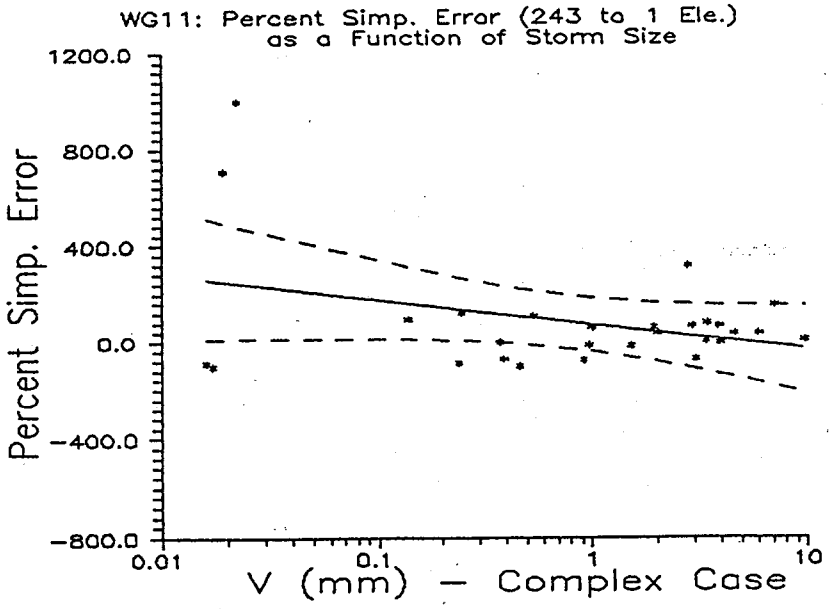

Figure 6.18 Simplification and Percentage Simplification Error (243 to 1 Ele.) Versus Runoff Volume for WG11

is examined (bottom portion of Figures 6.15 to 6.18), the null hypothesis (HYP 1A-2) must be rejected for the Lucky Hills watersheds and accepted for WG11. Therefore, for the Lucky Hills watersheds, we must conclude that the allowable level of geometric model simplification is a function of storm size as measured by complex model runoff volume. In WG11, the null hypothesis is accepted and the same conclusion cannot be drawn. Also note that in the Lucky Hills watersheds, the trend is an underestimation (negative percentage simplification error) of small events by the simple model. This trend can be explained by the averaging of infiltration related parameters that occurs during geometric model simplification as follows.

Variability in soils parameters is reduced during simplification and a more uniform basin representation is obtained even though $C_v > 0.0$. It was demonstrated in Chapter 2 (see Figure 2.5) that for small events, the more uniform the representation of infiltration, the greater the underestimation of runoff volume. However, as the event size increases, the response from a uniform infiltrating surface converges toward the response of a spatially variable surface (see Figure 2.6). Therefore, in the Lucky Hills watersheds, the percentage simplification error tends toward zero with increasing event size. If averaging causes a more uniform basin representation, it stands to reason that increasing C_v for the simplified system should compensate for this averaging. For the Lucky Hills watersheds, it was found that error in volume efficiency caused by simplification could be reduced by 68 percent by increasing C_v on the 1 element system.

Interpretations regarding the simplification errors as a function of storm size are not easily made for WG11. Both the simplification and percentage simplification error are much larger for WG11. This is not unexpected as reducing WG11 to a single element significantly alters the input spatial rainfall distribution. All channels have also been removed when the watershed is reduced to a single element. Significant differences in infiltration characteristics have also been averaged into the single remaining element. The reduction in average runoff ratios for WG11 can also be expected to contribute to simplification errors in WG11. The decrease in average runoff per unit area implies a greater degree of basin attenuating influence. When the basin influence dominates as compared to the climatic scale, errors due to geometric simplification of the basin representation can be expected to exert a greater influence on model performance.

6.5. Application of Study Results

Definition of model objectives will largely define how the results of this study are incorporated into modeling efforts. If modeling very large floods over small watersheds is the primary modeling task, significant geometric model simplification can be made. Modeling small events will require greater detail as long as the modeler does not attempt to estimate events where measurement error dominates the rainfall to runoff transformation. The application recommendations mentioned in this section are site-specific to the Walnut Gulch watershed until the methodology can be verified in other regions. The recommendations apply to the type of climatic

range represented by the calibration event sets with model performance measured by the Nash-Sutcliffe (1970) coefficient of efficiency.

An initial goal of this research was to provide guidelines to the applications modeler for selecting the proper level of geometric model complexity or level of basin discretization. The resolution and density of data available at Walnut Gulch will rarely be available for other rainfall-runoff modeling efforts, nor will the procedure followed in this investigation, starting with a very complex discretization level and simplifying, be economically feasible. Given commonly available data sources, the results of this study can aid modeling efforts in several ways.

The sensitivity to input rainfall distributions is very large and, therefore, the first task is assessment of the availability of rainfall data. Current gage networks are notoriously sparse, especially so in much of the arid Southwest, where thunderstorm rainfall is highly variable. A great deal of geometric model complexity is, therefore, unjustified. However, even with a single raingage, when channel processes become important, a single overland flow plane will not adequately model runoff and some channel processes must be incorporated (see the middle portion of Figure 6.14). The availability of higher resolution rainfall data should improve in the foreseeable future for large portions of North America with the installation of NEXRAD radar systems. These systems are capable of providing space-time estimates of rainfall intensities at a scale comparable with the suggested support area of WG11 in Table 6.5 (1 km^2).

If available rainfall data justify finer basin discretization, an average channel support area equal to roughly 15 percent of the basin area is recommended for watersheds with areas greater than 1 hectare (see Table 6.5). For a more thorough initial investigation to define required model complexity, the ratio of the channel to total equilibrium storage (ST_c/ST_t) could be computed. It is envisioned that Digital Elevation Models (DEM data) available from the U. S. Geological Survey for much of North America could be used to define the storage ratio as a function of increasing basin area. To do so, contributing overland flow areas with initial roughness estimates could be generated directly from the DEM data. Rough estimates of channel cross sections and roughness as a function of stream order could be obtained from sparse field measurements or prior studies. This would provide sufficient information to define impervious watershed geometries so that the (ST_c/ST_t) ratio could be computed. The support area corresponding to a stabilization of this ratio defines the required drainage density and level of geometric model complexity to adequately maintain model routing characteristics. Additional geometric model complexity would be warranted for cases where significant soils or land use changes impart large degrees of spatial infiltration variability.

These guidelines will establish an initial level of acceptable geometric model complexity. If rainfall-runoff data exist for the watershed under investigation (or a nearby comparable watershed), a parsimonious model calibration can be conducted to refine initial parameter estimates. Every effort must be made to obtain reliable calibration and verification data sets. The amount of time spent ensuring data

reliability should not be small in comparison to the overall modeling effort. Without trustworthy data, modeling results and study interpretations may bear little resemblance to the actual field situation. Modeling efforts can easily be rendered worthless by using unreliable data. When reasonable faith in data has been achieved, calibration can proceed. However, a large number of free calibration parameters is not warranted. An unparsimonious parameter set, like large data uncertainty, will most likely result in biased and/or inaccurate model interpretations.

It is hoped that these recommendations will help avoid unsupported or excess model complexity in distributed rainfall-runoff studies that is merely the result of having large-scale base maps available for initial basin discretization. This is especially true for urban rainfall-runoff studies where large-scale maps are available. It is believed that the application recommendations stated above will transfer reasonably well to urban studies as long as kinematic routing assumptions are not violated. This belief must, of course, be verified. The availability of 30 X 30 m DEM data will also fuel the fires of unnecessary distributed geometric model complexity in more general watershed settings. If nothing else, it is hoped that rainfall-runoff modelers will garner the realization that overkill in basin discretization is unwarranted from this study.

6.6. Conclusions

The results presented in this chapter indicate a degradation in model performance with increasing basin scale as measured by the Nash-Sutcliffe (1970)

forecast coefficient of efficiency. Much of the loss in model performance can be attributed to greater uncertainties associated with modeling at the larger scale in semi-arid regions, such as Walnut Gulch. They include greater spatial variability of rainfall and a lack of knowledge of initial channel conditions when channel losses are critical. Other important factors include an increase in the proportion of instrument measurement error to overall modeling error, as well as an increase in basin attenuation in relation to climatic scales that are typical of a losing watershed environment (influent streams) such as Walnut Gulch. However, the mean and standard deviation of model-predicted runoff volumes and peak runoff rates are well preserved as basin scale increases. This indicates that the model could be used with confidence to transform rainfall data into runoff frequency estimates.

Results also indicate that in arid and semi-arid regions, runoff response does not become more linear with increasing basin scale. The evidence presented here would support the argument that runoff response becomes more nonlinear with increasing basin scale. This occurs because of the decrease in climatic influence relative to the increasing role of basin attenuating influence resulting from routing and infiltration losses with increasing watershed scale.

As watershed scale increases, an increasing influence of channel processes is noted. However, the importance of runoff production on overland flow areas is critical throughout the entire range of basin scales examined. Incorporation of model representation of the small-scale infiltration variability becomes more important with

increasing watershed scale due to greater soils/rainfall interaction in space as large-scale spatial variability of rainfall increases.

The input rainfall field, and an accurate representation of it, remains the most important factor in determining runoff response due to the lack of any long time scale response related to groundwater in the ephemeral watersheds of Walnut Gulch. Infiltration is the second most important factor in runoff response. Model sensitivity to routing factors is third in importance in reproducing runoff response. This justifies a greater degree of infiltration process model complexity and fewer research exercises to improve routing. Given these observations, coupled with the increasing nonlinearity of runoff response and increasing spatial rainfall variability with increasing basin scale, it is unlikely that Unit Hydrographs concepts can be successfully applied to the basins examined in this study.

The ability to use average overland flow parameters to model runoff response is inversely proportional to basin size and directly proportional to storm size. The same proportionalities apply to the allowable level of geometric model simplification to maintain a specified level of model performance. An average channel support area of approximately 15 percent of the overall watershed area for basins with drainage areas roughly between 1.5 and 630 hectares is recommended for the basins studied. This will define the basin drainage density and level of basin discretization.

The ratio of channel to total equilibrium storage can also be used to predict, a priori, an acceptable level of basin discretization that maintains appropriate model routing of overland and channel flow. It should be noted that KINEROSR does not

currently model compound trapezoidal channel geometries and, therefore, channel overbank storage is not computed. This is not considered a problem as the majority of channels in the watersheds studied are highly incised. Stabilization of the channel to total equilibrium storage ratio provides a good measure to define the transition from hillslope to channel-dominated runoff response. Many of the results obtained from the analysis presented in this chapter are applicable to general rainfall-runoff modeling efforts and, in many cases, they can be incorporated to improve those efforts. To reiterate, it is hoped that these recommendations will help avoid unsupported or excess model complexity in distributed rainfall-runoff studies that is merely the result of having large-scale base maps available for initial basin discretization.

CHAPTER 7

CONCLUSIONS AND RECOMMENDATIONS

7.1 Major Conclusions and Contributions

Primary research conclusions are enumerated in succinct form and additional, important, discussion regarding the conclusions follows. The enumerated conclusions should not be interpreted without carefully reading the associated discussion. The techniques developed in this research effort were not verified on watersheds other than Walnut Gulch due to resource limitations. Therefore, the conclusions drawn from this study, except where noted, are offered with the caveat of applicability to comparable semi-arid watersheds, subjected to similar climatic forcing, over the range of basin scales examined in this study.

Under the umbrella of this caveat, the following conclusions appear to be justified by the analysis performed in this study:

(1) Modeling of small-scale infiltration variability is most critical for runoff events with small runoff/rainfall ratios at small spatial scales and increases in importance for larger spatial scales where spatial rainfall gradients are large. The model representation of Woolhiser and Goodrich (1988) with eight strips treats small-scale infiltration variability in a parsimonious, relatively efficient manner without added spatial discretization.

(2) Stabilization of the channel to total equilibrium storage ratio provides a powerful, a priori, measure of an acceptable level of

basin discretization which translates into an average first order channel support area equal to approximately 15% of basin area for catchments greater than 1.4 hectares and smaller than 630 hectares.

(3) Excellent rainfall-runoff modeling results were obtained for a quasi-physically-based model after parsimonious calibration, contrary to the findings of Loague and Freeze (1985) and Loague (1990).

(4) Rainfall-runoff response does not become more linear with increasing basin scale but appears to become more nonlinear.

The first conclusion highlights the importance of rainfall/soils interactions in runoff production and overall watershed response. The sensitivity analysis presented in Chapter 6 demonstrates that an accurate representation of the input rainfall field remains the most important factor in determining runoff response due to the lack of any long-term, highly-damped, response related to ground water in ephemeral watersheds. Infiltration is the second most important factor in runoff response determination. Model sensitivity to routing factors is third in importance in reproducing runoff response. This justifies a greater degree of infiltration process model complexity and fewer research exercises to improve routing.

With regard to the second conclusion, the importance of watershed equilibrium storage as a measure of characteristic basin response (Wu et al., 1978)

is demonstrated in Chapters 4 through 6. This measure integrates the effects of topography, slope convergence, and hydraulic roughness. The use of storage, to provide order to the complex interactions of topography, flow convergence, and roughness, further aids our understanding of runoff response in a fashion reflected by Bronowski (1972). He stated "All science is the search for unity in hidden likenesses . . . The progress of science is the discovery at each step of a new order which gives unity to what had long seemed unlike . . . For order does not display itself of itself . . . What we see, as we see it, is mere disorder."

Equilibrium storage also plays a pivotal role in the geometric model simplification procedure. The hydraulic response characteristics of a complex elementary basin representation are largely preserved by a simple equivalent overland flow plane by distorting the hydraulic roughness to maintain equilibrium storage. The dominance of overland flow routing and runoff production for a simple open book elementary watershed (Chapter 3) justifies the removal of the channel and incorporation of channel routing effects into an equivalent overland flow plane. Simplification is further justified if available data sources, especially distributed rainfall data, are not defined to a commensurate level of complexity with the level of geometric model complexity (Hromadka 1987, 1987a; Hughes, 1989; Hughes and Beater, 1989; Bras and Rodriguez-Iturbe, 1976; Troutman, 1986). The methods developed in this study to determine a suitable level of geometric model complexity can be applied with relative ease to other distributed modeling efforts.

The third conclusion addresses the ability of a quasi-physically-based model (KINEROSR) to reproduce runoff results. The poor quasi-physically-based modeling results of Loague and Freeze (1985) have been widely quoted in the hydrologic literature to attack the utility of such models (Hughes, 1989; Hughes and Beater, 1989; and Beven, 1989; to name a few). An oft-cited criticism is the plethora of parameters required for such models, of which many must be calibrated (Beven, 1989). The parsimonious calibration procedure developed in this study, resulting in only three fitting parameters, aptly addresses these concerns. Loague (1990) and Beven (1989) argued that if any model calibration is done, our so-called "physically-based" models reduce to merely black box conceptual models. This study argues that because it is impossible to measure initial model parameters perfectly in the field, some calibration is justified.

The parsimonious distributed model calibration procedure developed in this study produced excellent calibration results as measured by the Nash-Sutcliffe forecast coefficient of efficiency over the set of calibration events for all four study basins, of which the range in drainage area covers over three orders of magnitude. Verification results were also very good for the three smaller Lucky Hills watersheds. Individual events were simulated very well for medium to large events in Lucky Hills with internal distributed model integrity. Small events are not simulated well, as rainfall and runoff measurement uncertainty becomes a dominant part of the runoff response signal (Pilgrim et al., 1988). Verification simulations degraded with increases in basin scale to WG11. Because of the semi-arid setting of Walnut Gulch,

a decrease in runoff per unit area is encountered with increasing watershed scale (influent). As mean runoff volume per unit area approaches rainfall measurement resolution, measurement uncertainty will again become a large portion of the runoff signal. The ability to simulate runoff will, therefore, decrease.

The influent semi-arid watershed environment of Walnut Gulch largely explains conclusion four. Increasing nonlinearity in runoff response with increasing basin scale occurs because of the decrease in climatic influence relative to the increasing role of basin attenuating influence resulting from routing and infiltration losses with increasing watershed scale. This finding also explains why the importance of small-scale infiltration variability, model performance, and the allowable level of geometric model simplification is dependent on the continuum of relative basin attenuation in relation to climate or storm size.

Small-scale infiltration variability is important until the storm size increases to the point where rainfall intensities overwhelm the nonlinearities associated with infiltration. In this case, the uniform infiltration model representation converges toward more complex infiltration model representations. The allowable level of geometric model simplification is directly proportional to the climatic scale (storm size) and inversely proportional to basin scale. For small storms with large basin attenuation due to high initial hydraulic roughness or large infiltration abstraction, greater error is introduced upon geometric model aggregation. For large storms with minor basin attenuating capabilities, where the climate is dominant, larger spatial

averaging of infiltration related parameters and routing simplification will not impart significant uncertainty into the modeling process.

Model performance is also directly related to storm size and inversely related to basin scale as the level of basin attenuation increases. For large storms, the nonlinearities associated with infiltration and routing are largely overwhelmed resulting in a strong input-output (rainfall-runoff) signal. This is much more easily modeled than a very small runoff event where the ratio of basin attenuation to storm size influence is large, resulting in small runoff ratios. In this case, the input-output signal is very weak, and measurement error becomes a large percentage of overall modeling error. In a water quality modeling context, Beck (1987) also concluded that any type of modeling will be extremely difficult unless the process has a well-defined input-output relationship. For increasing basin scales, the loss of input-output proportionality, coupled with the increasing nonlinearity of runoff response and increasing rainfall spatial variability, implies that the application of Unit Hydrograph concepts is inappropriate for the basins examined in this study (see also Amorocho, 1961).

After review of this research effort, with conclusions and associated discussion in hand, several contributions can be identified. They are:

(1) Definition of the required level of geometric model complexity (basin discretization) and hydrologic subprocess domination specifically as a function of basin scale for distributed rainfall-runoff modeling.

(2) Development of an objective methodology to define a justifiable level of distributed geometric model complexity.

(3) Compilation of a carefully checked set of rainfall-runoff data, with associated watershed characteristics, for a range of watershed scales with sufficient detail to allow ready use by other investigators.

It should be noted that the second contribution and its associated conclusion (number 2) should be widely transferable to other watershed modeling situations where the primary basis for catchment discretization is identification of a support area at which channel processes become critical. Widespread applicability of this procedure should present little difficulty. An impervious watershed representation, with channel cross section information and initial roughness estimates, are all that is required to derive equilibrium storage ratios. The generality of the procedure is also enhanced as it is independent of the uniform rainfall rate used to obtain the storage. However, watersheds with significant backwater effects and significant overbank storage were not treated in this study; therefore, application of the research methodology to this class of basins requires further investigation.

7.2 Recommendations for Future Research

This research effort has raised many more questions than it has answered. Various frustrations with current capabilities have also surfaced throughout the

course of this study. The following future research objectives are offered to focus continuing efforts and to attempt to answer some of the scientific questions raised during the study:

(1) Develop algorithms to automatically extract overland flow and channel element geometries from digital elevation data.

(2) Incorporate initial channel moisture conditions to assess whether model performance can be improved for watersheds where channel losses are significant (WG11 and larger).

(3) Extend the methodology to larger basin scales within Walnut Gulch and to other watersheds in different climatic regions.

(4) Develop and test the ability of new measures to identify hydrologic subprocess domination as a function of basin and climatic scales.

(5) Assess how distributed simplification methodology would impact sediment and chemical transport model performance.

(6) Investigate hydrologic subprocess model simplification (nonlinear to linear routing, for example).

(7) Investigate the applicability of simplification methodology to interstorm hydrologic modeling.

(8) Investigate more thoroughly the issues of linearity, including Unit Hydrographs concepts, and nonlinearity as a function of basin scale.

(9) Investigate the tradeoffs between simplicity and complexity for both geometric and process modeling efforts in terms of economic advantages or disadvantages (Warwick, 1989).

The future research efforts outlined must be firmly grounded in realism. The continuing exponential increase in computing capability is allowing "simulation" modeling to be conducted at ever more complex levels of both geometric and process sophistication. Before continuing down the road to modeling nirvana with supercomputer in tow, commensurate levels of verification data must exist to justify the exercise.

APPENDIX A

DETAILED DESCRIPTION OF HYDROLOGIC DATA FOR STUDY BASINS

APPENDIX A

DETAILED DESCRIPTION OF HYDROLOGIC DATA FOR STUDY BASINS

A.1 Introduction

The purpose of this appendix is to summarize much of the data used in this research effort. Also included is a summary of procedures for developing many of the initial parameter estimates from field data. All of the data and procedures are not described in detail in this document as much of the information will be presented in a forthcoming publication. The majority of the data will also be made available in electronic format. The quantity of rainfall-runoff data and distributed watershed input data is too great to present here. It is hoped that by making the entire data set available in electronic format, other investigators will readily use this data, and that data entry errors resulting from transcribing the data from printed form will be avoided.

The following data will not be discussed in detail in this document but will be included in electronic format:

(1) Daily rainfall data for 11 raingages and basin-wide monthly meteorological data to compute estimates of initial relative soil moisture (SI in KINEROSR) at the beginning of rainfall-runoff events (see also Appendix B);

(2) Breakpoint rainfall data for the 12 raingages (and the raingage coordinates) for each of the study events;

(3) Time discharge runoff data for each of the four flumes for each of the study events;

(4) Digital elevation data for each of the study basins;

(5) KINEROSR input parameter files for each of the four study basins (they contain watershed geometric parameters and soils information: see also Woolhiser et al., (1990) for a further description of this information);

(6) Digital soils boundaries for each of the study watersheds.

A.2 Summary Runoff Data

Tables A.1 through A.4 contain summary information for each of the runoff events for each of the four watersheds used in this study. Corresponding time-discharge data for each of the events will be presented in electronic form.

A.3 Watershed Parameters

A.3.1 Computational Parameters

These parameters were estimated by way of methods discussed in Woolhiser et al. (1990). They include DELT, the computational time step, and THETA, the spatial weighting parameter in the four-point finite difference scheme used in KINEROSR. TFIN, the total computational time, is event dependent, and was chosen sufficiently large to ensure a near zero simulated discharge at TFIN. In KINEROSR, TFIN is included in the rainfall input file and not the parameter input

Table A.1. Lucky Hills - 106 (LH-106) Runoff Data

Date (d/m/y)	Event Number	Total Volume (mm)	Q Peak (mm/hr)	Time to Peak (min)
14/ 7/73	48	1.4	10.7	46
27/ 7/73	49	15.1	67.2	22
19/ 7/74	50	7.7	35.1	36
28/ 7/74	51	5.0	38.1	12
29/ 7/74	52	0.6	3.2	28
30/ 7/74*	53	1.9	12.3	24
1/ 8/74	54	4.1	20.9	16
12/10/74	56	1.2	11.2	27
22/10/74	58	2.5	17.3	16
29/10/74	59	0.5	1.7	124
5/ 7/75*	60	2.4	32.1	11
8/ 7/75	61	0.6	4.4	94
12/ 7/75*	62	11.0	86.3	23
17/ 7/75	63	47.6	151.1	11
7/ 9/75	64	1.2	10.7	15
13/ 9/75*	64A	4.5	20.9	17
6/ 9/76	65	6.9	47.0	29
10/ 9/76	66	1.5	10.7	22
13/ 7/77	67	0.8	6.6	14
23/ 7/77*	69	0.5	3.7	64
31/ 7/77*	70	0.9	7.4	26
1/ 8/77*	71	1.2	5.8	65
15/ 8/77*	72	0.9	7.4	12
16/ 8/77*	73	9.1	74.8	20
1/ 9/77	74	0.7	2.4	36
26/ 9/77	75	8.5	20.9	137
26/ 9/77*	75A	14.6	96.7	38

* Calibration Event

Table A.2. Lucky Hills - 102 (LH-102) Runoff Data

Date (d/m/y)	Event Number	Total Volume (mm)	Q Peak (mm/hr)	Time to Peak (min)
14/ 7/73	48	2.4	14.6	45
27/ 7/73	49	15.0	66.1	23
19/ 7/74	50	6.2	29.2	29
28/ 7/74	51	4.5	33.8	10
29/ 7/74	52	0.4	2.2	34
30/ 7/74*	53	1.3	8.7	36
1/ 8/74	54	4.5	21.2	21
12/10/74	56	1.3	14.6	14
22/10/74	58	2.5	16.1	13
29/10/74	59	0.4	2.2	120
5/ 7/75*	60	2.0	20.3	10
8/ 7/75	61	0.4	4.1	93
12/ 7/75*	62	10.8	85.3	17
17/ 7/75	63	41.1	107.4	14
7/ 9/75	64	2.5	23.1	15
13/ 9/75*	64A	5.1	18.6	29
6/ 9/76	65	7.0	33.8	29
10/ 9/76	66	1.5	8.7	19
13/ 7/77	67	1.5	11.9	13
23/ 7/77*	69	0.6	4.9	62
31/ 7/77*	70	1.5	11.8	24
1/ 8/77*	71	2.0	7.2	66
15/ 8/77*	72	1.4	11.8	12
16/ 8/77*	73	6.9	44.2	22
1/ 9/77	74	3.8	11.1	35
26/ 9/77	75	10.4	25.0	164
26/ 9/77*	75A	13.6	64.4	37

* Calibration Event

Table A.3. Lucky Hills - 104 (LH-104) Runoff Data

Date (d/m/y)	Event Number	Total Volume (mm)	Q Peak (mm/hr)	Time to Peak (min)
14/ 7/73	48	2.2	14.2	47
27/ 7/73	49	17.3	76.0	22
19/ 7/74	50	6.6	32.1	30
28/ 7/74	51	4.5	33.0	12
29/ 7/74	52	0.4	2.2	30
30/ 7/74*	53	1.6	9.7	37
1/ 8/74	54	5.0	21.3	21
12/10/74	56	1.3	15.2	16
22/10/74	58	-.-	-.-	-.-
29/10/74	59	0.1	0.3	134
5/ 7/75*	60	-.-	-.-	-.-
8/ 7/75	61	0.3	2.4	98
12/ 7/75*	62	10.4	86.4	19
17/ 7/75	63	47.8	134.9	31
7/ 9/75	64	1.7	16.7	18
13/ 9/75*	64A	4.9	20.5	30
6/ 9/76	65	5.4	36.2	29
10/ 9/76	66	1.1	9.2	23
13/ 7/77	67	0.6	6.4	19
23/ 7/77*	69	0.2	2.2	65
31/ 7/77*	70	0.8	8.4	26
1/ 8/77*	71	1.1	5.5	71
15/ 8/77*	72	0.9	10.1	12
16/ 8/77*	73	6.0	47.0	22
1/ 9/77	74	0.4	2.0	37
26/ 9/77	75	7.4	18.6	166
26/ 9/77*	75A	12.3	62.6	39

* Calibration Event

-.- Events excluded due to data errors

Table A.4. Walnut Gulch Subwatershed 11 (631 ha) Runoff Data

Date	Vol(mm)	Qp(mm/hr)	Tp(min)
*06AUG66	3.8	5.2	113
05AUG68	4.6	14.2	46
12AUG71	3.4	5.6	95
24AUG71	1.3	5.3	28
12JUL73	2.1	6.0	53
16JUL73	1.7	3.7	60
*27JUL76	4.9	8.4	45
22JUN77	3.4	5.6	153
01AUG78	3.3	7.4	44
*21OCT78	0.4	0.6	121
*04AUG80	5.8	14.4	72
16JUL81	0.7	1.5	77
29JUL81	1.3	2.3	98
30JUL81	2.5	1.8	243
31JUL82	1.0	2.2	75
10SEP83	1.2	3.9	55
15SEP83	1.2	4.3	53
20SEP83	3.3	5.0	164
26SEP83	1.2	2.8	75
*27SEP83	1.2	1.1	149
25AUG84	0.4	0.7	70
17JUL85	1.7	3.5	61
*24JUN86	0.4	0.6	117
15JUL86	0.4	0.7	70
*09AUG86	2.7	4.5	69
*10AUG86	0.8	2.5	51
*14AUG86	2.5	3.1	108
17AUG86	2.9	3.3	448
29AUG86	7.8	8.8	147
20AUG88	0.6	0.7	72

* Calibration Event

file as it is in KINEROS (Woolhiser et al., 1990). The resistance law used throughout the study was Manning's. This is denoted by selecting NRES = 1. English units were used for rainfall-runoff computations (NUNITS = 1), and minutes were used for the time step (NTIME = 2).

A.3.2 Topographic (Geometric) Model Parameters

The watersheds were segmented in a manner described in Chapter 4 to obtain overland flow and channel model elements. For WG11, a 1 inch = 400 foot, 10-foot contour interval orthophoto maps were used as base maps. These maps were compiled by the Orthoshop-Tucson, Arizona, from photography dated 4/30/88. For the Lucky Hills watershed, a 1 inch = 40 foot, 1 foot contour interval orthophoto map was used as a base map. This map was compiled by Cooper Aerial Survey Co., Tucson, Arizona, from photography dated 12-10-75, and Arizona State Plane Coordinates (ft) were transferred to this map from the WG11 maps.

As described in Chapter 4, the area, flow length, and slope for each overland flow element was determined by hand digitizing. For channel elements, the length and slope were also determined by digitizing. In addition, the approximate centroid coordinates (by eye) of each model element were digitized to facilitate the rainfall interpolation procedure (see Appendix C).

Channel geometry (bottom width and side slopes) was measured directly in the field for each channel segment. For this analysis, it was assumed that the area of the channel was the measured bottom width multiplied by the digitized channel

length. To maintain the proper digitized basin area, the area of one of the lateral contributing overland flow planes was reduced to account for the added channel area. This was accomplished by adjusting the length of the contributing overland flow plane.

A.3.3 Hydraulic Roughness Parameters (Manning's)

These parameters were estimated in the field for each channel and overland flow area by inspection using Woolhiser et al. (1990) as a guide. An effort was made to maintain relative differences in roughness based on the vegetation and rock cover of the areas surveyed. Because a multiplier on hydraulic roughness was used in the model calibration procedure, these relative differences are maintained even if an incorrect "base" roughness was selected.

A.3.4 Soils Parameters

Many of the soil parameters required for KINEROSR were estimated from textural soils information. For the Lucky Hills watersheds, 17 soils samples were taken. Soil texture class and percentages of sand, silt, clay, and rock (> 2mm) for each of these samples is shown in Table A.5. The samples were taken at the coordinate locations shown in Table A.6.

Saturated hydraulic conductivity estimates (Ks'; FMIN in KINEROSR) were determined after a multistep procedure. In the first step, Ks (in/hr) (column (1) of Table A.6) is estimated from the percent clay as follows:

Table A.5. Lucky Hills Soil Textural Information

Sample	Soil Texture Class	% Sand	% Clay	% Rock (> 2mm)	% Rock *
LH6-1	Sandy Loam	61.6	11.7	22.0	14.6
LH6-2	Sandy Loam	62.9	17.1	52.0	39.6
LH6-3	Sandy Loam	69.6	17.1	52.0	39.6
LH6-4	Sandy Loam	57.6	18.4	57.0	44.5
LH6-5	Sandy Loam	57.6	14.4	41.0	29.6
LH6-6	Sandy Loam	57.6	15.7	43.0	31.4
LH4-1	Loam	50.0	22.0	41.0	30.0
LH4-2	Sandy Loam	58.0	18.0	60.9	49.0
LH4-3	Sandy Loam	58.0	20.0	61.5	49.0
LH4-4	Sandy Loam	62.0	17.0	58.2	46.0
LH4-5	Sandy Loam	67.0	14.0	53.4	41.0
LH4-6	Sandy Loam	68.0	14.0	48.1	36.0
LH2-1	Loam	51.0	20.0	44.0	32.0
LH2-2	Sandy Loam	60.0	19.0	63.0	51.0
LH2-3	Sandy Loam	71.0	15.0	44.0	32.0
LH2-4	Sandy Clay Loam	61.0	18.0	29.0	20.0
LH2-5	Sandy Loam	64.0	16.0	53.0	41.0

* This column is percent rock by volume as computed from percent rock by weight in the previous column with an assumed specific gravity of rock = 2.65 and bulk density of soil matrix = 100 lbs/ft^3

Table A.6. Adjustments to Obtain Saturated Hydraulic Conductivity

Sample	Location (ft) (AZ State Plane) North	East	(1) Ks (in/hr)	(2) Total Porosity	(3) Ks_r (in/hr)	(4) Ks_c[1] (in/hr)
LH6-1	535149	269989	0.63	0.453	0.480	1.416
LH6-2	535200	270057	0.30	0.453	0.140	0.403
LH6-3	535266	270115	0.63	0.453	0.287	0.845
LH6-4	535269	270003	0.26	0.453	0.105	0.311
LH6-5	535291	269921	0.42	0.453	0.237	0.701
LH6-6	535223	269933	0.35	0.453	0.191	0.562
LH4-1	535326	269777	0.18	0.463	0.101	0.298
LH4-2	535527	269675	0.27	0.453	0.112	0.330
LH4-3	535590	269742	0.22	0.453	0.079	0.234
LH4-4	535761	269747	0.30	0.453	0.118	0.345
LH4-5	535457	269917	0.44	0.453	0.194	0.572
LH4-6	535744	269946	0.44	0.453	0.217	0.634
LH2-1	535499	270102	0.22	0.463	0.117	0.346
LH2-2	535569	270285	0.24	0.453	0.082	0.243
LH2-3	535711	270418	0.39	0.453	0.208	0.613
LH2-4	535639	270099	0.27	0.398	0.191	0.564
LH2-5	535724	270172	0.34	0.453	0.151	0.446

[1] For overland flow planes

$$Ks = 80.709\ (\%clay)^{-1.972} \tag{A.1}$$

This regression was derived from mean percent clay and mean Ks for each soil texture class in Table 2 of Rawls et al. (1982). The mean total porosity (column (2) of Table A.6) based on texture class was also obtained from Table 2 of Rawls et al. (1982). These values were used for the parameter POR in KINEROSR. The following relationship from Bouwer and Rice (1984) was then used to obtain a rock corrected Ks value (Ks_r, column (3) of Table A.6).

$$Ks_r = Ks\left(\frac{e_b}{e_s}\right) = \frac{(1-\varepsilon)(1-V_r)}{1-\varepsilon(1-V_r)} \tag{A.2}$$

where:

e_b = void ratio of field soil

e_s = void ratio of fine earth fraction (<2 mm)

ϵ = total porosity (column (2), Table A.6)

V_r = percent rock by volume (last column in Table A.5).

Cover corrections based on the work of Stone et al. (unpublished, refer to reference list for address to obtain this document) for erosion pavement and

vegetation were then applied to Ks_r via the following relationship to obtain Ks_c (column (4) Table A.6);

$$Ks_c = Ks_r \, e^{0.09(GC)} \, e^{0.0105(CC)} \tag{A.3}$$

where:

GC = percent ground cover = (1 - % bare soil)

CC = percent canopy cover.

Estimates of GC and CC were obtained from point scale measures on rainfall simulator plots (3.5 X 10 m) located approximately 150 m south of the rough center of LH-104. For channel model elements CC was assumed to equal zero. Using equation A.3 and the point scale data, $Ks_c = Ks_r * (2.95)$ for the overland flow planes and $Ks_c = Ks_r * (2.10)$ for channels. The factors 2.95 and 2.10 are the cover terms (COV in KINEROSR) used for overland and channel elements, respectively, for the Lucky Hills watersheds. The Ks values in column (4) of Table A.6 were used for model input values in Lucky Hills. These values were assigned to individual plane and channel model elements using a Thiessen weighting based on the soil sample locations.

Manpower limitations did not permit soil sampling on WG11. Instead, information from a new, high resolution soil survey (unpublished at this time) was

used to delineate soil boundaries. Soil pits dug during this soil survey were used to obtain percent clay and percentage of rock. Equations (A.1) and (A.2) were then used to obtain rock corrected Ks_r values.

A discernible transition in vegetation occurs within WG11. The lower end of the watershed is desert brush. A transition to range grassland occurs approximately midway up the watershed. Fortunately, detailed cover information on rainfall simulation plots exists for each vegetation type (Simanton et al, 1985). The "Hathaway Natural" simulator plot is covered by desert brush, and the "Benardino Natural" plot is representative of the range grassland. Average ground and cover data from 1981 for both plots were used to define CC and GS. Data from 1982-1984 were not used because the added artificial rainfall from the simulator caused significant growth. Table A.7 summarizes the soils and cover information on WG11. The areas of WG11 covered by the soils/Ks categories in Table A.7 are shown in Figure A.1.

The suction term G in KINEROSR was not field estimated but was internally computed using the first equation in Table 2.1. SMAX, the maximum relative soil saturation under imbibition, was estimated by soil texture class from Table 2 in Woolhiser et al. (1990). The initial relative soil saturation (SI) was obtained using CREAMS (Knisel, 1980). The procedure use to obtain SI is explained in more detail in Appendix B.

Table A.7. WG11 Soils/Ks Categories

Category	Soil Type	Ks_r (in/hr)	Rainfall Sim. Plot	COV Factor	Ks_c (in/hr)
A	Tombstone V.G.[1] Sandy Loam	0.100	Hathaway N.	2.98	0.298
B	Tombstone E.G.[2] Sandy Loam	0.111	Hathaway N.	2.98	0.330
C	Tombstone E.G. Sandy Loam	0.111	Bernardino N.	3.14	0.348
D	Tombstone V.G. Sandy Loam	0.100	Bernardino N.	3.14	0.314
E	Nolan V.G. Sandy Loam	0.104	Bernardino N.	3.14	0.327
F	Sand	8.3	---	-.-	8.3

Categories A,B,C,D apply to areas of WG11 show in Figure A.1
Category E applies to swale channel elements
Category F applies to incised channel elements

[1]V.G. stands for very gravely
[2]E.G. stands for extremely gravely

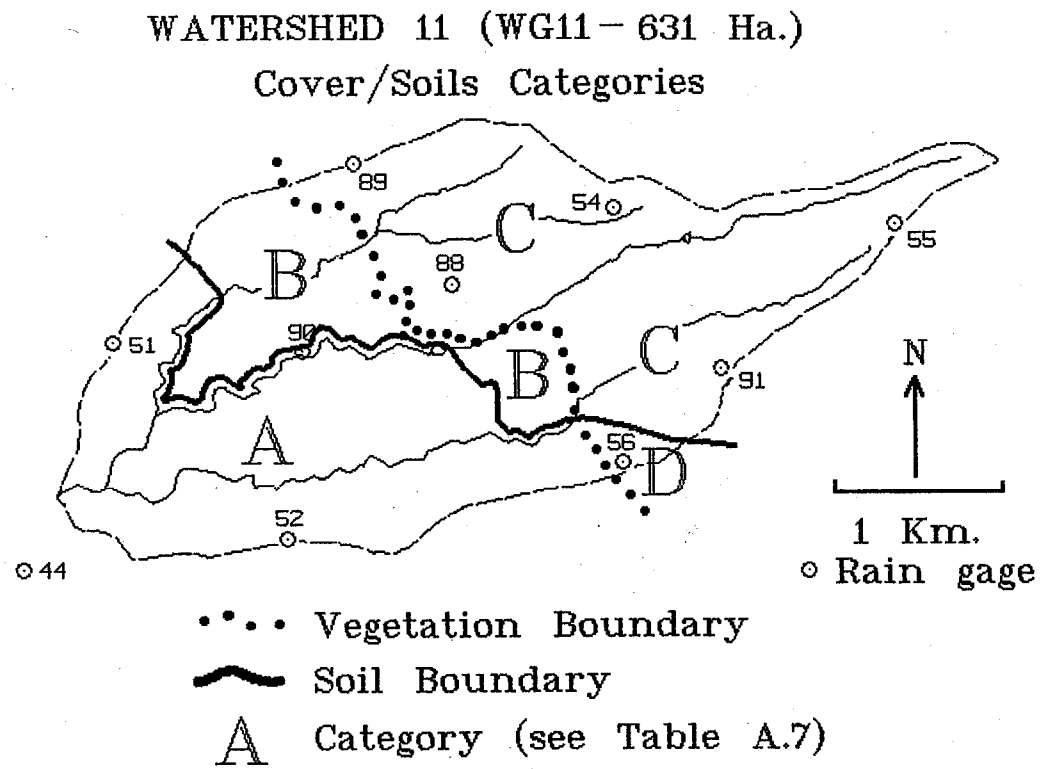

Figure A.1. Watershed WG11 - Areas for Soil/Ks Categories

A.3.5 Other Parameters

Interception (DINTR in KINEROSR) was estimated using data from Tromble (1983). Tromble estimated intercepted rainfall depth on tarbush. Tromble's average estimate was multiplied by the percentage of canopy cover obtained from the representative rainfall simulator plots (Simanton et al., 1985). A value of 0.36 mm was obtained and was used for all model overland flow plane elements. Interception was set to zero for all channel elements.

The coefficient of variation of Ks (CVF in KINEROSR) is used to define a lognormal distribution of Ks. With this distribution, small-scale infiltration variability can be modeled (see Chapter 2). This parameter was set to 0.8 for all overland flow elements and 0.0 for channel elements. This estimate was based on a variety of field data collected and reviewed in EPRI Report EA-4428 (1985). Insufficient information existed from Walnut Gulch to estimate this parameter from local information. Therefore, a multiplier on CVF (M_C) was used in calibrating the model for each watershed.

The infiltration recession factor (RECS in KINEROSR, see Woolhiser et al., 1990) was estimated from stereophotogrammetric data of the rainfall simulator plots (unpublished). Five digital elevation, cross-slope profiles on an undisturbed plot near Lucky Hills were used as the basis of this estimate. A line was fitted to each profile by standard linear regression where the cross-slope position was the independent variable and elevation was the dependent variable. Twice the standard deviation of the residuals about the regression line was assumed to equal RECS. The average

RECS value of the five profiles (20 mm) was used for all overland flow elements. RECS was set to zero for all channel elements. Photogrammetric data were only available for the simulator plot near the Lucky Hills watersheds; therefore, the same value of RECS was also used for WG11.

APPENDIX B

ESTIMATION OF INITIAL SOIL MOISTURE FOR RUNOFF EVENTS

APPENDIX B

ESTIMATION OF INITIAL SOIL MOISTURE FOR RUNOFF EVENTS

The purpose of this appendix is to briefly describe the methods used to obtain initial relative soil moisture (SI) estimates for the rainfall-runoff events used in this study. Because KINEROSR is an event-based model, SI estimates are required to define soil moisture conditions at the onset of rainfall causing the runoff event of interest. CREAMS (Knisel et al., 1980) was used to provide SI estimates.

CREAMS uses a daily time step to perform a multilayer soil water balance. Input parameters are used to describe soil textural characteristics, plant rooting depth, and mean monthly changes in solar radiation, temperature, and leaf area index. Readers are referred to Knisel et al. (1980) and Lane (1984) for a more detailed description of CREAMS and related input parameters.

One of the primary inputs to CREAMS is daily rainfall depth for a given raingage. Therefore, SI values were computed on a raingage by raingage basis. For the Lucky Hills watersheds, raingage 83 was used for the CREAMS simulations. CREAMS simulations were performed for each of the 10 raingages used in the Walnut Gulch subwatershed 11 (WG11) rainfall-runoff simulations. For WG11, SI values were then derived for each of the overland flow and channel elements used in KINEROSR by the spatial interpolation method described in Appendix C.

Three input parameter files for CREAMS were developed that reflected the primary vegetation types encountered in the Lucky Hills watersheds and WG11. In

all cases, the soils fall primarily into a sandy loam textural class. The three vegetation zones are desert brush, semi-arid grasslands, and a transition between the brush and grasslands. The input parameters were derived in consultation with experienced CREAMS users from the USDA-ARS Aridland Watershed Management Research Unit. These users also have extensive knowledge of the Walnut Gulch Experimental Watershed. Table B.1 lists the CREAMS input file used for each raingage. CREAMS input parameter files for each of the raingages listed in Table B.1 will be made available in electronic format in the near future.

CREAMS performs a water balance over seven soil layers from the surface to the rooting depth. Because of the short duration of thunderstorms causing runoff in Walnut Gulch, CREAMS was modified to compute the average soil water content (SW) based on the top three layers. SW was obtained from CREAMS for midnight on the day prior to the storm of interest. The midnight SW was adjusted to obtain an SW at the start time of the rainfall event. To do so, the one-day change in SW on the day prior to the rainfall event of interest was assumed to change at the rate depicted in Figure B.1. If rainfall occurred on the day prior to the event of interest, another day in the CREAMS simulation at roughly the same time of year with the same SW was selected to obtain a one-day change in SW. Once SW at the start time of the event is obtained, SI is computed by dividing SW by the soil porosity.

If intervening rainfall occurred between midnight and the start time of the event of interest, another adjustment was made to obtain SI. If the intervening rainfall did not cause runoff, SW was adjusted to mimic one-day changes in SW for

Table B.1. CREAMS Input Files for Study Raingages

Raingage	Vegetation Type	CREAMS Input File[1]	Watershed
83	Brush	RG83.PAR	Lucky Hills (106, 102, 104)
44	Brush	RG44.PAR	WG11
90	Brush	RG90.PAR	WG11
51	Brush	RG51.PAR	WG11
52	Brush	RG52.PAR	WG11
56	Brush/Grass Transition	RG56.PAR	WG11
89	Brush/Grass Transition	RG89.PAR	WG11
88	Grass	RG88.PAR	WG11
91	Grass	RG91.PAR	WG11
54	Grass	RG54.PAR	WG11
55	Grass	RG55.PAR	WG11

[1] These files will be made available in electronic format in the near future.

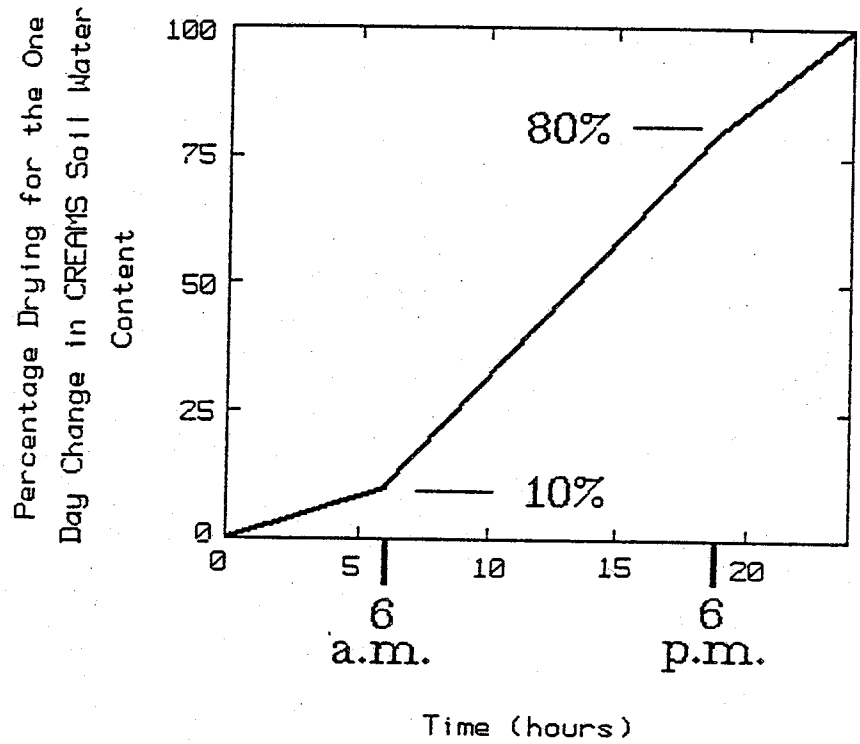

Figure B.1. Percentage of Cummulative Drying Versus Time of Day

the measured amount of intervening rainfall. Drying was assumed to continue following the pattern shown in Figure B.1 from the end of the intervening rainfall to the start time of the event of interest. If intervening rainfall produced runoff, SI was computed in a method consistent with KINEROSR when a rainfall hiatus occurs (Woolhiser et al., 1990). The hiatus was assumed to occur from the end of intervening runoff to the start time of the rainfall causing the runoff event of interest.

The computed initial relative soil saturations (SI) for all of the study events, for each raingage, are contained in input rainfall files. In addition, these files contain raingage coordinates (state plane coordinates, feet), and breakpoint rainfall data for each gage. These input files and the daily rainfall totals for each raingage (required to run CREAMS) are not contained in this document but will be made available in electronic format in the near future.

APPENDIX C

SPACE-TIME RAINFALL INTERPOLATION

APPENDIX C

SPACE-TIME RAINFALL INTERPOLATION

The air mass thunderstorm rainfall that causes the majority of runoff events in Walnut Gulch is highly variable in both time and space. The dense raingage network in the USDA-ARS Walnut Gulch Experimental Watershed affords a unique opportunity to incorporate a relatively detailed description of this highly variable rainfall into runoff modeling. To take advantage of these detailed rainfall data, a simple space-time rainfall interpolation scheme was developed. This appendix describes the interpolation algorithm.

A typical schematic, planimetric, location diagram of three raingages and several model element (overland flow plane or channel) centroids is shown in Figure C.1. Several basic rules were defined to establish the raingage or raingages used to interpolate rainfall. If the centroid of the model element, such as E2, falls within one of the shaded regions shown in Figure C.1, then the breakpoint rainfall data from the nearest raingage (G2) are applied to the entire area of element E2, and no interpolation is done. If the element centroid (E1) is in the interior of the triangle formed by three surrounding raingages (G1-G2-G3), then all three raingages are used in the interpolation to define the storm rainfall pattern for element E1. If the element centroid (E3) is outside of the triangular region (G1-G2-G3), and is not in one of the shaded zones, the nearest two raingages (G1 and G3 for element E3) are used in the interpolation.

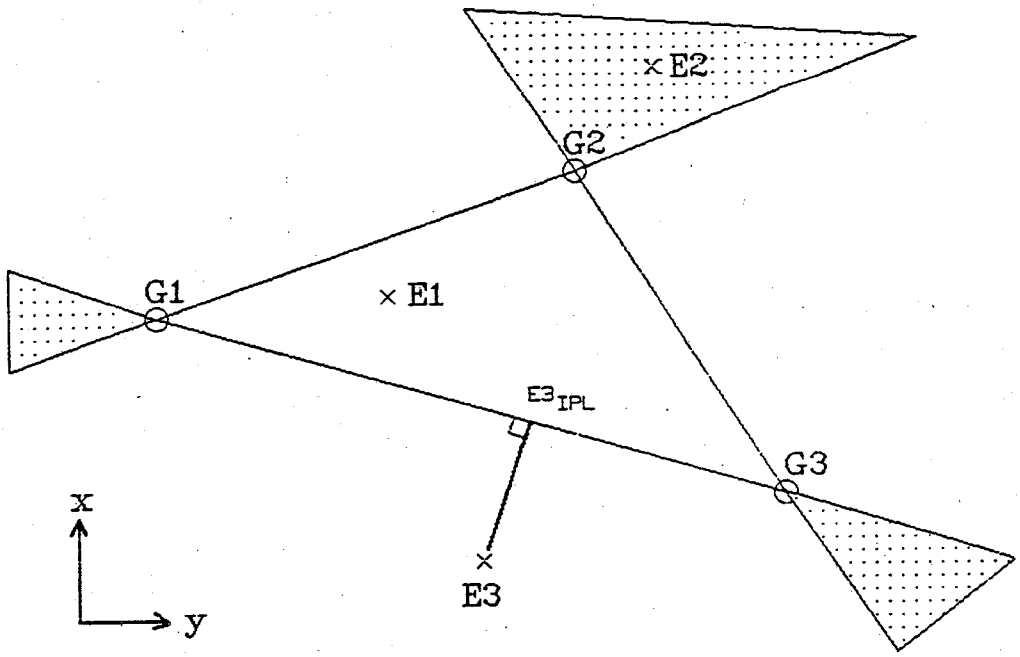

Figure C.1. Planimetric Raingage - Model Element Centroid Diagram

The interpolated rainfall intensity for element centroid E1 at two different times is shown in Figure C.2. For this case, the three surrounding raingages (G1 - G2 - G3) are used in the interpolation. At time (t), three intensities ($I1_t$, $I2_t$, and $I3_t$), computed from breakpoint rainfall data, exist for each of the three raingages. The (X,Y) raingage coordinates with the intensity values $I1_t$, $I2_t$, and $I3_t$ (Z intensity coordinates) are used to form the equation of the "intensity plane" at time (t). This intensity plane is shown as the shaded region in Figure C.2. With the equation of the intensity plane defined, the (x,y) coordinates of the element centroid (E1) can be substituted into this equation to compute the intensity which is be applied to element E1 ($IE1_t$). As soon as the intensity changes at any of the three raingages (time t + Δ t), a new intensity plane is computed as well as a new element intensity ($IE1_{t+\Delta t}$).

If only two raingages are used to interpolate an element intensity (E3 in Figure C.1), an "intensity plane" is also computed. In this case, the plane will pass through the $(X,Y,I_t)_{G1}$; $(X,Y,I_t)_{G3}$ coordinates and an arbitrary third coordinate that is not colinear with line G1-G3. The perpendicular line from the element centroid $(x,y)_{E2}$ to the line from G1 to G3 in the I = 0 plane defines the interpolation location for element E3 ($E3_{IPL}$) in the two- raingage interpolation case. The (x,y) coordinates of $E3_{IPL}$ are then substituted into the intensity plane for the two-gage case. The resulting intensity, $IE3_t$, is then applied to the entire area of element E3.

This interpolation scheme is easily implemented but does have several shortcomings. In cases where significant storm motion is present, the scheme will reduce peak rainfall intensities if either the two- or three-raingage interpolation case

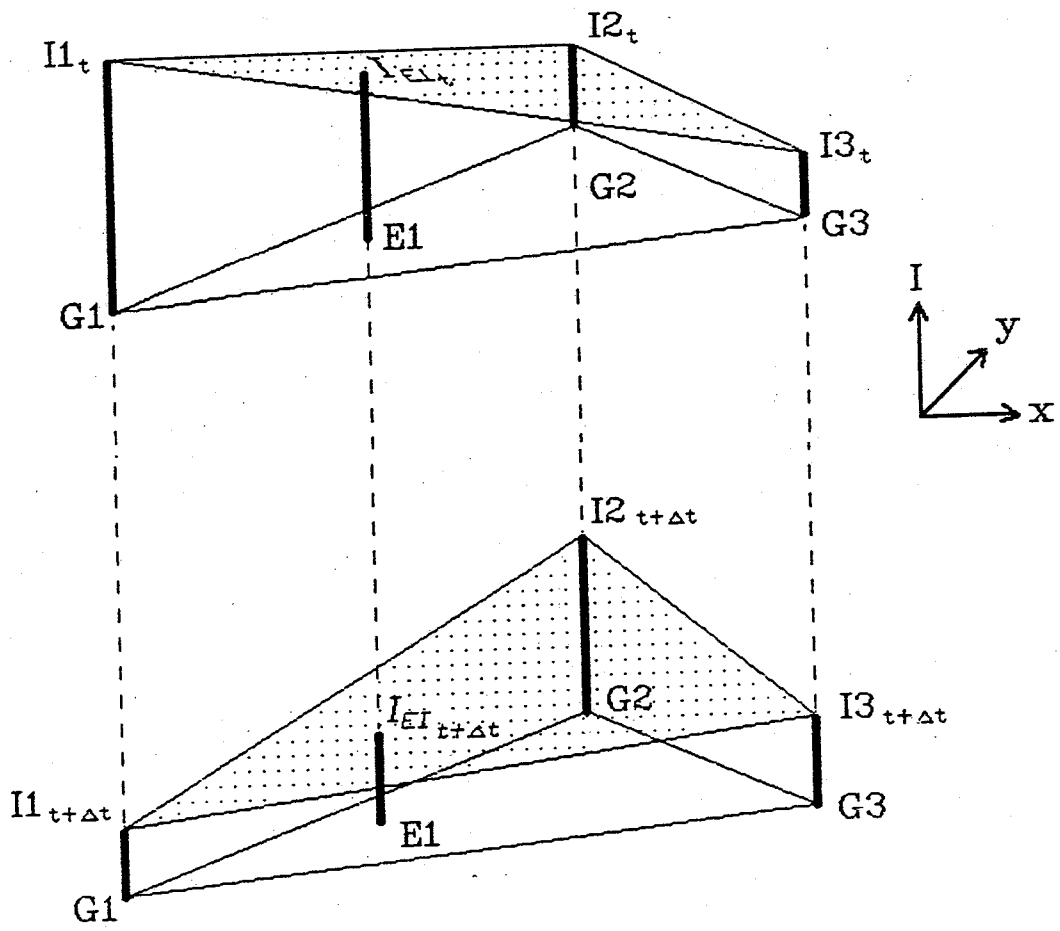

Figure C.2. Time-Space Rainfall Intensity Interpolation for a Model Element Centroid Surrounded by Three Raingages

occurs. Fitting of a higher order surface to the intensity coordinates might alleviate this problem to a certain extent. However, a higher order surface was not justified when the Walnut Gulch raingage density and the observed steep rainfall gradients are considered.

LIST OF REFERENCES

Abbott, M.B., Bathurst, J.C., Cunge, J.A., O'Connell, P.E., and Rasmussen, J.R., 1986a. An introduction to European Hydrological System--Systeme Hydrologique European-(SHE), 1: History and philosophy of a physically-based distributed modeling system. *Journal of Hydrology*, Vol. 87:45-59.

Abbott, M.B., Bathurst, J.C., Cunge, J.A., O'Connell, P.E., and Rasmussen, J.R., 1986b. An introduction to European Hydrological System--Systeme Hydrologique European-(SHE), 2: Structure of a physically-based distributed modeling system. *Journal of Hydrology*, Vol. 87:61-77.

Ahuja, L.R., Naney, J.W., and Nielsen, D.R., 1984. Scaling soil water properties and infiltration modeling. *Soil Science Society of America* Journal, 48:970-973.

Ahuja, L.R., Norziger, D.L., Swartzendruber, D., and Ross, J.D., 1989. Relationship between Green and Ampt parameters based on scaling concepts and field-measured hydraulic data. *Water Resources Research*, 25(7):1766-1770.

Aitken, A.P., 1973. Assessing systematic errors in rainfall-runoff models. *Journal of Hydrology*. 20:121-136.

Alley, W.M., and Smith, P.E., 1982. Distributed routing rainfall-runoff model--version II. Computer program documentation user's manual, USGS-WRD Open-File Report 82-344, Gulf Coast Hydroscience Center, NSTL Station, Mississippi.

Amorocho, J., 1961. Discussion of "Predicting storm runoff on samll experimental watersheds", by N.E. Minshall, *Journal of Hydraulics Division*, ASCE, 87(HY2):185-191.

Anderson, P.W., 1972. More is different, *Science*, 177(4047):393-396.

Anderson, M.G., Bosworth, D. and Kneale, P.E., 1981. Controls on overland flow generation. In: Catchment Experiments in Fluvial Geomorphology, Ed. by T.P. Burt and D.E. Walling, Geo Books, Norwich, pp 21-34.

ASCE Task Committee on Quantifying Land-Use Change Effects of the Watershed Management and Surface-Water Committees of the Irrigation and Drainage Division, 1985. Evaluation of hydrologic models used to quantify major land-use change effects. ASCE, *Journal of Irrigation and Drainage Division*, Vol. III(1):1-17.

Bathurst, J.C., 1986a. Physically-based distributed modeling of an upland catchment using the Systeme Hydrologique European. *Journal of Hydrology*, Vol. 87:79-102.

Bathurst, J.C., 1986b. Sensitivity analysis of the Systeme Hydrologique European for an upland catchment. *Journal of Hydrology*, Vol. 87:103-123.

Beck, M.B., 1987. Water quality modeling: a review of the analysis of uncertainty. *Water Resources Research*, 23(8):1393-1442.

Bell, N.C., Wheater, H.S., and Johnston, P.M., 1989. Evaluation of overland flow models using laboratory catchment data. II. Identification of physically-based models. *Hydrologic Sciences Journal*, 34(3):289-317.

Beven, K.J., 1979. On the generalized kinematic routing method. *Water Resources Research*, 15(5):1238-1242.

Beven, K.J., 1986. Runoff production and flood frequency in catchments of order n: An alternative approach. Scale Problems in Hydrology. D. Reidel Publishing Company, Boston, Massachusetts, pp. 107-132.

Beven, K.J., 1988. Lecture I: Scale Considerations. Section III-Current modeling issues and technological trends, NATO Advanced Study Institute, Sintra, Portugal, August.

Beven, K.J., 1988a. Lecture I: Interflow, NATO Advanced Study Institute, Sintra, Portugal, August.

Beven, K.J., 1988b. Lecture I: Infiltration and soil moisture, interception and surface detention, unsaturated flow. In Section II-State of the art in modeling components of the hydrological cycle: facts and assumptions. NATO Advanced Study Institute, Sintra, Portugal, August.

Beven, K.J., Wood, E.F., and Sivapalan, M., 1988. On hydrological heterogeneity-catchment morphology and catchment response. *Journal of Hydrology*, 100:353-375.

Beven, K.J., 1989. Changing ideas in hydrology--the case of physically-based models. *Journal of Hydrology*. 105:157-172.

Binley, A., Beven, K. and Elgy, J., 1989. A physically-based model of heterogeneous hillslopes 2. Effective hydraulic conductivities, *Water Resources Research*, 25(6):1227-1233.

Blackie, J.R., and Eeles, C.W.O., 1985. Lumped catchment models, in M. G. Anderson and T.P. Burt, Editors, Hydrological Forecasting, Wiley and Sons.

Bonell, M., and Williams, J., 1986. The two-parameter Phillips infiltration equation: their properties and spatial and temporal heterogeneity in red earth of tropical semi-arid Queensland. *Journal of Hydrology*, Vol. 87:9-31.

Bouwer, H., and Rice, R.C., 1984. Hydraulic Properties of Stony Vadose Zones. *Groundwater*, 22(6):696-705.

Branson, F.A., Gifford, G.F., Renard, K.G., and Hadley, R.F., 1981. Rangeland Hydrology, 2nd Edition, Published by Kendall/Hunt Publishing Company, Dubuque, Iowa, pp. 38-45.

Bras, R.L., and Rodriguez-Iturbe, I., 1976. Rainfall network design for runoff prediction, *Water Resources Research*, 12(2):1197-1208.

Bras, R.L., 1979. Sampling of interrelated random fields: the rainfall-runoff case. *Water Resources Research*, 15(6):1767-1780.

Bronowski, J., 1972. Science and Human Values, Harper and Row, New York.

Casti, J.L., 1985. On system complexity: identification, measurement, and management. Complexity, Language and Life: Mathematical Approaches. Academic Press, London, Chapter 6.

Chery, D.L., and Beaver, D.G., 1976. Resolutions of analog rainfall records relative to chart scales. Hydrology and Water Resources in Arizona and the Southwest, 6:215-225.

Chow V.T., 1959, Open Channel Hydraulics. McGraw-Hill, Inc., New York, N.Y., pp. 108-114.

Connors, K.F., Gardner, T.W., and Day, R.L., 1989. Deriving stream parameters for hydrologic modeling from digital elevation data. IAHS Pub. No. 181, pp. 397-406.

Cordova, J.R., and Rodriguez-Iturbe, I., 1983. Geomorphologic estimation of extreme flow probabilities. *Journal of Hydrology*, Vol. 65:159-173.

Diaz-Granados, M., Bras, R.L., and Valdes, J.B., 1986. Incorporation of channel losses in the geomorphological IUH. Scale Problems in Hydrology. D. Reidel Publishing Company, Boston, Massachusetts, pp. 217-243.

Diskin, M.H., 1973. The role of lag in a quasi-linear analysis of the surface runoff system. In Proc. Sec. Intern. Sym. on Hydrology. Water Resour. Pub., Ft. Collins, Colorado, pp. 133-144.

Diskin, M. H., and E. S. Simpson, 1978. A quasi-linear spatially distributed cell model for the surface runoff system. *Water Resources Bulletin*, 14(4):903-917.

Dooge, J. C. I., 1981. Parameterization of hydrologic processes. Presented at the JSC Study Conf. on Land Surface Processes in Atmosph. Gen. Circulation Models, Greenbelt, MD, USA, Jan. pp. 243-283.

Dooge, J. C. I., 1986. Looking for hydrologic laws. *Water Resources Research*, Vol. 22(9):46S-58S.

El-Kadi, A. I., 1987. Variability of infiltration under uncertainty in unsaturated zone parameters. *Journal of Hydrology*, 90:61-80

Engman, E. T., 1974. A partial area model for simulation surface runoff from small watersheds. Ph.D. Dissertation, Pennsylvania State University, University Park, Pennsylvania. 154 p.

EPRI (Electrical Power Research Institue) Report EA-4428, 1985. Spatial variability of soil physical properties in solute migration: A critical literature review. Prepared by University of California at Riverside, W. A. Jury, Principal Investigator, pp. 2-5.

Freeze, R. A., 1980. A stochastic-conceptual analysis of rainfall-runoff processes on a hillslope. *Water Resources Research*, Vol. 16(2):391-408.

Golany P., and Larson, C. L., 1971. Effects of channel characteristics on time parameters for small watershed runoff hydrographs. Water Resources Research Center, University of Minnesota, Bulletin 31., pp. 104-118.

Goodrich, D. C., Woolhiser, D.A., and Sorooshian, S., 1989. Model complexity required to maintain hydrologic response. Proc. ASCE Nat. Conf. Hydr. Div., Colo. Springs, CO, Aug. 8-12, pp. 431-436.

Goodrich, D. C., Woolhiser, D.A., and Sorooshian, S., 1989. Geometric model simplification with efficient parameterization of the saturated hydraulic conductivity, *EOS,* Transactions, American Geophysical Union, 70(15):343.

Goodrich, D. C., 1990. Geometric simplification of a distributed rainfall-runoff model over a range of basin scales. Ph.D. Dissertation, Department of Hydrology and Water Resources, University of Arizona, Tucson, Arizona, 1990.

Grah, O. J., Hawkins, R.H., and Cundy, T.W., 1983. Distribution of infiltration on a small watershed. *Advances in Irrigation and Drainage*, pp. 44-54.

Gray, D. M., 1961. Synthetic unit hydrographs for small watersheds. Proc. ASCE. *Journal of Hydrology Division*, Vol. 87, No. HY4, pp. 33-54.

Green I. R. A., 1984. WITWAT stormwater drainage program version II. Univ. of the Witwatersrand, Dept. of Civil Engineering, Report No. 2.

Gupta, V. K., E. Waymire, and C. T. Wang, 1980. A representation of an instantaneous unit hydrograph from geomorphology, *Water Resources Research*, 16(5):855-862.

Gupta, V. K., and Waymire, E., 1983. On the formulation of an analytical approach to hydrologic response and similarity at the basin scale. *Journal of Hydrology*, Vol. 65:95-123.

Gupta, V. K., Rodriguez-Iturbe, I., and Wood, E. F. (editors), 1986. Scale Problems in Hydrology. D. Reidel Publishing Company, Boston, Massachusetts.

Hager W. H., 1985. Analysis of non-linear rainfall-runoff process. *Nordic Hydrology*, Vol. 16, pp. 291-308.

Hamlin, M. J., 1983. The significance of rainfall in the study of hydrological processes at basin scale. *Journal of Hydrology*, Vol. 65:73-94.

Hanson, C. L., 1989. Precipitation catch measured by the Wyoming shield and the dual-gauge system. *Water Resources Bulletin*, 25(1):159-164.

Heil, R.J., and Brych, S.M., 1978. An approach for consistent topographic representation of varying terrain. Proceedings of the ASP-ACSM Digital Terrain Modeling Symposium, May 9-11, St. Louis, Missouri.

Hjelmfelt, A. T., Jr., 1981. Overland flow from time-distributed rainfall. *Journal of the Hydraulics Division*, American Society of Civil Engineers 107 HY2, pp. 227-238.

Hjelmfelt, A. T., Jr., and R. E. Burwell, 1984. Spatial variability of runoff. ASCE *Irrigation and Drainage Division*, 110(1):46-54.

Hromadka, T. V. II, 1987. Use of subareas in rainfall-runoff models, I: Development of a multi-linear runoff model approximation. *Hydrological Science and Technology*, 3(1-2):25-35.

Hromadka, T. V. II, 1987a. Use of subareas in rainfall-runoff models, II: reducing model uncertainty. *Hydrological Science and Technology*, 3(1-2):37-45.

Hughes, D.A., and A. B. Beater, 1989. The applicability of two single event models to catchments with different physical characteristics. *Hydrologic Sciences Journal,* 34, 1,2/1989, pp. 63-78.

Hughes, D.A. 1989. Estimation of the parameters of an isolated event conceptual model from physical catchment characteristics. Hydrologic Sciences Journal, 35, 5,10/1989 p. 539-557.

Ishihara, T., and T. Takasao, 1963. A study of runoff pattern and its characteristics. Bull. Disaster Prev. Res. Inst., No. 65.

Iwagaki, Y., and T. Takasao, 1956. On the effects of rainfall and drainage basin characteristics on runoff relation. Memorial Papers of the 5th Anniversary of the Disaster Prevention Institute, Kyoto University, Kyoto, Japan, pp. 191-201.

Izzard, C. F., 1946. Hydraulics of runoff from developed surfaces. Proc. Highway Res. Board, 26:129-146.

Jain S. C., Kumar, S., Whelan, G., and Croley, T. E., II, 1982. IIHR distributed parameter watershed model. Iowa Institute of Hydraulic Research Report No. 244.

James, W., 1972. Developing simulation models. *Water Resources Research,* 8(6):1590-1592.

James, W., and Robinson, M., 1985. Time and space resolution for continuous dynamic storm and runoff model studies. Proceedings of ASCE Hydraulic Division, Hydraulics and Hydrology in the Small Computer Age, Vol. 2, pp. 1160-1165, Lake Buena Vista, Florida, Aug. 12-17, 1985.

James, L. D., and S. J. Burges, 1982. Selection, calibration and testing of hydrologic models, in Hydrologic Modeling of Small Watersheds, Ed. by C. T. Haan, H. P. Johnson, and D. L. Brakensiek, Amer. Soc. of Agric. Engr., St. Joseph, Mich.

Johnston, P. R. and D. H. Pilgrim, 1976. Parameter optimization for watershed models. Water Resour. Res., 12(3):477-486.

Jun, X., 1989. Parameter identifiability of hydrological models with implicit structure: a numerical approach. Hydrological Sciences J., 34(1):1-19.

Keppel, R. V., and Renard, K. G., 1962. Transmission losses in ephemeral stream beds. *Journal of the Hydraulics Division,* American Society of Civil Engineers, Vol. 88, No. HY 3, pp. 59-68.

Khan, M. H., 1989. Evaluation of rainfall-discharge models with discrimination. J. Hydrol., 108:63-78.

Kirkby, M., 1976. Tests of the random network model and its application to basin hydrology. Earth Surf. Process., 1:197-212.

Kirkby, M., 1986. A runoff simulation model based on hillslope topography. Scale Problems in Hydrology. D. Reidel Publishing Company, Boston, Massachusetts, pp. 39-56.

Kirkby, M., 1988. Hillslope runoff processes and models. *Journal of Hydrology*, 100:315-339.

Klein, M., 1984. Effect of catchment size on runoff relationships-a comment. *Journal of Hydrology*, Vol. 71:191-195.

Klemes, V., 1982. Empirical and causal models in hydrology. Scientific Basis of Water Resource Management. Nat. Academy Press, pp. 95-104.

Klemes, V., 1983. Conceptualization and scale in hydrology. *Journal of Hydrology*, Vol. 65:1-23.

Klemes, V., 1988. A hydrologic perspective. *Journal of Hydrology*. 100:3-28.

Knisel, W. G. (Editor), 1980. CREAMS: A Field Scale Model for Chemicals, Runoff, and Erosion from Agricultural Management Systems, U.S. Department of Agriculture, Science and Education Administration, Conservation Research Report 26, 643 p.

Lane, L. J., Woolhiser, D.A., and Yevjevich, V., 1975. Influence of simplification in watershed geometry in simulation of surface runoff. Hydrology Paper No. 81, Colorado State University, Ft. Collins, Colorado, Dec., 50 p.

Lavee, A., 1986. A deterministic simulation model for rainfall-runoff relationship of arid hillslopes. *Zeitschrift fur Geomorphologie*. 58:35-46.

Li, A. E., 1975. A model to define hydrologic response units based on characteristics of the soil-vegetation complex within a basin. Master's Thesis, Virginia Polytech. Institute and State University, Blacksburg, Virginia, May.

Liggett J. A., and Woolhiser D. A., 1967. The use of the shallow water equations in runoff computation. Proceedings of the Third Annual American Water Resources Conference, San Francisco, California, pp. 117-126.

Lima, J. L. M. P., 1989. The influence of the angle of incidence of the rainfall on the overland flow process. Proceedings of the Baltimore Symposium, IAHS Publication 181:73-82.

Loague, K. M., and Freeze, R. A., 1985. A comparison of rainfall runoff modeling techniques on small upland catchments. *Water Resources Research*, Vol. 21(2):229-248.

Loague, K. M., 1986. An assessment of rainfall-runoff modeling methodology. Ph.D. Dissertation, University of British Columbia, Vancouver, pp. 140-161.

Loague, K. M., 1990. R-5 Revisited: 2. Re-evaluation of a quasi-physically based rainfall-runoff model with supplemental information. *Water Resources Research*, (In press).

Lyngfelt, S., 1985. On urban runoff modeling: the application of numerical models based on the kinematic wave theory. Report Series A:13, Dept. of Hydraulics, Chalmers University of Technology, Vol. 1, pp. 124-125.

Martinec, J., and Rango, A., 1989. Merits of statistical criteria for the performance of hydrologic models. *Water Resources Bulletin*. 25(2):421-432.

McCuen, R. H., and W. M. Synder, 1975. A proposed index for comparing hydrographs. *Water Resources Research*, 11:1021-1024.

Merzougui, M., 1982. The effect of instrument type in measuring infiltration rates on spatial variability patterns. M.S. Thesis, Watershed Science Dept., Utah State University, Logan, Utah.

Mesa, O. J., and E. R. Mifflin, 1986. On the relative role of hillslope and network geometry in hydrologic response. Scale Problems in Hydrology. D. Reidel Publishing Company, Boston, Massachusetts, pp. 1-18.

Miller, S. A., and Mantey, R.J., 1982. Suitability of single event-steady state hydrologic models for Michigan watersheds. ASAE Winter Meeting, Dec. 14-17, Paper 2602.

Minshall, N. E., 1960. Predicting storm runoff on small experimental watersheds. *Journal of Hydraulics Division*, ASCE, 86(HYB):17-38.

Moglen, G. E., 1989. On the effects of spatial variability of overland flow parameters. Proc. Ninth Annual AGU Hydrology Days, Hydrology Days Pub., Ft. Collins, CO., April 18-21, pp.1-12.

Moore, R. J., 1985. The probability-distributed principle and runoff production at point and basin scales. *Hydrologic Sciences Journal,* Vol. 30, 2(6):273-297.

Nash, J. E., and J. V. Sutcliffe, 1970. River flow forecasting through conceptual models, I. A discussion of principles. *Journal of Hydrology,* 10:282-290.

Nelder, J. A., and R. Mead, 1965. A simplex method for function minimization. *The Computer Journal,* 7(4):308-313.

Neff, E. L., 1977. How much rain does a raingage gage? *Journal of Hydrology,* 35:213-220.

Neuman, S. P., and Carrera, J., 1985. Maximum-likelihood adjoint-state finite-element estimation of groundwater parameters under steady and nonsteady-state conditions. *Applied Mathematics and Computation,* 17:405-432.

Nielsen, D. R., Biggar, J.W., and Erh, K.T., 1973. Spatial variability of field measured soil-water properties. *Hilgardia,* 42:215-260.

O'Connell, P. E., and Clarke, R. T., 1981. Adaptive hydrological forecasting--a review. *Hydrological Sciences Bulletin,* Vol. 26(2):179-205.

Olson, V. M., 1975. Autocorrelation and visual map complexity. *Annuls of Association Geographers,* Vol. 65(2):189-204.

Osborn, H. B., and L. J. Lane, 1969. Precipitation-runoff relationships for very small semiarid rangeland watersheds. *Water Resources Research,* 5(2):419-425.

Osborn, H. B., L. J. Lane, and R. S. Kagan, 1971. Determining significance and precision of estimated parameters for runoff from semiarid watersheds. Water Resour. Bull., 7(3):484-494

Osborn, H. B., K. G. Renard, and J. R. Simanton, 1979. Dense networks to measure convective rainfall in the southwestern United States. *Water Resources Research,* 15(6):1701-1711.

Osborn, H. B., E. D. Shirley, D. R. Davis, and R. B. Koehler, 1980. Model of time and space distribution of rainfall in Arizona and New Mexico. USDA-SEA Agric. Reviews and Manual, ARM-W-14, 27.

Osborn, H. B., and J. R. Simanton, 1981. Maximum rainfall intensities of southwestern thunderstorms. Proc. Fourth Conf. on Hydromet., Amer. Met. Soc., Reno, NV, p. 166-173.

Osborn, H. B., 1982. Quantifiable differences in air-mass and frontal convective rainfall in the southwest. In: Statistical Analysis of Rainfall and Runoff. Intern. Sym. on Rainfall/Runoff Modeling, Miss. State Univ., MS, p.21-32.

Osborn, H. B., and K. G. Renard, 1988. Rainfall intensities for Southeastern Arizona. ASCE, J. Irr. and Drain. Eng. 114(1):195-199.

Pilgrim, D. H., Cordery, I., and Baron, B. C., 1982. Effect of catchment size on runoff relationships. *Journal of Hydrology*, Vol. 58:205-221.

Pilgrim, D. H., 1986. Bridging the gap between flood research and design practice. *Water Resources Research* (supplement), 22(9):1655-1765.

Pilgrim, D. H., T. G. Chapman and D. G. Doran, 1988. Problem of rainfall-runoff modeling in arid and semiarid regions. *Hydrological Sciences Journal*, 33(4):379-399.

Press, W. H., Flannery, B.P., Teukolsky, S.A., and Vetterling, W.T., 1986. Numerical Recipes, Cambridge University Press, New York, N.Y., pp. 114-120.

Rajendran R., and Mein, R.G., 1986. Determination of rainfall excess on spatially variable catchments. *Journal of Hydrology*, 83:67-89.

Rawls, W. J., Brakensiek, D.L., and Saxton, K.E., 1982. Estimation of soil water properties. *Transactions of the American Society of Agricultural Engineers*, Vol. 25 SW, pp. 1316-1320, 1328.

Renard, K. G., 1970. The hydrology of semiarid rangeland watersheds. USDA-ARS pub. 41-162.

Renard, K. G., Rawls, W. J., and Fogel, M. M., 1982. Currently available models in Hydrologic Modeling of Small Watersheds. Edited by Haan, C. T., Johnson, H. P., and Brakensiek, D. L., pp. 507-522, American Society of Agricultural Engineers, St. Joseph, Michigan.

Rogowski, A. S., 1972. Watershed physics: soil variability criteria. *Water Resources Research*, 8(4):1015-1023.

Rosenblueth, A., and Wiener, N., 1945. The role of models in science. *Philosophy of Science*, 12(4):316-321.

Rovey, E. W., Woolhiser, D. A., and Smith, R. E., 1977. A distributed kinematic model of upland watersheds. Hydrology Paper No. 93, Colorado State University, Ft. Collins, Colorado, 52 p.

Russo, D., and Bresler, E., 1981. Soil conductivity properties as stochastic processes: I. An analysis of field spatial variability. *Soil Science Society of America*, 45:682-687.

Schilling, W, and Fuchs, L., 1986. Errors in stormwater modeling--a quantitative assessment. *Journal of Hydraulic Engineering*, ASCE 112(2):111-123.

Shanholtz, V. O., B. B. Ross and J. C. Carr, 1981. Effect of spatial varibility on the simulation of overland and channel flow. Trans. ASAE 24(1):124-133, 138.

Sharma, M. L., Gander, G. A., and Hunt, C. G., 1980. Spatial variability of infiltration in a watershed. *Journal of Hydrology*, Vol. 45:101-122.

Sharon, D., 1980. The distribution of hydrologically effective rainfall incident on sloping ground. *Journal of Hydrology*, 46:165-188.

Shirley, E. D. Rainfall intensity accuracy from a weighing raingage. Unpublished

Simanton, J. R., C. W. Johnson, J. W. Nyhan, and E. M. Romney, 1985. Rainfall simulation on rangeland erosion plots. Proc. of the Rainfall Simulator Workshop, Ed. L. J. Lane, Jan. 14-15, Tucson AZ, Pub. by Soc. for Range Manag., Denver, CO, pp 11-17. (related Walnut Gulch plot data in Appendix C of same document pp. 63-68).

Singh, V. P., and Woolhiser, D.A., 1976. Sensitivity of linear and nonlinear surface runoff models to input errors. *Journal of Hydrology*, 29:243-249.

Singh, V. P., and Woolhiser, D.A., 1976a. A nonlinear kinematic wave model for watershed surface runoff. *Journal of Hydrology*, 31(1976):221-243.

Sivapalan M., and Wood, E. F., 1986. Spatial heterogeneity and scale in the infiltration response of catchments. Scale Problems in Hydrology. D. Reidel Publishing Company, Boston, Massachusetts, pp. 81-106.

Smith, R. E., and Hebbert, R. H. B., 1979. A Monte-Carlo analysis of the hydrologic effects of spatial variability of infiltration. *Water Resources Research*, Vol. 15:419-429.

Smith, R. E., and Parlange J.-Y., 1978. A parameter-efficient hydrologic infiltration model. *Water Resources Research*, 14(33):533-538.

Smith, R. E., 1987. Personal Communication.

Smith, R. E., Goodrich, D.C., and Woolhiser, D.A., 1990. Areal effective infiltration dynamics for runoff of small catchments. Proceedings of the ISSS Congress, Kyoto, Japan, August (in press).

Sorooshian, S., and Dracup, J. A., 1980. Stochastic parameter estimation procedures for hydrologic rainfall-runoff models: correlated and heteroscedastic error cases. *Water Resources Research,* 16(2):430-442.

Sorooshian, S., 1982. Parameter identification of compartmental models: case of hydrologic rainfall-runoff models. Proceedings of the 6th IFAC Symposium on Identification and Systems Parameter Estimations, Washington, D.C., June 7-11, pp. 1397-1402.

Sorooshian, S., Gupta, V. K., and Fulton, J. L., 1983. Evaluation of maximum likelihood parameter estimation techniques for conceptual rainfall-runoff models: influence of calibration data variability and length on model credibility. *Water Resources Research,* 19(1):251-259.

Sorooshian, S., and Gupta, V. K., 1983. Automatic calibration of conceptual rainfall-runoff models: the question of parameter observability and uniqueness. *Water Resources Research,* 19(1):260-268.

Sorooshian, S., and Gupta, V. K., 1985. The analysis of structural identifiability: theory and application to conceptual rainfall-runoff models. *Water Resources Research,* 21(4):487-495.

Sorooshian, S., and Huerte, A., 1989. Utilization of Eos data in quantifying the processes controlling the hydrologic cycle in arid/semi-arid regions. NASA Interdisciplinary Investigation Eos Proposal, A.O. No. OSSA-1/88, University of Arizona, Tucson, Arizona.

Stone, J. J., L. J. Lane, and E. D. Shirley. Brief user manual for program IRS. Unpublished user manual that may be obtained from USDA-ARS, 2000 E. Allen Rd., Tucson, AZ

Tromble, J. M., 1983. Interception of rainfall by tarbush. *Journal of Range Management,* 36(4):525-526.

Troutman, B. M., 1983. Runoff prediction errors and bias in parameter estimation induced by spatial variability of precipitation. *Water Resources Research,* Vol. 19(3):791-810.

Troutman, B. M., 1985. Errors and parameter estimation in precipitation-runoff modeling, 1. Theory, *Water Resources Research*, 21(8):1195-1213.

Troutman, B. M., and Karlinger, M. R., 1986. Averaging properties of channel networks using methods in stochastic branching theory. Scale Problems in Hydrology. D. Reidel Publishing Company, Boston, Massachusetts, pp. 185-216.

Truschel, A. D., and M. E. Campana, 1983. A parametric model for peak flow prediction in ungaged ephemeral watersheds. Water Resour. Res. Center, Desert Res. Instit., Univ. of Nev., Reno, Nev., Pub. No. 41083, pp. 108.

Wang, C. T., V. K. Gupta, and E. Waymire, 1981. A geomorphologic synthesis of nonlinearity in surface runoff. *Water Resources Research*, 17(3):545-554.

Warrick, A. W., G. J. Mullen, and D. R. Nielsen, 1977. Scaling field-measured soil hydraulic properties using similar media concept. *Water Resources Research*, 15:419-429.

Warwick, J. J., 1989. Interplay between parameter uncertainty and model aggregation error. *Water Resources Bulletin*, 25(2):275-283.

Wheater H. S., Bell, N.C., and Johnston, P.M., 1989. Evaluation of overland flow models using laboratory catchment data. III. Comparison of conceptual models. *Hydrological Sciences Journal*, 34(3):319-337.

Willmott, C. J., 1982. Some comments on the evaluation of model performance. *Bulletin of the American Meteorological Society*, 63:1309-1313.

Willmott, C. J., Ackleson, S. G., Davis, R. E., Feddema, J. J., Klink, K. M., Legates, D. R., O'Donnell, J., and Rowe, C. M., 1985. Statistics for the evaluation and comparison of models. *Journal of Geophysical Research*, 90(C5):8995-9005.

Wood, E. F., Sivapalan, M., Beven, K., and Band, L., 1987. Effects of spatial variability and scale with implications to hydrologic modeling. U.S.A.-Japan Seminar on Hydrology, Honolulu, Hawaii, Jan. 5-7.: Pub. later in *Journal of Hydrology*, 102(1988):29-47, 1988.

Wooding, R. A., 1965a. A hydraulic model for the catchment-stream problem, I. Kinematic-wave theory. *Journal of Hydrology*, Vol. 3, pp. 254-267.

Woolhiser, D. A., Osborn, H.B., and Hershenhorn, J., 1983. Disaggregation of daily rainfall. Proceedings, Natural Resources Modeling Symposium, Pingree Park, Colorado, Oct. 16-21, pp. 304-306.

Woolhiser, D. A., and Osborn, H.B., 1985. A stochastic model of dimensionless thunderstorm rainfall. *Water Resources Research*, 21(4): pp. 511-522.

Woolhiser, D. A., 1986. Sensitivity of calculated peak-runoff rates to rainfall-sampling frequency. In: Integrated Design of Hydrologic Networks, IAHS Pub. No. 158, Proc., Budapest Symposium, pp. 161-171.

Woolhiser, D. A., and Osborn, H.B., 1986. Point storm disaggregation: seasonal and regional effects. Proceedings of 4th International Hydrology Symposium on Multivariate Analysis of Hydrologic Processes, 1985, Colorado State University, Ft. Collins, Colorado, pp. 105-120.

Woolhiser, D. A., and Goodrich, D.C., 1988. Effect of storm rainfall intensity patterns on surface runoff. *Journal of Hydrology*, (102):335-354.

Woolhiser, D. A., Smith, R.E., and Goodrich, D.C., 1990. KINEROS, A kinematic runoff and erosion model: documentation and user manual. U.S. Department of Agriculture, ARS, ARS-77, 130 pp.

Wu, Y., Yevjevich, V., and Woolhiser, D. A., 1978. Effects of surface roughness and its spatial distribution on runoff hydrographs. Hydrology Paper No. 93, Colorado State University, Ft. Collins, Colorado, 47 p.

Zaghloul, N. A., 1981. SWMM model and level of discretization. ASCE, Vol. 107, No. HY11, pp. 1535-1545.

Zaghloul, N. A., 1983. Sensitivity analysis of the SWMM runoff-transport parameters and the effects of catchment discretization. *Advances Water Resources*, Vol. 6, Dec. pp. 214-223.

APPENDIX B

ESTIMATION OF INITIAL SOIL MOISTURE FOR RUNOFF EVENTS

APPENDIX B

ESTIMATION OF INITIAL SOIL MOISTURE FOR RUNOFF EVENTS

The purpose of this appendix is to briefly describe the methods used to obtain initial relative soil moisture (SI) estimates for the rainfall-runoff events used in this study. Because KINEROSR is an event-based model, SI estimates are required to define soil moisture conditions at the onset of rainfall causing the runoff event of interest. CREAMS (Knisel et al., 1980) was used to provide SI estimates.

CREAMS uses a daily time step to perform a multilayer soil water balance. Input parameters are used to describe soil textural characteristics, plant rooting depth, and mean monthly changes in solar radiation, temperature, and leaf area index. Readers are referred to Knisel et al. (1980) and Lane (1984) for a more detailed description of CREAMS and related input parameters.

One of the primary inputs to CREAMS is daily rainfall depth for a given raingage. Therefore, SI values were computed on a raingage by raingage basis. For the Lucky Hills watersheds, raingage 83 was used for the CREAMS simulations. CREAMS simulations were performed for each of the 10 raingages used in the Walnut Gulch subwatershed 11 (WG11) rainfall-runoff simulations. For WG11, SI values were then derived for each of the overland flow and channel elements used in KINEROSR by the spatial interpolation method described in Appendix C.

Three input parameter files for CREAMS were developed that reflected the primary vegetation types encountered in the Lucky Hills watersheds and WG11. In

all cases, the soils fall primarily into a sandy loam textural class. The three vegetation zones are desert brush, semi-arid grasslands, and a transition between the brush and grasslands. The input parameters were derived in consultation with experienced CREAMS users from the USDA-ARS Aridland Watershed Management Research Unit. These users also have extensive knowledge of the Walnut Gulch Experimental Watershed. Table B.1 lists the CREAMS input file used for each raingage. CREAMS input parameter files for each of the raingages listed in Table B.1 will be made available in electronic format in the near future.

CREAMS performs a water balance over seven soil layers from the surface to the rooting depth. Because of the short duration of thunderstorms causing runoff in Walnut Gulch, CREAMS was modified to compute the average soil water content (SW) based on the top three layers. SW was obtained from CREAMS for midnight on the day prior to the storm of interest. The midnight SW was adjusted to obtain an SW at the start time of the rainfall event. To do so, the one-day change in SW on the day prior to the rainfall event of interest was assumed to change at the rate depicted in Figure B.1. If rainfall occurred on the day prior to the event of interest, another day in the CREAMS simulation at roughly the same time of year with the same SW was selected to obtain a one-day change in SW. Once SW at the start time of the event is obtained, SI is computed by dividing SW by the soil porosity.

If intervening rainfall occurred between midnight and the start time of the event of interest, another adjustment was made to obtain SI. If the intervening rainfall did not cause runoff, SW was adjusted to mimic one-day changes in SW for

Table B.1. CREAMS Input Files for Study Raingages

Raingage	Vegetation Type	CREAMS Input File[1]	Watershed
83	Brush	RG83.PAR	Lucky Hills (106, 102, 104)
44	Brush	RG44.PAR	WG11
90	Brush	RG90.PAR	WG11
51	Brush	RG51.PAR	WG11
52	Brush	RG52.PAR	WG11
56	Brush/Grass Transition	RG56.PAR	WG11
89	Brush/Grass Transition	RG89.PAR	WG11
88	Grass	RG88.PAR	WG11
91	Grass	RG91.PAR	WG11
54	Grass	RG54.PAR	WG11
55	Grass	RG55.PAR	WG11

[1] These files will be made available in electronic format in the near future.

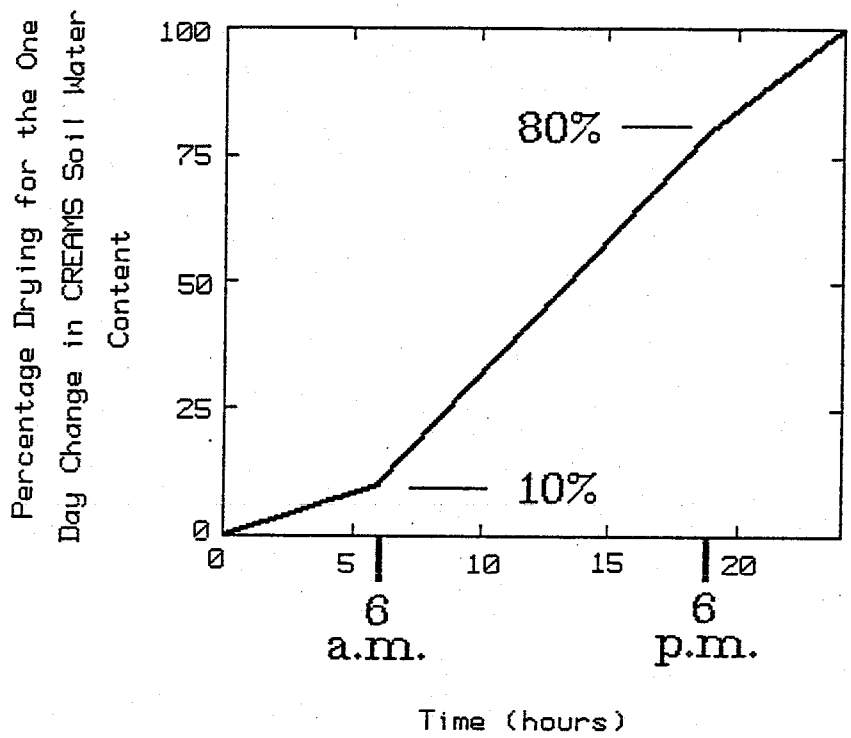

Figure B.1. Percentage of Cummulative Drying Versus Time of Day

the measured amount of intervening rainfall. Drying was assumed to continue following the pattern shown in Figure B.1 from the end of the intervening rainfall to the start time of the event of interest. If intervening rainfall produced runoff, SI was computed in a method consistent with KINEROSR when a rainfall hiatus occurs (Woolhiser et al., 1990). The hiatus was assumed to occur from the end of intervening runoff to the start time of the rainfall causing the runoff event of interest.

The computed initial relative soil saturations (SI) for all of the study events, for each raingage, are contained in input rainfall files. In addition, these files contain raingage coordinates (state plane coordinates, feet), and breakpoint rainfall data for each gage. These input files and the daily rainfall totals for each raingage (required to run CREAMS) are not contained in this document but will be made available in electronic format in the near future.

APPENDIX C

SPACE-TIME RAINFALL INTERPOLATION

APPENDIX C

SPACE-TIME RAINFALL INTERPOLATION

The air mass thunderstorm rainfall that causes the majority of runoff events in Walnut Gulch is highly variable in both time and space. The dense raingage network in the USDA-ARS Walnut Gulch Experimental Watershed affords a unique opportunity to incorporate a relatively detailed description of this highly variable rainfall into runoff modeling. To take advantage of these detailed rainfall data, a simple space-time rainfall interpolation scheme was developed. This appendix describes the interpolation algorithm.

A typical schematic, planimetric, location diagram of three raingages and several model element (overland flow plane or channel) centroids is shown in Figure C.1. Several basic rules were defined to establish the raingage or raingages used to interpolate rainfall. If the centroid of the model element, such as E2, falls within one of the shaded regions shown in Figure C.1, then the breakpoint rainfall data from the nearest raingage (G2) are applied to the entire area of element E2, and no interpolation is done. If the element centroid (E1) is in the interior of the triangle formed by three surrounding raingages (G1-G2-G3), then all three raingages are used in the interpolation to define the storm rainfall pattern for element E1. If the element centroid (E3) is outside of the triangular region (G1-G2-G3), and is not in one of the shaded zones, the nearest two raingages (G1 and G3 for element E3) are used in the interpolation.

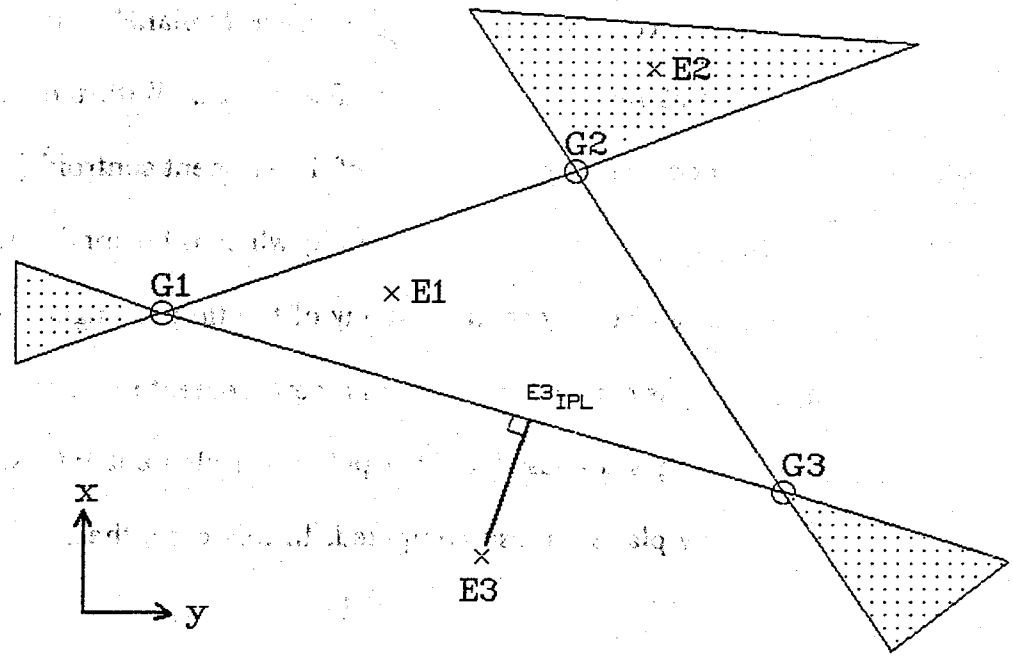

Figure C.1. Planimetric Raingage - Model Element Centroid Diagram

The interpolated rainfall intensity for element centroid E1 at two different times is shown in Figure C.2. For this case, the three surrounding raingages (G1 - G2 - G3) are used in the interpolation. At time (t), three intensities ($I1_t$, $I2_t$, and $I3_t$), computed from breakpoint rainfall data, exist for each of the three raingages. The (X,Y) raingage coordinates with the intensity values $I1_t$, $I2_t$, and $I3_t$ (Z intensity coordinates) are used to form the equation of the "intensity plane" at time (t). This intensity plane is shown as the shaded region in Figure C.2. With the equation of the intensity plane defined, the (x,y) coordinates of the element centroid (E1) can be substituted into this equation to compute the intensity which is be applied to element E1 ($IE1_t$). As soon as the intensity changes at any of the three raingages (time t + Δt), a new intensity plane is computed as well as a new element intensity ($IE1_{t+\Delta t}$).

If only two raingages are used to interpolate an element intensity (E3 in Figure C.1), an "intensity plane" is also computed. In this case, the plane will pass through the $(X,Y,I_t)_{G1}$; $(X,Y,I_t)_{G3}$ coordinates and an arbitrary third coordinate that is not colinear with line G1-G3. The perpendicular line from the element centroid $(x,y)_{E2}$ to the line from G1 to G3 in the I = 0 plane defines the interpolation location for element E3 ($E3_{IPL}$) in the two- raingage interpolation case. The (x,y) coordinates of $E3_{IPL}$ are then substituted into the intensity plane for the two-gage case. The resulting intensity, $IE3_t$, is then applied to the entire area of element E3.

This interpolation scheme is easily implemented but does have several shortcomings. In cases where significant storm motion is present, the scheme will reduce peak rainfall intensities if either the two- or three-raingage interpolation case

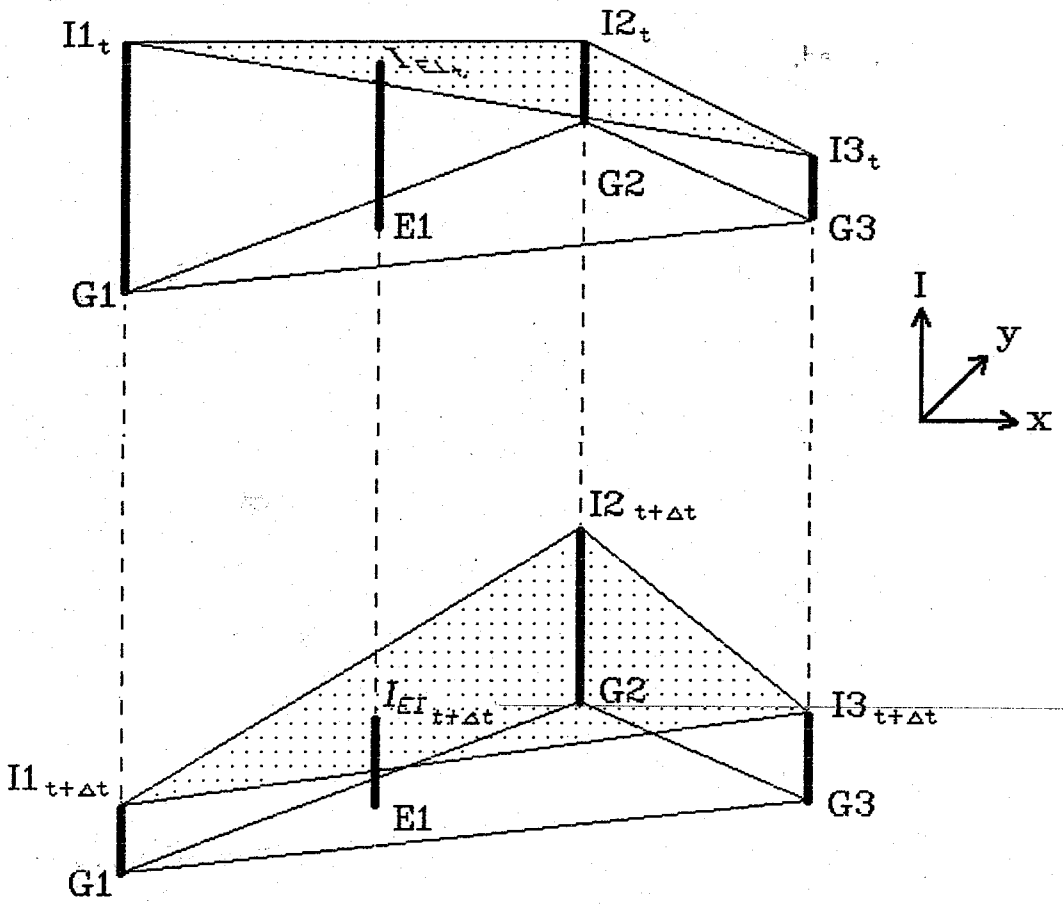

Figure C.2. Time-Space Rainfall Intensity Interpolation for a Model Element Centroid Surrounded by Three Raingages

occurs. Fitting of a higher order surface to the intensity coordinates might alleviate this problem to a certain extent. However, a higher order surface was not justified when the Walnut Gulch raingage density and the observed steep rainfall gradients are considered.